Quels Processus Physiologiques Pilotent l'Acidité de la Banane Dessert (sp. Musa) en Pré et Post Récolte? Modélisation Ecophysiologique et Analyse Expérimentale de l'Effet du Génotype et des Conditions de Croissance du Fruit.

Audrey Etienne

Ecole Doctorale de l'Université des Antilles et de la Guyane

THESE

Pour l'obtention du titre de

Docteur De l'Université Antilles Guyane

Discipline : Sciences Agronomiques, biotechnologiques agro-alimentaires

Présentée par

Audrey ETIENNE

Quels Processus Physiologiques Pilotent l'Acidité de la Banane Dessert (sp. *Musa*) en Pré et Post Récolte? Modélisation Ecophysiologique et Analyse Expérimentale de l'Effet du Génotype et des Conditions de Croissance du Fruit.

CIRAD Martinique - Unité Mixte de Recherche "Qualisud"

Soutenue publiquement le 27 février 2014 devant le jury composé de :

Delphine LUQUET, Chargée de Recherches CIRAD, Montpellier	Rapporteur
Gerhard BUCK-SORLIN, Professeur AgroCampus Ouest, Angers	Rapporteur
Harry OZIER-LAFONTAINE, Directeur de Recherches INRA, Guadeloupe	Examinateur
Alexandra JULLIEN, Maître de Conférence AgroParisTech, Grignon	Examinateur
Félicie LOPEZ-LAURI, Maître de Conférence Université d'Avignon	Examinateur invité
Christophe BUGAUD, Chargé de Recherches CIRAD, Martinique	Encadrant de thèse
Michel GENARD, Directeur de Recherches INRA, Avignon	Directeur de thèse

Quels processus physiologiques pilotent l'acidité de la banane dessert (sp. *Musa*) en pré et post récolte?

Modélisation écophysiologique et analyse expérimentale de l'effet du génotype et des conditions de croissance du fruit.

RESUME

Chez la banane dessert, les saveurs sucrée et acide, caractéristiques importantes pour les consommateurs, sont pilotées par les teneurs en acides citrique et malique. Ce travail a donc porté sur l'étude des processus physiologiques qui pilotent l'accumulation de ces acides dans la pulpe de banane (*Musa* sp. AA) en combinant analyse expérimentale et modélisation écophysiologique. Nous nous sommes notamment intéressés à l'effet du génotype et des conditions de croissance du fruit en adoptant une approche intégrative liant les **phases pré et post récolte**.

Les effets de **la charge en fruit, de la fertilisation potassique, et du stade de récolte** sur l'accumulation du citrate et du malate dans la pulpe ont été étudiés expérimentalement. La **variabilité génotypique** a été prise en compte en choisissant trois génotypes présentant des acidités contrastées à maturité. Des différences d'évolution des teneurs en acides, dues à des modifications métaboliques, ont été observées entre les génotypes pendant les phases pré et post récolte. Le stade de récolte a eu un effet significatif sur les teneurs en acides des fruits pendant la maturation post récolte. La charge en fruit et la fertilisation potassique n'en ont eu aucun.

Des **modèles écophysiologiques** ont été développés pour prédire différents critères d'acidité de la banane en pré et post récolte. Le pH et l'acidité titrable ont été prédits par un modèle d'équilibres acido-basiques, la teneur en malate par un modèle de stockage vacuolaire, et la teneur en citrate par un modèle du cycle de Krebs. Ces modèles ont permis d'identifier les processus physiologiques clés qui pilotent l'acidité de la banane. Des paramètres génotypiques ont été identifiés liés à l'activité de l'enzyme malique mitochondriale et à celle des transporteurs mitochondriaux du malate pour le modèle citrate, et à l'activité des pompes à protons vacuolaire ATPases pour le modèle malate. Ces modèles ont également permis de disséquer l'effet des conditions de croissance du fruit sur l'acidité de la banane.

L'intégration des modèles développés dans un modèle d'élaboration de l'acidité et son utilisation potentielle pour l'amélioration variétale sont discutées.

Mots-clés: Acidité ; banane ; écophysiologie ; génotype ; modélisation ; pré et post récolte

Which physiological processes control banana acidity (sp. *Musa*) during pre and post-harvest stages?

Ecophysiological modeling and experimental analysis of the effects of genotype and fruit growth conditions.

ABSTRACT

Citric and malic acids determine the sourness and sweetness of banana pulp, which are the two main determinants of consumer preferences. The present work focused on the physiological processes controlling the accumulation of citric and malic acids in banana pulp (*Musa* sp. AA) using experimental analysis and ecophysiological modeling. We chose an integrative approach linking the **pre and post-harvest stages**, and focused on the effect of genotype and fruit growing conditions.

Experiments were conducted to study the effect of **fruit load, potassium fertilization and fruit age at harvest** on the accumulation of citrate and malate in banana pulp. To account for **genotypic variability**, three genotypes with contrasting acidity at the eating stage were studied. Major differences in the pattern of citrate and malate accumulation were found in the three cultivars both during growth and post-harvest ripening and were shown to be the result of metabolic changes. The harvest stage had a significant effect on the concentrations of acids during post-harvest ripening. Fruit load and potassium fertilization had no effect.

Ecophysiological models were developed to predict several banana acidity criteria during the pre and post harvest stages. pH and titratable acidity were predicted by a model of acid-base reactions; malate content by a model of vacuolar storage; and citrate content by a model of the TCA cycle. These models led to the identification of the key physiological processes that control banana acidity. Genotypic parameters were identified, which were related to the activity of the mitochondrial malic enzyme and of the malate mitochondrial carriers in the citrate model, as well as to the activity of the vacuolar proton pump, ATPase, in the malate model. The two models were also used to analyze the effects of fruit growth conditions on banana acidity.

Combining the three models in a global model of banana acidity, and the possible use of this model for varietal improvement are discussed.

Key Words: Acidity; banana; ecophysiology; genotype; modeling; pre and post-harvest

Remerciements

Mon premier remerciement va à Michel Génard pour avoir accepté de diriger cette thèse. Je ne saurai assez le remercier pour sa présence constante et ses encouragements au cours de ces trois années malgré la distance (vive Skype !). Ces années passées à travailler à ses côtés ont été un vrai plaisir (malgré les quelques moments de doute et de déprime inhérents à une thèse!) et une belle aventure humaine. J'ai appris à ses côtés la rigueur, la ténacité et la curiosité d'esprit.

Un très grand merci à mon encadrant Christophe Bugaud avec qui le travail rime avec bonne humeur. Merci pour ton accueil chaleureux, ton soutien, tes conseils, et tes bonnes blagues ! Elle nous en aura fait voir de toutes les couleurs la banane !

Merci à Philippe Lobit pour ses lumières sur le monde compliqué des acides organiques et pour son implication dans l'écriture de plusieurs articles de cette thèse.

Je remercie les membres du jury pour avoir bien voulu étudier et évaluer ce travail : merci à Delphine Luquet et Gerhard Buck-Sorlin d'avoir accepté la lourde mission de rapporteurs. Merci à Harry Ozier-Lafontaine, Alexandra Jullien et Félicie Lopez-Laurie pour leur participation au jury.

Je remercie Marie-Odette Daribo et Doriane Bancel pour leur aide précieuse dans l'acquisition des données. Que d'échantillons broyés, filtrés, dosés !

Un grand merci à Mohammed et Thomas (qui a pris la relève !) pour tous les programmes qu'ils ont si gentiment accepté de faire tourner sur leurs ordis.

Merci à mes petites mains, Sophie, Marielle, Géraldine, Earvin, Marion, Florian, Yasmina, Vanessa pour les longues heures passées dans les bananeraies ou dans le labo.

Au moment de conclure ce travail, je pense à tous mes amis du PRAM qui se sont succédés durant ces 3 années: Soline, Benjamin, Sophie, Gina, Aude, Florian, Chachou, Alice, Gaëlle et tous les autres…

Je remercie le personnel du PRAM pour son accueil et son aide ; je pense en particulier à Dominique pour son aide dans les bananeraies.

Merci à mes nunuches Céline, Camille, les Julies et Amandine pour avoir toujours été présentes malgré la distance et pour être venues me rendre visite pour celles qui le pouvaient.

Merci à Gigi pour m'avoir tenue compagnie les journées pluvieuses et les soirs de rédaction devant l'ordinateur…et merci pour les petites surprises ramenées dans l'appartement !

Merci à ma famille chérie pour m'avoir encouragée et soutenue même si mon travail leur a toujours semblé mystérieux !

Et pour terminer, merci à Romain qui a rendu ces 3 années magiques…

« *Il faut avoir du chaos en soi pour accoucher d'une étoile qui danse*. » Nietzsche

Sommaire

Liste des annexes

Liste des tableaux

Liste des figures

Introduction Générale

1 Contexte de la thèse

La banane dessert est la deuxième production fruitière mondiale (106 millions de tonnes (MT) en 2011) et la première production agricole des Antilles françaises (298 000 T en 2011) (FAOSTAT). La filière banane dessert des Antilles françaises, qui comprend essentiellement des variétés du sous-groupe Cavendish (Musa spp AAA), est exportée en totalité au sein de l'Union européenne (Loeillet, 2008), et se caractérise donc par des phases de production et de maturation bien distinctes. ***On parle ainsi de phase pré récolte pour décrire la période de croissance du fruit sur la plante, et de phase post récolte pour décrire la période de transport, stockage et maturation des fruits après récolte*** (*Fig. 1*)**.** La banane étant un fruit climactérique, l'initiation de la maturation après récolte est déclenchée par un traitement à l'éthylène.

La filière banane dessert des Antilles doit faire face à plusieurs enjeux : d'une part une concurrence accrue avec les pays d'Amérique latine et d'Afrique (Maillard, 2002), et d'autre part une pression parasitaire importante due à la sensibilité du sous-groupe Cavendish aux cercosporioses jaune et noire, deux maladies fongiques foliaires importantes du bananier présentes aux Antilles (Jeger *et al.*, 1995). Dans ce contexte, la création de variétés de banane dessert présentant des qualités gustatives différentes de celle du standard Cavendish (Bugaud *et al.*, 2011) et une résistance aux principales maladies (Abadie *et al.*, 2007) apparaît comme une voie privilégiée pour accroître la viabilité et la durabilité de la filière. Depuis une vingtaine d'années, le Centre de Coopération Internationale en Recherche Agronomique pour le Développement (CIRAD) travaille donc sur la création d'hybrides alliant ces deux caractéristiques, mais les hybrides proposés jusqu'ici ont été rejetés par les consommateurs pour cause de défauts sensoriels. ***Il apparaît alors nécessaire de comprendre les mécanismes impliqués dans l'élaboration de la qualité sensorielle de la banane*** afin de pouvoir proposer des hybrides répondant aux exigences des consommateurs**.**

Les saveurs sucrée et acide jouent un rôle crucial dans l'acceptabilité des fruits par les consommateurs (Mehinagic *et al.*, 2012). Récemment, une étude multivariétale a montré l'importance de ces saveurs dans l'expression de la diversité sensorielle de variétés de bananes dessert (Bugaud *et al.*, 2011). Chez de nombreux fruits, et notamment la banane, les saveurs sucrée et acide sont principalement pilotées par les concentrations en acides organiques (Esti *et al.*, 2002; Harker *et al.*, 2002; Tieman *et al.*, 2012), essentiellement le malate et le citrate (Bugaud *et al.*, 2013; Seymour *et al.*, 1993). ***La compréhension de***

l'élaboration de la qualité sensorielle de la banane passe donc par l'étude des mécanismes impliqués dans l'accumulation de ces deux acides organiques.

La majeure partie du citrate et du malate stockés dans les cellules de la pulpe des fruits est synthétisée au sein du fruit (Bollard, 1970; Sweetman *et al.*, 2009; Ulrich, 1970). Ces deux acides sont impliqués dans de nombreuses voies métaboliques et jouent donc un rôle important dans la physiologie du fruit. Le malate et le citrate sont synthétisés et dégradés au travers de différentes voies métaboliques localisées dans différents compartiments cellulaires. Dans la mitochondrie se déroule le cycle de Krebs, une des voies métaboliques centrales pour la vie cellulaire, et au sein duquel le malate et le citrate peuvent être produits ou dégradés (Sweetlove *et al.*, 2010). Dans le cytosol, le malate est produit par la carboxylation du phosphoénolpyruvate (PEP), un intermédiaire de la glycolyse, et est dégradé en PEP, par la voie métabolique inverse, ou bien en pyruvate (Sweetman *et al.*, 2009). Dans le cytosol, le citrate peut être dégradé au travers de deux voies cataboliques : le GABA shunt qui conduit à la synthèse du γ-aminobutirate (Bown and Shelp, 1997), et la voie de synthèse de l'acetyl-CoA conduisant *in fine* à la synthèse de flavoinoids et isoprenoids (Fatland *et al.*, 2002). Dans le glyoxysome se déroule le cycle du glyoxylate dont la fonction finale est de convertir les acides gras en glucose et au sein duquel le malate et le citrate participent en tant qu'intermédiaires (Pracharoenwattana and Smith, 2008). La localisation de ces voies métaboliques dans différents compartiments cellulaires implique l'existence de mécanismes de transports permettant aux métabolites de transiter entre chacun d'eux. Ainsi, chez les plantes, plusieurs types de transporteurs ont été mis en évidence sur la membrane mitochondriale interne (Haferkamp and Schmitz-Esser, 2012), ainsi que sur la membrane du glyoxysome (Rottensteiner and Theodoulou, 2006). Le citrate et le malate sont stockés dans la vacuole des cellules de la pulpe du fruit grâce à un système de transports membranaires extrêmement complexe gouverné par les lois thermodynamiques de transport de solutés au travers d'une membrane biologique et faisant intervenir différentes types de transporteurs (Shiratake and Martinoia, 2007). ***La compréhension des mécanismes d'accumulation du citrate et du malate dans le fruit nécessite donc d'étudier le métabolisme et le stockage vacuolaire de ces acides afin d'identifier les principaux processus contrôlant leurs accumulation.***

Plusieurs études ont mis en lumière le rôle des facteurs génétiques sur l'accumulation du citrate et du malate dans la pulpe des fruits (cf. (Etienne *et al.*, 2013b)). Chez de nombreuses espèces de fruits, des phénotypes dits « doux » et « acides » ont été identifiés et des études de transcriptomique, protéomique, ou encore métabolomique ont mis en évidence certains gènes et enzymes potentiellement à l'origine de ces différences phénotypiques

(Berüter, 2004; Chen *et al.*, 2009; Sadka *et al.*, 2000a; Yao *et al.*, 2009). Concernant la banane, il a été montré que les concentrations en malate et citrate de la pulpe varient de manière significative entre cultivars (Bugaud *et al.*, 2013), ce qui met en évidence une forte composante génétique dans la détermination de l'acidité de la banane. ***Cependant, il n'existe à ce jour aucune information sur les origines physiologiques d'une telle variabilité génotypique.***

L'accumulation des acides organiques dans la pulpe des fruits est sous l'influence de facteurs agro-environnementaux. Ainsi, il a été montré que la température ainsi que la disponibilité hydrique avaient une influence sur l'acidité de fruits tels que la tomate (Veit-Köhler *et al.*, 1999), la pomme (Mills *et al.*, 1996) ou encore les agrumes (Kallsen *et al.*, 2011; Thakur and Singh, 2012). Certaines pratiques culturales, telles que la manipulation du rapport feuille : fruit et la fertilisation potassique, ont également une influence sur l'acidité des fruits tels que la pêche (Wu *et al.*, 2002), la mangue (Léchaudel *et al.*, 2005b), l'ananas (Spironello *et al.*, 2004), ou encore le citron (Alva *et al.*, 2006). Plusieurs études ont révélé l'influence des facteurs pré récolte sur l'acidité de la banane pendant la maturation post récolte. Ainsi, il a été montré que l'altitude de même que le site et la période de production ont un effet significatif sur les concentrations en citrate et malate dans la banane mûre après récolte (Bugaud *et al.*, 2006; Bugaud *et al.*, 2009). Ramesh Kumar et Kumar (2007) ainsi que Vadivel et Shanmugavelu (1978) ont observé que la fertilisation potassique des bananiers entraînait une diminution significative de l'acidité titrable des bananes mûres après récolte. L'âge physiologique du fruit à la récolte semble aussi avoir un effet sur l'accumulation des acides pendant la maturation post récolte puisque une étude a montré que les fruits mûrs (après maturation post récolte) récoltés plus tôt avaient des concentrations plus élevées en malate et moins élevées en citrate que les fruits récoltés plus tard (Bugaud *et al.*, 2006). ***Il semble donc que les conditions de production en pré récolte peuvent affecter les concentrations en citrate et malate dans la pulpe de banane après récolte, d'où l'importance d'adopter une approche intégrative liant les phases pré et post récolte*** *(Fig. 1).* L'acquisition de connaissances sur les facteurs pré récolte qui influencent l'acidité de la banane au cours de la maturation post récolte est nécessaire pour innover en matière de pratiques culturales permettant d'obtenir des fruits mûrs présentant un niveau d'acidité satisfaisant.

Depuis quelques années, l'utilisation de modèles écophysiologiques se révèle être un outil puissant pour étudier les effets du génotype et de l'environnement sur la physiologie de la plante (Génard *et al.*, 2007; Hammer *et al.*, 2006; Struik *et al.*, 2005). Les modèles écophysiologiques ont pour but de décomposer une variable très intégrative en processus

élémentaires et permettent ainsi d'identifier les mécanismes physiologiques qui pilotent cette variable et de voir à quels niveaux jouent les facteurs environnementaux. Les modèles écophysiologiques contiennent un certain nombre de paramètres indépendants de l'environnement et pouvant prendre des valeurs différentes selon le génotype, et sont donc un outil intéressant pour analyser la variabilité génotypique d'un trait (Quilot and Génard, 2005; Wu *et al.*, 2012). A l'échelle du fruit, plusieurs modèles écophysiologiques ont été proposés permettant de prédire différents critères de sa qualité tels que l'accumulation des sucres (Dai *et al.*, 2009; Génard and Souty, 1996), de la matière sèche (Léchaudel *et al.*, 2005a; Lescourret *et al.*, 1998) et de l'eau (Fishman and Génard, 1998; Léchaudel *et al.*, 2007; Liu and Génard, 2007). Bien que l'acidité soit un critère important de la qualité du fruit, plus rares sont les modèles qui s'attachent à décrire son élaboration. A ce jour, aucun modèle décrivant la variabilité génotypique et environnementale de l'acidité de la banane n'a été proposé. Cependant, des modèles écophysiologiques permettant de prédire les concentrations en citrate et malate dans le fruit ont été développés chez la pêche. Ils représentent de manière simplifiée les principaux mécanismes cellulaires impliqués dans l'accumulation de ces deux acides (Lobit *et al.*, 2006; Lobit *et al.*, 2003; Wu *et al.*, 2007) et permettent de prédire les changements de teneurs en acides au cours du développement du fruit en réponse à certains facteurs agro-environnementaux. ***Ils peuvent donc constituer une base pour la construction de tels modèles adaptés aux particularités liées à l'espèce Musa et à son mode de production. L'utilisation de ces modèles pourra permettre d'apporter des éléments de réponse sur les origines de la variabilité génotypique et sur les déterminants physiologiques de l'accumulation du malate et du citrate dans la pulpe de banane au cours de la croissance et de la maturation post récolte du fruit.***

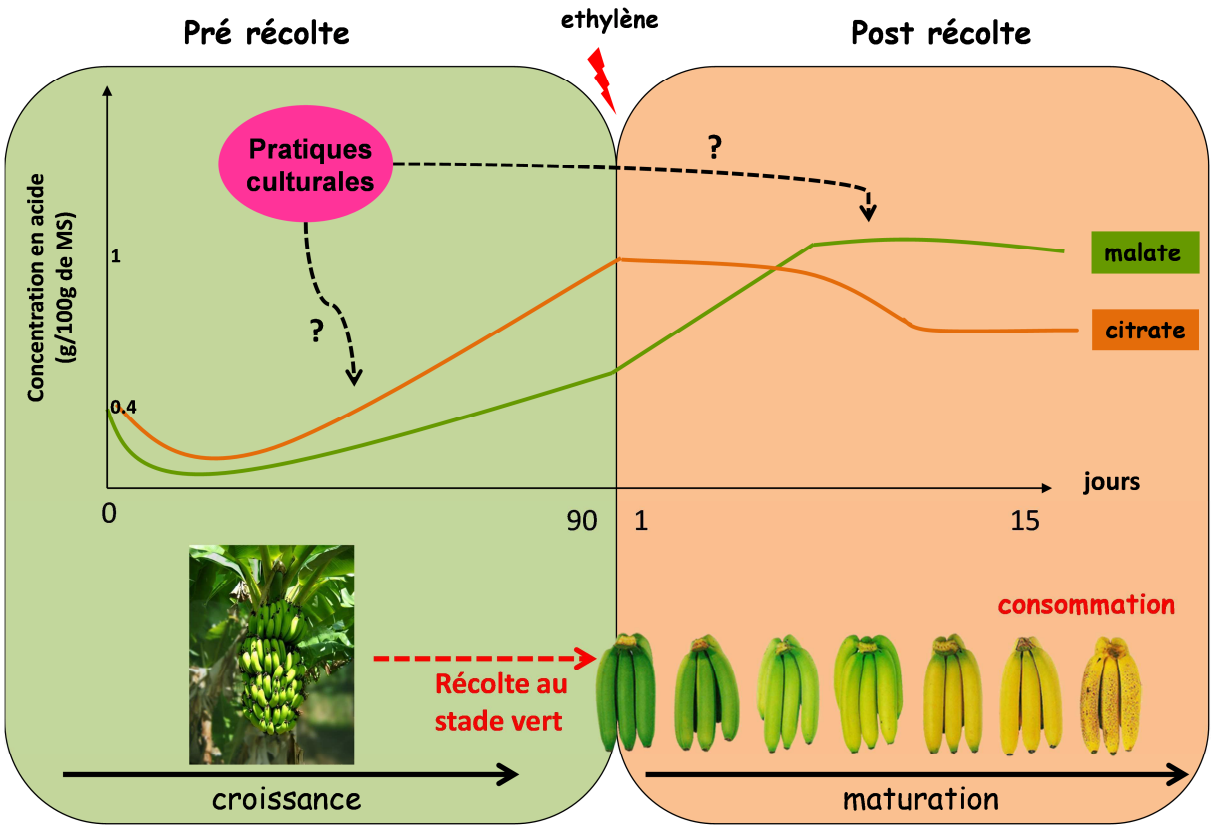

Figure 0-1 Cultural practices might affect organic acids concentrations both during the pre and postharvest stages of banana development.

2 Objectifs de la thèse

Mon travail de thèse a porté sur la compréhension des processus physiologiques impliqués dans l'accumulation du citrate et du malate chez la banane dessert. Les facteurs génotypiques et agro-environnementaux pouvant avoir une forte influence sur l'acidité des fruits (cf. Contexte de la thèse), je me suis notamment intéressée à leur influence sur l'accumulation des acides organiques chez la banane dessert. La démarche choisie dans ce travail a été de combiner analyse expérimentale et modélisation, en adoptant une approche intégrative liant les phases pré et post récolte (associée à la phase de consommation). L'accent a été mis sur l'étude de l'effet de la charge en fruit, de la fertilisation potassique et du stade de récolte, trois facteurs agronomiques couramment manipulés par les producteurs de banane et connus pour affecter l'acidité des fruits (cf. Contexte de la thèse).

Dans un premier temps, des connaissances ont donc été acquises sur l'effet de ces trois pratiques agronomiques sur l'accumulation du citrate et du malate dans la pulpe de banane durant les phases pré et post récolte, au travers d'expérimentations agronomiques. Afin de prendre en compte la variabilité génotypique, trois génotypes de banane dessert présentant des acidités contrastées à maturité ont été étudiés.

Dans un deuxième temps, l'intégration des données expérimentales acquises dans des modèles écophysiologiques de prédiction des concentrations en citrate et malate dans la pulpe de banane, a permis de proposer des hypothèses sur les origines des différences génotypiques au niveau cellulaire et sur l'effet des facteurs agronomiques observés expérimentalement. Les modèles ont été construits sur la base de ceux proposés par Lobit et al. (2006; 2003; 2002) pour la pêche. L'étude a porté à la fois sur les phases pré et post récolte afin de voir quels pourraient être les origines physiologiques des différences de profils d'accumulation en acides organiques entre ces deux phases.

La finalité de cette thèse est d'apporter des éléments de compréhension sur les mécanismes de régulation de l'accumulation du citrate et du malate chez la banane dessert, et notamment de fournir des pistes sur l'origine de la variabilité génotypique.

3 Plan de la thèse

Cette thèse est organisée en trois chapitres principaux. Le chapitre I est une **synthèse bibliographique** sur les mécanismes cellulaires impliqués dans l'accumulation du citrate et du malate dans les cellules de la pulpe des fruits. L'objectif de cette synthèse est d'identifier les processus qui pilotent l'accumulation du citrate et du malate dans les cellules de la pulpe du fruit. Les effets de différents facteurs agro-environnementaux (température, disponibilité hydrique, charge en fruit, fertilisation) sur l'acidité des fruits sont également analysés pour tenter de comprendre sur quels mécanismes cellulaires ils agissent. Les conclusions de cette synthèse seront mobilisées par la suite pour la construction des modèles écophysiologiques.

Le chapitre II présente les **résultats expérimentaux** des effets de la charge en fruit, de la fertilisation potassique et du stade de récolte sur l'accumulation du citrate et du malate chez trois génotypes de banane dessert présentant des acidités contrastées. Cette étude nous a permis de voir si ces facteurs influencent les teneurs en acides organiques de la même manière chez les trois cultivars, et quelles phases de développement, à savoir croissance et/ou maturation post récolte, sont affectées.

Le chapitre III décrit le développement de **modèles écophysiologiques** permettant de prédire différents critères d'acidité du fruit. Cette approche, basée sur l'intégration des données expérimentales acquises, a permis de proposer des hypothèses sur les processus physiologiques qui pilotent l'acidité de la banane et sur les origines de la variabilité génotypiques au niveau cellulaire. L'étude a porté à la fois sur les phases pré et post récolte afin de voir quels pourraient être les origines physiologiques des différences de profils d'accumulation en acides organiques entre ces deux phases. Ce chapitre est organisé en trois

parties. La première partie présente un **modèle de prédiction du pH et de l'acidité titrable** de la pulpe de banane à travers la représentation des équilibres acido-basiques (Lobit *et al.*, 2002). La deuxième partie présente un **modèle d'accumulation du malate** dans la pulpe de banane basé sur une représentation simplifiée du mécanisme de transport du malate dans la vacuole (Lobit *et al.*, 2006). La troisième partie présente un **modèle d'accumulation du citrate** dans la pulpe de banane basé sur une représentation simplifié du cycle de Krebs dans la mitochondrie.

Enfin, la **conclusion générale** des travaux présentés débouche sur des perspectives ouvertes. L'intégration des trois modèles développés est présentée et son utilisation potentielle est abordée. L'utilisation d'un tel modèle écophysiologique, combiné à des données génétiques, dans le cadre de la sélection variétale est discutée.

4 Publications et communications scientifiques

Publications dans des revues scientifiques soumises à comité de lecture

Etienne A., Génard M., Lobit P., Mbéguié-A-Mbéguié D., Bugaud C., 2013. What controls fleshy fruit acidity? A review of malate and citrate accumulation in fruit cell. Journal of Experimental Botany; 64(6):1451-1469.

Etienne A., Génard M., Bancel B., Benoit S., Nonone M., Bugaud C., 2013. A model approach revealed the relationship between banana pulp acidity and composition during growth and post-harvest ripening. Scientia Horticulturae; 162:125-134.

Etienne A., Génard M., Bancel B., Benoit S., Bugaud C., (accepté dans Scientia Horticultuare). Citrate and malate accumulation in banana fruit (*Musa* sp. AA) is highly affected by genotype and fruit age, but not by cultural practices.

Etienne A., Génard M., Bugaud C., (soumis à Plant Physiology). A model of TCA cycle functioning to analyze citrate accumulation in pre and post-harvest fruits: application to banana fruit (*Musa* sp. AA).

Etienne A., Génard M., Lobit P., Bugaud C., (à soumettre en février-mars). Modeling the vacuolar storage of malate shed lights on malate accumulation in pre and post-harvest banana (*Musa* sp. AA).

Communication orale

Etienne A., Génard M., Bancel B., Benoit S., Nonone M., Barre F., Bugaud C., 2012. Modeling changes in pH and titratable acidity during the maturation of dessert banana. 2nd International Symposium on Horticulture in Europe - SHE2012, Angers, France, July 1-5 2012.

Chapitre I Qu'est ce qui Contrôle l'Acidité des Fruits ?

Synthèse Bibliographique sur l'Accumulation du Malate et du Citrate dans les Cellules du Fruit

Objectifs

Ce chapitre est une synthèse bibliographique sur les avancées faites dans la compréhension des mécanismes cellulaires impliqués dans l'accumulation du citrate et du malate dans les cellules de la pulpe des fruits charnus, en mettant l'accent sur les origines possibles des différences variétales ainsi que sur l'influence des facteurs agro-environnementaux. Les conclusions de cette synthèse seront mobilisées par la suite pour la construction des modèles écophysiologiques. Ce chapitre a fait l'objet d'une publication dans **Journal of Experimental Botany** sous la forme d'une review intitulée « What controls fleshy fruit acidity? A review of malate and citrate accumulation in fruit cells ».

Principaux résultats

- L'accumulation du citrate et du malate dans la pulpe des fruits est le résultat de l'interaction complexe entre métabolisme et stockage vacuolaire.
- L'accumulation du citrate semble être pilotée par le cycle de Krebs et donc par la respiration, alors que l'accumulation du malate semble être pilotée par le stockage vacuolaire.
- Plusieurs facteurs environnementaux (température et disponibilité en eau) et pratiques culturales (charge en fruit, fertilisation potassique) affectent l'acidité des fruits en agissant sur différents mécanismes cellulaires (métabolisme, stockage vacuolaire, accumulation d'eau).

What controls fleshy fruit acidity? A review of malate and citrate accumulation in fruit cells

A. Etienne[1], M. Génard[2], P. Lobit[3], D. Mbeguié-A-Mbéguié[4], C. Bugaud[1]

[1] Centre de Coopération International en Recherche Agronomique pour le Développement (CIRAD), UMR QUALISUD, Pôle de Recherche Agronomique de Martinique, BP 214, 97 285 Lamentin Cedex 2, France

[2] INRA, UR 1115 Plantes et Systèmes de Cultures Horticoles, F-84914 Avignon, France

[3] Instituo de investigaciones Agropecuarias y Forestales, Universidad Michoacana de San Nicolas de Hidalgo, Tarimbaro, Michoacan, CP. 58880, Mexico

[4] Centre de Coopération International en Recherche Agronomique pour le Développement (CIRAD), UMR QUALISUD, Station de Neufchâteau, Sainte-Marie, 97130 Capesterre Belle-Eau, Guadeloupe

Abstract

Fleshy fruit acidity is an important component of fruit organoleptic quality and is mainly due to the presence of malic and citric acids, the main organic acids found in most ripe fruits. The accumulation of these two acids in fruit cells is the result of several interlinked processes that take place in different compartments of the cell and appear to be under the control of many factors. This review combines analyses of transcriptomic, metabolomic, and proteomic data, and fruit process-based simulation models of the accumulation of citric and malic acids, to further our understanding of the physiological mechanisms likely to control the accumulation of these two acids during fruit development. The effects of agro-environmental factors, such as the source: sink ratio, water supply, mineral nutrition, and temperature on citric and malic acid accumulation in fruit cells have been reported in several agronomic studies. This review sheds light on the interactions between these factors and the metabolism and storage of organic acids in the cell.

1 Introduction

Fleshy fruit acidity, as measured by titratable acidity and/or pH, is an important component of fruit organoleptic quality (Bugaud *et al.*, 2011; Esti *et al.*, 2002; Harker *et al.*, 2002). Fruit acidity is due to the presence of organic acids, and malic and citric acids are the main acids found in most ripe fruits (Seymour *et al.*, 1993). Understanding the factors that influence the concentration of these acids in fruit cells is thus of primary importance for fruit quality improvement.

The predominant organic acid in ripe fruit varies among species. Malic acid is dominant in apple (Yamaki, 1984), loquat (Chen *et al.*, 2009), and pear (Lu *et al.*, 2011), whereas citric acid is dominant in citrus fruits (Yamaki, 1989). In many fruit species, differences in total acidity or in the balance of organic acids among cultivars are also observed, e.g. in loquat (Yang *et al.*, 2011), peach (Etienne *et al.*, 2002), pear (Lu *et al.*, 2011), citrus (Albertini *et al.*, 2006), pineapple (Saradhuldhat and Paull, 2007), apricot (Gurrieri *et al.*, 2001) and banana (Bugaud *et al.*, 2011).

The processes involved in the metabolism and accumulation of malic and citric acids in mesocarp cells are under both genetic and environmental control. Transcriptomics (Cercos *et al.*, 2006; Deluc *et al.*, 2007; Etienne *et al.*, 2002), metabolomics (Deluc *et al.*, 2007; Katz *et al.*, 2011), proteomics (Famiani *et al.*, 2005; Katz *et al.*, 2007), and QTLs (Lerceteau-Köhler *et al.*, 2012; Schauer *et al.*, 2006; Xu *et al.*, 2012) studies have helped decipher some of the mechanisms that control acidity, and intervene at cellular level. Many agronomic studies have shown the impacts of cultural practices, including irrigation (Thakur and Singh, 2012; Wu *et al.*, 2002), mineral fertilization (Cummings and Reeves, 1971; Ramesh Kumar and Kumar, 2007; Spironello *et al.*, 2004), thinning (Léchaudel *et al.*, 2005b; Souty *et al.*, 1999; Wu *et al.*, 2002), and environmental factors like temperature (Burdon *et al.*, 2007; Gautier *et al.*, 2005; Wang and Camp, 2000), on fruit acidity, but how they affect malic and citric acid accumulation in the cell is still not clear.

In the last few years, process-based simulation models (PBSMs) of fruit have been increasingly used to simulate the metabolic and biophysical aspects of cell behavior (Martre *et al.*, 2011) and appear to be a powerful tool to study genotype x environment interactions (Bertin *et al.*, 2010). Fruit PBSMs of the accumulation of citric acid (Lobit *et al.*, 2003; Wu *et al.*, 2007) and malic acid (Lobit *et al.*, 2006) have been developed to predict citric and malic acid concentrations in the whole fruit during development in peach.

The aim of this review is to elucidate the physiological mechanisms that probably control citric and malic acid accumulation during fruit development and their possible

regulation by genetic and agro-environmental factors. To this end, the review combines analyses of transcriptomic, metabolomic, and proteomic data related to malic and citric acid metabolism, and also the PBSMs of citric and malic acids. The three first sections describe the cell mechanisms involved in malic and citric acid accumulation and their regulation. The last section deals with the effects of agro-environmental factors (source: sink ratio, mineral fertilization, water supply, and temperature) on citric and malic acid accumulation and the related cell mechanisms they may affect.

In this review, the terms "malate" and "citrate", which usually describe the conjugate base of malic and citric acids, refer to all physiological forms of each compound.

2 Several pathways exist for malate and citrate metabolism in the mesocarp cells of fleshy fruits

Even though some organic acids are supplied by the sap, variations in the acidity of fleshy fruits are mainly due to the metabolism of malate and citrate in the fruit itself (Bollard, 1970; Sweetman *et al.*, 2009; Ulrich, 1970). This section presents the metabolic pathways involved in the metabolism of the dicarboxylate malate and the tricarboxylate citrate. We first describe the pathways responsible for the initial formation of organic acids (carboxylation of phosphoenolpyruvate (PEP) in the cytosol), then the pathways responsible for the degradation of organic acids (decarboxylation of malate and oxaloacetate (OAA) in the cytosol), and finally those that allow conversion between tri- and di-carboxylates (the TCA cycle in the mitochondria, the glyoxylate cycle in the glyoxysome, and citrate catabolism in the cytosol) (*Fig. I.1*).

2.1 First step in organic acids synthesis: PEP carboxylation in the cytosol

Formation of acidity involves the synthesis of organic acids, mostly malate and citrate, which can be stored in the vacuole in large amounts. As citrate is produced from dicarboxylates (mostly malate) (see following section), the first step in the development of acidity is the synthesis of dicarboxylates, namely malate and OAA. These require fixation of CO_2 on a carbon skeleton derived from hexose catabolism (Hardy, 1968; Young and Biale, 1968), which is achieved by the carboxylation of PEP, catalyzed by the phosphoenolpyruvate carboxylase (PEPC). This reaction takes place in the cytosol, since PEP is an intermediate of the glycolysis pathway, and produces OAA, which can then be reduced into malate by the cytosolic NAD-dependant malate dehydrogenase (NAD-cytMDH) (Givan, 1999) or supplied the TCA cycle if replenishment is necessary (Leegood and Walker, 2003) (*Fig. I.1*).

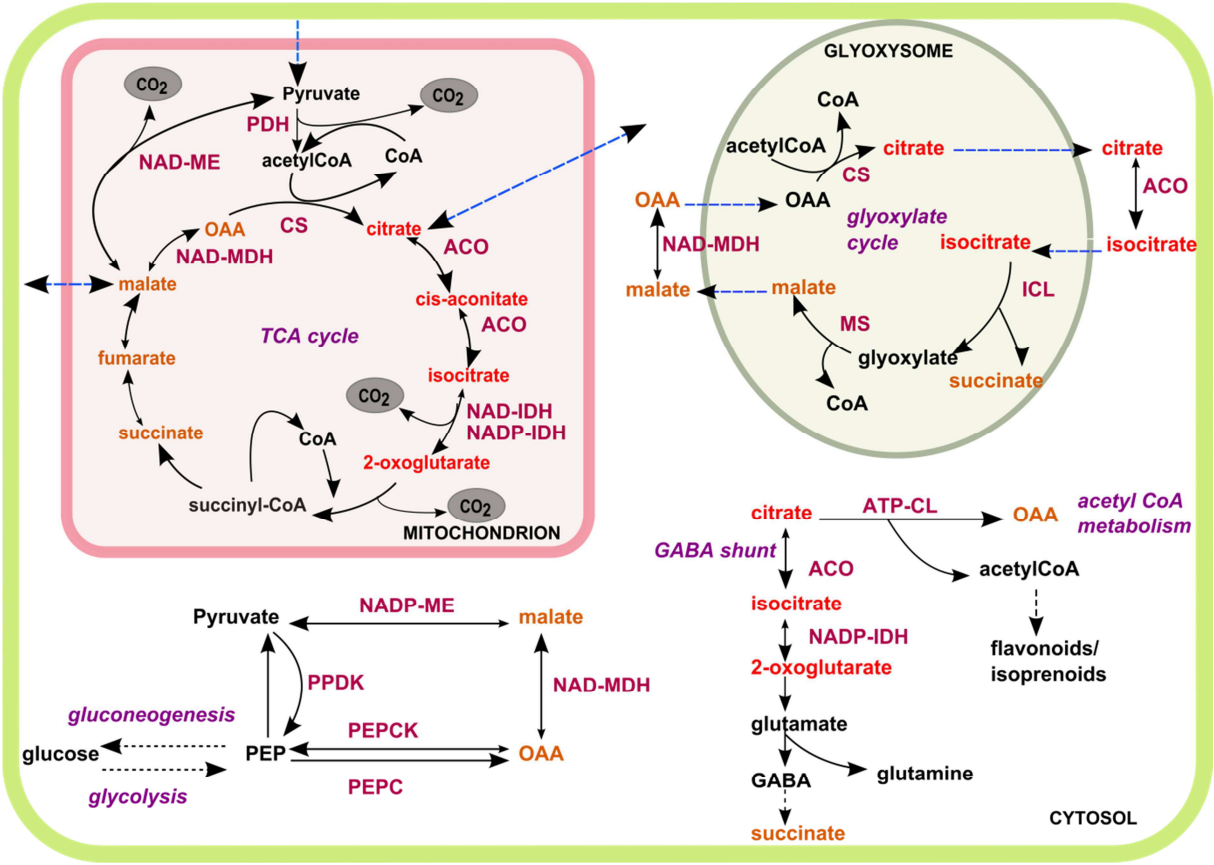

Figure I-1 Citrate and malate metabolic pathways in fruit mesocarp cells. Only the enzymes described in the paper are shown. ACO: aconitase; ATP-CL: ATP-citrate lyase; CS: citrate synthase; ICL: isocitrate lyase; MS: malate synthase; NAD-MDH: NAD-malate dehydrogenase; NAD-ME: NAD-malic enzyme; NAD-IDH: NAD-isocitrate dehydrogenase; NADP-ME: NADP-malic enzyme; NADP-IDH: NADP-isocitrate dehydrogenase; PDH: pyruvate dehydrogenase; PEPC: phosphoenolpyruvate carboxylase; PEPCK: phosphoenolpyruvate carboxykinase; PPDK: pyruvate orthophosphate dikinase. The probable direction of reversible reactions is indicated by the large arrow. Dashed blue arrows indicate malate and citrate transport. Names in orange are dicarboxylates and names in red are tricarboxylates.

Multiple PEPC isoforms have been detected in fruits and are possibly the result of transcriptomic (Sweetman *et al.*, 2009; Yao *et al.*, 2009) and/or post-translational regulations (Sweetman *et al.*, 2009). PEPC is controlled by both cytosolic pH and malate concentration (Davies, 1986; Lakso and Kliewer, 1975a; Possner *et al.*, 1981) in a way that stabilize the cytosolic pH (Smith and Raven, 1979). In grape berries, transcriptomic analysis (Or *et al.*, 2000; Terrier *et al.*, 2005) and measurement of enzymatic activity (Diakou *et al.*, 2000; Hawker, 1969; Ruffner *et al.*, 1976) pointed to the role of PEPC in malate accumulation throughout fruit development. Several studies based on analyses of transcriptomic and enzymatic activity suggest that PEPC is not responsible for the difference in malate content between low and high acid peach cultivars (Moing *et al.*, 2000), apple (Yao *et al.*, 2009), and loquat (Chen *et al.*, 2009).

NAD-cytMDH catalyzes the reversible conversion of malate into OAA, the most likely direction being the synthesis of malate (Sweetman *et al.*, 2009; Yao *et al.*, 2011). Even if a mitochondrial form is also present in fruit cells (see following section), it has been shown in several fruits that NAD-cytMDH represents 70% to 80% of total NAD-dependant MDH (Abou-Zamzama and Wallace, 1970; Taureilles-Saurel *et al.*, 1995), explaining why total NAD-dependant MDH activity is generally related to malate synthesis in fruits (Chen *et al.*, 2009; Martınez-Esteso *et al.*, 2011; Zhao *et al.*, 2007). Yao *et al.* (2011) showed that over expression of the apple MdcyMDH gene encoding NAD-cytMDH resulted in an increase in malate, fructose and sucrose content, suggesting its direct involvement in malate synthesis. Over expression of MdcyMDH also resulted in the up regulation of several malate-related genes/enzymes, suggesting an indirect role in malate accumulation.

2.2 Organic acids degradation: malate and OAA decarboxylation in the cytosol

Loss of acidity implies decarboxylation of carboxylates, which can occur through the conversion of tricarboxylates into dicarboxylates (described later in the review), but also through decarboxylation of the dicarboxylates malate and OAA leading to the degradation of organic acids (*Fig. I.1*). Decarboxylation of OAA and malate allows the production of PEP and is linked to the activation of gluconeogenesis (Sweetman *et al.*, 2009). Gluconeogenesis is a metabolic pathway that results in the generation of glucose from PEP. It occurs mostly during fruit ripening when sugars accumulate rapidly (Sweetman *et al.*, 2009). In the past few years, proteomics (Katz *et al.*, 2011), transcriptomics and metabolite (Carrari *et al.*, 2006; Deluc *et al.*, 2007; Fait *et al.*, 2008) analyses have provided evidence for a shift from the accumulation of organic acids to sugar synthesis during the final stage of development in several fruit species.

PEP can originate from OAA through the activity of phosphoenol carboxykinase (PEPCK) which catalyzes the reversible reaction, the most likely direction being the synthesis of PEP (Leegood and Walker, 2003). This reaction requires a source of OAA that could be supplied by the oxidation of malate by NAD-cytMDH. This hypothesis is supported by the fact that PEPCK is involved in the dissimilation of malate in the flesh of several fruits (Famiani *et al.*, 2005) and possibly in the lack of malate in low acid apple cultivars (Berüter, 2004).

PEP can also originate from the conversion of pyruvate through pyruvate orthophosphate dikinase (PPDK) activity (Sweetman *et al.*, 2009). The pyruvate required for PPDK may be supplied through the carboxylation of malate by cytosolic NADP-dependant malic enzyme (NADP-cytME), which catalyzes a reversible conversion, the most likely

direction being the decarboxylation of malate (Sweetman *et al.*, 2009). NADP-cytME appears to be involved in the decrease in malate content during the ripening of several fruit species (Chen *et al.*, 2009; Dilley, 1962; Goodenough *et al.*, 1985; Sweetman *et al.*, 2009). Involvement of NADP-cytME during the early stage of fruit growth differs between species. Thus, in young tomato and apple fruits, NADP-cytME does not appear to play an important role in malate accumulation (Dilley, 1962; Goodenough *et al.*, 1985) whereas in young grape berries the use of a proteomics approach suggested the opposite (Martınez-Esteso *et al.*, 2011). The contribution of NADP-cytME to the lack of malate in ripe pulp of low acid cultivars has been demonstrated in apple (Yao *et al.*, 2009), and loquat (Chen *et al.*, 2009). Studies of different fruit species suggest that NADP-cytME is regulated at the post translational level (Bahrami *et al.*, 2001; Famiani *et al.*, 2000; Yang *et al.*, 2011; Yao *et al.*, 2009) by cytosolic pH and malate concentration, among others (Davies, 1986; Lakso and Kliewer, 1975a; Possner *et al.*, 1981).

Decarboxylation of malate and OAA may also be linked to fermentative metabolism as it can occur in ripening fruit if the cytosol becomes too acidic (for review see (Sweetman *et al.*, 2009)).

2.3 Conversions between di- and tri-carboxylic acids: multiple compartments, multiple pathways

Once malate and OAA have been synthesized in the cytosol, they can be converted into tricarboxylates, mostly citrate, or other dicarboxylates through two metabolic pathways, the TCA cycle and the glyoxylate cycle. In its turn, citrate can be converted into dicarboxylates via several pathways (TCA cycle, glyoxylate cycle, GABA shunt, and acetyl CoA catabolism). All these conversion reactions can modify the acidity of fruit cells.

2.3.1 The TCA cycle in the mitochondria: conversions between di- and tricarboxylates

The TCA cycle results in the oxidation of pyruvate into CO_2 and a reduction in co-enzymes through a series of conversions between organic acids including malate and citrate (*Fig. I.1*). The cycle begins with the condensation of OAA and acetyl CoA, the latter provided by the action of pyruvate dehydrogenase on mitochondrial pyruvate. The input of acetyl CoA allows the TCA cycle to maintain a cyclic flux mode under which it is not able to catalyze net synthesis of cycle intermediates. Therefore, export of intermediates implies non-cyclic flux modes that are known to occur in plants and have been evidenced in citrus fruit (Katz *et al.*, 2011), and are likely to be controlled by ATP demand (Sweetlove *et al.*, 2010). The

maintenance of the pools of TCA cycle intermediates implies that for each metabolite exported, one is imported and vice versa. These exchanges are achieved by a variety of mechanisms mediated by mitochondrial carrier proteins (for review see (Haferkamp and Schmitz-Esser, 2012; Laloi, 1999)) that obey the general principles behind the transport of ionic species across a biological membrane (*Fig. I.2 and I.3*). In fruits, mitochondrial dicarboxylate/tricarboxylate transporters have been characterized at the gene level in citrus (Deng *et al.*, 2008) and grape berry (Regalado *et al.*, 2013), and at the protein level in citrus (Katz *et al.*, 2007).

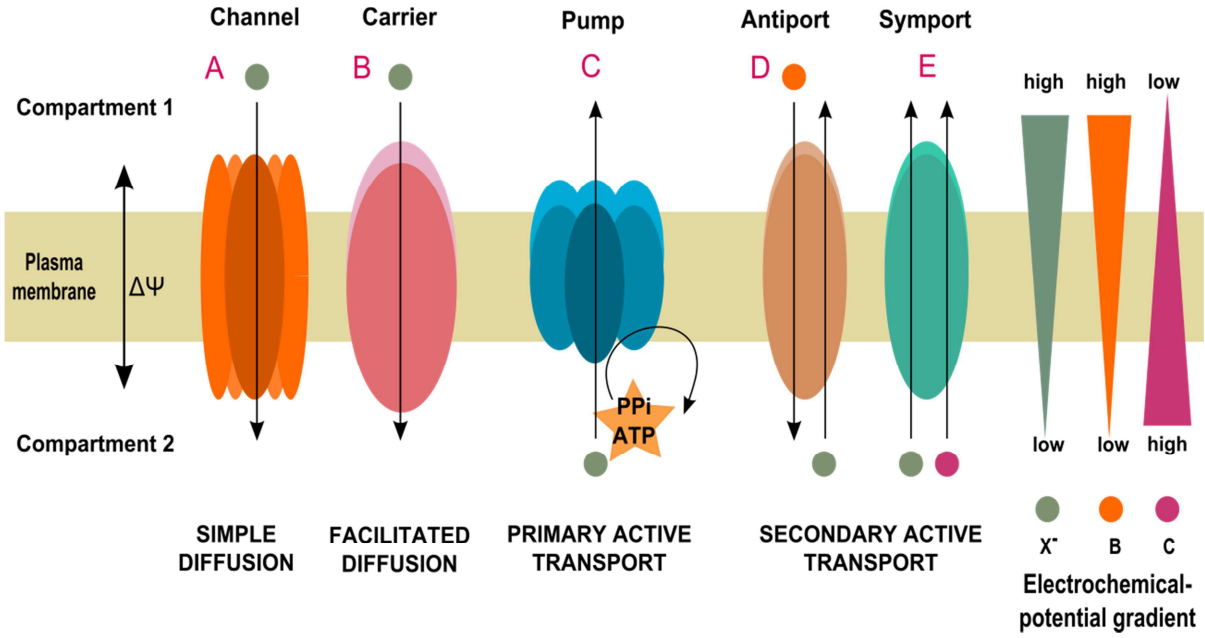

Figure I-2 Mechanisms of transport of ionic species across a biological membrane. Membrane transport is mediated by three types of membrane proteins: channels, carriers, and pumps. Channels function as selective pores through which molecules or ions can diffuse across the membrane. Carriers catalyze either the transport of a single solute, or the coupled transport of two solutes. Pumps catalyze the coupled transport of a solute with a chemical reaction. Three mechanisms allow the transport of an ionic species (X^-) across a biological membrane (from compartment 1 to compartment 2) and are governed by a general principle of thermodynamics stating that the variation in free energy of the transport reaction ($\Delta G_{1\text{-}2}$) has to be negative. (i) Diffusion (simple or facilitated) is mediated by channels (A) in the case of simple diffusion, or by carriers (B) in the case of facilitated diffusion. This kind of transport allows the spontaneous movement of X^- down its electrochemical-potential gradient ($\Delta G(X^-)_{1\text{-}2}<0$), which depends on the electric potential gradient of the membrane ($\Delta\psi$) and on the gradient of concentrations of X^- on the two sides of the membrane. $\Delta G_{1\text{-}2}= \Delta G(X^-)_{1\text{-}2} = zF\Delta\psi + RT\ln([X^-]_2/[X^-]_1) <0$ where z is the electric charge of the ionic species transported; F is Faraday's constant; R is gas constant; T is temperature. (ii) Primary active transports are mediated by a specific class of proteins called pumps (C). This kind of transport allows the movement of X^- against its electrochemical-potential gradient ($\Delta G(X^-)_{2\text{-}1} >0$) using the energy released from the hydrolysis of ATP or PPi (ΔGATP (or PPi) <0). $\Delta G_{2\text{-}1}=\Delta G_{ATP\ (or\ PPi)} + \Delta G(X^-)_{2\text{-}1} <0$. (iii) Secondary active transports are mediated by two types of carrier proteins: antiports (D) and symports (E). This kind of transport allows the movement of X^- against its electrochemical-potential gradient ($\Delta G(X^-)_{2\text{-}1} >0$) using the energy dissipated by the downhill movement of a molecule across the membrane ($\Delta G(B)_{1\text{-}2} <0$ in the case of antiport, $\Delta G(C)_{2\text{-}1} <0$ in the case of symport). Antiport: $\Delta G_{2\text{-}1}= \Delta G(X^-)_{2\text{-}1} + \Delta G(B)_{1\text{-}2} <0$. Symport: $\Delta G_{2\text{-}1}= \Delta G(X^-)_{2\text{-}1} + \Delta G(C)_{2\text{-}1}<0$.

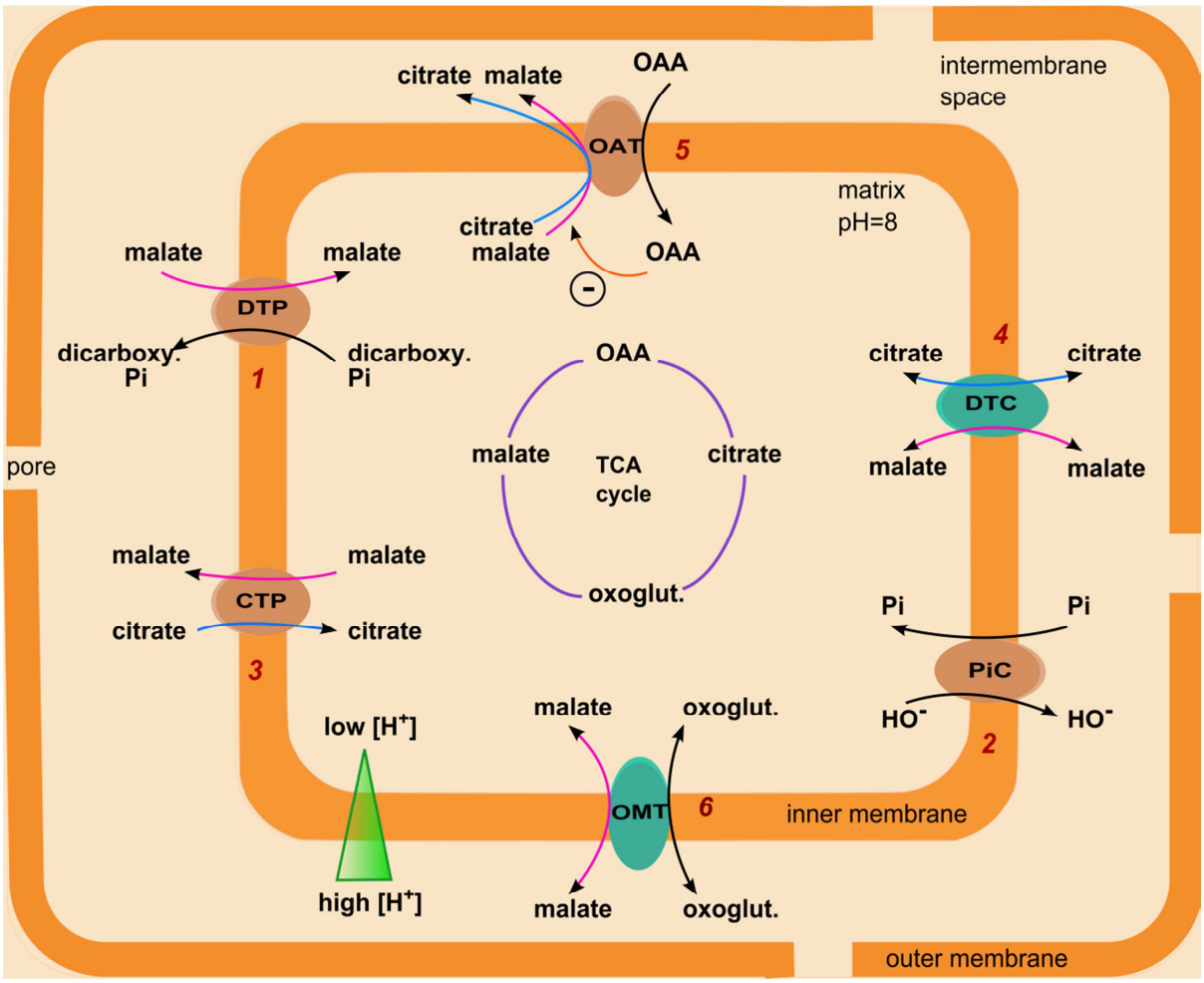

Figure I-3 Mitochondrial carriers involved in citrate and malate transport. CTP: citrate transport protein; DTC: dicarboxylate-tricarboxylate carrier; DTP: dicarboxylate transport protein; OAT: oxaloacetate-malate transporter; OMT: oxoglutarate-malate translocator; PiC: phosphate carrier. The orange arrow represents the inhibition of malate efflux through the OAT by OAA. The electrochemical potential gradient of protons (green triangle) generates an electric potential gradient (negative inside) and a pH gradient (alkaline inside) that both play a role in the transport of organic acids between the cytosol and the mitochondria.

Non-cyclic flux modes allow conversion of di- and tricarboxylates (Steuer *et al.*, 2007; Sweetlove *et al.*, 2010) and are sustained by the activities of the TCA cycle enzymes. The enzymes that directly control citrate synthesis are the mitochondrial citrate synthase (mtCS), and citrate degradation, the mitochondrial aconitase (mtACO), and the mitochondrial NAD-dependant isocitrate dehydrogenase (NAD-mtIDH) (*Fig. I.1*). mtCS activity is positively correlated with citrate accumulation in citrus (Sadka *et al.*, 2001; Wen *et al.*, 2001) and strawberry (Iannetta *et al.*, 2004), but transcriptomics and protein studies suggested that this enzyme is not responsible for the difference in citrate content between low and high acid cultivars of several fruit species (Canel *et al.*, 1996; Etienne *et al.*, 2002; Sadka *et al.*, 2001; Saradhuldhat and Paull, 2007; Tang *et al.*, 2010). The involvement of mtACO, which catalyzes the conversion of citrate into isocitrate (the most likely direction in mitochondria due to the way the cycle functions), in citrate accumulation has been described by Sadka

(2000a). He showed that in sour lemon, mtACO activity decreases in the early stage of fruit growth and could thus be responsible for the increase in citrate concentration observed during fruit growth. Two forms of isocitrate dehydrogenase, an NADP-dependant form (NADP-IDH) and an NAD-dependant form (NAD-IDH) can catalyze the conversion of isocitrate into 2-oxoglutarate (the most likely direction in mitochondria like for mtACO). NAD-IDH is only found in mitochondria but has rarely been characterized in fruits and no links with citrate accumulation have been found (Sha *et al.*, 2011). NADP-IDH is mainly localized in the cytosol (NADP-cytIDH), but is also found in mitochondria (NADP-mtIDH) and peroxisomes (Chen, 1998; Gálvez and Gadal, 1995). In sour lemon, Sadka (2000a) observed that NADP-mtIDH activity decreased in the early stage of fruit growth in parallel with a decrease in mtACO activity (Sadka *et al.*, 2000a; Sadka *et al.*, 2000b). This could reflect a general reduction in citrate metabolism in the mitochondria. Malate can be oxidized in fruit mitochondria either in OAA by mitochondrial NAD-dependant malate dehydrogenase (NAD-mtMDH) (the most likely direction in mitochondria (Sweetman *et al.*, 2009)), which feeds the cycle, or in pyruvate by mitochondrial NAD-dependant malic enzyme (NAD-mtME), which interrupts the cycle (Macrae and Moorhouse, 1970) (*Fig. I.1*). These two competing metabolic pathways affect fruit acidity in different ways. While malate oxidation by NAD-mtMDH leads mainly to citrate production (Steuer *et al.*, 2007; Sweetlove *et al.*, 2010), hence affecting the malate:citrate ratio of fruit cells, malate oxidation by NAD-mtME leads to the degradation of acidity since organic acids must be imported into the mitochondria to compensate for the loss of malate. Malate metabolism in the mitochondria therefore depends on NAD-mtMDH and NAD-mtME activity, both of which are regulated by the concentration of NADH and the pH (Day *et al.*, 1984; Douce, 1985; Palmer *et al.*, 1982). In young tomato fruit, the majority of malate degradation could be due to NAD-mtME (Bahrami, 2001). Transcriptomics and proteomics analyses suggest that NAD-mtMDH is involved in malate degradation during grape berry ripening (Martınez-Esteso *et al.*, 2011; Sweetman *et al.*, 2009).

2.3.2 Catabolism of citrate in the cytosol: conversion of citrate into dicarboxylates

Once citrate has been produced by the TCA cycle, it can be degraded in the cytosol through two metabolic pathways. One is the gamma-aminobutyrate (GABA) synthesis pathway, also called GABA shunt, which leads to succinate synthesis, and the other is cleavage into OAA and acetyl-CoA (*Fig. I.1*). As these two pathways produce dicarboxylic acids, they are responsible for a decrease in fruit acidity.

The GABA synthesize pathway is a part of the amino acid metabolism since it produces two amino acids (glutamate and GABA). This pathway also leads to the production of succinate that can then enter the TCA cycle. Two major enzymes are involved in the catabolism of citrate through the GABA shunt: cytosolic aconitase (cytACO), which catalyzes the reversible conversion of citrate into isocitrate, and cytosolic NADP-dependant isocitrate dehydrogenase (NADP-cytIDH), which catalyzes the reversible conversion of isocitrate into 2-oxoglutarate (*Fig. I.1*). The involvement of the GABA shunt in citrate degradation during the ripening of citrus fruits was evidenced by proteomics and metabolite analyses (Katz *et al.*, 2011), gene expression analyses (Cercos *et al.*, 2006; Sadka *et al.*, 2000b) and enzymatic activity analysis (Degu *et al.*, 2011; Sadka *et al.*, 2000b). Activation of the GABA shunt could partially account for the lack of citrate in sweet lemon since activation of the genes involved in the degradation of 2-oxoglutarate, the precursor for GABA synthesize, was observed (Aprile *et al.*, 2011). Activation of the GABA shunt also appears to occur during post-harvest ripening of banana since an increase in 2-oxoglutarate content, NADP-IDH activity, mainly attributable to the cytosolic form (Chen and Gadal, 1990), and total ACO gene expression, was observed (Liu *et al.*, 2004; Medina-Suárez *et al.*, 1997). It is likely that the rate of citrate degradation through the GABA shunt is mainly controlled by cytACO and NADP-cytIDH activities. In several genotypes of citrus, the pattern of expression of two genes encoding cytACO was associated with the timing of acid content reduction in fruits (Terol *et al.*, 2010). In tomato fruit, genetic and transgenic approaches demonstrated the key role of cytACO in the control of citrate content in ripe fruit (Morgan *et al.*, 2013). In sour lemon, NADP-cytIDH gene expression and NADP-cytIDH activity increase during fruit development and could thus be involved in the decrease in citrate content (Sadka *et al.*, 2000a).

The alternative citrate breakdown pathway cleaves citrate into OAA and acetyl-CoA through the activity of the ATP-citrate lyase (ATP-CL) and leads to the synthesis of flavonoids and isoprenoids (*Fig. I.1*). During ripening, these compounds accumulate in the fruit (Giovannoni, 2004), so it is likely that citrate catabolism through this pathway is activated during this phase. Evidence for such activation was found in mango fruit. Indeed, ATP-CL activity increased considerably during ripening while there was a decrease in citrate content (Mattoo and Modi, 1970). Proteomics analysis identified ATP-CL in mature citrus fruit (Katz *et al.*, 2007). However, this result is in contradiction with the decrease in the levels of mRNA in this gene during ripening of citrus fruits observed by Cercos (Cercos *et al.*, 2006). Thus, the role of this pathway in the decrease in acid in citrus fruit requires further investigation.

2.3.3 The glyoxylate cycle: conversion of succinate and malate

The function of the glyoxylate cycle is to convert the acetyl CoA produced in the peroxisomes by β-oxidation of fatty acids into succinate via a series of reactions involving malate and citrate (*Fig. I.1*). Succinate is then converted into malate through the TCA cycle (Pracharoenwattana and Smith, 2008). Malate can then enter the gluconeogenesis pathway to produce glucose. In this way, the glyoxylate cycle decreases fruit acidity since it leads to the consumption of malate.

The five key enzymes involved in this metabolic pathway are located in either glyoxysome (citrate synthase, isocitrate lyase (ICL), malate synthase (MS)) or cytosol (cytACO, NAD-cytMDH) (Pracharoenwattana and Smith, 2008) (*Fig. I.1*). The location of the enzymes requires several intermediates of the cycle to cross the glyoxysomial membrane, but which transport systems are involved is still not clear (Rottensteiner and Theodoulou, 2006).

The glyoxylate cycle is possibly involved in malate accumulation in young grape berry and ripening banana fruit (Pua *et al.*, 2003; Terrier *et al.*, 2005). Activation of the glyoxylate cycle during post harvest ripening of banana fruit could be a way to provide substrates for gluconeogenesis at a period when sugar accumulation is high (Liu *et al.*, 2004; Surendranathan and Nair, 1976). However, the involvement of the glyoxylate cycle in organic acid accumulation during fruit development could be specific to certain fruit species since no ICL proteins were detected in the flesh of several berry fruits at any stage of development (Famiani *et al.*, 2005).

3 The complex mechanism of vacuolar storage of organic acids

Most of the citrate and malate content of fruit is found in the vacuole (Moskowitz and Hrazdina, 1981; Yamaki, 1984), which occupies 90% of most mature fruit cells (Etxeberria *et al.*, 2012; Fontes *et al.*, 2011). This section is devoted to the mechanisms allowing their transport in and out of the vacuole.

3.1 The "acid trap" mechanism

The mechanism that allows the accumulation of citrate and malate in the vacuole has been described as the "acid trap", and is enabled by the fact that these two weak acids can dissociate (Martinoia *et al.*, 2007). In the cytosol, at neutral or slightly alkaline pH, almost all malate is in the form of dianion and almost all citrate in the form of trianion. In the vacuole, where the pH is acidic, the dominant species is either the protonated form or the monoanion

(a significant proportion of the acids may remain in the dianion form, or even in the trianion form in the case of citrate, only in fruits with high vacuolar pH). Only dianion malate and trianion citrate can be transported into the vacuole (Lüttge and Ball, 1979; Oleski *et al.*, 1987; Rentsch and Martinoia, 1991) because the transport systems involved are specific to these chemical forms (Brune *et al.*, 1998; Martinoia *et al.*, 2007). Once they have crossed the tonoplast and reached the acidic vacuole, they are immediately protonated, which maintains their electrochemical-potential gradient and allows their continuous transport into the vacuole (*Fig. I.4.A*). It should be pointed out that trapping efficiency depends on both vacuolar pH and on the electric potential gradient across the tonoplast ($\Delta\psi$). On one hand, the lower the pH, the more effective the protonation and trapping mechanism, on the other hand, the $\Delta\psi$ contributes strongly to the electrochemical potential gradient of the di- and trianion. Efflux of the protonated forms of malate and citrate probably occurs through specific carriers, but little is known on this subject (see following sections).

The sustained transport of organic anions must be accompanied by a simultaneous influx of the equivalent amount of cations to maintain the electroneutral state of the vacuole. This is achieved by the transport of either mineral cations (mostly potassium) or protons (released from the dissociation of weak acids in the cytosol), only the latter being responsible for the acidification of the vacuole.

3.2 Malate crosses the tonoplast by facilitated diffusion

Vacuolar dianion malate uptake occurs by facilitated diffusion (Maeshima, 2001; Rea and Sanders, 1987) (*Fig. I.2.B*). In Arabidopsis, vacuolar malate transport is mediated at least by a tonoplast malate transporter (AttDT) (Emmerlich *et al.*, 2003) (*Fig. I.4.A, n°1*) and two members of the aluminium-activated malate transporter (ALMT) family, the AtALMT9 and AtALMT6 channels (Kovermann *et al.*, 2007; Meyer *et al.*, 2011) (*Fig. I.4.A, n°2*). An AttDT homolog has been identified in grape berries and could play a role in malate transport (Terrier *et al.*, 1998). ALMTs may be responsible for vacuolar malate transport in fruits since four candidate genes homologous to AtALMT9 have been identified in grape berry (Rongala, 2008), and two ALMT-like genes have been discovered in apple (Bai *et al.*, 2012).

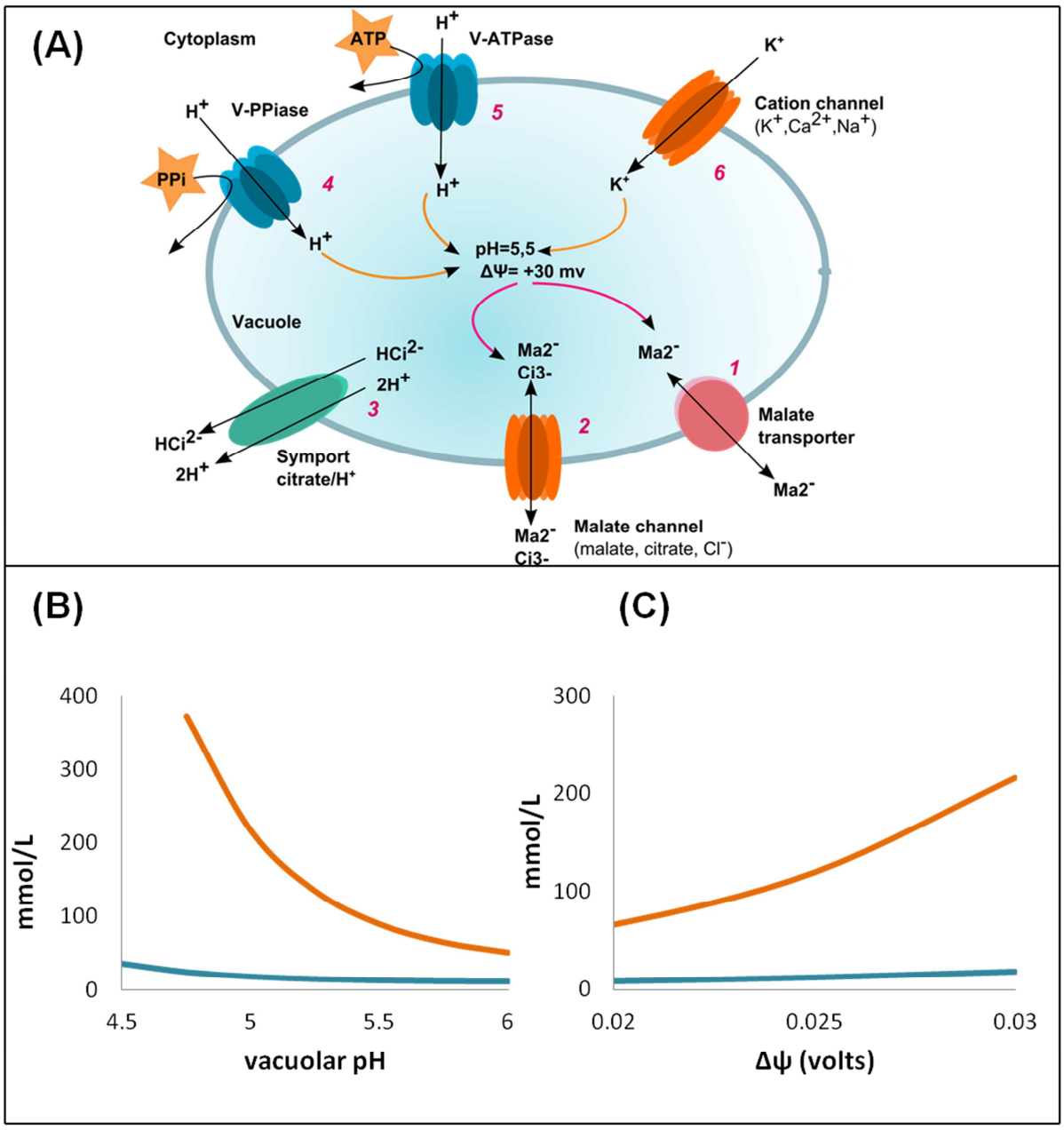

Figure I-4 (A) "Acid trap" mechanism of vacuolar organic acid storage in fruit cells. Several tonoplastic carriers are involved in the transport of malate and citrate across the tonoplast. Once the dianions or trianions have crossed the tonoplast, they are immediately protonated due to the acid pH of the vacuole according to the following equations: Malate: $H_2Mal \leftrightarrow HMal^- + H^+ \leftrightarrow Mal^{2-} + 2H^+$, (pKa1~3.40, pKa2~5.10). Citrate: $H_3Cit \leftrightarrow H_2Cit + H^+ \leftrightarrow HCit^{2-} + 2H^+ \leftrightarrow Cit^{3-} + 3H^+$, (pKa1~3.10, pKa2~4.70, pKa3~6.40). The two vacuolar proton pumps are responsible for the acid pH of the vacuole and for the electric potential gradient across the tonoplast (Δψ). The cation channel is also involved in the regulation of the Δψ. (B) Theoretical changes in citrate (orange line) and malate (blue line) concentrations in the vacuole as a function of the pH of the vacuole. The concentrations were calculated using the Nernst equation (that is ΔG_{Mal}^{2-} and ΔG_{Cit}^{3-} are equal to zero, assuming that the dianion malate and trianion citrate are in thermodynamic equilibrium across the tonoplast) and the dissociation equations of the two organic acids with a vacuolar pH ranging from 4.5 to 6, and a Δψ equal to 30 mV (Martinoia et al., 2007). We did not consider any limitation by tonoplastic carriers.

***Nernst equations*:**

$$(Mal^{2-})_{vac} = (Mal^{2-})_{cyt} * exp^{\frac{2*F*\Delta\psi}{R*T}}$$

$$(Cit^{3-})_{vac} = (Cit^{3-})_{cyt} * exp^{\frac{3*F*\Delta\psi}{R*T}}$$

Dissociation equations:

$$[Mal^{2-}] = \frac{K'_{m1} * K'_{m2}}{h^2 + (h * K'_{m1}) + (K'_{m1} * K'_{m2})}[Mal]$$

$$[Cit^{3-}] = \frac{K'_{c1} * K'_{c2} * K'_{c3}}{h^3 + (h^2 * K'_{c1}) + (h * K'_{c1} * K'_{c2}) + (K'_{c1} * K'_{c2} * K'_{c3})}[Cit]$$

where Δψ is the tonoplastic electric potential gradient; $(Mal^{2-})_{cyt}$ is the cytosolic activity of the dianion malate that is equal to the product of the cytosolic concentration and activity coefficient of the dianion malate; $(Cit^{3-})_{cyt}$ is the cytosolic activity of the trianion citrate; $[Mal^{2-}]_{vac}$ is the vacuolar concentration of the dianion malate; $[Cit^{3-}]_{vac}$ is the vacuolar concentration of the trianion citrate; F is Faraday's constant; R is gas constant; T is temperature; K'_{m1}, K'_{m2}, are apparent acidity constants of malate; K'_{c1}, K'_{c2}, K'_{c3}, are apparent acidity constants of citrate; $h=10^{-pH}$ (Lobit *et al.*, 2002). Since malate and citrate are stored in the vacuole, their cytosolic concentrations are low and were set at 1 mM (Gout *et al.*, 1993; Lobit *et al.*, 2006). (C) Theoretical changes in citrate (orange line) and malate (blue line) concentrations in the vacuole as a function of the Δψ. The concentrations were calculated using the same equations as in (B), with the vacuolar pH set at 5, and the Δψ ranged from 20 to 30 mv.

Malate currents through AtALMT9 and AtALMT6 are strongly inward-rectifying, that is, malate transport occurs only in the presence of a Δψ (positive inside the vacuole) (Epimashko *et al.*, 2004; Hafke *et al.*, 2003; Hurth *et al.*, 2005; Meyer *et al.*, 2011). As Δψ is expected to decrease with a decrease in vacuolar pH (see following section), these channels may close at low vacuolar pH when the acid trap mechanism would be most effective, perhaps as a mechanism to prevent over-acidification of very acidic vacuoles. AttDT appears to play a role in the import and export of malate (Hurth *et al.*, 2005), consequently, this transporter could be less rectifying than the malate channel. AttDT also appears to be involved in the regulation of cytosolic pH homeostasis (Hurth *et al.*, 2005).

3.3 Citrate crosses the tonoplast by facilitated diffusion and secondary active transport

In most species of fleshy fruit, vacuolar trianion citrate uptake occurs by facilitated diffusion (*Fig. I.2.B*), possibly through the malate channel (Oleski *et al.*, 1987; Rentsch and Martinoia, 1991) (*Fig. I.4.A, n°2*).The thermodynamic conditions are more favorable for the uptake of citrate than of malate at any vacuolar pH and Δψ (*Fig. I.4.B and I.4.C*). Thus, citrate appears to be easily transported into the vacuole as soon as its cytosolic concentration increases sufficiently (Gout *et al.*, 1993). AttDT could also play a role in the transport of citrate into the vacuole, but according to Hurth *et al.* (2005) it is not the main tonoplast citrate carrier since AttDT knock-out vacuoles contain much more citrate than wild-type vacuoles, and the transport rate of citrate was higher in AttDT knock-out plants. In citrus, several authors proposed that an ATP-dependant citrate pump may operate in addition to the malate channel. However, further investigation is needed to provide complete evidence that citrate transport is coupled to ATP hydrolysis though a single transporter and not through the tonoplastic pH

gradient (ΔpH) and Δψ setting up by the V-ATPase (see following section) (Brune *et al.*, 1998; Canel *et al.*, 1995; Ratajczak *et al.*, 2003).

Citrate content generally decreases during fruit ripening (Léchaudel *et al.*, 2005b; Saradhuldhat and Paull, 2007; Shimada *et al.*, 2006; Wu *et al.*, 2005) meaning that citrate is exported from the vacuole. The existence of a symporter involved in citrate efflux has been evidenced in citrus (*Fig. I.2.E*). This carrier (CsCit1) is able to mediate the electroneutral co-transport of H^+ and $CitH^{2-}$ outside the vacuole of juice cells (Shimada *et al.*, 2006) (*Fig. I.4.A, n°3*).

3.4 Setting up the electric potential and pH gradient across the tonoplast

The main determinants of malate and citrate accumulation in the vacuole are vacuolar pH (always acidic) and the inside-positive Δψ, with values commonly ranging between 20 and 30 mV (Taiz and Zeiger, 2010). Proton pumping into the vacuole contributes to the generation of both acid vacuolar pH and positive Δψ (*Fig. I.4.A, n°4 and 5*). Two types of proton pumps are present in fruit vacuoles: the H^+-ATPase (V-ATPase) (Ratajczak, 2000), characterized in several fruit species (Müller *et al.*, 1997; Müller *et al.*, 1996; Suzuki *et al.*, 2000; Terrier *et al.*, 1998), and the H^+-PPiase (V-PPase) (Maeshima, 2000), also characterized in several fruit species (Suzuki *et al.*, 2000; Terrier *et al.*, 1998). These enzymes catalyze chemiosmotic coupling between the hydrolysis of a high energy phosphate bond (ATP or pyrophosphate (PPi)) and proton transport into the vacuole. The thermodynamic conditions of these reactions are determinant for the activity of the pumps. Protons can be pumped into the lumen only if the variation in free energy of the chemiosmotic coupling (ΔG) is negative (*Fig. I.2.C*).

$$\Delta G = \Delta G_{ATP\ or\ PPi} + \Delta G_{H^+} \leq 0 \text{ (Equation 1)}$$

where ΔG_{ATP} and ΔG_{PPi} are the free energy of the substrate hydrolysis, and ΔG_{H+} is the free energy of proton transport. ΔG_{H+} can be written (derived from the diffusion equation of ionic species, see *Fig. I.2*) as:

$$\Delta G_{H^+} = n(F\Delta\psi + 2.3RT\Delta pH) \text{ (Equation 2),}$$

where $\Delta\psi = \psi_{vac} - \psi_{cyt}$, $\Delta pH = pH_{cyt} - pH_{vac}$, and n is the coupling ratio (that is, the number of protons transported during the hydrolysis of one phosphate bond).

The thermodynamic constraints impose a limit on the Δψ that can be achieved at a given ΔpH, as shown by combining Equation 1 and 2:

$$\Delta\psi \leq \frac{-\Delta G_{ATP\ or\ PPi}}{nF} - \frac{2.3RT}{F}\Delta pH \text{ (Equation 3)}$$

The free energy of the substrate hydrolysis (ΔG_{ATP} and ΔG_{PPi}) are negative but may fluctuate with the cytosolic concentrations of their substrates (Davies *et al.*, 1993). The coupling ratio

(determined by electrophysiology experiments) is 1 for the V-PPase (Maeshima *et al.*, 1994). For the V-ATPase, the coupling ratio is variable and decreases with an increase in ΔpH (Davies *et al.*, 1994; Rienmüller *et al.*, 2012). In lemon fruits, Müller *et al*. (2002) also reported for the V-ATPase a coupling ratio that decreases from 2 to 1 with an increase in ΔpH. Assuming a model cytosol with a composition assumed to be representative of a plant cell, Davies *et al.* (1993) modeled the ΔpH obtained as a function of Δψ and showed that both pumps are able to sustain vacuolar pH as low as in the most acidic fruits, but that Δψ dropped to zero.

Apart from these thermodynamic limitations, various mechanisms are involved in regulating the proton pumps, including gene expression and substrate availability. Several studies of organic acid-related genes and enzymes suggested that the difference in organic acid content between species and between cultivars of fruits could be linked to differences in their proton pumps (Echeverria *et al.*, 1997; Etienne *et al.*, 2002; Lu *et al.*, 2011; Yang *et al.*, 2011). The contribution of the V-ATPase and V-PPase to proton pumping also varies during fruit development. In the grape berry and in pear, the V-PPase is most active in young tissues, but subsequently decreases, and the V-ATPase dominates during fruit ripening (Shiratake *et al.*, 1997; Suzuki *et al.*, 2000; Terrier *et al.*, 2001). The high V-PPase activity in young fruits may be explained by the need to scavenge the PPi, a by-product and inhibitor of several polymerization reactions (synthesis of RNA, proteins, cellulose, and starch) (Maeshima, 2000). In mature tissues, PPi production may decrease as these syntheses slow down while ATP is constantly supplied by cell respiration.

The transport of potassium (K^+) across the tonoplast also plays a role in the regulation of the Δψ and of the vacuolar pH. Since the concentration of cytosolic K^+ is controlled homeostatically (Leigh, 2001) and because of the small size of the cytosol, most of the K^+ supplied to the fruit cell has to be transported to the vacuole. Facilitated diffusion through vacuolar cation channels is the most likely mechanism (Isayenkov *et al.*, 2010). However, in fruit with a high K^+ content like banana, it can be calculated using the Nernst equation (*Fig. I.4.B*), with a cytosolic concentration of K^+ of around 100 mM (Leigh, 2001), and a Δψ of 30 mV (Martinoia *et al.*, 2007), passive transport accounts for accumulation of up to 30 mM of K^+ in the vacuole. This is very far from the 80 mM found in ripe banana (Chandler, 1995). Thus, in such fruits, active transport is required. The most likely mechanism is a K^+/H^+ antiport, as identified in the tonoplast of tomato plants (Leidi *et al.*, 2010). Cation channels help reach a positive Δψ (Isayenkov *et al.*, 2010), since the passive influx of K^+ hyperpolarizes the tonoplast (*Fig. I.4.A, n°6*). In contrast, the K^+/H^+ antiport, which mediates an electroneutral exchange, has no effect on Δψ. Concerning acidity, transporting K^+ as the

balancing charge for organic anions is equivalent to storing not the acid, but its conjugated base, which leads to an increase in pH. In the case of the K^+/H^+ antiport, there is an additional effect on pH due to protons leaving the vacuole.

4 Citrate accumulation could be driven by metabolism and malate accumulation by vacuolar storage

In the previous sections, we showed that both metabolism and vacuolar storage play a role in the accumulation of malate and citrate in fruit cells. A relevant question is whether their accumulation in fruit cells is primarily controlled by metabolism or vacuolar storage.

Concerning malate, we showed that the thermodynamic conditions of its transport into the vacuole may limit its accumulation. Therefore, one can hypothesize that malate accumulation in fruit cells is mainly controlled at the level of vacuolar storage, and that metabolism responds appropriately to regulate the cytosolic concentration of malate since it plays a fundamental role in the regulation of cytosolic pH (Smith and Raven, 1979). Several authors agree with this hypothesis. When comparing two apple cultivars with different acidity, Berüter and al. (2004) reported higher vacuolar accumulation of ^{14}C labeled malate in the high-acid cultivar. The higher rate of malate degradation in the low-acid cultivar may only be a consequence of its impaired capacity to store malate. In interspecific introgression lines of tomato, Schauer *et al*. (2006) showed that the V-PPase gene colocalized with the QTL for malate content. In apple, Bai *et al.* (2012) suggested that one of the two ALMT-like genes discovered, *Ma1*, could be the major determinant of malate content in fruit. The relation between malate accumulation and vacuolar functioning has been modeled in peach by Lobit *et al.* (2006). The model predicts malate accumulation in peach based on the calculation of the thermodynamic constraints on both proton and malate transports, and model results were in good agreement with experimental data, thus reinforcing the hypothesis of control by tonoplastic transports.

Concerning citrate, we showed that its accumulation in the vacuole is unlikely to be limited by thermodynamic conditions. However, the rate of citrate transport into the vacuole may be limited by the activity of its transport system, given that the malate channel transports citrate much more slowly than malate (Hafke *et al.*, 2003). Thus, it is likely that citrate accumulation in the vacuole is controlled by its cytosolic concentration and consequently by its metabolism. Among several possible pathways related to citrate metabolism, the TCA cycle is the only one that allows citrate synthesis, so that citrate accumulation is likely controlled by respiration. A fruit PBSM based on a representation of the TCA cycle reactions

and their responses to temperature and respiration (Lobit, 1999; Wu *et al.*, 2007) led to predictions that were in agreement with observed data. In particular, this model reproduced the increase in citrate content during the early stage of fruit development and the subsequent decrease during the later stage (Albertini *et al.*, 2006; Léchaudel *et al.*, 2005a; Saradhuldhat and Paull, 2007; Wu *et al.*, 2005). The fact that citrate synthesis is positively linked to fruit respiration during the green stage, and negatively during ripening may reflect a change in the respiratory substrates used by the TCA cycle from malate (or other intermediates) to citrate. It should be noted that dilution due to pulp growth is required to explain the variations in the concentration of organic acids (Wu *et al.*, 2007).

5 Influence of agro-environmental factors on malate and citrate accumulation in the mesocarp cells of fleshy fruits

The literature shows that the plant source: sink ratio, mineral fertilization, water supply, and temperature are the agro-environmental factors that have the most impact on fruit acidity. This section focuses on their effects on malate and citrate accumulation in fruits considering the mechanisms described above.

5.1 The source: sink ratio influences fruit acidity by modifying the supply of sugars

Orchard management practices like fruit thinning, plant pruning or defoliation affect the source: sink ratio of the plant, which usually results in altered sugar supply and fruit growth. These practices also affect fruit acidity (*Table I-1*). In peach and mango it has been observed that an increase in the source: sink ratio increases citrate content early in fruit development, and decreases it near maturity (Léchaudel *et al.*, 2005b; Souty *et al.*, 1999; Wu *et al.*, 2002). The opposite effects have been reported for malate, with a decrease during early stages followed by an increase near maturity (Léchaudel *et al.*, 2005b; Wu *et al.*, 2002).

It can be hypothesized that during the green stages, large amounts of sugars imported from the leaves are available for the production of malate via glycolysis and its conversion to citrate via the TCA cycle. It is well known that fruits grown with a high sugar supply, due to a high source: sink ratio, are bigger and consequently have a higher respiration rate. Therefore, in these stages, an increase in fruit respiration due to a high supply of sugars may stimulate glycolysis and conversion of malate into citrate. In contrast, during ripening, sugars may no longer be available for respiration since they are stored in the vacuole (Coombe, 1976), causing a shift from sugars to organic acids (in particular citrate) as respiratory substrate. During this stage, an increase in respiration (due to bigger fruit in response to the high source:

sink ratio) may stimulate the conversion of citrate into malate to maintain the pool of TCA cycle intermediates constant. This behavior has been represented in the PBSM of citrate accumulation (Lobit *et al.*, 2003; Wu *et al.*, 2007), the results of which are in agreement with observations made in field trials (Génard and Bruchou, 1993; Génard *et al.*, 1991; Génard *et al.*, 1999; Génard *et al.*, 1994).

5.2 Different but strong effects of mineral fertilization on fruit acidity

Potassium fertilization has an impact on fruit acidity, but agronomic observations are contradictory (*Table I-1*). Some authors reported that potassium fertilization increased fruit titratable acidity (TA) (which is the amount of weakly bound hydrogen ions that can be released from the acids by NaOH titration) (Alva *et al.*, 2006; Du Preez, 1985; Embleton *et al.*, 1978; Spironello *et al.*, 2004), others that potassium fertilization decreased fruit acidity (Ramesh Kumar and Kumar, 2007; Vadivel and Shanmugavelu, 1978), and still others that it had no significant effect (Cummings and Reeves, 1971). At cellular level, different mechanisms allow K^+ to affect the metabolism and storage of organic acids. Organic anions are synthesized in the vegetative parts to buffer the excess of organic cations absorbed from the soil (Lopez-Bucio *et al.*, 2000). As a result, the K^+ supplied to the fruit by the sap is necessarily accompanied by an equivalent amount of organic anions, mostly malate, and to a lesser extent, citrate (Burström, 1945). Without any further metabolism in the fruit, this would amount to adding conjugated bases to the fruit, increasing pH, which is consistent with the positive correlation found between K^+ content and pH of grape berry juice (Mpelasoka *et al.*, 2003). However, in this case, TA would not be affected, since no protonated forms would be added to the fruit. Thus, a modification in fruit TA in response to the supply of K^+ implies that K^+ affects the synthesis or the vacuolar storage of organic acids within the fruit itself. The regulation of tonoplastic transport may be an essential contributor to the effect of K^+. In fruits that contain little K^+, K^+ transport is probably passive and thus contributes to the $\Delta\psi$ (Allen and Sanders, 1997), which in turns stimulates the transport of organic anions into the vacuole. In fruits with a high concentration of K^+, K^+ transport is probably mediated by an electroneutral K^+/H^+ antiport (Leidi *et al.*, 2010). In this case, increasing K^+ accumulation would no longer increase the $\Delta\psi$ but instead increase vacuolar pH, reducing the transport of organic anions. Finally, K^+ is known to be involved in the regulation of various enzymes (including the tonoplastic proton pumps), either directly (Maeshima, 2000; Wyn Jones and Pollard, 1983) or by modifying cytosolic pH (Wyn Jones and Pollard, 1983). However, this is unlikely to play an important role, because of the homeostasis of cytosolic K^+ (Leigh, 2001).

Table I-1 Impact of agro-environmental factors (source: sink ratio, mineral fertilization, water supply, and temperature) on malate and citrate concentrations, and titratable acidity (TA) in the ripe fruits of several species. Citrate content, malate content, and TA are expressed in meq/100 g FW. The protocol of each study is summarized as two contrasted treatments applied (A and B). Differences between treatment A and B are either significant at p<0.05 (*) or non-significant (NS). Concerning mineral fertilization, the total quantity of K, Mg, N or P applied during the experimental period is given.

	Protocol	Malate content		Citrate content		TA		References
		A	B	A	B	A	B	
SOURCE:SINK RATIO								
Peach (cv. Suncrest)	A: 30 leaves/fruit B: 10 leaves/fruit	8.8*	7.8*	1.5*	3.5*			Wu et al., 2002 (data from 1997)
	A : 30 leaves/fruit B : 6 leaves/fruit	9.0*	8.4*	1.2*	4.9*	9.5*	7.4*	Souty et al., 1999
Mango (cv. Lirfa)	A :100 leaves/fruit B: 10 leaves/fruit	0.04 (NS)	0.04 (NS)	0.08*	0.12*			Lechaudel et al., 2005
POTASSIUM FERTILIZATION								
Pineapple (cv. Smooth Cayenne)	A: 0 g of K/plant B: 19.1 g of K/plant					9.6*	13.8*	Spironello et al., 2004
Peach (cv. Elberta)	A: 90 g of K/tree B: 600 g of K/tree					6.1 (NS)	6.9 (NS)	Cummings and Reeves, 1971
Banana (cv. Ney Poovan)	A: 0% SOK spray B: 1.5% SOK spray					6.0*	3.4*	Ramesh Kumar et al., 2007
Banana (cv. Robusta)	A: 0 g of K/plant B: 274 g of K/plant					6.1*	3.4*	Vadivel et al., 1978
Citrus	A: 65 kg of K/ha B: 230 kg of K/ha					10.9*	11.7*	Alva et al., 2006
MAGNESIUM FERTILIZATION								
Peach (cv. Elberta)	A: 14 g of Mg/tree B: 220 g of Mg/tree					6.7 (NS)	6.3 (NS)	Cummings and Reeves, 1971
NITROGEN FERTILIZATION								
Peach (cv. Redhaven)	A:150 g of N/tree B: 610 g of N/tree					7.2 (NS)	6.3 (NS)	Cummings and Reeves, 1971
Apricot (cv. Canino)	A: 213 g of N/tree B: 400 g of N/tree					26.0*	31.4*	Radi et al., 2003
Orange (cv. Valencia)	A: 540 g of N/tree B: 1000 g of N/tree					13.7*	14.7*	Reitz et al., 1957
Pineapple (cv. Smooth Cayenne)	A: 0 g of N/plant B: 23 g of N/plant					14.5*	11.4*	Spironello et al., 2004
PHOSPHOROUS FERTILIZATION								
Peach (cv. Loring)	A: 0 kg of P/ha B: 141 kg of P/ha					8.2*	8.4*	Cummings and Reeves,1971

Pineapple (cv. Smooth Cayenne)	A: 0 g of P/plant B: 10 g of P/plant					13.0 (NS)	12.5 (NS)	Spironello et al., 2004
WATER SUPPLY								
Peach (cv. Suncrest)	A: Irrigated B: Non irrigated	7.9 (NS)	8.9 (NS)	3.4 (NS)	3.1 (NS)			Wu et al., 2002
Pear (cv. Williams)	A: No water stress B: Early water stress	0.26 (NS)	0.1 (NS)	2.2 (NS)	3.4 (NS)	3.3 (NS)	3.6 (NS)	Hudina et al., 2000
Tomato (cv. Vanessa)	A: Watered to 70% maximum water holding capacity B: Watered to 50% maximum water holding capacity					5.1*	6.0*	Veit Khöler et al., 1999
Apple (cv. Braeburn)	A: Irrigated B: Non irrigated					6.7*	7.5*	Mills et al., 1996
Mandarin (cv. Satsuma)	A: Well watered B: Severely drought stress					29.6*	46.9*	Yakushiji et al., 1998
Nectarine (cv. Spring Bright)	A: Irrigated B: Deficit irrigation (33% of irrigation in "A")	4.6*	3.1*	4.7 (NS)	4.7 (NS)			Thakur et al., 2012
Clementine (cv. de Nules)	A: Irrigated B: Deficit irrigation (reduced to 25% of crop evapotranspiration)					13.1*	17.1*	Gonzales-Altozano et al., 1999 (data from 1995)
Orange (cv. Navel)	A: Irrigated B: Late water stress					17.2*	21.9*	Kallsen et al., 2011 (data from 2007)
Grape (cv. Monastrell)	A: Irrigated B: Non irrigated					7.3*	8.9*	De La Hera Orts et al., 2005
Grape (cv. Sauvignon Blanc)	A: No water stress B: Water stress	2.2*	3.4*			7.0*	9.2*	Des Gachons et al., 2005 (data from 1998)
TEMPERATURE								
Tomato (cv. Cervil)	A: Not heated B: Heated (fruit temperature: +1,1°C during the day, +1,3°C during the night)					11.7*	10.5*	Gautier et al., 2005
Strawberry (cv. Kent)	A: 18/12 day/night temperature (°C) B: 25/22 day/night temperature (°C)					14.0*	12.5*	Wang et al., 2000

The PBSM proposed by Lobit *et al.* (2006), which is based on the assumption that malate accumulation is controlled by vacuolar pH, only takes the contribution of K^+ to the acid-basic reactions in the vacuole into account. The model predicted that at low vacuolar pH (in the early stages of fruit growth), an increase in K^+ content would reduce malate accumulation, while at higher pH (during fruit ripening) it would stimulate it.

Contradictory effects of nitrogen nutrition on fruit acidity have also been reported (*Table I-1*). Some authors found a negative correlation between nitrogen nutrition and TA (Spironello *et al.*, 2004), others found a positive correlation between nitrogen nutrition and both TA (Reitz and Koo, 1960) and organic acid content (Jia *et al.*, 1999; Radi *et al.*, 2003; Ruhl, 1989), and still others that it had no significant effect (Cummings and Reeves, 1971). Nitrogen fertilization may have an indirect impact on fruit acidity by stimulating the vegetative growth of plants. Increased vegetative growth may affect the fruit in various ways: by shading them (which would lower their temperature and reduce transpiration), or by diverting assimilates towards vegetative growth (which would reduce the supply of assimilates to the fruits). The effect of nitrogen on fruit acidity may also depend on the form of nitrogen applied (NO_3^- or NH_4^+). NO_3^- fertilization is likely to have a positive impact on the concentration of organic anions in the phloem sap since nitrate assimilation in the leaves requires the coordinated synthesis of organic acids (Benzioni *et al.*, 1971; Scheible *et al.*, 1997; Smith and Raven, 1979), which are then transported in the phloem sap together with K^+. Conversely, NH_4^+ fertilization does not cause the synthesis of organic anions, and may affect cation uptake by roots, like K^+, as observed in banana (Sathiamoorthy and Jeyabaskaran, 2001).

Very few studies have been conducted on the effects of other mineral elements on fruit acidity (*Table I-1*). However, magnesium has been shown to have no significant effect on fruit acidity (Cummings and Reeves, 1971), and phosphorous nutrition appears to have little effect on fruit acidity (Cummings and Reeves, 1971; Spironello *et al.*, 2004).

5.3 Water supply influences fruit acidity probably due to modifications in fruit water content and osmotic adjustment

The impact of water supply on fruit acidity has been widely studied (*Table I-1*). In most cases, water supply was shown to be negatively correlated with TA, and organic acid content in ripe fruits (Gonzales-Altozano and Castel, 1999; Hudina and Stampar, 2000; Kallsen *et al.*, 2011; Mills *et al.*, 1996; Veit-Köhler *et al.*, 1999; Wu *et al.*, 2002; Yakushiji *et al.*, 1998). However, some authors reported a positive relationship between water supply and both TA and organic

acid content in ripe fruits (De la Hera-Orts *et al.*, 2005; des Gachons *et al.*, 2004; Esteban *et al.*, 1999; Thakur and Singh, 2012). Even if water supply modifies fruit acidity, there is apparently no change in the seasonal patterns of the accumulation of organic acids (De la Hera-Orts *et al.*, 2005; Thakur and Singh, 2012; Wu *et al.*, 2002). Taken together, these data suggest that water stress tends to increase organic acid content and TA in ripe fruits through a simple dilution/dehydration effect (Gonzales-Altozano and Castel, 1999). Another mechanism through which the plant water status may interfere with fruit acidity is osmotic adjustment: under water stress, all plant tissues accumulate solutes, mainly sugars and organic acids (Hummel *et al.*, 2010), to lower their osmotic potential and prevent a drop in cell turgor pressure. As water stress increases the accumulation of organic acids in the leaves and xylem fluid (Andersen, 1995; Hummel, 2010), it may also increase imports of organic acids to the fruit.

5.4 Temperature influences fruit acidity by affecting both metabolism and vacuolar storage of organic acids

Increasing the temperature during fruit growth or storage decreases fruit TA (Gautier *et al.*, 2005; Kliewer, 1973; Rufner, 1982; Wang and Camp, 2000) (*Table I-1*) as well as malate and citrate concentrations, as shown in the grape berry (Buttrose *et al.*, 1971; Kliewer, 1973; Rufner, 1982) and in banana (Bugaud *et al.*, 2009). Nevertheless, all organic acids do not appear to be equally sensitive to temperature (Rufner, 1982; Wang and Camp, 2000).

Modifications in organic acid metabolism in response to temperature probably result from the impact of temperature on the reaction rates of glycolysis and of the TCA cycle (Araujo *et al.*, 2012) by modifying enzyme activities (Lakso and Kliewer, 1975b), and also on the kinetic properties of the mitochondrial transport systems involved (Halestrap, 1975). The main effect of increasing temperature would be to stimulate respiration, with the above mentioned effects on citrate metabolism (increasing citrate production during green stages and decreasing citrate production during ripening) (see previous section). Results of the fruit PBSM developed by Lobit *et al.* (2003), which models net citrate production as a function of temperature, fruit mesocarp weight, and respiration, were in good agreement with experimental data. Further simulations showed that temperature can affect fruit acidity in different ways depending on the fruit cultivar or species (Wu *et al.*, 2007).

Temperature probably affects vacuolar storage of organic acids via several mechanisms. Temperature is a key variable in the thermodynamic equations that limit the operation of the proton pumps and the diffusion of organic anions through the tonoplast. In

the PBSM of malate accumulation in fruit developed by Lobit *et al.* (2006), increasing the temperature reduced the ability of the fruit to accumulate malate, which is in accordance with observations made in agronomic studies. Temperature also affects membrane fluidity by modifying lipid properties (Murata and Los, 1997). Thus, high temperatures may change the tonoplastic permeability of fruit cells, which could increase leakage of solutes like protons, or protonated forms of organic acids. The increase in tonoplastic permeability could explain the increased activity of vacuolar proton pumps observed in grape berry cells in response to an increase in temperature (Terrier *et al.*, 1998). The increase in proton pump transport activity may compensate for the leakage of solutes, which is known to occur during grape berry ripening (Terrier et al., 2001), but only partially, resulting in a net efflux of malic and citric acid to the cytosol and their further degradation (because of the cytosolic pH homeostasis), leading to a decrease in fruit acidity.

6 Conclusions

This review showed that accumulation of malate and citrate is the result of interactions between metabolism and vacuolar storage, and identified the main mechanisms likely to drive them. It also showed that agro-environmental factors affect the acidity of fleshy fruit by acting on various cellular mechanisms. To increase our understanding of the development of acidity in fleshy fruit, we believe that integrative approaches would be particularly appropriate (Génard *et al.*, 2010; Struik *et al.*, 2005). The combination of PBSMs and molecular data, as a tool for model parameterization, could advance our understanding of the response of citrate and malate accumulation to environmental fluctuations and genetic control.

Chapitre II Etude Expérimentale de l'Effet du Génotype et des Conditions de Croissance du Fruit sur l'Acidité de la Banane (*Musa* sp. AA)

Objectifs

Dans ce chapitre, sont présentés les effets du génotype et des conditions de croissance du fruit (charge en fruit, fertilisation potassique, stade de récolte) sur l'accumulation du citrate et du malate dans la pulpe de banane pendant les phases pré et post récolte. La concentration en acides organiques dans la pulpe résulte à la fois de l'accumulation en eau, de l'accumulation en matière sèche (composés de stockage tels que l'amidon et les sucres), et du métabolisme et stockage vacuolaire des acides, et peut donc être décomposée en trois composantes : la teneur en eau de la pulpe, la teneur en matière sèche non structurale, et la concentration de chaque acide par gramme de matière sèche structurale. L'effet des différents facteurs agronomiques sur chaque composante est quantifié. Ce chapitre a été accepté par le journal **Scientia Horticulturae** sous la forme d'un article intitulé «Citrate and malate accumulation in banana fruit (*Musa* sp. AA) is highly affected by genotype and fruit age, but not by cultural practices».

Principaux résultats

- D'importantes différences de profils d'accumulation du citrate et du malate existent entre les trois génotypes étudiés aussi bien pendant la croissance que pendant la maturation post récolte des fruits.
- Une diminution de la charge en fruit et un niveau élevé de fertilisation potassique ont un effet positif sur la croissance des fruits mais n'ont pas d'effet sur les concentrations en citrate et malate, aussi bien pendant la croissance que pendant la maturation post récolte.
- Une date de récolte tardive augmente légèrement la concentration en citrate dans les fruits mûrs après récolte, et diminue celle en malate.

Citrate and malate accumulation in banana fruit (Musa sp. AA) is highly affected by genotype and fruit age, but not by cultural practices

A. Etienne[1], M. Génard[2], D. Bancel[2], S. Benoit[1], G. Lemire[1], C. Bugaud[1]

[1] Centre de Coopération International en Recherche Agronomique pour le Développement (CIRAD), UMR QUALISUD, Pôle de Recherche Agronomique de Martinique, BP 214, 97 285 Lamentin Cedex 2, France

[2] INRA, UR 1115 Plantes et Systèmes de Cultures Horticoles, F-84914 Avignon, France

Abstract

Sourness and sweetness are major drivers of consumer preference for banana fruits and are mainly linked to the presence of citrate and malate. The objectives of the present work were to determine how agro-environmental and genotypic factors affect the concentrations of citrate and malate in banana pulp during growth and post-harvest ripening. Changes in citrate and malate concentrations in the pulp during the development of the fruit were investigated in relation to fruit age, fruit load, and potassium fertilization in three cultivars of dessert banana presenting contrasted acidity at the eating stage. Major differences in the pattern of citrate and malate accumulation were found in the three cultivars both during growth and post-harvest ripening. The fruit growth rate was greater when the fruit load was reduced, but this treatment had no effect on the accumulation of organic acids in any of the three cultivars. A high potassium supply increased fruit growth but had no effect on organic acid accumulation in any of the three cultivars. Late harvested fruits had higher citrate and lower malate concentrations in the pulp at the eating stage. Our results showed that the concentration of organic acids in banana pulp is mainly controlled by genotype and that this may be an interesting trait to target in breeding programs to improve the organoleptic quality of new cultivars. The physiological mechanisms likely to control the accumulation of citrate and malate during banana fruit development are discussed.

1 Introduction

Banana is an important high-value food crop but the international banana market is almost completely restricted to the Cavendish variety, which is sensitive to the main diseases of banana. The breeding history of banana has therefore focused on disease resistance (Yellow Sigatoka Disease and Black Leaf Streak Disease), without taking sensory characteristics into consideration. As a result, new hybrids have been rejected by consumers owing to sensory shortcomings among other characteristics. To improve the sensory characteristics of new hybrids it is crucial to understand the determinants of the organoleptic quality of banana fruits.

Sourness and sweetness are major drivers of consumer preference for banana fruits, and these characteristics are mainly linked to the presence of organic acids in fruit cells (Esti et al., 2002; Harker et al., 2002; Tieman et al., 2012). Citrate and malate, the most abundant acid metabolites in banana fruit, have been shown to be good predictors of pulp sourness and sweetness (Bugaud et al., 2013). Banana fruit has the particularity of having separate growth and ripening phases, during which significant changes in the concentration of organic acids take place in the fruit. Banana fruits accumulate both citrate and malate during growth and these determine fruit acidity at harvest (Jullien et al., 2008). The concentrations of organic acids still change considerably during post-harvest ripening with an increase in pulp acidity (Etienne et al., 2013a; Mustaffa et al., 1998; N'Ganzoua et al., 2010), and considerable variations in the acidity of ripe fruits among dessert banana cultivars (Bugaud et al., 2013). Thus, any attempts to understand the determinants of banana pulp acidity must include a study of the dynamics of organic acid concentrations during fruit growth but also during post-harvest ripening.

The concentrations of organic acids in fruit pulp are the result of several processes. First, the transport and metabolic processes of organic acids, which involve several interconnected metabolic pathways and transport mechanisms through several compartments, control the amount of citrate and malate in the pulp (Etienne *et al.*, 2013b). Second, the accumulation of water and dry matter in the fruit influences the concentration of organic acids in the pulp due to dilution (Léchaudel *et al.*, 2005b; Souty *et al.*, 1999). Dilution by dry matter is the result of the import of assimilates in the fruit that are used for the storage of starch, sugars and organic acids. However, the imported assimilates can also be used to produce cell walls. Hence, the ratio of storage compounds (also called non-structural dry matter) to cell wall material (also called structural dry matter) plays a major role in the concentration of organic acids in the pulp (Léchaudel *et al.*, 2005b).

Agro-environmental factors, including fruit load, water supply, mineral fertilization and temperature, are known to affect fruit acidity by acting on the transport and metabolic processes of organic acids (Etienne *et al.*, 2013b), and/or by modifying the water content of the pulp (Léchaudel et al., 2002). Only a few studies have been conducted on the effect of orchard management on banana pulp acidity. They showed that potassium fertilization decreased the titratable acidity of ripe banana fruits (Ramesh Kumar and Kumar, 2007; Vadivel and Shanmugavelu, 1978), but these studies provided no information on the direct effect of potassium fertilization on the concentration of organic acids.

The objectives of the present work were to advance our understanding of the roles played by agro-environmental factors and genotype in the concentrations of citrate and malate in banana pulp during growth and post-harvest ripening. To this end, we studied the effect of fruit age, fruit load, and potassium fertilization on the accumulation of malate and citrate in three cultivars of dessert banana with contrasting acidity at the eating stage. To better understand how cultural practices and genotype affect organic acid concentrations in the pulp, we analyzed changes in concentrations of citrate and malate by breaking them down into components related to transport and metabolic processes, and to the accumulation of water and dry matter. This approach was shown to be a good way to study the influence of irrigation and of the ratio of leaf to fruit on mango fruit quality (Léchaudel *et al.*, 2005b).

2 Materials and methods

2.1 Field experiment and treatments

Three dessert banana cultivars (*Musa* spp.) diploids AA, differing in predominant organic acid at eating stage: Indonesia 110 (IDN), Pisang Jari Buaya (PJB), and Pisang Lilin (PL) were studied during the 2011 and 2012 growing seasons (*Appendix 1*). All the bananas were grown at the *Pôle de Recherche Agroenvironnementale de la Martinique* (PRAM, Martinique, French West Indies; latitude 14°37N, longitude 60°58W, altitude 16 m) on continental alluvial soil. In the two growing seasons, irrigation was adjusted to the amount of rainfall to supply at least 5 mm of water per day, and non-systemic fungicide was applied to control foliar diseases. During the first period of bunch growth (March–November 2011) the mean daily temperature was 27 °C ± 1.2 °C. During the second period of bunch growth (February-August 2012) the mean daily temperature was 26 °C ± 0.9 °C. Bunches were left uncovered in both growing seasons.

2011 experiment: Effect of fruit load on banana pulp acidity

For each cultivar, 36 plants were randomly chosen and tagged at inflorescence emergence. Two contrasted fruit loads were used: 18 plants of each cultivar were used as the control treatment i.e. high fruit load, and 18 other plants were highly pruned i.e. low fruit load. In the control treatment, the number of leaves and hands left on the plants were calculated in order to have the same leaf area: fruit ratio among cultivars (approximately equal to 0.5 cm^2 leave. g $fruit^{-1}$). Thus, 15 days after inflorescence emergence, 8, 6, and 5 leaves were left on the plant for cultivars IDN, PL, and PJB respectively, and the top 10, 5 and 7 hands were left on the bunch for cultivars IDN, PL, and PJB respectively. To ensure the situation was the same among the three cultivars, fruit pruning in low fruit load treatment was calculated to increase the leaf area: fruit ratio by approximately 2.5. Consequently, 15 days after inflorescence emergence, the top 4, 2, and 3 hands were left on the bunch for cultivars IDN, PL, and PJB respectively. Banana plants received 12 g of nitrogen, 1.7 g of phosphorus, and 23 g of potassium at 4-week intervals during fruit growth.

2012 experiment: Effect of potassium fertilization on banana pulp acidity

Two plots containing 50 banana plants of each cultivar were planted. Two contrasted levels of potassium fertilization were started six months before the beginning of fruit sampling. For each cultivar, one plot received 124 g of potassium per plant (high potassium fertilization) at 4-week intervals, while the other received no potassium at all. All the banana plants received 12 g of nitrogen and 10 g of phosphorus at 4-week intervals. Twenty-four plants of each cultivar were randomly chosen in each plot and tagged at inflorescence emergence. At 15 days after inflorescence emergence, 9, 7, and 9 leaves were left of cultivars IDN, PL, and PJB respectively, which corresponds to the average leaf number in 2012, and the top 10, 5, and 7 hands were left on the bunch of cultivars IDN, PL, and PJB respectively, which correspond to a high fruit load. Leaf and soil analyses were performed at the beginning and end of the experiment. In each plot, lamina 3 of 10 randomly selected banana plants was sampled according to the international reference method (Martin-Prével, 1977). In each plot, ten soil samples evenly distributed throughout the plot were collected. Soluble K, Mg, and Ca concentrations in the leaves and soil were determined by mass spectrometry (Martin-Prével et al., 1984), the concentration of Cl was determined by potentiometry using a Titroline alpha automatic titrator (Walinga et al., 1995), and soluble phosphorus was determined by colorimetry (Martin-Prével et al., 1984).

2.2 Fruit sampling procedure

Monitoring fruit growth

In the two growing seasons, six bunches of each cultivar-treatment combination were selected. At 15 day intervals, one fruit located in the internal row of the second proximal hand was collected for analyses. Natural ripening on standing plants, i.e. when the first yellow finger appeared, determined the end of sampling.

Monitoring post-harvest fruit ripening

In the 2011 experiment, two harvest stages were studied. For each cultivar, the harvest stages were calculated to be 70% and 90% of the average "flowering-to-yellowing time" of the bunch on the tree. Previous observations in the field informed us about the average flowering-to-yellowing time of each cultivar. For each harvest stage, six bunches per cultivar and per treatment were harvested. In the 2012 experiment, only one harvest stage was studied. For each cultivar, the harvest stage was calculated for each cultivar to be 75% of the average flowering-to-yellowing time of the bunch on the tree. Six bunches per cultivar and per treatment were harvested.

After the bunches were harvested, the second proximal banana hand on each bunch was rinsed and dipped in fungicide (bitertanol, 200 $mg.L^{-1}$) for 1 min. The fruits were placed in a plastic bag with 20 μm respiration holes and stored in boxes for 6 days at 18 °C. The fruits were then stored in a room at 18 °C and underwent ethylene treatment (1 $mL.L^{-1}$ for 24 h) to trigger the ripening process. After 24 h, the room was ventilated. Bananas were maintained at 18 °C for 13 days and a banana fruit was sampled before ethylene treatment (day 0), and at day 3, 6, 9 and 13. The fruit storage potential – called the green life – was estimated as the time between harvest and the climacteric rise (Chillet et al., 2008).

2.3 Determination of banana pulp composition

The fresh pulp of each fruit sampled was weighed. Dry matter was determined by freeze-drying the pulp and then weighing it. The dried pulp was then mixed to obtain a dry powder and citrate and malate concentrations were determined according to the method described in Etienne et al. (2013a). Concentrations of starch and soluble sugars (glucose, fructose, sucrose) were assessed according to Gomez et al. (2007) using an enzymatic method and a microplate reader. Soluble K, Mg, and Ca in the pulp were determined by mass spectrometry and soluble phosphorus was measured by colorimetry (Martin-Prével et al., 1984).

The concentration of malate and citrate was considered to be the product of three components obtained from the following equation:

$$C_x = \frac{W_x}{FW} = \frac{DW}{FW} * \frac{W_x}{DW} = \frac{DW}{FW} * \frac{SDW}{DW} * \frac{W_x}{SDW} = \left(1 - \frac{WW}{FW}\right) * \left(1 - \frac{NSDW}{DW}\right) * \frac{W_x}{SDW} \quad (1)$$

where C_x is the concentration (in g.100g FW^{-1}) and W_x is the weight (in g) of the compound x in fruit pulp; FW is fresh weight, DW is dry weight, WW is water weight, SDW is structural dry weight, and NSDW is non-structural dry weight of the pulp (in g).

The ratio of water weight to fresh weight represents the water content of the pulp and is related to water dilution; the ratio of non-structural to total dry weight is related to the accumulation and storage of compounds; and the ratio of the weight of compound x to structural dry weight is related to the transport and metabolic processes of organic acids. Water weight was calculated as the difference between fresh and dry weight. Non-structural dry weight was calculated as the difference between dry weight and structural dry weight. Structural dry weight was calculated as the difference between dry weight and the sum of the weights of the main non-structural compounds (soluble sugars, starch, acids).

In order to compare the dynamics of organic acid concentrations among cultivars during fruit growth, fruit age was expressed as a percentage of the flowering-to-yellowing time of the bunch.

2.4 Statistical Analysis

Linear mixed-effects models [LMMs (Gałecki and Burzykowski, 2013)] were used to examine the relationship between response variables (pulp citrate and malate concentration) and explanatory variables (fruit age, cultivar, treatment), and interactions. We used quadratic and cubic terms of fruit age when the curve passed through a maximum and had an asymmetrical shape. We used the lme function in the 'nlme' library (Pinheiro et al., 2013) in the statistical program R 2.14.0. "Banana plant" was treated as a random effect because banana plants were assumed to contain unobserved heterogeneity which is impossible to model. A temporal correlation structure was used to account for temporal pseudo-replication. Model selection was made using the top-down strategy (Zuur et al., 2009): starting with a model in which the fixed component contains all the explanatory variables and interactions, we found the optimal structure of the random component. We then used the F-statistic obtained with restricted maximum likelihood (REML) estimation to find the optimal fixed structure. Finally, the significance of each factor kept in the optimal model was assessed using the F-statistic obtained with REML estimation.

3 Results and discussion

3.1 Fruit age and cultivar strongly affected the accumulation of organic acids during fruit growth

Organic acid concentrations in the pulp can be broken down into three components, pulp water content, the ratio of non-structural to total dry weight, and the ratio of organic acids to structural dry weight. In 2011 and 2012, fruit age had a significant effect on these three components, and consequently on the concentrations of malate and citrate in the pulp (*Table II-1*).

The concentration of malate in the pulp and the ratio of malate to structural dry weight increased throughout fruit growth (*Fig. II.1.B, D, H, J*). In a previous paper, we suggested that malate accumulation in the fruit is controlled at the level of vacuolar storage, and that, in response, malate metabolism maintains the cytosolic pH constant (Etienne *et al.*, 2013b). Thus, the increase in the concentration of malate during banana fruit growth may be due to more favorable thermodynamic conditions for the transport of malate into the vacuole as the fruit grows. Lobit et al. (2006) showed that the concentration of malate in the vacuole of fruit cells is determined by vacuolar pH and by the electric potential gradient across the tonoplast ($\Delta\psi$). The tonoplast proton pumps are the main contributors to $\Delta\psi$ and vacuolar pH (Martinoia et al., 2007) and could thus be responsible for the accumulation of malate during banana fruit growth.

The concentration of citrate in the pulp and the ratio of citrate to structural dry weight increased throughout fruit growth (*Fig. II.1.A, C, G, I*). Citrate is produced through the TCA cycle, a metabolic pathway located in the mitochondria that is responsible for the oxidation of respiratory substrates that drive ATP synthesis (Sweetlove et al., 2010). We suggested that citrate accumulation in the fruit is controlled by the TCA cycle and consequently by fruit respiration rate (Etienne *et al.*, 2013b). The increase in the concentration of citrate during banana fruit growth implies that the TCA cycle is acting in a non-cyclic flux mode that probably converts malate into citrate. Citrate production during banana growth may be due to an increase in mitochondrial citrate synthase activity (Iannetta et al., 2004; Sadka et al., 2001; Wen et al., 2001), and/or to a decrease in cytosolic and/or mitochondrial aconitase activity (Morgan *et al.*, 2013; Sadka *et al.*, 2000a).

Pulp water content decreased linearly up to 50% of flowering-to-yellowing time, then decreased slowly between 50% and 80% of flowering-to-yellowing time, and finally increased slightly until the end of growth as previously reported by Bugaud et al. (2012) (*Fig. II.1.E and K*). The ratio of non-structural to total dry weight increased markedly up to 50% of

flowering-to-yellowing time and then only slightly (*Fig. II.1.F and L*). Thus, in the second half of the flowering-to-yellowing period, dilution by water and by the accumulation and storage of compounds, (mainly starch) (Jullien *et al.*, 2001b), did not play an important role in the determination of the concentration of organic acids in the pulp.

There were significant differences among cultivars in the patterns of citrate and malate accumulation in the pulp in both 2011 and 2012. The PL cultivar had significantly higher citrate and malate concentrations in the pulp than the IDN and PJB cultivars (*Table II-1*, *Fig. II.1.A, B, G and H*). There were major differences in the ratio of citrate and malate to structural dry weight among cultivars, and slight differences in pulp water content and in the ratio of non-structural to total dry weight (*Table II-1, Fig. II.1.C, D, E, F, I, J, K and L*), meaning that differences among the three cultivars in the accumulation of organic acids during fruit growth were mainly the result of differences in the metabolism and/or vacuolar storage of organic acids. Based on total citrate and malate concentrations, the PL cultivar had a much higher total organic acid concentration than the PJB and IDN cultivars. As citrate is mainly produced from malate through the TCA cycle, this means that malate production in the cytosol was highest in the PL cultivar. Concerning the ratio of citrate to malate concentrations, the IDN and PJB cultivars had twice to three times higher concentrations of citrate than of malate, whereas in the PL cultivar, the ratio was close to one. As citrate is more easily transported into the vacuole than malate (Etienne *et al.*, 2013b), there may be an advantage for fruit cells to store citrate rather than malate. The particularity of the PL cultivar in storing equal amounts of citrate and malate may be the consequence of differences in vacuolar transport and/or in the rate of conversion of malate into citrate through the TCA cycle.

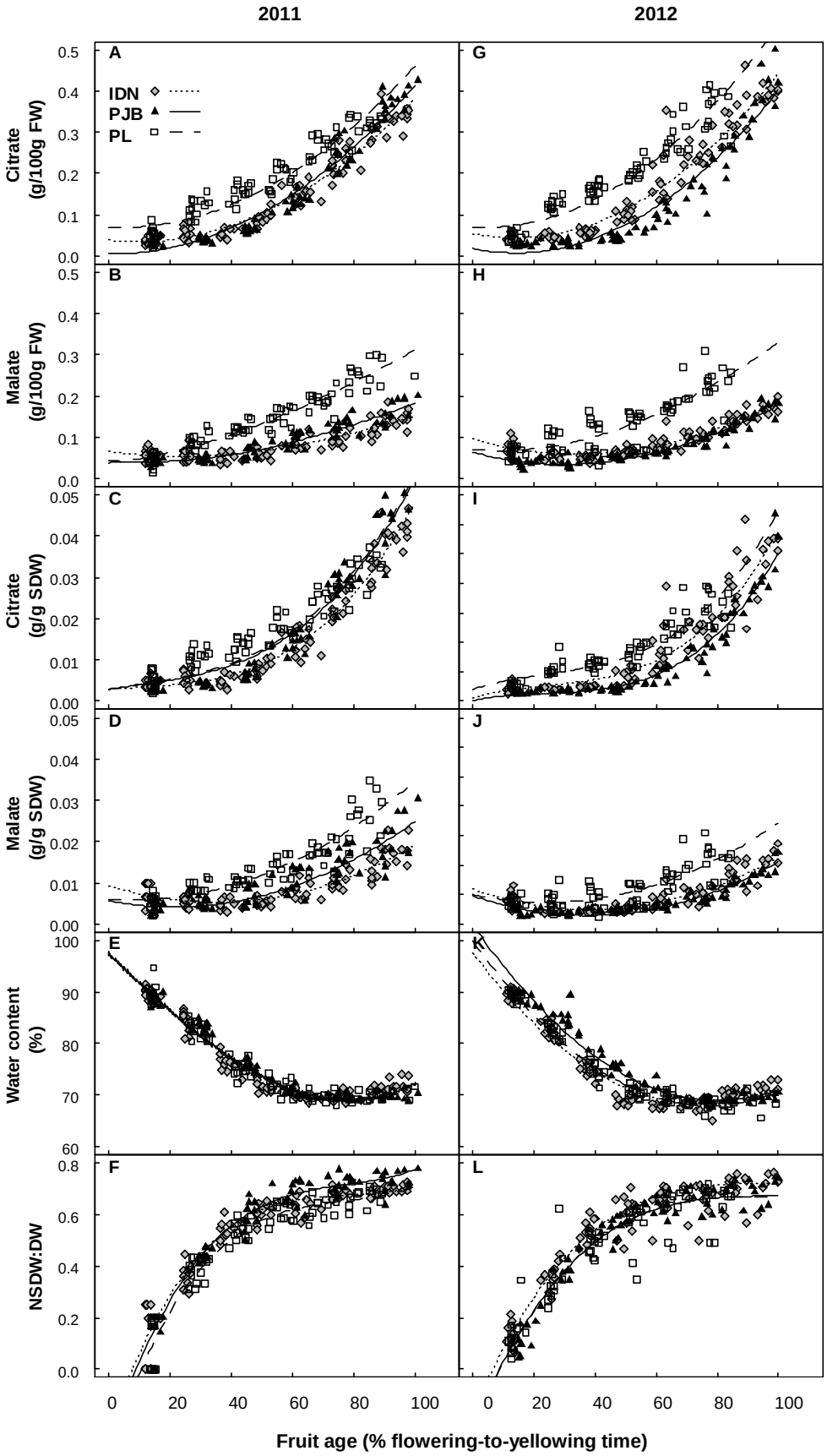

Figure II-1 Seasonal variations in pulp citrate concentration (A, G), pulp malate concentration (B, H), ratio of citrate to structural dry weight (C, I), ratio of malate to structural dry weight (D, J), water content (E, K), and ratio of non-structural to total dry weight (F, L) during the 2011 and 2012 experimental period in the three cultivars (IDN, PJB, and PL). Each symbol represents a fruit. Lines are those of the fitted linear mixed model.

Table II-1 LMM analysis of banana pulp fresh weight (g), citrate concentration (g.100 g FW^{-1}), malate concentration (g.100 g FW^{-1}), water content (%), non-structural: total dry weight ratio (NSDW: DW), citrate: structural dry weight ratio (citrate: SDW), and malate: structural dry weight ratio (malate: SDW) during fruit growth. The factors studied were fruit age, cultivar and pruning treatment in the 2011 experiment, and fruit age, cultivar and potassium fertilization treatment in the 2012 experiment.

		F-value [a] and significance [b]						
Year	Factors [c]	Pulp fresh weight	Citrate concentration	Malate concentration	Water content	NSDW : DW	Citrate : SDW	Malate : SDW
2011								
	c	67***	16***	79***	Ns	16***	Ns	17***
	p	32***	Ns	Ns	8**	Ns	Ns	Ns
	a	6117***	2703***	1599***	3738***	1655***	1493***	702***
	a^2	262***	184***	44***	967***	399***	224***	87***
	a^3	9**	Ns	9**	14***	40***	6*	Ns
	p : a	36***	Ns	Ns	Ns	Ns	Ns	Ns
	c : p	Ns	Ns	Ns	Ns	Ns	Ns	Ns
	c : a	76***	7***	155***	Ns	4*	14***	50***
	c: p : a	Ns	Ns	Ns	Ns	Ns	Ns	Ns
2012								
	c	13***	28***	92***	18***	7*	6**	22***
	f	Ns	Ns	Ns	Ns	Ns	6*	4*
	a	4043***	1603***	560***	3562***	520***	936***	3623***
	a^2	106***	142***	70***	950***	115***	233***	145***
	a^3	34***	Ns	6**	Ns	5*	21**	Ns
	c : f	Ns	Ns	Ns	Ns	Ns	3*	2*
	c : a	15***	8***	54***	19***	Ns	3*	19***
	f: a	Ns	Ns	Ns	Ns	Ns	Ns	Ns
	c: f: a	6***	Ns	Ns	Ns	Ns	Ns	Ns

[a] The F-value is given only for the factors kept in the optimal model.

[b] *** p-value < 0.001; ** p-value < 0.01; * p-value<0.05 ; Ns : not significant.

[c] Codes for factors: c=cultivar; p=pruning treatment; a=fruit age (in % of flowering-to-yellowing time); f=potassium fertilization treatment.

3.2 Ripening stage and cultivar strongly affected the accumulation of organic acids during post-harvest fruit ripening

During post-harvest ripening, the ripening stage and the cultivar had a significant effect on the ratio of organic acids to structural dry weight and pulp water content in 2011 and 2012. The ratio of non-structural to total dry weight was significantly affected by the cultivar only in 2011, and by the ripening stage and the cultivar in 2012 (*Table II-2*). Consequently, the ripening stage and the cultivar had a significant effect on the concentrations of malate and citrate in the pulp in 2011 and 2012. Differences in the concentrations of total organic acids in the pulp in the three cultivars at the eating stage (day 6 to 13) were greater than 0.3 g.100g FW^{-1}, which is sufficient for a detectable difference in sourness and sweetness (Bugaud et al., 2013).

The patterns of citrate concentration in the pulp and the ratio of citrate to structural dry weight were the same in the IDN and PL cultivars with an overall decrease during ripening, whereas there was an overall increase in the PJB cultivar (*Fig. II.2.A, C, G and I*). At the end of ripening, PJB had the highest citrate concentration and PL the lowest. Several mechanisms may explain the decrease in citrate concentration observed in the PL and IDN cultivars during ripening. One could be the activation of the GABA shunt, a cytosolic pathway of citrate catabolism known to occur during banana ripening (Chen and Gadal, 1990; Liu et al., 2004; Medina-Suárez et al., 1997). Another possible reason for the decrease in the concentration of citrate could be a shift from the use of malate to citrate as respiratory substrate by the TCA cycle. The different pattern of citrate accumulation observed in the PJB cultivar may be due to the use of malate as respiratory substrate instead of citrate, or to less active catabolism of citrate in the cytosol.

The patterns of malate concentration in the pulp and the ratio of malate to structural dry weight were the same in all three cultivars with an increase from day 0 to day 6, and a slight decrease after that (*Fig. II.2.B, D, H and J*). At the end of ripening, the PL cultivar had the highest concentration of malate, followed by the PJB and IDN cultivars. The accumulation of malate from day 0 to day 9 may be due to more favorable thermodynamic conditions for malate transport into the vacuole or to a higher capacity for malate synthesis. The slight decrease in malate concentration at the very end of ripening could be due to an increase in tonoplast permeability leading to leakage of anions, as observed during grape berry ripening (Terrier et al., 2001). It is known that membrane permeability increases during banana ripening (Sacher, 1966). The malate arriving in the cytosol from the vacuole could be further degraded by pH homeostasis leading to a decrease in the concentration of malate.

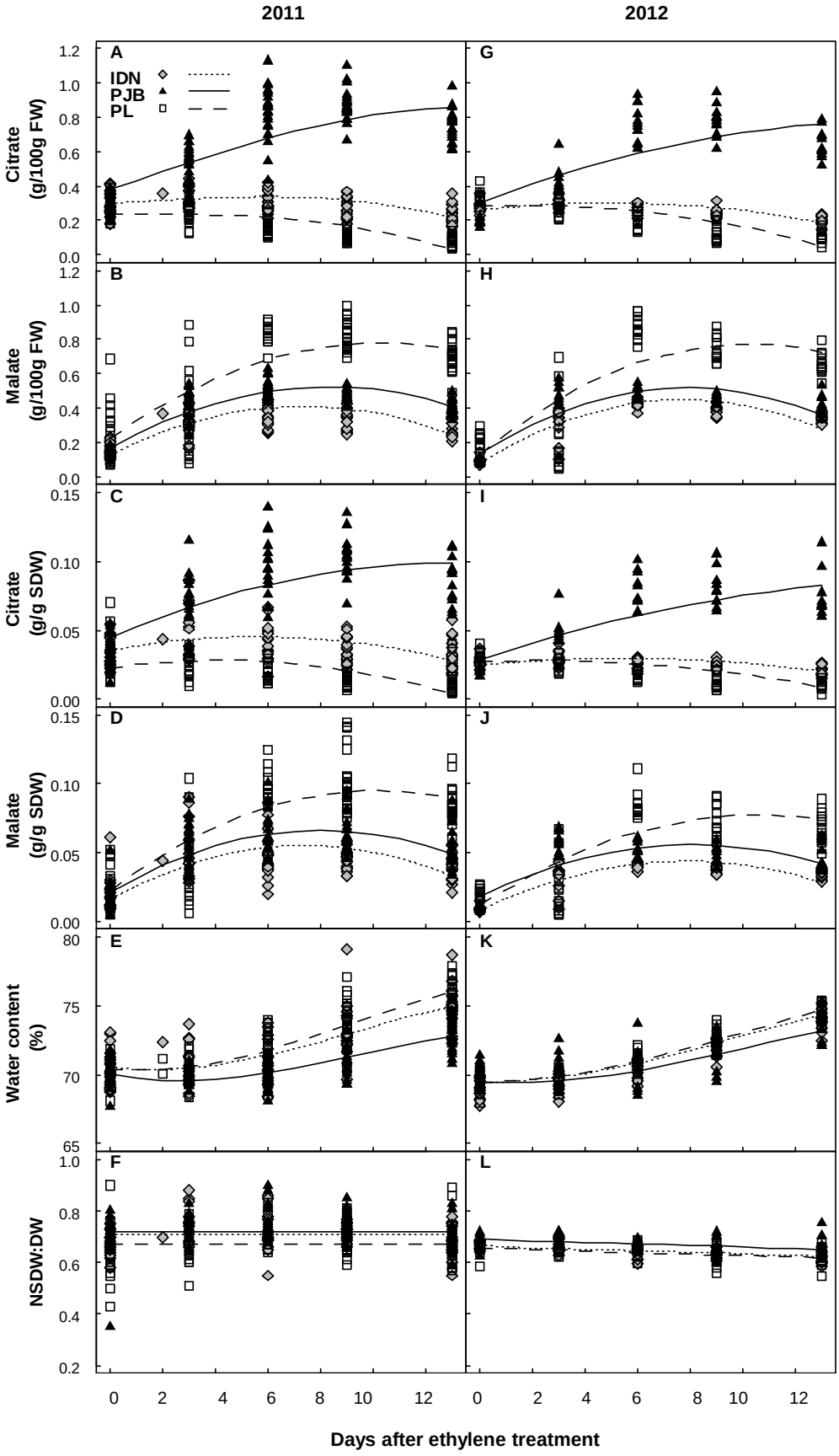

Figure II-2 Variations in pulp citrate concentration (A, G), pulp malate concentration (B, H), ratio of citrate to structural dry weight (C, I), ratio of malate to structural dry weight (D, J), water content (E, K), and ratio of non-structural matter to total dry weight (F, L) during post-harvest ripening of banana in 2011 and 2012 in the three cultivars (IDN, PJB, and PL). Each symbol represents a fruit. Lines are those of the fitted linear mixed model.

Differences in pulp malate concentration among cultivars may be related to differences in tonoplast proton pump activity or to differences in the activities of the enzymes involved in malate metabolism (Etienne *et al.*, 2013b).

The increase in pulp water content during post-harvest ripening in all three cultivars was due to osmotic migration of water from peel to pulp because of the higher concentration of sugar in the latter (John and Marchal, 1995). Dilution by water was lower in PJB and thus widened the gap in the concentration of citrate in the pulp between PJB and the two other cultivars (*Fig. II.2.E and K*). The ratio of non-structural to total dry weight remained constant during ripening and there was little difference among the three cultivars, meaning that this component did not play an important role in the determination of organic acid concentrations (*Fig. II.2.F and L*).

3.3 Fruit age at harvest affected the accumulation of organic acids during post-harvest fruit ripening

The two harvest stages studied corresponded to very contrasted fruit age since at 90% of flowering-to-yellowing time, the IDN, PJB, and PL cultivars had a green life of 9±6, 17±2, and 8±3 days respectively, whereas at 70% of flowering-to-yellowing time, the IDN, PJB, and PL cultivars had a green life of 37±7, 42±14, and 50±10 days respectively (data not shown). In accordance with the patterns of citrate and malate accumulation during fruit growth, fruits harvested later had higher citrate and malate concentrations at harvest (day 0) (*Fig. II.3*). Fruit age at harvest had a significant effect on the ratio of organic acids to structural dry weight, and to a lesser extent on water content and on the ratio of non-structural to total dry weight during ripening (*Table II-2*). Consequently, fruit age at harvest had a significant effect on the concentrations of malate and citrate in the pulp during post harvest ripening. Concerning malate concentrations, there were additional effects of fruit age at harvest x ripening stage interaction, and of fruit age at harvest x cultivar interaction.

The concentration of citrate in the pulp and the ratio of citrate to structural dry weight (data not shown) were higher throughout ripening in fruits harvested at 90% of flowering-to-yellowing time (*Fig. II.3.A, B and C*). These results are in agreement with those obtained by Bugaud et al. (2006) in the Cavendish cultivar. These authors reported that the concentration of citrate in the pulp of ripe fruit increased with fruit age at harvest. Lobit et al. (2003) showed that citrate accumulation in peach pulp can be predicted by a model linked to pulp citrate concentration at harvest, fruit pulp respiration, temperature, and pulp weight. During banana ripening, the temperature remained constant as did the pulp weight, since the banana

fruit was detached from the plant. Pulp weight and pulp respiration were higher in fruits harvested later (data not shown). So this model means that the harvest stage probably affected citrate concentration in banana pulp by impacting both citrate metabolism and dilution during post-harvest ripening.

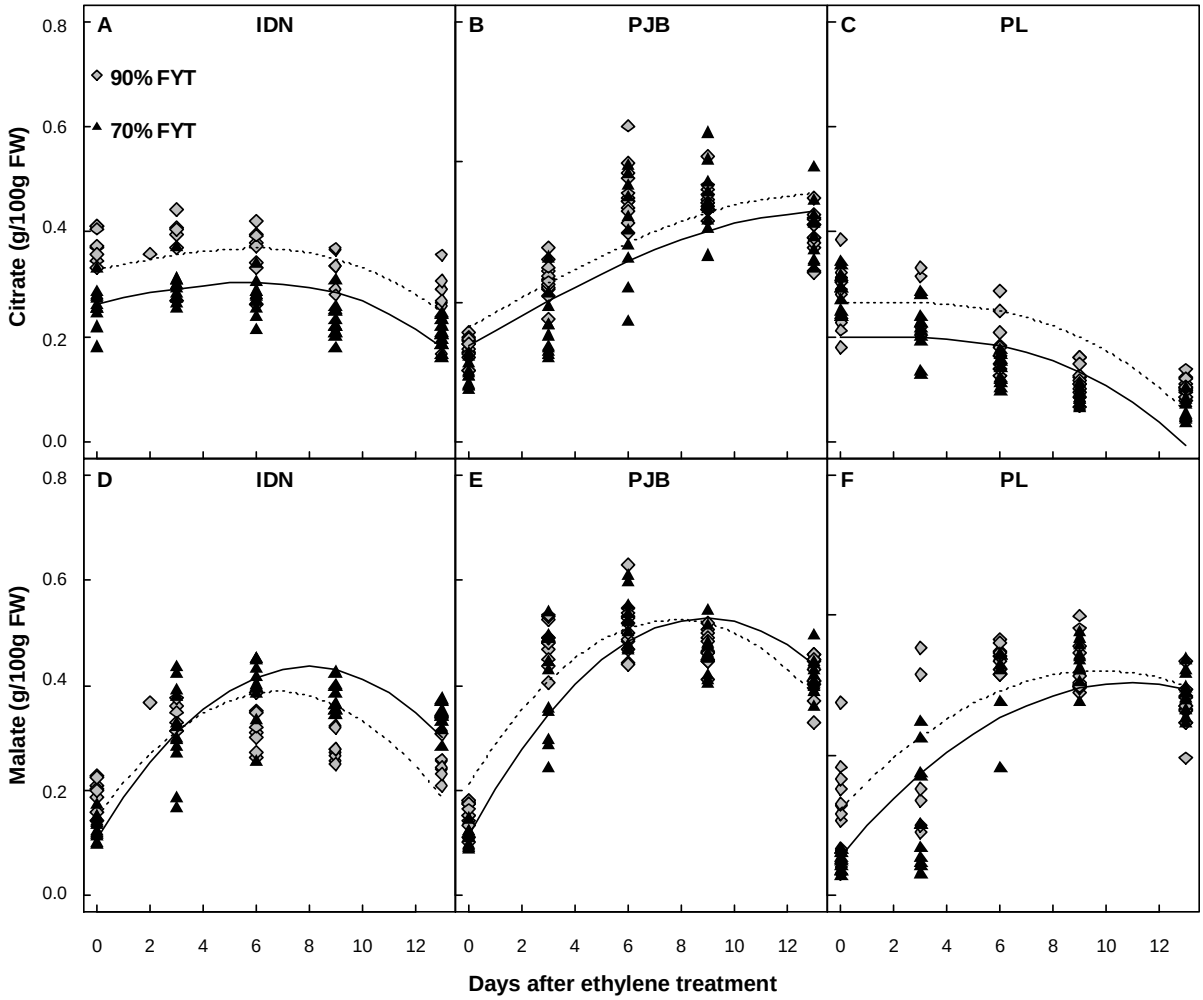

Figure II-3 Variations in pulp citrate (A, B, C) and malate (D, E, F) concentrations during post-harvest ripening of banana in 2011 vs. fruit age at harvest (90% and 70% of flowering-to-yellowing time (FYT)) in the three cultivars (IDN, PJB, and PL). Each symbol represents a fruit. Lines are those of the fitted linear mixed model.

The concentration of malate in the pulp and the ratio of malate to structural dry weight (data not shown) were higher in fruits harvested at 90% of flowering-to-yellowing time until day 3 in the IDN cultivar and until day 9 in the PJB cultivar, after which the trend reversed (*Fig. II.3.D and E*). In the PL cultivar, the malate concentration and the ratio of malate to structural dry weight were higher throughout ripening in fruits harvested at 90% of flowering-to-yellowing time but the effect decreased with time (*Fig. II.3.F*). These results are in agreement with the results obtained by Bugaud et al. (2006) in the cultivar Cavendish.

Table II-2 LMM analysis of banana pulp fresh weight (g), citrate concentration (g.100 g FW^{-1}), malate concentration (g.100 g FW^{-1}), water content (%), non-structural: total dry weight ratio (NSDW: DW), citrate: structural dry weight ratio, and malate: structural dry weight ratio during post-harvest fruit ripening. The factors studied were ripening stage, fruit age at harvest, cultivars and pruning treatment in the 2011 experiment, and ripening stage, cultivars and potassium fertilization treatment in the 2012 experiment.

		F-value [a] and significance [b]						
Year	Factors [c]	Pulp fresh weight	Citrate concentration	Malate concentration	Water content	NSDW : DW	Citrate : SDW	Malate : SDW
2011								
	c	39***	496***	284***	24***	8**	249***	100***
	p	10**	Ns	Ns	12**	Ns	Ns	Ns
	a	98***	23***	11**	Ns	8**	24***	14***
	r	44***	21***	327***	1509***	Ns	13***	227***
	r^2	Ns	45***	241***	161***	Ns	44***	161***
	r^3	Ns	5*	Ns	23***	Ns	Ns	Ns
	p :a	Ns	Ns	Ns	Ns	Ns	Ns	Ns
	p :c	Ns	Ns	Ns	Ns	Ns	Ns	Ns
	p :r	7**	Ns	Ns	5*	Ns	Ns	Ns
	a :c	5**	Ns	15***	4**	Ns	Ns	11***
	a :r	6*	Ns	15***	37***	Ns	Ns	12***
	c :r	5**	212***	50***	56***	Ns	94***	34***
	p :a :c	Ns	Ns	Ns	Ns	Ns	Ns	Ns
	p:a:r	Ns	Ns	Ns	Ns	Ns	Ns	Ns
	a:c:r	Ns	Ns	Ns	Ns	Ns	Ns	Ns
	p:a:c:r	Ns	Ns	Ns	Ns	Ns	Ns	Ns
2012								
	c	37***	252***	73***	Ns	13***	88***	39***
	f	Ns	Ns	Ns	Ns	Ns	Ns	Ns
	r	29***	6*	386***	1533***	43***	10**	343***
	r^2	5*	29***	184***	80***	Ns	25***	130***
	r^3	Ns	Ns	Ns	7**	Ns	Ns	Ns
	c : f	Ns	Ns	Ns	Ns	Ns	Ns	Ns
	c : r	Ns	104***	51***	16***	Ns	74***	48***
	f : r	Ns	Ns	Ns	Ns	Ns	Ns	Ns
	c:f : r	Ns	Ns	Ns	Ns	Ns	Ns	Ns

[a] The F-value is given only for the factors retained from the optimal model.

[b] *** p-value < 0.001; ** p-value < 0.01; * p-value<0.05 ; Ns : not significant.

[c] Codes for factors: c=cultivar; p=pruning treatment; a=fruit age at harvest; r=ripening stage; f=potassium fertilization treatment.

These authors reported that the concentration of malate in the pulp of ripe fruit decreased with fruit age at harvest. The higher concentration of malate in late harvested fruits during the first days of ripening may be due to more favorable vacuolar storage conditions leading to a higher accumulation of malate in the vacuole. As we found no differences in pulp pH between the two harvest stages in the three cultivars (data not shown), we suggest that differences in $\Delta\psi$ may be responsible for the differences in malate accumulation. At the end of ripening, late harvested fruits had a lower concentration of malate, which may be the consequence of a higher rate of malate leakage across the tonoplast.

3.4 Fruit load affected fruit growth but had no effect on the accumulation of organic acids

As expected, low fruit load significantly increased the pulp fresh weight during fruit growth in all three cultivars (Bugaud *et al.*, 2012; Jullien *et al.*, 2001b) (*Table II-1, Fig. II.4.A, B and C*). The same result was observed during post harvest ripening (*Table II-2*). The pruning treatment had no significant effect on pulp citrate and malate concentrations in the pulp during fruit growth and ripening in all three cultivars (*Table II-1 and II-2*). Considering the different components of Equation 1, it appeared that only the water content of the pulp was significantly reduced by the pruning treatment during fruit growth and ripening. However, the effect was very limited since the pruning treatment only decreased pulp water content by 4% on average at the end of fruit growth and by 3% on average during ripening (data not shown) and consequently had no impact on the concentration of organic acids in the pulp. Several agronomic studies reported an effect of the leaf: fruit ratio on the malate and citrate concentrations of pulp fruits, probably linked to modifications in fruit respiration. During mango growth, a high leaf: fruit ratio decreased malate and citrate concentrations in the pulp (Léchaudel *et al.*, 2005b), whereas it had no effect during post-harvest ripening (Joas et al., 2012). Lechaudel et al. (2005b) showed that a high leaf: fruit ratio decreased pulp water content, had no effect on the ratio of non-structural to total dry weight, and reduced the ratio of citrate and malate to structural dry weight. In peach, a high leaf: fruit ratio increased pulp citrate concentration early in fruit development, but decreased it near maturity. The opposite effects were observed for malate (Souty et al., 1999; Wu et al., 2002). In the present study, the fruit load was only increased by a factor of 2.5 whereas in the studies mentioned above it was increased by at least a factor of 4, which could explain why in our case, the pruning treatment had no effect on citrate and malate concentrations in banana pulp. However, a physiological explanation is also possible. In fruit containing a lot of starch, like banana at the green stage,

it is likely that organic acids play an important role as osmoticum since very few soluble sugars are stored in the vacuole. Thus, we hypothesize that the accumulation of organic acids in the vacuole is tightly linked to water accumulation, meaning that their concentration cannot vary significantly with pulp fresh weight.

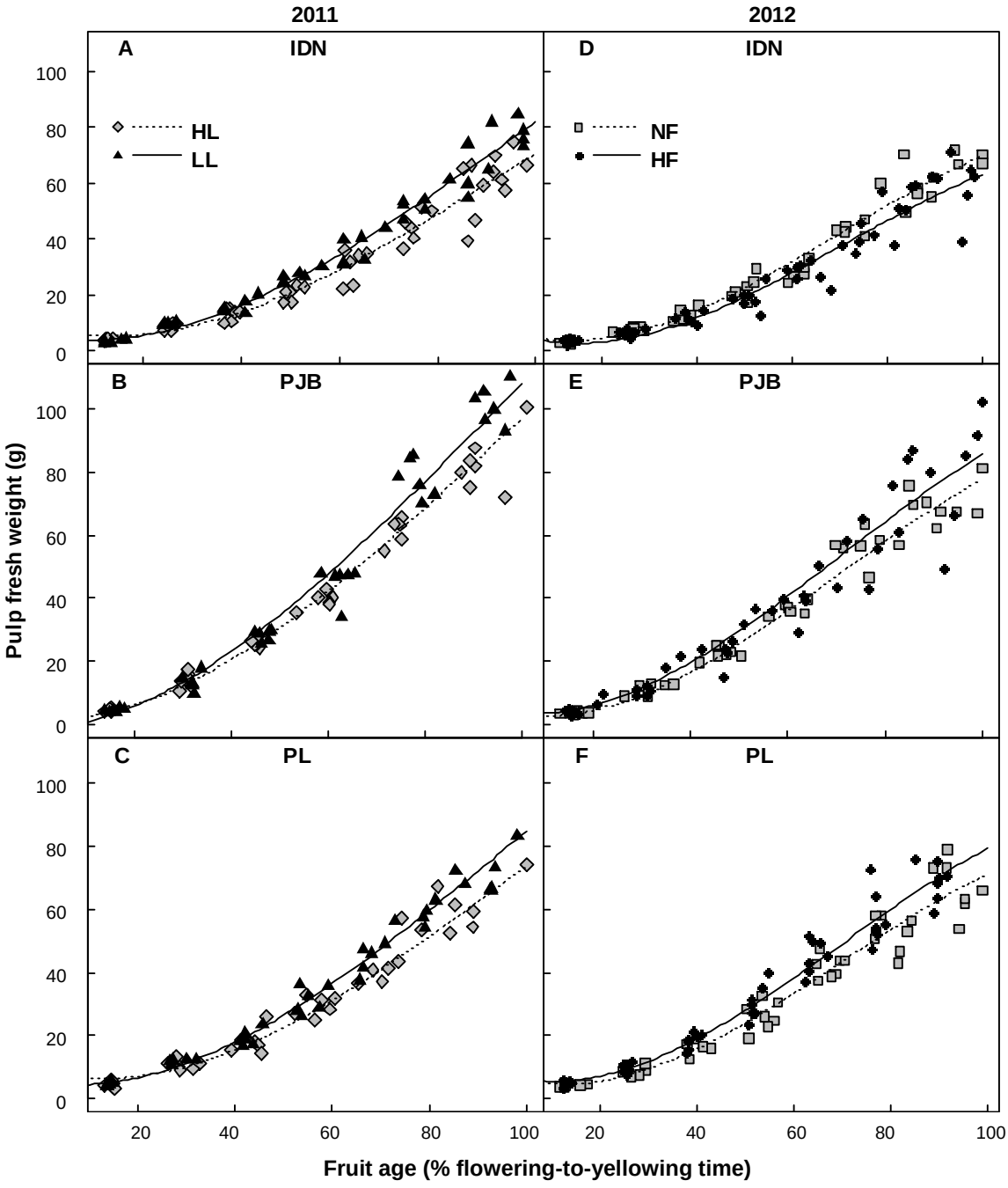

Figure II-4 Seasonal variations in pulp fresh weight in the three cultivars (IDN, PJB, and PL) vs. fruit load (LL=low fruit load; HL=high fruit load) during the 2011 growing season (A, B, C), and potassium fertilization (HF=high level of potassium fertilization; NF=no potassium fertilization) during the 2012 growing season (D, E, F). Each symbol represents a fruit. Lines are those of the fitted linear mixed model.

3.5 Potassium fertilization affected fruit growth but had no effect on the accumulation of organic acids

The K concentrations found in the soils sampled in the different blocks were in the low range of values found in other soils in Martinique (Bugaud *et al.*, 2009) (*Table II-3*). Soils in the blocks with the high potassium fertilization treatment had a higher K concentration than soils in the blocks with no potassium fertilization, which had an impact on banana plant nutrition since leaves from plants in the blocks with high potassium fertilization had higher K concentrations than leaves from plants in the blocks with no potassium fertilization (*Table II-4*). The concentrations of K in the leaves of all three cultivars were in the range found by Moreira and al. (1986) in 42 cultivars of dessert bananas.

There was a significant effect of the interaction between potassium fertilization, cultivar, and fruit age on pulp fresh weight during fruit growth (*Table II-1*). Thus, fruits from PJB and PL cultivars grown with high potassium fertilization treatment had higher pulp fresh weight than fruits from the same cultivars grown with no potassium fertilization, whereas the opposite was the case for fruits from the IDN cultivar (*Fig. II.4.D, E and F*). However, the effects were low since, at the end of fruit growth, potassium fertilization only decreased pulp fresh weight by 7% in the IDN cultivar, and increased pulp fresh weight by 16% in the PJB and by 10% in the PL cultivars. As a consequence, in the fruits from plots with high potassium fertilization and no potassium fertilization harvested at 75% of flowering-to-yellowing time there was no significant difference in pulp fresh weight in the three cultivars (*Table II-2*). The positive effect of potassium supply on the pulp fresh weight in the PL and PJB cultivars is in agreement with several studies on fruits (Ashraf et al., 2010; Hunsche et al., 2003; Lester et al., 2010; Quaggio et al., 2011). Low potassium supply is known to decrease the translocation of carbohydrates from leaves to banana fruit, and to reduce their conversion into starch (Martin-Prével, 1973). Concerning the negative effect of potassium supply on the pulp fresh weight in the IDN cultivar, the decrease was very small, and could simply be due to a sampling artifact. IDN banana plants may be less sensitive to potassium shortage than PL and PJB plants, and IDN fruits may be able to reach their full potential growth using the potassium already present in the soil.

During fruit growth, among the three components that determine the concentrations of organic acids in banana pulp, only the ratio of organic acids to structural dry weight was significantly affected by potassium fertilization and by its interaction with the cultivar (*Table II-1*). In the IDN cultivar, fruit from plots with high potassium fertilization had a lower ratio

of organic acids to structural dry weight than fruit from plots with no potassium fertilization, whereas there was no difference in fruits from the PJB and PL cultivars (*Fig. II.5*).

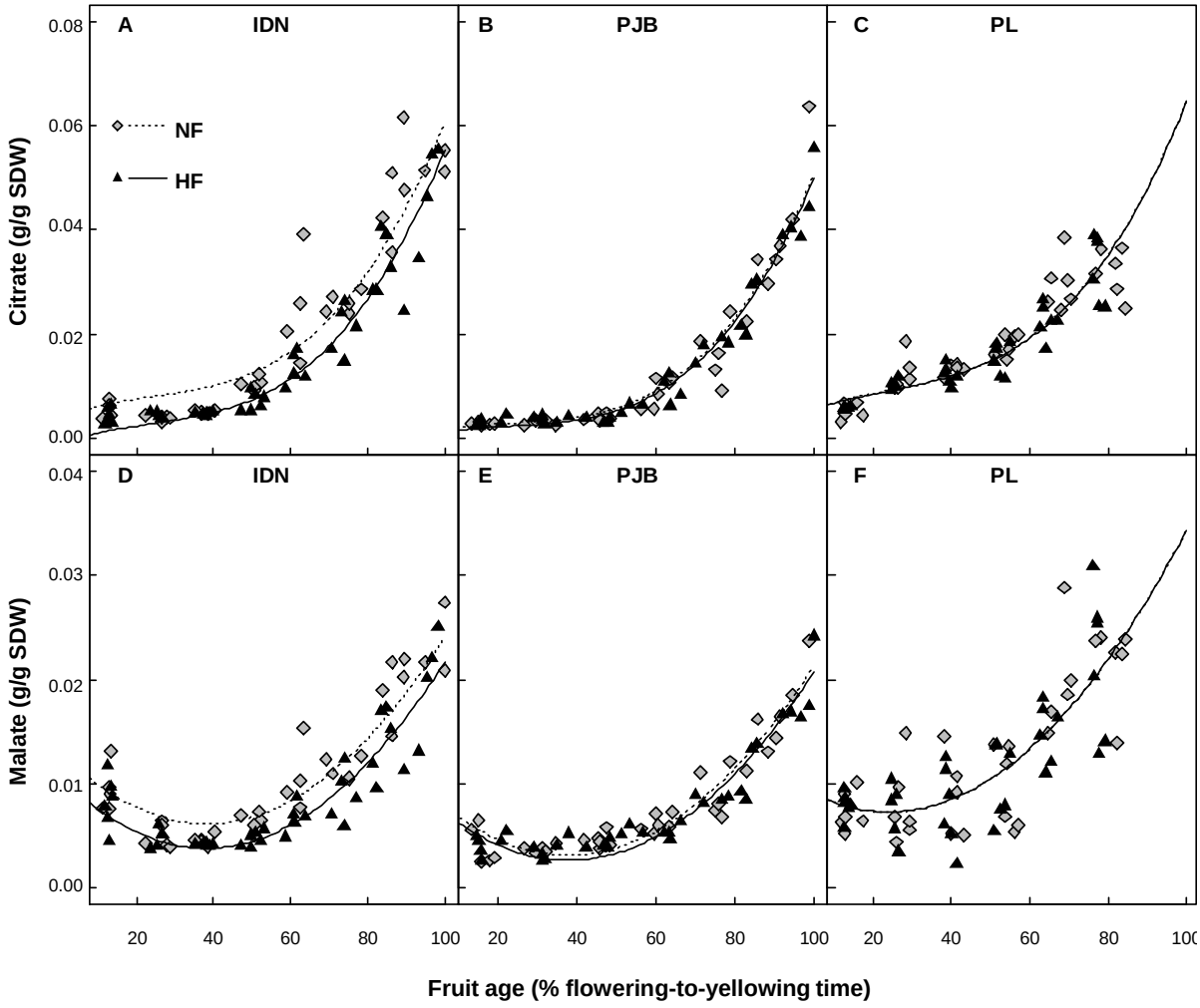

Figure II-5 Seasonal variations in the ratios of citrate content to structural dry weight (A, B, C) and of malate content to structural dry weight (D, E, F) in the three cultivars (IDN, PJB, and PL) vs. potassium fertilization (HF=high level of potassium fertilization; NF=no potassium fertilization) during the 2012 growing season. Each symbol represents a fruit. Lines are those of the fitted linear mixed model.

However, the effects observed in the IDN cultivar were very small and consequently did not affect the concentrations of organic acids in the pulp. Fruits from the PL cultivar grown with the high potassium fertilization treatment had a significantly higher concentration of K in the pulp (16%) than fruits from the PL cultivar grown with no potassium treatment, and the same trend was observed in the PJB cultivar even if the difference was not significant (*Table II-4*). Therefore, it appears that in the PL and PJB cultivars, potassium fertilization slightly increased the accumulation of K in fruit pulp but had no effect on the concentration of organic acids. As mentioned previously, K and organic acids are the main osmoticums in green banana fruit and this possibly explains why their concentrations cannot vary significantly with potassium supply since their concentrations are tightly linked to water accumulation. In

contrast, the concentration of K in the pulp of fruits grown with high potassium fertilization or no potassium fertilization were the same in the IDN cultivar (*Table II-4*), meaning that potassium fertilization had no effect on K accumulation in the fruit. Thus, the decrease in the ratio of organic acids to structural dry weight in IDN fruits grown with high potassium fertilization can probably not be attributed to potassium fertilization and is consequently difficult to explain.

During post-harvest ripening, potassium fertilization had no effect on the concentration of organic acids in the pulp, or on the components of Equation 1, which is in accordance with the results observed during fruit growth (*Table II-2*). These results are in contradiction with those of studies by Ramesh Kumar and Kumar (2007), and Vadivel and Shanmugavelu (1978), who reported a decrease in titratable acidity in ripe banana fruit grown with a high potassium supply. These contradictory results are difficult to explain since the same levels of potassium fertilization were applied in the study of Vadivel and in ours, so further studies are needed to clarify this issue.

Table II-3 Soil chemical properties of the blocks used in the 2012 experiment. Values are the means of the two sampled dates ±s.d, except for the blocks HF of cultivar PJB and for the calcium content of blocks NF for cultivar IDN for which there was only one sample date.

Cultivar	Treatment [a]	pH	Cation-exchange capacity	K	Ca	Mg
				($mEq.100g^{-1}$)		
IDN	HF	5.4±0.3	41.9±9.2	0.96±0.2	16.2±0.6	7.18±1.2
	NF	5.4±0.2	44.1±5.3	0.44±0.1	13.1	6.46±0.8
PJB	HF	5.7	49.0	0.87	16.1	6.65
	NF	5.4	35.6	0.48±0.1	14.0	5.96
PL	HF	5.5±0.3	35.2±3.5	0.75±0.1	16.6±0.3	7.58±1.2
	NF	5.5±0.1	44.9±1.3	0.40±0.0	16.0±0.8	7.24±1.2

[a] Code for treatment: HF= high potassium fertilization; NF=no potassium fertilization

Table II-4 Soluble mineral content of leaves (g.100 g DW^{-1}) and fruit pulp (g.100 g FW^{-1}) for the three cultivars (IDN, PJB, and PL) and the two treatments, high potassium fertilization (HF) and no potassium fertilization (NF) in the 2012 experiment. For leaves, values are the mean of two sampling dates ±s.d. For fruit pulp, values are the mean of six fruits at harvest (green fruit) ±s.d. For fruit pulp, letters 'a–b' indicate results of Tukey's HSD test at p = 0.05 for a given mineral element.

Organ	Cultivar	Treatment [a]	K	Ca	Mg	P	Cl
Leave							
	IDN	HF	2.86±0.4	1.52±0.6	0.38±0.0	0.17±0.1	0.97±0.2
		NF	2.38±0.3	1.09±0.1	0.35±0.1	0.19±0.0	0.87±0.2
	PJB	HF	2.76±0.0	1.74±0.7	0.29±0.0	0.18±0.1	1.01±0.4
		NF	1.96±0.2	1.37±0.1	0.40±0.1	0.18±0.0	0.95±0.1
	PL	HF	2.59±0.4	1.75±0.6	0.29±0.0	0.20±0.0	1.19±0.3
		NF	1.84±0.2	1.56±0.1	0.39±0.2	0.18±0.0	1.05±0.2
Pulp fruit at harvest							
	IDN	HF	0.30±0.02 b	0.03±0.02 a	0.02±0.01 a	0.02±0.0 a	-
		NF	0.30±0.01 b	0.02±0.02 a	0.02±0.01 a	0.02±0.0 a	-
	PJB	HF	0.32±0.03 ab	0.02±0.01 a	0.02±0.01 a	0.01±0.0 b	-
		NF	0.28±0.03 b	0.02±0.02 a	0.02±0.01 a	0.01±0.0 b	-
	PL	HF	0.35±0.03 a	0.03±0.01 a	0.02±0.01 a	0.01±0.0 b	-
		NF	0.30±0.01 b	0.02±0.01 a	0.03±0.00 a	0.01±0.0 b	-

[a] Code for treatment: HF= high potassium fertilization; NF=no potassium fertilization

4 Conclusions

The concentrations of citrate and malate in the pulp of banana fruits were significantly affected by genotype and fruit age, but not by cultural practices. However, it is important to note that these results were obtained under particular soil and climatic conditions, and now need to be confirmed by further studies in other sites. Nevertheless, the results of this study strongly suggest that the concentration of organic acids in banana pulp is mainly determined by genetic factors. Consequently, banana pulp acidity probably has high heritability and may be an interesting trait to target in breeding programs aimed at improving the organoleptic quality of new cultivars.

Chapitre III Modélisation écophysiologique de l'acidité de la banane (*Musa* sp. AA) en pré et post récolte

Dans ce chapitre, des modèles écophysiologiques permettant de prédire différents critères d'acidité du fruit (pH, acidité titrable, concentrations en malate et citrate de la pulpe) sont développés afin de comprendre les processus qui pilotent l'acidité de la banane et de proposer des pistes sur les origines de la variabilité observée entre génotypes (c.f. Chapitre II). L'analyse de sensibilité de ces modèles a permis de simuler l'effet de certains facteurs agro-environnementaux sur l'acidité de la banane. L'étude porte à la fois sur les phases pré et post récolte afin de voir quelles pourraient être les origines physiologiques des différences d'acidité observées entre ces deux phases (c.f. Chapitre II).

Un premier modèle utilisé (Lobit *et al.*, 2002) prédit le **pH et l'acidité titrable** de la pulpe, deux paramètres importants de la qualité organoleptique de la banane (Bugaud *et al.*, 2013), à travers la représentation des équilibres acido-basiques de la vacuole.

Pour prédire la concentration en **malate** dans la pulpe de banane, nous nous sommes basés sur l'une des conclusions de la synthèse bibliographique (c.f. chapitre I) qui est que l'accumulation du malate dans le fruit est pilotée par les conditions de son stockage dans la vacuole. Le modèle d'accumulation du malate présenté est donc basé sur une représentation simplifiée du mécanisme de transport du malate dans la vacuole et adapté du modèle de Lobit et al. (2006). Ce modèle intègre le modèle de prédiction du pH.

Enfin, pour prédire la concentration en **citrate** dans la pulpe de banane, nous nous sommes basés sur l'une des conclusions de la synthèse bibliographique (c.f. chapitre I) qui est que l'accumulation du citrate dans le fruit est pilotée par le fonctionnement du cycle de Krebs dans la mitochondrie. Le modèle d'accumulation du citrate présenté est donc basé sur une représentation simplifiée de ce cycle.

1 Modélisation du pH et de l'acidité titrable de la pulpe par un modèle d'équilibres acido-basiques

Objectifs

Dans cette partie, la relation entre la composition (acides et minéraux solubles) et l'acidité de la pulpe (mesurée par le pH et l'acidité titrable) a été étudiée en adaptant le modèle de Lobit et al. (2002) développé sur la pêche. Les évolutions du pH et de l'acidité titrable chez trois génotypes de banane dessert contrastés en acidité ont pu ainsi être prédites en modélisant les équilibres acido-basiques présents dans la vacuole. La contribution des différents composés pris en compte par le modèle à l'acidité de la banane a été évaluée par une analyse de sensibilité à différents stade de développement du fruit. Cette partie a fait l'objet d'une publication dans **Scientia Horticulturae** sous la forme d'un article intitulé «A model approach revealed the relationship between banana pulp acidity and composition during growth and post harvest ripening ».

Principaux résultats

- Les prédictions du pH et de l'acidité titrable sont meilleures pendant la maturation post récolte que pendant la croissance.
- Durant la croissance de la banane, les principaux déterminants de l'acidité sont le citrate, le malate, l'oxalate et le potassium.
- Durant la maturation post récolte de la banane, les principaux déterminants de l'acidité sont le citrate, le malate et le potassium.

A model approach revealed the relationship between banana pulp acidity and composition during growth and post harvest ripening

A. Etienne[1], M. Génard[2], D. Bancel[2], S. Benoit[1], C. Bugaud[1]

[1] Centre de Coopération International en Recherche Agronomique pour le Développement (CIRAD), UMR QUALISUD, Pôle de Recherche Agronomique de Martinique, BP 214, 97 285 Lamentin Cedex 2, France

[2] INRA, UR 1115 Plantes et Systèmes de Cultures Horticoles, F-84914 Avignon, France

Abstract

Titratable acidity and pH are important chemical traits for the organoleptic quality of banana since they are related to the perception of sourness and sweetness. Banana fruit has the particularity of having separate growth and ripening stages, during which pulp acidity changes. A modeling approach was used to understand the mechanisms involved in changes in acidity during pulp growth and post harvest ripening. Changes in pH and titratable acidity were modeled by solving a set of equations representing acid/base reactions. The models were built using data from growth and post harvest ripening of three dessert banana cultivars with contrasting acidity. For each model, calculated values were compared to observed values. These models allowed the prediction of pH (R^2=0.34; RMSE=0.75, biais=0.05) and of titratable acidity (R^2=0.81, RMSE=2.05, biais=-1.44) during fruit growth and post harvest ripening. The sensitivity analyses showed that among acids, malic, citric and oxalic acids are the main contributors to banana pulp acidity, and that among soluble minerals, potassium also plays an important role. Studying the factors that affect the accumulation of organic acids (citric, malic, and oxalic acids) and potassium in banana pulp could be a relevant area of research with the objective of modifying banana fruit acidity.

1.1 Introduction

Fruit acidity is a topic of primary importance in improving fruit quality since it influences the perception of both sourness and sweetness (Bugaud *et al.*, 2011; Esti *et al.*, 2002). These two attributes are major drivers of consumer preferences for fruit (Lyon *et al.*, 1993), and are thus important traits to consider in breeding programs. Understanding the elaboration of fruit acidity is also important because acidity controls numerous enzyme activities (Madshus, 1988).

Fruit acidity is commonly measured using two chemical parameters: titratable acidity (TA) i.e. the amount of weakly bound hydrogen ions that can be released from the acids, and pH, the activity of free hydrogen ions. Fruit acidity is due to the acidity of the vacuole which represents about 90% of the volume of most mature fruit cells (Etxeberria *et al.*, 2012). The acidity of the vacuole is the result of its ionic composition, mainly organic acids and mineral cations that determine the vacuolar pH and TA (Etienne *et al.*, 2013b). Banana pulp contains three major organic acids, malic acid, citric acid, and oxalic acid, whose concentrations undergo marked changes during growth and ripening (John and Marchal, 1995; Jullien *et al.*, 2008) and phosphoric acid (Bugaud *et al.*, 2013). Banana pulp contains soluble minerals, mainly potassium (K), and to a lesser extent magnesium (Mg), calcium (Ca), and chloride (Cl) (John and Marchal, 1995). During post harvest ripening, mineral content can still change due to migration between the peel and the pulp (Izonfuo and Omuaru, 1988).

There are considerable differences in pH and TA among dessert banana cultivars and among post-harvest ripening stages (Bugaud et al., 2013; Chacón *et al.*, 1987), and the origins of these differences remain unclear. Quantifying the relations between pulp acidity and pulp ionic composition using a modeling approach, would advance our understanding of the determinants of banana acidity. Models of pH and TA predictions have been developed for peach (Lobit *et al.*, 2002) and proved to be powerful tools to understand the mechanisms underlying changes in acidity during peach development. The objective of the present work was to apply and validate these models on banana fruit, in which other ionic species than those found in peach need to be taken into account, and to throw light on the determinants of the changes in pH and TA that occur during the life of the banana pulp, i.e. from growth on the plant through post harvest ripening.

1.2 Materials and methods

1.2.1 Model Development

1.2.1.1 pH model

The model used for pH prediction was adapted from Lobit et al. (2002). Banana pulp can be considered as a concentrated aqueous solution of weak acids, mainly malic, citric, oxalic and phosphoric acids, and mineral cations, mainly potassium, magnesium, calcium and chloride. Other acids can be found in banana pulp but were not taken into account in the present study. Weak acids are partly in free form and partly dissociated to form salts with monovalent cations. Proton exchange reactions occur between acids and bases until equilibrium state is reached, which determines the pH and the concentrations of all ionic species. So, to predict the pH of banana pulp solution, the concentrations of the different chemical forms of the weak acids need to be calculated.

Acid/base equilibrium

The equilibrium state of a solution containing several acid/conjugate base pairs and cations in known amounts can be computed by solving a system consisting in the following sets of equations:

- *Equations of conservation*

The total amount of an acid is equal to the sum of the concentrations of all the ionic species formed by its dissociation:

Citric acid: $[Cit] = [H_3Cit] + [H_2Cit^-] + [HCit^{2-}] + [Cit^{3-}]$ (1a)

Malic acid: $[Mal] = [H_2Mal] + [HMal^-] + [Mal^{2-}]$ (1b)

Oxalic acid : $[Oxa] = [H_2Oxa] + [HOxa^-] + [Oxa^{2-}]$ (1c)

Phosphoric acid: $[PO_4] = [H_3PO_4] + [H_2PO_4^-] + [HPO_4^{2-}] + [PO_4^{3-}]$ (1d)

- *Equations of dissociation*

The dissociation reactions of the weak acids considered in the model are the following:

Citric acid: $H_3Cit \leftrightarrow H_2Cit + H^+ \leftrightarrow HCit^{2-} + 2H^+ \leftrightarrow Cit^{3-} + 3H^+$ (2a)

(pKa_1~3.10, pKa_2~4.70, pKa_3~6.40)

Malic acid: $H_2Mal \leftrightarrow HMal^- + H^+ \leftrightarrow Mal^{2-} + 2H^+$ (2b)

(pKa_1~3.40, pKa_2~5.10)

Oxalic acid: $H_2Oxa \leftrightarrow HOxa^- + H^+ \leftrightarrow Oxa^{2-} + 2H^+$ (2c)

(pKa_1~1.23, pKa_2~4.19)

Phosphoric acid: $H_3PO_4 \leftrightarrow H_2PO_4 + H^+ \leftrightarrow HPO_4^{2-} + 2H^+ \leftrightarrow PO_4^{3-} + 3H^+$ (2d)

(pKa_1~2.12, pKa_2~7.21, pKa_3~12.67)

If HA/A^- is an acid/base pair characterized by an acidity constant K_a, the equilibrium between the concentrations of the protonated and the dissociated form can be written as a function of pH and of the activity of the ionic species involved in the reaction: $K_a = (A^-)h/(HA)$, where (HA) and (A^-) are the activities of the conjugated acid and base, respectively; $h=(H^+)=10^{-pH}$ is the hydrogen ion activity, and $K_a=10^{-pKa}$ is the acidity constant.

In diluted solutions (concentrations below 10^{-2} mol.L^{-1}), activities can be considered equal to concentrations. In more concentrated solutions like fruit juice, they are less than concentrations: $(HA)=a_{HA}[HA]$ and $(A^-)=a_{A^-}[A^-]$, where [HA] and [A^-] are the concentrations of the acid and its corresponding base respectively, and a_{HA} and a_{A^-} are the activity coefficients, which depend on the ionic composition of the solution. So, the dissociation equilibrium can be written by introducing an apparent acidity constant: $[A^-]h/[HA] = Ka'$, where K'_a is the apparent constant of acidity defined as:

$$K'_a = K_a a_{HA}/a_{A^-} \quad (3)$$

- *Activity coefficient of ions*

The activity coefficients of each acid and conjugated base have to be computed to estimate the apparent acidity constants. In a solution that contains n ionic species S_i with electric charges z_i and at concentrations $C_{i1<i<n}$, an ion S with a charge z has an activity coefficient a_s that depends on the ionic strength (μ) of the medium. The ionic strength of the solution is the total concentration in ionic species, given by the following equation:

$$\mu = 1/2(\sum_i z_i^2 C_i) \quad (4)$$

In the case of an aqueous solution with a ionic strength of up to 1 M, a_s can be calculated by the equation of Davies (1962):

$$\log(a_s) = -0.509z^2((\sqrt{\mu}/(1+\sqrt{\mu})) - 0.3\mu) \quad (5)$$

- *Ionic balance*

The neutrality of the electrical solution in pulp cell implies that the algebraic sum of cationic and anionic charged must be null:

$$[H_2Cit^-] + 2*[HCit^{2-}] + 3*[Cit^{3-}] \quad (6)$$
$$+ [HOxa^-] + 2*[Oxa^{2-}]$$
$$+ [Hmal^-] + 2*[Mal^{2-}]$$
$$+ [H_2PO_4^-] + 2*[HPO_4^{2-}] + 3*[PO_4^{3-}] + [OH^-]$$

$+ [Cl^-] - [H^+]-[K^+]-2*[Mg^{2+}]-2*[Ca^{2+}] = 0$

$[OH^-]$ is expressed as a function of the pH: $[OH^-] = 10^{(pH-14)}$

Algorithm of the pH model

Combinations of equations 1 and 2 give the following set of equations that all depend on the apparent acidity constants and the pH:

$$[Cit^{3-}] = (K'_{cit1}K'_{cit2}K'_{cit3}/(h^3 + h^2K'_{cit1} + hK'_{cit1}K'_{cit2} + K'_{cit1}K'_{cit2}K'_{cit3}))[Cit] \quad (7a)$$

$$[HCit^{2-}] = (hK'_{cit1}K'_{cit2}/(h^3 + h^2K'_{cit1} + hK'_{cit1}K'_{cit2} + K'_{cit1}K'_{cit2}K'_{cit3}))[Cit] \quad (7b)$$

$$[H_2Cit^-] = (h^2K'_{cit1}/(h^3 + h^2K'_{cit1} + hK'_{cit1}K'_{cit2} + K'_{cit1}K'_{cit2}K'_{cit3}))[Cit] \quad (7c)$$

$$[H_3Cit] = (h^3/(h^3 + h^2K'_{cit1} + hK'_{cit1}K'_{cit2} + K'_{cit1}K'_{cit2}K'_{cit3}))[Cit] \quad (7d)$$

$$[Mal^{2-}] = (K'_{mal1}K'_{mal2}/(h^2 + hK'_{mal1} + K'_{mal1}K'_{mal2}))[Mal] \quad (7e)$$

$$[HMal^-] = (hK'_{mal1}/(h^2 + hK'_{mal1} + K'_{mal1}K'_{mal2}))[Mal] \quad (7f)$$

$$[H_2Mal] = (h^2/(h^2 + hK'_{mal1} + K'_{mal1}K'_{mal2}))[Mal] \quad (7g)$$

$$[Oxa^{2-}] = (K'_{oxa1}K'_{oxa2}/(h^2 + hK'_{oxa1} + K'_{oxa1}K'_{oxa2}))[Oxa] \quad (7h)$$

$$[HOxa^-] = (hK'_{oxa1}/(h^2 + hK'_{oxa1} + K'_{oxa1}K'_{oxa2}))[Oxa] \quad (7i)$$

$$[H_2Oxa] = (h^2/(h^2 + hK'_{oxa1} + K'_{oxa1}K'_{oxa2}))[Oxa] \quad (7j)$$

$$[PO_4^{3-}] = (K'_{pho1}K'_{pho2}K'_{pho3}/(h^3 + h^2K'_{pho1} + hK'_{pho1}K'_{pho2} + K'_{pho1}K'_{pho2}K'_{hpo3}))[PO_4] \quad (7k)$$

$$[HPO_4^{2-}] = (hK'_{pho1}K'_{pho2}/(h^3 + h^2K'_{pho1} + hK'_{pho1}K'_{pho2} + K'_{pho1}K'_{pho2}K'_{hpo3}))[PO_4] \quad (7l)$$

$$[H_2PO_4^-] = (h^2K'_{pho1}/(h^3 + h^2K'_{pho1} + hK'_{pho1}K'_{pho2} + K'_{pho1}K'_{pho2}K'_{hpo3}))[PO_4] \quad (7m)$$

$$[H_3PO_4] = (h^3/(h^3 + h^2K'_{pho1} + hK'_{pho1}K'_{pho2} + K'_{pho1}K'_{pho2}K'_{hpo3}))[PO_4] \quad (7n)$$

So, combining equations 3, 4, 5, 6 and 7, it is possible to calculate the ionic strength (μ) and the pH of the pulp by solving a system of two equations with two unknowns (pH and μ).

$$F_1(\mu, pH) = \sum Anions - \sum Cations = 0$$

$$F_2(\mu, pH) = \mu - 1/2 \sum z_i^2 [A_i] = 0$$

1.2.1.2 TA model

The TA of banana pulp was predicted by computing the amount of base (NaOH) needed to bring its pH to 8.1 (usual norm). Knowing the total concentrations of each acid and cation,

and the pH of the pulp (equal to 8.1), it is possible to calculate the ionic strength (μ) and the TA of the pulp by solving a system of two equations with two unknowns (NaOH and μ):

$$F_1(\mu, NaOH) = \sum Anions - \sum Cations = 0$$

$$F_2(\mu, NaOH) = \mu - 1/2 \sum z_i^2 [A_i] = 0$$

1.2.1.3 Model solving

The input data of the models were the acid and cation concentrations of the banana pulp, and the acidity constants of the malic, citric, phosphoric and oxalic acid. The models were computed using R software (R Development Core Team, http://www.r-project.org). For each sampling date, the system was solved to calculate the pH of the pulp sample (pH model) or the amount of NaOH added to reach a pH of 8.1 (TA model), using the "nleqslv" function of the R software (http://cran.r-project.org/web/packages/nleqslv/index.html).

1.2.2 Model Validation

1.2.2.1 Field experiment

Three dessert banana cultivars (Musa spp.) diploids AA, with different predominant organic acid at the eating stage were used in this study: Indonesia 110 (IDN 110), Pisang Jari Buaya (JB), and Pisang Lilin (PL). All bananas were grown at the *Pôle de Recherche Agroenvironnementale de la Martinique* (PRAM, Martinique, French West Indies; latitude 14°37N, longitude 60°58W, altitude 16 m) on continental alluvial soil.

Plants received 12 g of nitrogen, 1.7 g of phosphorus, and 20 g of potassium at 4-week intervals during fruit growth. Irrigation was adjusted to the amount of rainfall to supply at least 5 mm of water per day. The other cultural practices (desuckering, bunch management) were similar to those used in standard Cavendish production. During the period of bunch growth (March–November 2010) the mean daily temperature was 27 ± 1.2 °C. Non-systemic fungicide was applied during the experiment to control foliar diseases. For each cultivar, plants were tagged at inflorescence emergence. Bunches were not covered.

1.2.2.2 Preparation of samples

Monitoring fruit growth

Six bunches corresponding to six replicates of each cultivar were selected. One fruit located in the internal row of the second proximal hand was collected for analyses every 15 days.

Sampling before natural ripening on standing plants, i.e. when the first yellow finger appears, determined the end of monitoring.

Monitoring post-harvest fruit ripening

For each cultivar, six bunches were harvested between May and November 2011. For each cultivar, the harvest stage was calculated to be 70% of the flowering-to-yellowing time of the bunch on the tree. The second proximal banana hand per bunch was rinsed and dipped in fungicide (bitertanol, 200 mg L^{-1}) for 1 min. The fruits were placed in a plastic bag with 20 µm respiration holes and stored in boxes for 6 days at 18 °C. The fruits were then stored in a room at 18 °C and underwent ethylene treatment (1 mL L^{-1} for 24 h) to trigger the ripening process. After 24 h the room was ventilated and bananas were maintained at 18 °C for 13 days. A banana fruit was sampled at day 0 (before ethylene treatment), 3, 6, 9 and 13.

1.2.2.3 Chemical analyses

Pulp of the sampled fruit was freeze dried and mixed to obtain a dry powder. TA and pH were measured after dilution of 1 g of dry powdered banana pulp in 30 mL of distilled water. TA was determined by titration with NaOH (0.1N) at pH 8.1 and expressed in milli-equivalents of acid (mEq) per 100 g of fresh weight (FW). Two analytical replicates per sample were performed for each analysis. Citric acid and malic acid were extracted with a mixture of solvents (methanol/water/chloroform) and purified with PVPP according to Gomez et al. (2007). Starting from initial conditions described by Bergmeyer (1983), enzymatic assays were adapted to be performed in each well of a 96 well Microplate using a robotic platform (Freedom EVO 75, *TECAN*) equipped with a microplate reader (Infinite 200, *TECAN)*. All the following preparations were done for one microplate. Citric acid assay: a mixture was prepared containing 115 µg of malic acid dehydrogenase, 0.51 mg of lactate dehydrogenase and 5 mg of NADH in 12 mL of 0.6 mol L^{-1} glycylglycine buffer (pH 7.8). Then 100 µL of the mixture and 180 µL of extract or standard solution of citric acid (4 to 50 mg L^{-1}) were mixed in each well. Ten minutes later, absorbance was read at 340 nm (DO A) before 20 µL of citric acid lyase (6.4 U mL^{-1}) were added. The microplate was incubated for 3 h at room temperature and regularly shaken, before a second reading (DO B). Malic acid assay: a mixture was prepared with 6 mL of water and 6 mL of a 0.6 mol L^{-1} glycylglycine buffer (pH 10). Then 100 µL of the mixture, 20 µL of NAD (18 mg mL^{-1}), 20 µL of GOT (66.7 mg L^{-1}) and 100 µL of extract or standard malic acid solution (4 to 50 mg L^{-1}) were mixed in each well. Ten minutes later, absorbance was measured at 340 nm (DO A) before 20 µL of malic

acid dehydrogenase (33 µg mL^{-1}) were added. For the next 2h45min, the microplate was incubated at room temperature and shaken twice, after which absorbance was measured at 340 nm (DO B). The concentration of soluble oxalic acid was determined using the LIBIOS Oxalic acid assay kit. Soluble K, Mg, and Ca concentrations were determined by mass spectrometry (Martin-Prével *et al.*, 1984), and Cl concentration was determined by potentiometry using the automatic titrator TitroLine alpha (Walinga *et al.*, 1995). The concentration of phosphoric acid was estimated from soluble phosphorus (P) determined by colorimetry (Martin-Prével et al., 1984).

1.2.2.4 Statistical Analysis

Linear mixed-effects models [LMMs (Gałecki and Burzykowski, 2013)] were used to examine the relationship between the response variables (pulp acidity and composition) and the explanatory variables (fruit age, cultivar), and their interactions. We used quadratic and cubic terms of fruit age when the curve passed through a maximum and had an asymmetrical shape. We used the lme function in the 'nlme' library (Pinheiro *et al.*, 2013) in the statistical program R 2.14.0. "Banana plant" was treated as a random effect because banana plants were assumed to contain unobserved heterogeneity that cannot be modeled. A temporal correlation structure was used to account for temporal pseudo-replication. Model selection was made using the top-down strategy (Zuur *et al.*, 2009): starting with a model where the fixed component contains all explanatory variables and interactions, we found the optimal structure of the random component. Then, we used *F*-statistic obtained with REML estimation to find the optimal fixed structure. Finally, the optimal model is presented in this paper, using REML estimation.

The predictive quality of the pH and TA models was evaluated by the bias (mean of the difference between observed and predicted values), and the root mean squared error (RMSE), which describes the mean distance between simulation and measurement data (Kobayashi and Salam, 2000). The RMSE design was:

$$RMSE = \sqrt{\frac{(\sum(yi_p - yi_m)^2)}{n}}$$

Where yi_p is the predicted value of the fruit i, and yi_m is the measured value of the fruit i. n is the data number.

A sensitivity analysis of the pH and TA models was performed at two different stages of fruit development- green (before ethylene treatment) and ripe (9 days after ethylene treatment), according to the method of Monod et al. (2006). First, border values of each of the

eight input factors of the models were estimated as the extremes values of the dataset corresponding to the fruit stage considered for the sensitivity analysis. Then, for each input factor, their range of values was divided into five equal levels and a 5^8 factorial simulation design was created. Next, an analysis of variance (ANOVA) was performed on the model responses to study the contribution of each input factor to pH and TA variability. A sensitivity index (SI) of each input factor was calculated by dividing its sum of squares by the total sum of squares (Monod et al., 2006).

1.3 Results

1.3.1 Changes in pulp acidity

Fruit age and the cultivar had a significant effect on pH and TA during fruit growth (*Table III-1*). Throughout fruit growth, PL had the most acidic fruits (TA=3.5 meq 100 g FW^{-1} ±0.22; pH=5.5 ±0.13), IDN 110 fruits were intermediate (TA=2.8 meq 100 g FW^{-1} ±0.31; pH=5.7 ±0.17), and JB had the least acidic fruits (TA=2.3 meq 100 g FW^{-1} ±0.27; pH=5.9 ±0.28) (*Fig. III.1.A and B*). In all three cultivars, TA decreased slightly during the early stages of fruit growth and then increased slightly. pH increased throughout fruit growth in the three cultivars but most in JB.

Fruit age and the cultivar had a significant effect on pH and TA during post harvest fruit ripening (*Table III-1*). The general patterns of TA and pH during post harvest ripening were similar in the three cultivars (*Fig. III.2.A and B*): TA increased from day 0 to day 6 and then decreased slightly until day 13. pH showed the opposite trend. There were strong significant differences between the three cultivars in the levels of TA and pH at the end of ripening (*Fig. III.2.A and B*). At day 13, JB had the highest acidity (TA=12 meq 100 g FW^{-1} ±0.46; pH=4.3 ±0.05), followed by PL (TA=6 meq 100 g FW^{-1} ±0.32; pH=4.8 ±0.08) and lastly IDN 110 (TA=3.8 meq 100 g FW^{-1} ±0.43; pH=5.4 ±0.09).

1.3.2 Changes in organic acid and mineral contents

During fruit growth, citric and malic acid contents increased linearly in the three cultivars but at different rates leading to significant differences among cultivars (*Fig. III.1.C and D, Table III-1*).Thus, at the end of fruit growth, JB had the highest citric acid content (0.4 g 100 g FW^{-1} ±0.03), followed by PL (0.34 g 100 g FW^{-1} ±0.005) and IDN 110 (0.33 g 100 g FW^{-1} ±0.001). Concerning malic acid content, PL had the highest content (0.23 g 100 g FW^{-1} ±0.01) at the end of fruit growth, followed by JB (0.15 g 100 g FW^{-1} ±0.003) and IDN 110 (0.14 g 100 g FW^{-1} ±0.01). Soluble oxalic acid content decreased linearly during fruit growth in all three

cultivars (*Fig. III.1.E, Table III-1*). PL had a significantly lower soluble oxalic acid content than JB and IDN throughout fruit growth (*Table III-1*). K was the main mineral present in banana pulp in the three cultivars and K content increased during fruit growth (*Fig. III.3.A, Table III-1*).

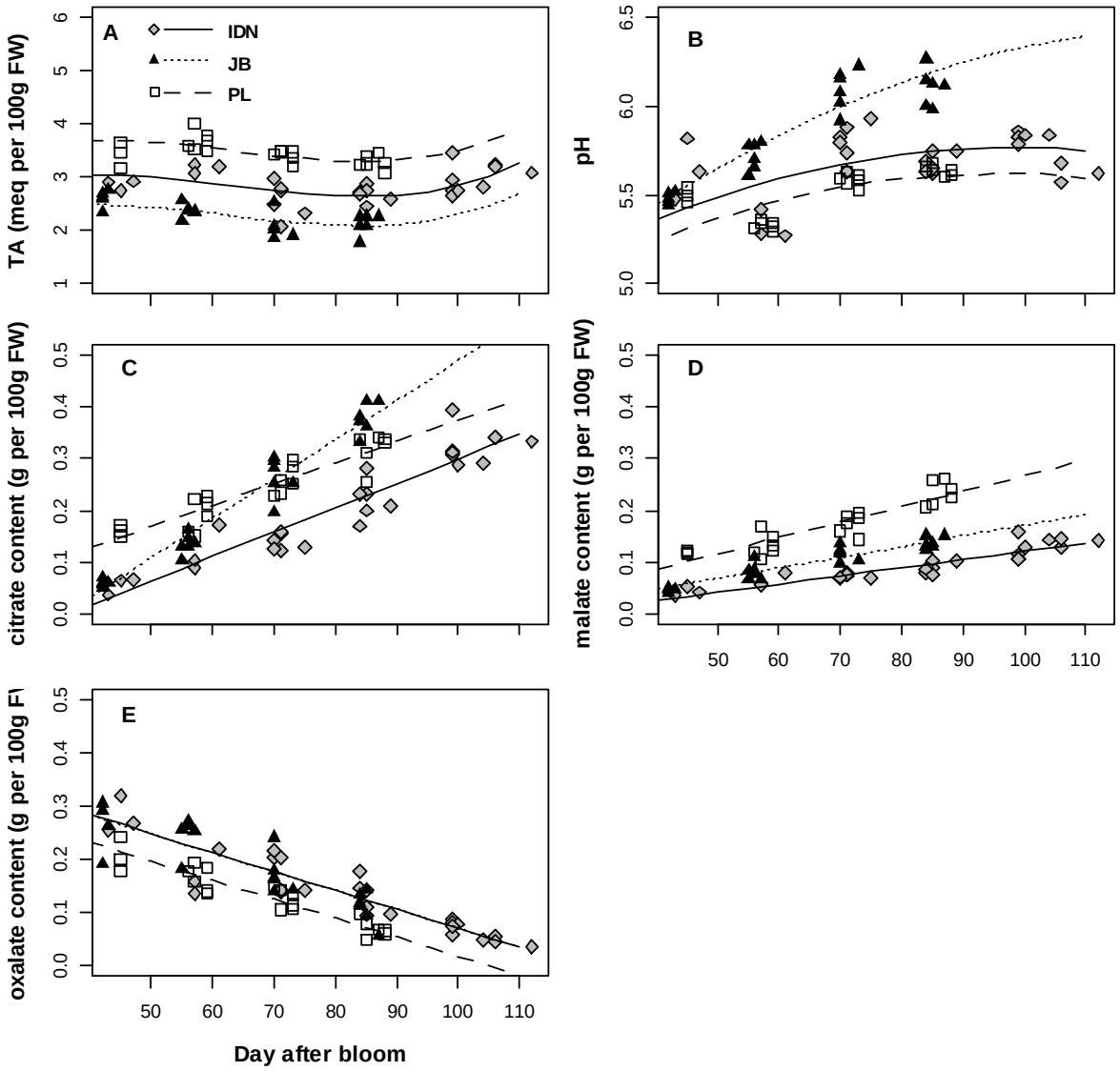

Figure III-1 Changes in TA (A), pH (B), citric acid content (C), malic acid content (D), and soluble oxalic acid content (E) of the pulp during fruit growth of the three cultivars of dessert bananas: Pisang Jari Buaya (JB), Pisang Lilin (PL), and Indonesia 110 (IDN 110). Each symbol represents a bunch. Lines are those of the fitted linear mixed model.

There were significant differences among cultivars (*Table III-1*): JB had the highest K content (0.30 g 100 g FW^{-1} ±0.02), followed by PL (0.26 g 100 g FW^{-1} ±0.03), and IDN 110 (0.25 g 100 g FW^{-1} ±0.02). The other mineral elements were present in lesser amounts (about ten times less) in banana pulp. Cl content increased from 0.05 to 0.07 g 100 g FW^{-1} during fruit growth and no differences were observed among the three cultivars whereas P content

decreased during fruit growth in all three cultivars (*Fig. III.3.B and C, Table III-1*). There were significant differences among cultivars throughout fruit growth and IDN 110 had a significantly higher P content (0.02 g 100 g FW^{-1} ±0.002) than JB (0.01 g 100 g FW^{-1} ±0.003) and PL (0.01 g 100 g FW^{-1} ±0.003) (*Fig. III.3.C, Table III-1*). Mg content decreased significantly during fruit growth in the three cultivars but most in PL (*Fig. III.3.D, Table III-1*). Throughout fruit growth, JB (0.03 g 100 g FW^{-1} ±0.001) and IDN 110 (0.03 g 100 g FW^{-1} ±0.004) had a significantly higher Mg content than PL (0.02 g 100 g FW^{-1} ±0.005). No clear pattern of Ca content was observed during fruit growth since the values varied greatly among bunches even within the same cultivar (*Fig. III.3.E, Table III-1).*

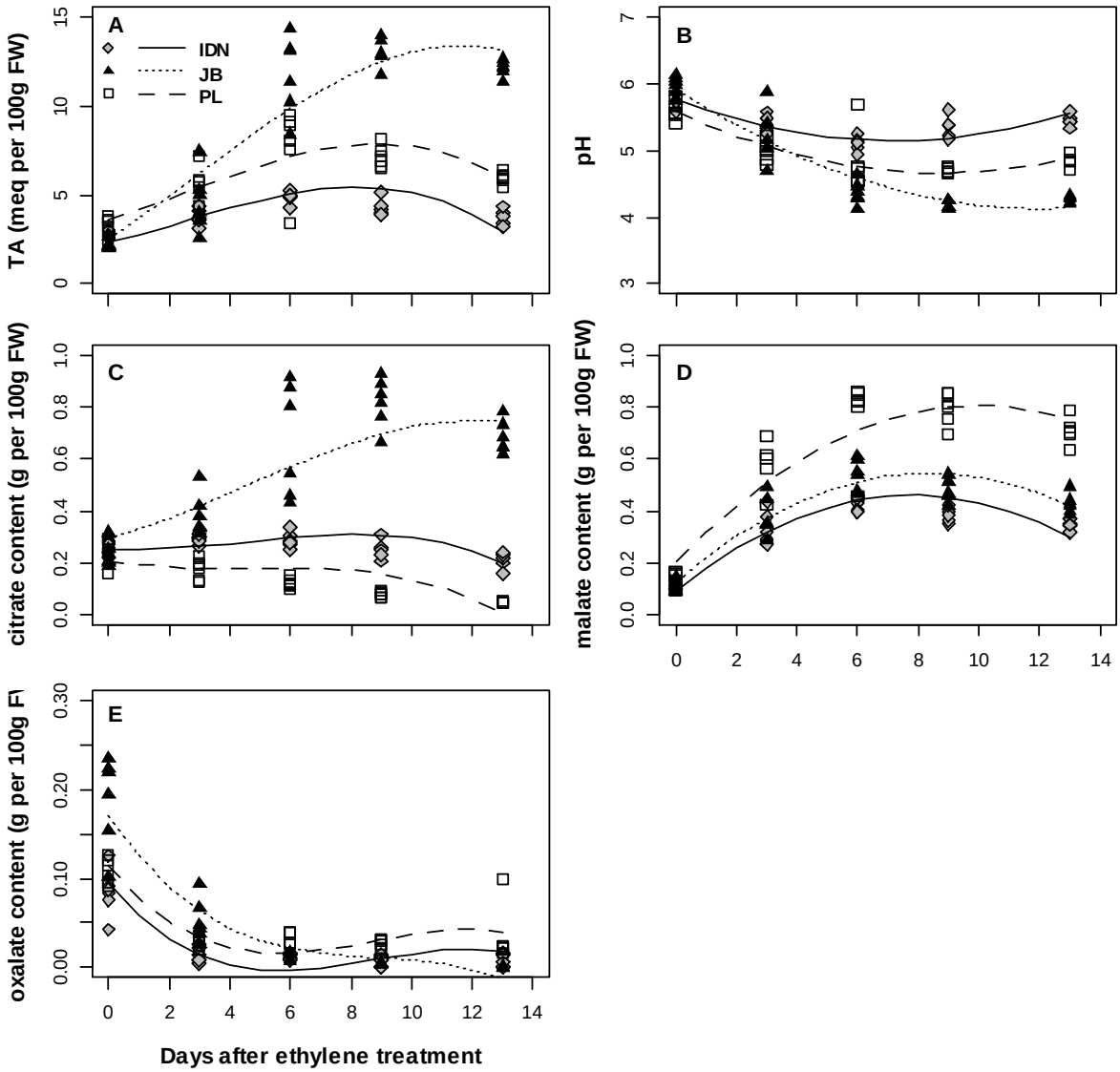

Figure III-2 Changes in TA (A), pH (B), citric acid content (C), malic acid content (D), and soluble oxalic acid content (E) of the pulp during post harvest ripening of the three cultivars of dessert bananas (JB, PL, and IDN 110). Each symbol represents a bunch. Lines are those of the fitted linear mixed model.

Table III-1 Linear mixed model analyses of TA, pH, malic acid content, citric acid content, soluble oxalic acid content, and mineral content during fruit growth and fruit post harvest ripening in relation to fruit age and the three cultivars used in this study.

Parameter	Fruit stage	*F*-value and significance				
		t	c	t^2	t^3	t:c
TA	growth	12.1***	126***	29.8***	7.0*	Ns
	ripening	179***	73.6***	49.4***	4.4*	66.5***
pH	growth	222***	69.9***	51.2***	Ns	16.0***
	ripening	184***	64.4***	79.4***	Ns	46.2***
Citric acid content	growth	602***	7.2**	Ns	Ns	20.7***
	ripening	9.90**	93.1***	11.1**	5.1*	65.9***
Malic acid content	growth	451***	98.4***	Ns	Ns	16.6***
	ripening	220***	59.1***	126***	Ns	20.3***
Oxalic acid content	growth	240***	24.5***	Ns	Ns	Ns
	ripening	162***	10.5**	58.9***	13.2***	12.3***
K content	growth	38.7***	20.6***	Ns	Ns	Ns
	ripening	Ns	Ns	Ns	Ns	Ns
P content	growth	66.6***	24.2***	Ns	Ns	Ns
	ripening	Ns	47.0***	Ns	Ns	Ns
Cl content	growth	76.0***	Ns	Ns	Ns	Ns
	ripening	21.4***	8.5**	8.3**	Ns	Ns
Mg content	growth	15.6**	5.1*	Ns	Ns	Ns
	ripening	Ns	5.4*	Ns	Ns	Ns
Ca content	growth	Ns	Ns	Ns	Ns	Ns
	ripening	Ns	Ns	Ns	Ns	Ns

[a] All models included one random effect: "plant". Codes for effects: t = fruit age; c = cultivar. *** p-value < 0.001; ** p-value < 0.01; * p-value<0.05 ; ns: not significant

During post harvest ripening, there were significant differences in the pattern of citric acid accumulation among the three cultivars (*Fig. III.2.C, Table III-1*). Citric acid accumulation was the same in IDN 110 and PL with an overall decrease during ripening, whereas in JB there was a significant increase until day 9 and a slight decrease at the end of ripening. As a consequence, JB had a significantly higher level of citric acid (0.68 g 100 g FW^{-1} ±0.06) than IDN 110 (0.21 g 100 g FW^{-1} ±0.03) and PL (0.05 g 100 g FW^{-1} ±0.003) at the end of ripening. The three cultivars showed the same pattern of malic acid accumulation with an increase from day 0 to day 6, followed by a slight decrease (*Fig. III.2.D*). There were significant differences among cultivars (*Table III-1*), so that at the end of ripening, PL had the highest malic acid content (0.71 g 100 g FW^{-1} ±0.05), followed by JB (0.43 g 100 g FW^{-1} ±0.04) and IDN 110 (0.34 g 100g FW^{-1} ±0.02). Soluble oxalic acid content was highest at the pre-climacteric stage (day 0) in all three cultivars with JB having a significantly higher oxalic acid content (0.19 g 100 g FW^{-1} ±0.05) than PL (0.14 g 100 g FW^{-1} ±0.09) and IDN 110 (0.08 g 100 g FW^{-1} ±0.03) (*Fig. III.2.E, Table III-1*). From day 3, soluble oxalic acid content decreased rapidly in all three cultivars to become inexistent at the end of ripening. K was the main mineral found in banana pulp during post harvest ripening with a mean K content of 0.30 g 100 g FW^{-1} ±0.05 (*Fig. III.4.A*). K content remained constant during ripening and there were no significant differences among cultivars (*Table III-1*). The other mineral elements such as Cl, Ca, Mg, and P were present in lower amounts (about ten times less) in the banana pulp. Cl content decreased slightly during ripening in all three cultivars and was significantly lower in PL (0.05 g 100 g FW^{-1} ±0.006) than in JB (0.07 g 100 g FW^{-1} ±0.008) and IDN 110 (0.06 g 100 g FW^{-1} ±0.01) (*Fig. III.4.B, Table III-1*). P content remained constant during ripening in the three cultivars, IDN 110 had a significantly higher P content (0.02 g 100 g FW^{-1} ±0.002) than PL (0.01 g 100 g FW^{-1} ±0.001) and JB (0.01 g 100 g FW^{-1} ±0.002) (*Fig. III.4.C, Table III-1*). Mg content remained constant during ripening in all three cultivars. PL had a significantly lower Mg content (0.02 g 100 g FW^{-1} ±0.005) than IDN 110 (0.03 g 100 g FW^{-1} ±0.005) and JB (0.03 g 100 g FW^{-1} ±0.004) (*Fig. III.4.D, Table III-1*). There was no clear pattern in Ca content during fruit ripening since there was significant variability between bunches belonging to the same cultivar (*Fig. III.4.E, Table III-1*).

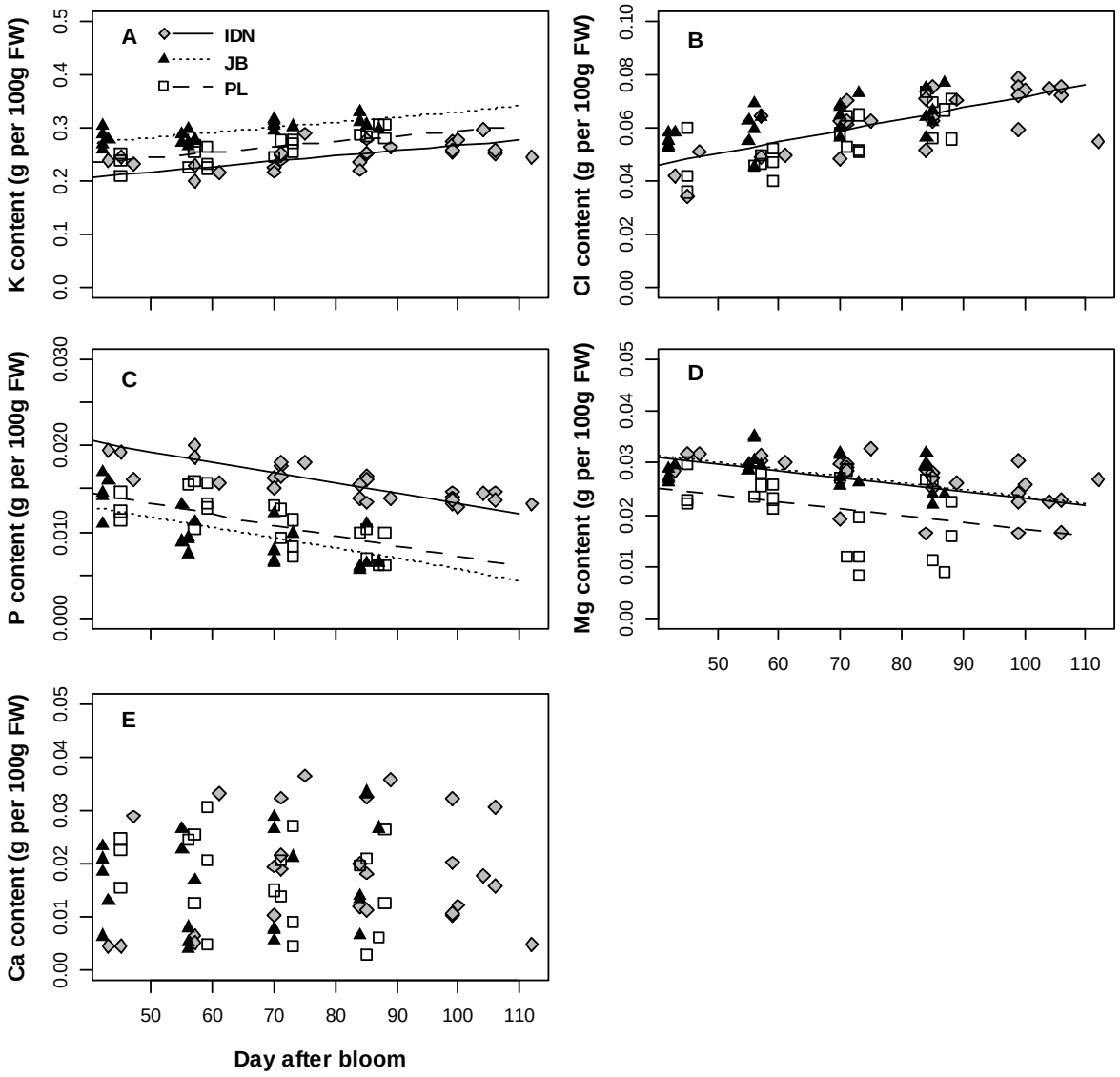

Figure III-3 Changes in K (A), Cl (B), P (C), Mg (D), and Ca (E) pulp content during fruit growth of the three cultivars of dessert bananas (JB, PL, and IDN 110). Each symbol represents a bunch. Lines are those of the fitted linear mixed model.

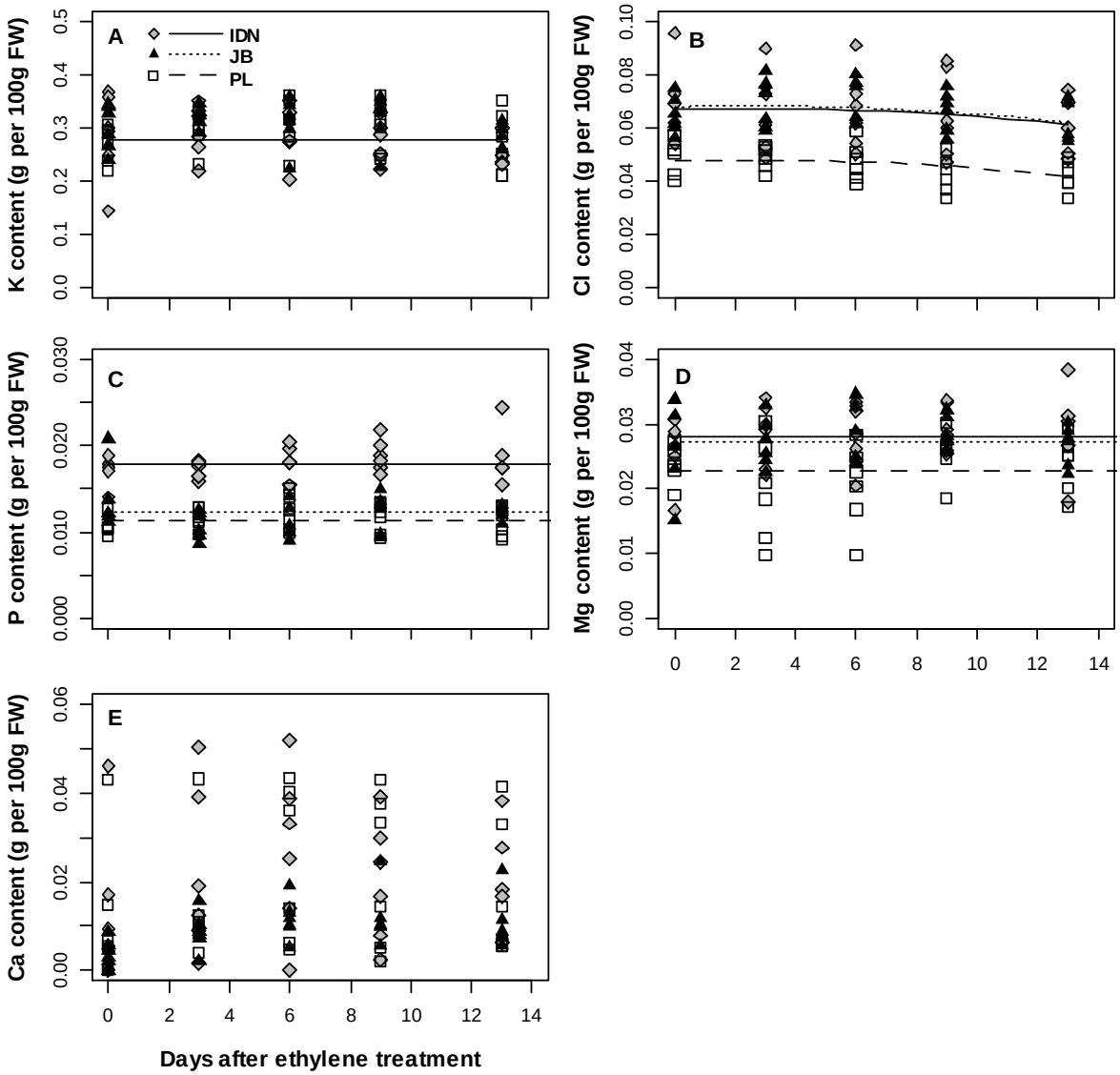

Figure III-4 Changes in K (A), Cl (B), P (C), Mg (D), and Ca (E) pulp content during post harvest ripening of the three cultivars of dessert bananas (JB, PL, and IDN 110). Each symbol represents a bunch. Lines are those of the fitted linear mixed model.

1.3.3 Model predictions and sensitivity analysis

Overall, the pH model predicted banana pulp pH with an average bias of 0.05 pH units and a R^2 of 0.34 (*Fig. III.5.A and B*). The RMSE, quantifying the goodness-of-fit, was acceptable with a mean value of 0.7 pH unit (*Table III-2*). However, the predictions were better for JB and PL than for IDN, and better during ripening than during fruit growth. For pH above 5, the discrepancies between observed and predicted values were sometimes higher than 1 pH unit. Overall, the TA model allowed prediction of banana pulp TA with an average bias of -1.44 meq 100 g FW^{-1} and a R^2 of 0.81 (*Fig. III.5.C and D*). Thus, the model underestimated TA most of the time. The RMSE was satisfactory with a mean value of 2 meq 100 g FW^{-1} (*Table III-2*). The predictions were better during ripening than during fruit growth.

Every input factor considered in the sensitivity analysis had a significant effect on pH and TA at both green and ripe stages (*Table III-3*). The sensitivity indices (SI) calculated represent the percentage of pH or TA variability explained by the factor considered. For both pH and TA, citric acid (SI=48% for pH and 63% for TA) and malic acid (SI=25% for pH and 21% for TA) were the most influential acids at the ripe stage, whereas phosphoric acid had little effect (SI=5.6% for pH and TA), and oxalic acid had almost no effect (SI=0.3% for pH and SI=0.2% for TA). In contrast, at the green stage oxalic acid was the most influential acid (SI=44% for pH and 48% for TA), whereas citric acid (SI=4.5% for pH and 6.9% for TA), malic acid (SI=0.9% for pH and 1.3 for TA), and phosphoric acid (SI=0.5% for pH and TA) had very little effect. Among soluble minerals, K was the main contributor to changes in pH at both stages, but its effect was more pronounced at the green stage (SI=39%) than at the ripe stage (SI=14%). K was also the main contributor to TA at the green stage (SI=37%), but its effect was greatly reduced at the ripe stage (SI=6.9%). Other soluble minerals had only a limited effect on pH and TA since they accounted for a total of 11% of their variability at the green stage and for a total of 6% and 3% for pH and TA respectively at the ripe stage.

Table III-2 Quality of prediction (RMSE and bias) of the pH and TA models.

Cultivar	Fruit stage	pH		TA	
		RMSE (units pH)	bias (units pH)	RMSE (meq.100g FW^{-1})	bias (meq.100g FW^{-1})
PL	growth	0.5	-0.2	1.5	-1.2
	ripening	0.5	-0.1	2.6	-1.9
JB	growth	0.6	0.1	1.3	-1.1
	ripening	0.6	-0.2	2	-1
IDN 110	growth	1	0.3	1.8	-1.5
	ripening	1	0.4	2.4	-1.7
All cultivars	growth	0.8	0.1	1.6	-1.3
	ripening	0.7	0	2.3	-1.5
All cultivars	All stages	0.7	0.05	2	-1.4

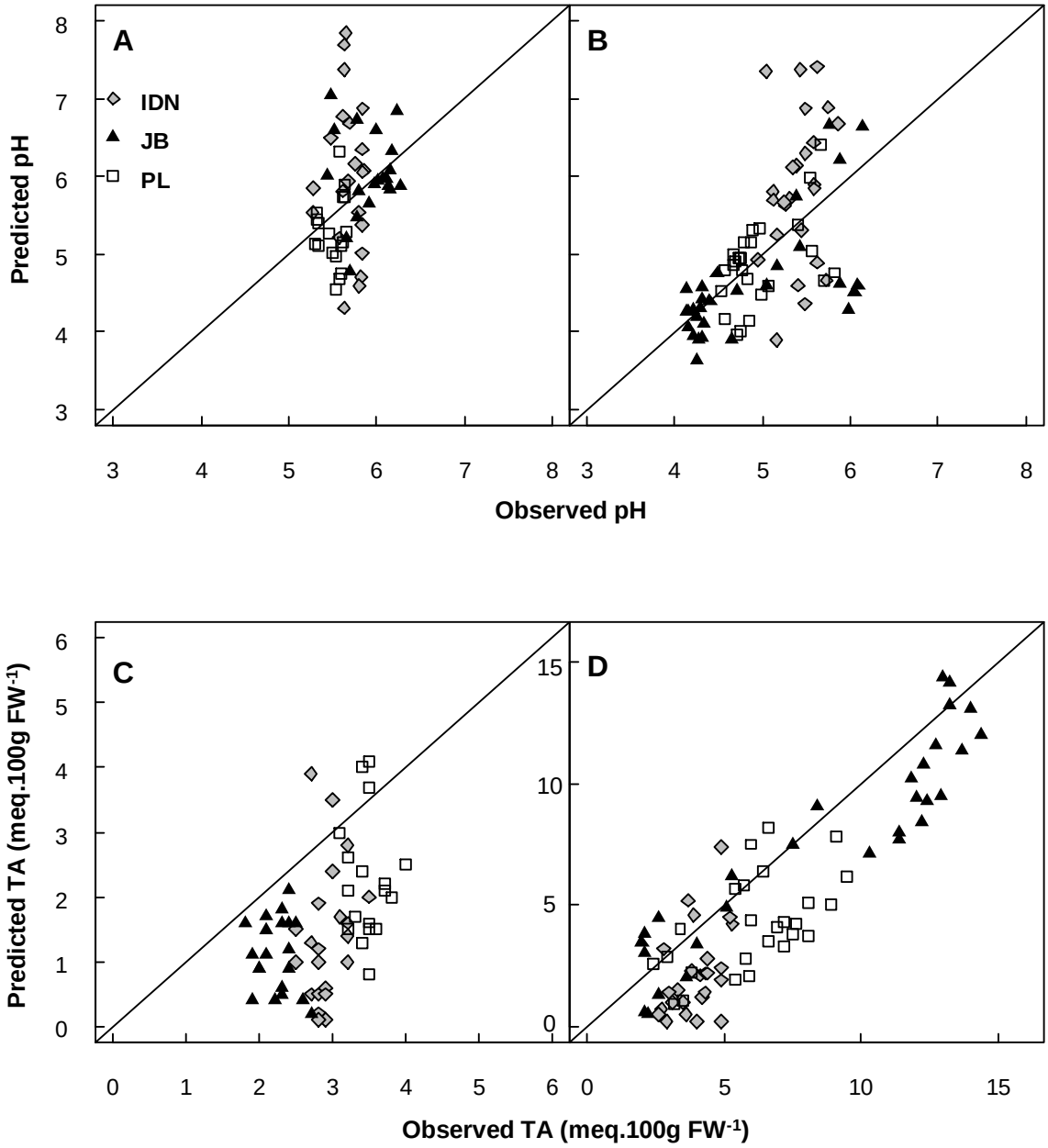

Figure III-5 Comparison between observed and predicted pH during fruit growth (A) and post harvest ripening (B), and between observed and predicted TA during fruit growth (C) and post harvest ripening (D) of the three cultivars of dessert bananas (JB, PL, and IDN 110).

Table III-3 Results of the sensitivity analysis of the pH and TA models for green (before ethylene treatment) and ripe fruits (9 days after ethylene treatment).

	Borders of the input factors		pH	TA
	Min. value (g.100 g FW^{-1})	Max. value (g.100 g FW^{-1})	SI (%)	SI (%)
Ripe fruit				
Citric acid	0.04	1.02	48.4***	62.9***
Malic acid	0.05	0.93	25.6***	21.3***
Oxalic acid	0.00	0.19	0.28***	0.16***
Phosphoric acid	0.01	0.03	5.59***	5.64***
Potassium	0.13	0.43	13.9***	6.89***
Chloride	0.03	0.10	1.47***	0.71***
Magnesium	0.01	0.04	1.99***	0.99***
Calcium	0.00	0.05	2.76***	1.38***
Green fruit				
Citric acid	0.05	0.41	4.55***	6.91***
Malic acid	0.04	0.35	0.96***	1.31***
Oxalic acid	0.02	0.29	43.7***	48.2***
Phosphoric acid	0.00	0.02	0.5***	0.55***
Potassium	0.22	0.33	39.3***	36.7***
Chloride	0.05	0.08	2.81***	2.80***
Magnesium	0.01	0.03	2.55***	2.59***
Calcium	0.00	0.04	5.84***	5.92***

The table gives the borders of the input factors, and the sensitivity indices (SI) with their significance.

*** p-value < 0.001

1.4 Discussion

1.4.1 Quality of prediction of the models

For the pH model, the lower the pH, the better the predictions, which explains why pH predictions were better during ripening than during fruit growth. This is due to the logarithm function of the pH which increases the sensitivity of the pH to input parameters with an increase in pH. Thus, imprecision in the determination of the chemical elements that are the main contributors to banana pulp acidity (organic acids and K) may be responsible for the difference between observed and predicted data, especially at high pH. For example, we calculated that for a pulp sample with a measured pH of 6, overestimating the K content by 10% impacts the prediction by about 2 pH units. In addition, some approximations were used for modeling, for example, considering that all the soluble phosphorus is in the form of phosphoric acid whereas in reality it is probably also present in the form of several other acidic compounds than phosphoric acid. We also considered that the acid content of banana pulp could be estimated by malic acid, citric acid, oxalic acid and phosphoric acid content only. pH has been previously modeled using the same approach to predict acidity of ripe harvested peaches (Lobit et al., 2002). Predictions were a little better than those obtained in the present study which can be explained by the fact that pH of ripe peaches was below 4.5, and thus within the range where the model predictions are best.

For the TA model, predictions were on average 1.5 meq lower than observed values. This is presumably because we did not consider free amino acids in the model and these can reach 0.1 g 100 g FW^{-1} and 0.15 g 100 g FW^{-1} in green and ripe bananas respectively (John and Marchal, 1995). Indeed, as the standard procedure is to measure TA at a pH of 8.1, not only carboxyl groups of amino acids are titrated but also some amine groups, probably leading to overestimation of the quantity of non-dissociated acids in fruit pulp. For ripe peaches, TA predictions were a little better than the ones obtained in the present study, probably due to the fact that amino acids were considered and approximated by the soluble nitrogen content of the pulp in the form of asparginine (Lobit et al., 2002). The authors calculated that at a pH of 8.1, free amino acids account for 8% of TA in ripe peach pulp. The better prediction of banana pulp TA during ripening was due to the fact that TA ranged from 3 to 15 meq 100 g FW^{-1} during this stage, whereas it only varied between 2 and 4 meq 100 g FW^{-1} during growth.

1.4.2 Link between banana pulp acidity and composition

The elaboration of banana fruit acidity is a continuous process that takes place throughout fruit growth and post harvest ripening. During its growth on the plant, the banana fruit accumulates both acids and minerals that determine the TA and pH of the pulp. Sensitivity analysis showed that during this phase, oxalic acid, which is present in large amounts, is the main determinant of banana pulp acidity because of its low pKas. Sensitivity analysis also showed that, among soluble minerals, K is the main contributor to banana acidity. K content increased during banana fruit growth, as also observed in mango (Léchaudel *et al.*, 2005b), and was the major mineral found in banana pulp in accordance with results of previous studies (John and Marchal, 1995). It is interesting to note that K, which is the main cation present in all fruit cell, affects fruit acidity not only by participating in the acid/base reactions but also by acting on enzyme regulation and vacuolar storage of organic acids (Etienne *et al.*, 2013b).

During post harvest ripening, banana pulp acidity underwent its greatest changes and there were marked differences among the three cultivars. JB and PL appeared to have a higher acidity than IDN 110 at the end of ripening, which is in accordance with the classification of dessert bananas cultivars made by Bugaud et al. (2011). According to Bugaud's classification, JB and PL belonged to the sourest cluster whereas IDN 110 belonged to the least sour cluster. The marked changes in pulp acidity during post harvest ripening are mainly the result of changes in malic and citric acid contents as shown by the results of the sensitivity analysis. Indeed, as the fruit ripened, soluble oxalic acid content decreased dramatically, hence its contribution to banana fruit acidity. While oxalic acid disappears during ripening, malic and citric acids become the main acids in banana pulp and hence the main contributors to its acidity. The decrease in soluble oxalic acid content during banana fruit ripening is probably linked to starch hydrolysis. Indeed, Osuji et al. (2005) observed that oxalic acid was mainly present in the form of calcium oxalate crystals inside the starch grains in the pulp of unripe banana fruit. As the fruit ripened, the starch grains were destroyed and calcium oxalate released, probably leading to oxalate catabolism. The same pattern of oxalic acid content has been observed in kiwi fruit with a maximum at early stages and a gradual decrease during fruit growth and also during storage (Watanabe and Takahashi, 1998). The major role of malic and citric acids in the acidity of ripe fruit has been reported in many species (Etienne *et al.*, 2013b). Marked differences in the pattern of citric acid content were observed among the three cultivars. Thus, there was a significant increase in citric acid content in JB throughout fruit ripening while there was a decrease in PL and IDN 110. The pattern of malic acid content was the same in the three cultivars although differences were observed, with PL

accumulating more malic acid than JB and IDN 110. Citric and malic acids are involved in the respiratory metabolism of fruit pulp cells through their involvement in the glycolysis and TCA cycle pathways (Etienne *et al.*, 2013b). As banana fruit, which is a climacteric fruit, showed a significant rise in their respiration rate in the first days after ethylene treatment, differences in pulp acidity among cultivars during ripening could be linked to respiratory metabolism. During post harvest ripening, K, P and Mg contents remained constant in all three cultivars, whereas Cl content decreased slightly. Migration of minerals from the pulp to the peel can occur in response to loss of water by the peel due to transpiration, but it is also possible that some minerals migrate with the water from the peel to the pulp (John and Marchal, 1995). In the present study, it appears that osmotic adjustment only significantly affected Cl content. There was a large variability of the soluble Ca content observed during ripening and growth but this is consistent with the high coefficient of variation of pulp Ca content that we found in previous studies. However, we showed that Ca did not play a major role in the determination of pH and TA, and so even if there was a large variability among samples in the measured Ca contents it did not have important repercussions on the predictions of the pH and TA models.

1.5 Conclusions

This study, which presents a model of banana pulp acidity for the first time, showed that among acids, malic, citric and oxalic acids are the main contributors to banana pulp acidity, and that among soluble minerals, K also plays an important role. Consequently, studying the factors that affect malic acid, citric acid, oxalic acid, and K accumulation in banana pulp appears to be an appropriate area of research to ultimately modify banana fruit acidity. In future work, the pH model will be incorporated in a more complex process-based simulation model to predict banana acidity. Process-based simulation models are powerful tools to study genotype*environment interactions and to design ideotypes adapted to consumer taste (Génard *et al.*, 2010; Quilot-Turion *et al.*, 2011).

2 Etude de l'accumulation du malate par un modèle de stockage vacuolaire

Objectifs

Dans cette partie, l'accumulation du malate dans la pulpe de banane a été modélisée dans le but (i) de comprendre les processus physiologiques qui pilotent la concentration en malate dans la pulpe de banane pendant la croissance et la maturation post récolte, (ii) de proposer des hypothèses sur les origines des différences génotypiques au niveau cellulaire, et (iii) d'étudier l'effet des conditions de croissance du fruit sur l'accumulation du malate. L'hypothèse de base de ce travail de modélisation est que l'accumulation du malate dans la pulpe est pilotée par les conditions de son stockage dans la vacuole (c.f. Chapitre I). Ainsi, un modèle mécaniste décrivant de manière simplifiée le stockage du malate dans la vacuole a été utilisé (Lobit *et al.*, 2006). Cette partie a été rédigée sous la forme d'un article intitulé «Modeling the vacuolar storage of malate shed lights on malate accumulation in pre and post-harvest banana (*Musa* sp. AA)» en vu d'être soumis à **Plos One**.

Principaux résultats

- Ce modèle permet de prédire la concentration en malate dans la pulpe pendant la croissance et la maturation post récolte de la banane et de décrire la variabilité entre génotypes.
- Le stockage vacuolaire du malate apparaît comme un processus clé de l'accumulation du malate dans la banane.
- Ce modèle suggère que les concentrations en acides organiques et potassium ont un effet important sur l'accumulation du malate dans la vacuole.
- Ce modèle suggère un effet négatif de la température sur le stockage du malate dans la vacuole pendant les phases pré et post récolte.
- La variation d'énergie libre d'hydrolyse de l'ATP et le pH vacuolaire pourraient être des déterminants important de l'accumulation du malate et pourraient expliquer les différences de concentrations en malate observées entre génotypes et entre les phases pré et post récolte.

Modeling the vacuolar storage of malate shed lights on malate accumulation in pre and post-harvest banana (*Musa* sp. AA)

A. Etienne[1], M. Génard[2], P. Lobit[3], C. Bugaud[1]

[1] Centre de Coopération International en Recherche Agronomique pour le Développement (CIRAD), UMR QUALISUD, Pôle de Recherche Agronomique de Martinique, BP 214, 97 285 Lamentin Cedex 2, France

[2] INRA, UR 1115 Plantes et Systèmes de Cultures Horticoles, F-84914 Avignon, France

[3] Instituo de investigaciones Agropecuarias y Forestales, Universidad Michoacana de San Nicolas de Hidalgo, Tarimbaro, Michoacan, CP. 58880, Mexico

Abstract

Malate concentration is a crucial determinant of the perception of banana sourness and sweetness, two major drivers for consumer preferences. Banana fruit has the particularity of having separate growth and ripening stages, with contrasting evolutions of pulp malate concentration. Our objective was to simulate these evolutions by adapting the mechanistic model of malate vacuolar storage by Lobit et al. (2006). The model was calibrated and validated using data sets from three cultivars of dessert banana contrasting in terms of malate accumulation, grown under different fruit load and potassium supply, and harvested at different stages. It predicted the post-harvest dynamic of malate concentration with a fairly good accuracy for the three cultivars (mean RRMSE=0.25), but was less good during banana growth (mean RRMSE=0.42). The sensitivity of the model to parameters and input variables was analyzed. According to the model, vacuolar composition, in particular potassium and organic acids concentrations, had an important effect on malate accumulation. The model suggested that raising temperature depressed malate accumulation. The model also helped to dissect differences of malate concentration among cultivars and between the pre and post-harvest phases by highlighting the likely importance of proton pumps activity and in particular of the free energy of ATP hydrolysis and vacuolar pH. Finally, the present adaptation of the malate model initially developed on peach, to banana fruit highlights the possible generic quality of the model and its suitability for fleshy fruit.

2.1 Introduction

In banana, malate is the most abundant organic acid present in the pulp together with citrate (Etienne *et al.*, 2013a; Jullien *et al.*, 2008), and is a good predictor of pulp sourness and sweetness (Bugaud *et al.*, 2013), two major drivers of consumer preferences. Malate concentration varies considerably among banana cultivars (Bugaud *et al.*, 2013). Malate accumulation in fruit cells is a complex phenomenon because it involves several metabolic pathways and transport mechanisms across different compartments, mainly cytosol, mitochondria, and vacuole (for review see (Etienne *et al.*, 2013b)). Several transcriptomic, metabolomic, proteomic, and QTL studies have begun to elucidate the complexity of this system (for review see (Sweetman *et al.*, 2009)), but much remains unclear. Given the complexity of the processes, ecophysiological process-based simulation models (PBSMs) could advance our understanding of the mechanisms underlying malate accumulation in banana and their interactions. PBSMs could also help to elucidate the differences in malate accumulation among cultivars, as was the case for sugar accumulation in peach (Wu *et al.*, 2012), and grape berry (Dai *et al.*, 2009).

Despite the importance of pulp malate concentration for fruit quality, attempts to mechanistically model it are rare. To our knowledge, the only PBSM was proposed by Lobit et al. (2006) to simulate malate concentration in peach. This model, which was based on the assumption that malate accumulation was controlled at the level of vacuolar storage, is in agreement with several later studies (for review see (Etienne *et al.*, 2013b)), and still appears to be a good framework to study malate accumulation in fleshy fruit.

In the present study, we adapted Lobit's model to banana fruit in order to study the accumulation of malate in banana using a mechanistic model-based analysis. Banana fruit has the particularity of having separate growth and post-harvest ripening stages, during which malate concentration undergoes substantial changes (Etienne *et al.*, 2013a). For this reason, we modeled the dynamics of malate concentration during both the pre and post-harvest stages. The concentration of malate in banana pulp varies greatly among genotypes (Bugaud *et al.*, 2013; Etienne *et al.*, 2014). The physiological age of the fruit at harvest is also known to affect the concentration of malate in the pulp of banana during post-harvest ripening (Bugaud *et al.*, 2006). Fruit pruning and potassium fertilization, two cultural practices commonly used by the banana growers, can also impact the concentration of malate in fleshy fruits (for review see (Etienne *et al.*, 2013b)). Consequently, we chose to calibrate and validate the model on three cultivars with contrasting acidity under different fruit loads, potassium supplies, and harvest stages. To study how these factors could affect malate accumulation, we analyzed the sensitivity of the model to parameters and input variables. The model enabled us to: improve

our understanding of malate accumulation during growth and post-harvest ripening of banana fruit; propose a possible explanation for differences in malate accumulation among cultivars; study the possible effects of fruit growth conditions on malate accumulation.

2.2 Material and Methods

2.2.1 Model description

The model of malate accumulation proposed by Lobit et al. (2006) assumes that the accumulation of malate in fleshy fruits is mainly determined by the conditions of its storage in the vacuole of pulp cells. The model provides a simplified representation of the functioning of the tonoplast (*Fig. III.6*).

The transport of malate across the tonoplast is passive and occurs by facilitated diffusion of the di-anion form through specific ion channels (De Angeli *et al.*, 2013; Kovermann *et al.*, 2007; Meyer *et al.*, 2011) and transporters (Emmerlich *et al.*, 2003; Terrier *et al.*, 1998). It follows the electrochemical potential gradient of the di-anion across the tonoplast, defined as follows:

$$\Delta G_{Mal^{2-}} = -2F\Delta\psi + RT\ln\left(\frac{(Mal^{2-}_{vac})}{(Mal^{2-}_{cyt})}\right) \quad (1)$$

where (Mal^{2-}_{cyt}) and (Mal^{2-}_{vac}) are the activities of the di-anion malate in the cytosol and in the vacuole respectively (mol.L^{-1}), $\Delta\psi$ is the electric potential gradient across the tonoplast (ψ_{vac}-ψ_{cyt}; V), T is temperature (K), R is the gas constant (J.mol^{-1}.K^{-1}), and F is Faraday's constant (C.mol^{-1}).

This implies that the accumulation of malate in the vacuole is controlled mainly by the ratio of the di-anion malate activity across the tonoplast and the $\Delta\psi$.

The activity of the di-anion is the product of its activity coefficient a_{Mal}^{2-} (dimensionless) and of its concentration [Mal^{2-}] (mol.L^{-1}):

$$(Mal^{2-}) = a_{Mal^{2-}} * [Mal^{2-}] \quad (2)$$

In the cytosol, the concentration of the di-anion malate is unlikely to vary much because it plays a fundamental role in the regulation of cytosolic pH (Smith and Raven, 1979). In addition, its activity coefficient, which depends only on the ionic strength of the cytosol, is also unlikely to vary much (Lobit et al., 2006). Therefore, in the model, (Mal^{2-}_{cyt}) is considered as a constant.

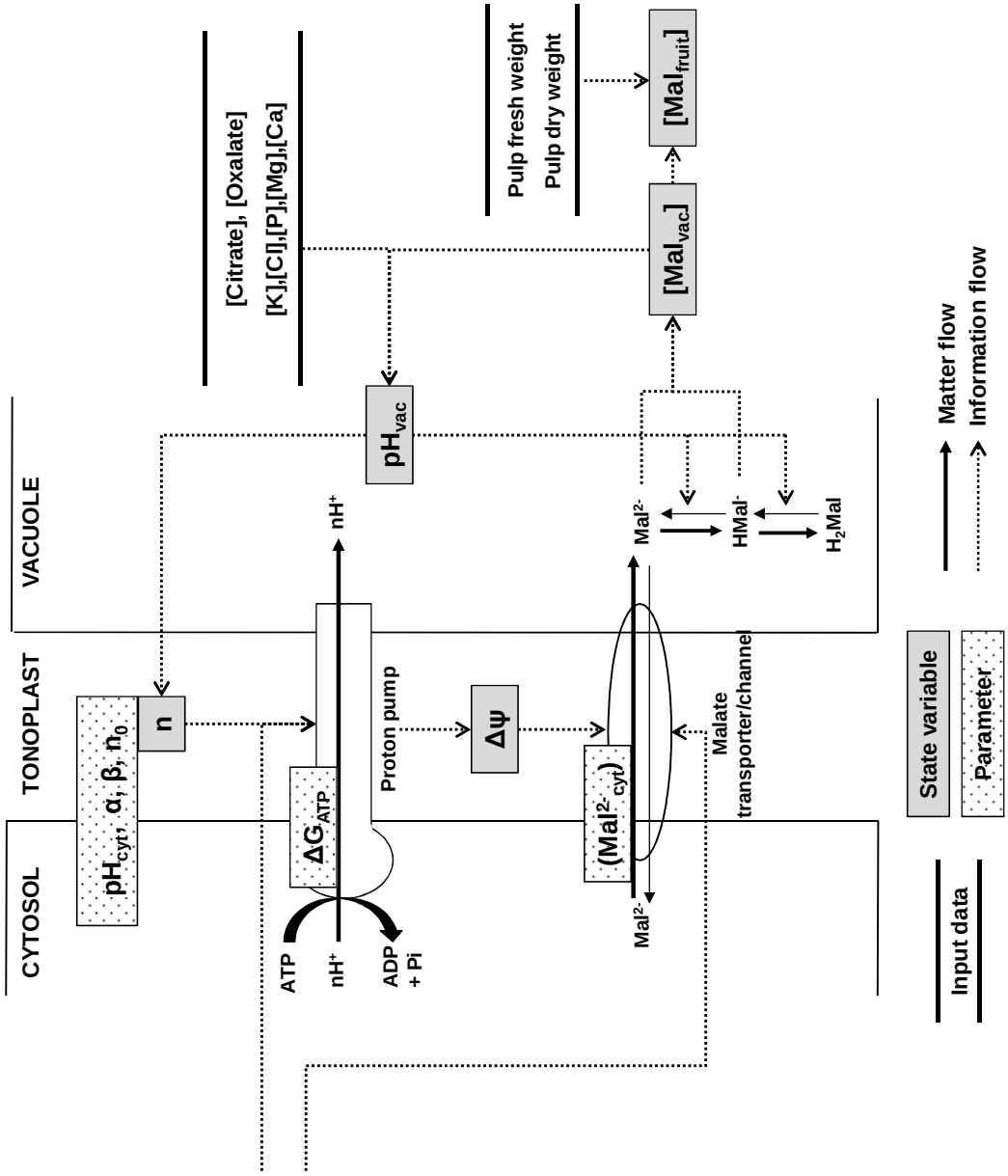

Figure III-6 Schematic representation of the model of vacuolar malate storage proposed by Lobit et al. (2006). State variables: $[Mal_{fruit}]$ = concentration of malate in the pulp; $[Mal_{vac}]$ = concentration of malate in the vacuole; pH_{vac} = vacuolar pH; $\Delta\psi$ = electric potential gradient across the tonoplast; n = coupling ratio of the proton pump ATPase. Model parameters: pH_{cyt} = cytosolic pH; ΔG_{ATP} = free energy of ATP hydrolysis; α, β, and n_0 = fitted parameters of the coupling ratio equation (Eq. 5); (Mal^{2-}_{cyt}) = cytosolic activity of the di-anion malate.

In the vacuole, the activity coefficient of the di-anion malate ($a_{Mal}{}^{2-}{}_{vac}$) is related to the concentration of all ionic species (Etienne *et al.*, 2013a), while its concentration is proportional to the total malate concentration and is controlled by the dissociation equation, since malate is a weak acid:

$$[Mal_{vac}^{2-}] = [Mal_{vac}] * \frac{K_1' K_2'}{h^2 + hK_1' + K_1' K_2'} \quad (3)$$

where $[Mal_{vac}]$ is the total concentration of malate in the vacuole (mol.L^{-1}), h=10^{-pHvac}, and K'$_1$ and K'$_2$ are the apparent acidity constants of malate (mol.L^{-1}).

In plant cells, $\Delta\psi$ is mainly generated by the tonoplastic proton pumps, which catalyze the active transport of protons into the vacuole. Two types of pumps are present on the tonoplast of fruit cells: the ATPase (Ratajczak, 2000) and the PPiase (Maeshima, 2000), which respectively hydrolyze ATP and PPi as a source of energy. Both are known to be active in most fruits (Müller *et al.*, 1997; Suzuki *et al.*, 2000; Terrier *et al.*, 1998), but for the sake of simplicity, only ATPase was taken into account in the model. Proton pumping can occur only if the variation in free energy of the chemiosmotic reaction ΔG_{ATPase} defined below is negative:

$$\Delta G_{ATPase} = \Delta G_{ATP} + nF\Delta\psi - nRT\ln(10) * (pH_{vac} - pH_{cyt}) \quad (4)$$

where ΔG_{ATP} is the free energy of ATP hydrolysis (J.mol^{-1}), n is the coupling ratio i.e. the number of protons pumped by hydrolyzed ATP, pH_{vac} and pH_{cyt} are vacuolar and cytosolic pH respectively.

The pH gradient across the tonoplast plays a role in this equation, both directly, and because it affects the coupling ratio n. Lobit et al. (2006) fitted the following equation to the data of Davies et al. (1994) to calculate the coupling ratio:

$$n = n_0 + \alpha(pH_{vac} - 7) + \beta 10^{(pH_{cyt} - 7)} \quad (5)$$

where n_0, α, and β are fitted parameters.

The approach used in this model is to represent changes in vacuolar composition as a succession of stationary states during which malate concentration, pH_{vac}, and $\Delta\psi$ can be considered to be constant. The assumption is that the transport of the di-anion malate and protons operate in conditions close to their respective thermodynamic equilibrium.

Assuming that the di-anion malate is at thermodynamic equilibrium across the tonoplast implies that $\Delta G_{Mal}{}^{2-}$=0. So rewriting and combining equations 1, 2 and 3 gives:

$$[Mal_{vac}] = \frac{1}{a_{Mal_{vac}^{2-}}} * \frac{h^2 + hK_1' + K_2' K_1'}{K_2' K_1'} * \left(Mal_{cyt}^{2-}\right) * \exp^{\frac{2F\Delta\psi}{RT}} \quad (6)$$

Assuming that proton transport occurs at thermodynamic equilibrium implies that ΔG_{ATPase}=0. So, rewriting and combining equations 4 and 5 gives:

$$\Delta\psi = \frac{-\Delta G_{ATP}}{(n_0+\alpha(pH_{vac}-7)+\beta 10^{(pH_{cyt}-7)})F} + \frac{RT}{F}\ln(10) * (pH_{vac} - pH_{cyt}) \quad (7)$$

The acid/base composition of the vacuole determines $a_{Mal^{2-}vac}$, K'_1, K'_2, and pH_{vac}. These variables are calculated using a model of pH prediction that was described and validated on banana fruit in a previous paper (Etienne *et al.*, 2013a). As input variables, the model requires the concentrations of the three main organic acids present in banana pulp, citrate, malate, and oxalate (oxalate being present in large amounts at the green stage (Etienne *et al.*, 2013a)), and of the main soluble mineral elements, namely potassium, magnesium, chloride, calcium, and phosphorus.

Solving the malate model means solving a system of equations with two unknowns, $[Mal_{vac}]$ and pH_{vac}, and six parameters, pH_{cyt}, (Mal^{2-}_{cyt}), ΔG_{ATP}, n_0, α, and β. Once the concentration of malate in the vacuole is determined, the concentration of malate in the pulp can be calculated by assuming that the volume of water in the vacuole is equal to the water mass of the pulp:

$$[Mal_{fruit}] = [Mal_{vac}] * \frac{FW-DW}{FW} * 1000 \quad (8)$$

where $[Mal_{fruit}]$ is the concentration of malate in the pulp (mmol.Kg FW^{-1}), FW and DW are the pulp fresh weight and pulp dry weight respectively (g).

2.2.2 Changes in ΔG_{ATP} during banana development

According to the sensitivity analysis of the model performed by Lobit et al. (2006) on peach, malate accumulation is strongly dependent on ΔG_{ATP}. According to the literature, ΔG_{ATP} can vary considerably depending on cytosolic conditions (Davies *et al.*, 1993; Roberts *et al.*, 1985), so that one may expect ΔG_{ATP} to vary during banana development. The possible variation of ΔG_{ATP} required (according to the model) to sustain malate accumulation during banana growth and post-harvest ripening was assessed by reorganizing and combining equations 6 and 7, and by assuming that pH_{cyt}=7 (common notion of a neutral cytosol), (Mal^{2-}_{cyt}) = 0.001 mol.L^{-1} (reasonable value according to Lobit et al. (2006)), $a_{Mal^{2-}vac}$ =0.3 (average value found by the banana pH model (Etienne *et al.*, 2013a)), and parameters n_0=4, α=0.3, and β=-0.12 (to calculate n with equation 5) (Lobit *et al.*, 2006).

$$\Delta G_{ATP} = nRT\ln(10) * \left(pH_{vac} - pH_{cyt}\right) - \frac{nRT}{2}\ln\left(\frac{K'_2K'_1[Mal_{vac}]a_{Mal^{2-}_{vac}}}{(h^2+hK'_1+K'_2K'_1)\left(Mal^{2-}_{cyt}\right)}\right) \quad (9)$$

Changes in ΔG_{ATP} over time, calculated with equation 9 and using 12 datasets including three cultivars, two developmental stages (pre- and post-harvest stage), and 2 years, were plotted. During fruit growth, ΔG_{ATP} varied little (*Fig. III.7.A*) whereas during post-harvest ripening, there was a negative relationship between ΔG_{ATP} and the number of days after ethylene

treatment in all three cultivars (*Fig. III.7.B*). Thus, we considered ΔG_{ATP} as a constant during fruit growth and simulated the observed relationship with days after ethylene treatment during ripening by the following function:

$$\Delta G_{ATP} = G_1 * DAE^2 + G_2 * DAE + G_3 \quad (10)$$

where DAE is the day after ethylene treatment, and G_1 (J.mol^{-1}.day^{-2}), G_2 (J.mol^{-1}.day^{-1}), and G_3 (J.mol^{-1}) are fitted parameters.

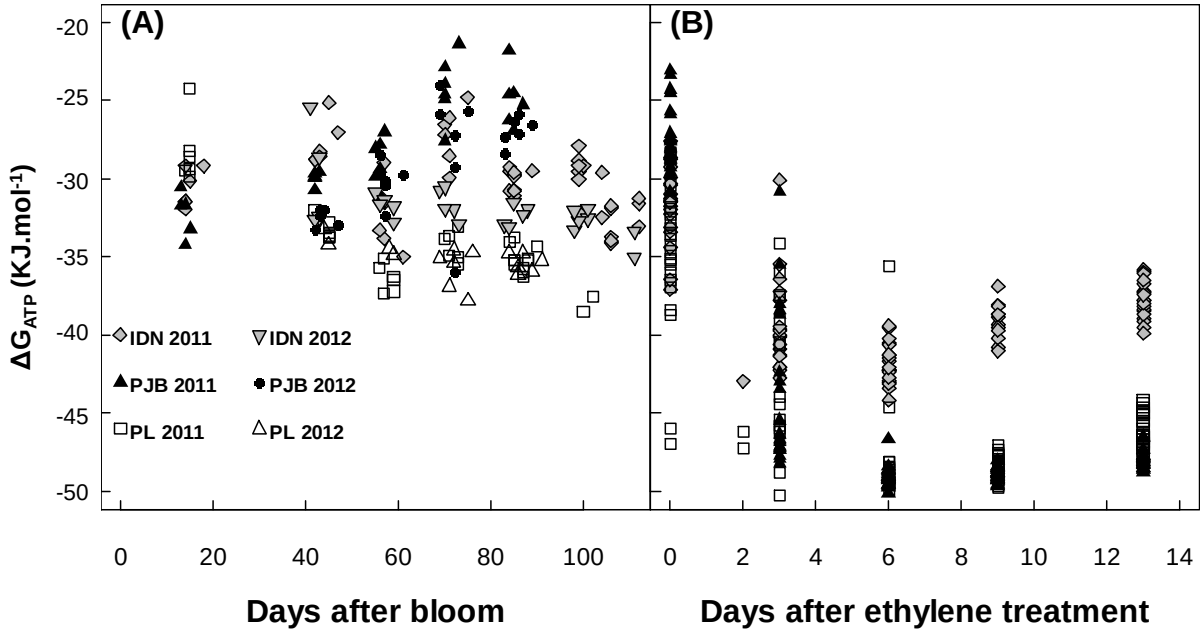

Figure III-7 Variations in ΔG_{ATP} as a function of (A) days after bloom during fruit growth, and (B) days after ethylene treatment during post-harvest ripening for cultivars IDN, PJB, and PL. These values were calculated with equation 9 using the data for the three cultivars for 2011 and 2012.

2.2.3 Model inputs

The input variables required were temperature (T; K), pulp fresh weight (FW; g), pulp dry weight (DW; g), pulp potassium content (K; mol.L^{-1}), pulp magnesium content (Mg; mol.L^{-1}), pulp phosphorus content (P; mol.L^{-1}), pulp calcium content (Ca; mol.L^{-1}), pulp chloride content (Cl; mol.L^{-1}), pulp citrate content (mol.L^{-1}), and pulp oxalate content (mol.L^{-1}).

2.2.4 Plant materials and experimental conditions

All experiments were conducted at the *Pôle de Recherche Agroenvironnementale de la Martinique* (PRAM, Martinique, French West Indies; latitude 14°37N, longitude 60°58W, altitude 16 m) using three cultivars of dessert banana (Musa spp.) diploids AA, differing in predominant organic acid at the eating stage: Indonesia 110 (IDN), Pisang Jari Buaya (PJB),

and Pisang Lilin (PL). Experiments were conducted during the 2011 and 2012 growing seasons on continental alluvial soil. In both growing seasons, irrigation was adjusted to the amount of rainfall to supply at least 5 mm of water per day, and non-systemic fungicide was applied to control foliar diseases. During the first period of bunch growth (March–November 2011) the mean daily temperature was 27 ± 1.2 °C. During the second period of bunch growth (February-August 2012) the mean daily temperature was 26± 0.9 °C.

2011 experiment: effect of fruit load on banana pulp acidity

For each cultivar, 36 plants were randomly chosen and tagged at inflorescence emergence. Two contrasted fruit loads were used: 18 plants of each cultivar were used as the control treatment i.e. high fruit load, and 18 other plants were highly pruned i.e. low fruit load. In the control treatment, the number of leaves and hands left on the plants were calculated in order to have the same leaf area: fruit ratio among cultivars (approximately equal to 0.5 cm^2 leave. g $fruit^{-1}$). Thus, 15 days after inflorescence emergence, 8, 6, and 5 leaves were left on the plant for cultivars IDN, PL, and PJB respectively, and the top 10, 5 and 7 hands were left on the bunch for cultivars IDN, PL, and PJB respectively. To ensure the situation was the same among the three cultivars, fruit pruning in low fruit load treatment was calculated to increase the leaf area: fruit ratio by approximately 2.5. Consequently, 15 days after inflorescence emergence, the top 4, 2, and 3 hands were left on the bunch for cultivars IDN, PL, and PJB respectively. Banana plants received 12 g of nitrogen, 1.7 g of phosphorus, and 23 g of potassium at 4-week intervals during fruit growth.

2012 experiment: effect of potassium fertilization on banana pulp acidity

Two plots containing 50 banana plants of each cultivar were planted. Two contrasted levels of potassium fertilization were started six months before the beginning of fruit sampling. For each cultivar, one plot received 124 g of potassium per plant (high potassium fertilization) at 4-week intervals, while the other received no potassium at all. All the banana plants received 12 g of nitrogen and 10 g of phosphorus at 4-week intervals. Twenty-four plants of each cultivar were randomly chosen in each plot and tagged at inflorescence emergence. At 15 days after inflorescence emergence, 9, 7, and 9 leaves were left on cultivars IDN, PL, and PJB respectively, which corresponded to the average leaf number in 2012, and the top 10, 5, and 7 hands were left on the bunch of cultivars IDN, PL, and PJB respectively, which corresponded to a high fruit load.

Monitoring fruit growth

In the two growing seasons, six bunches were selected for each cultivar*treatment combination. One fruit located in the internal row of the second proximal hand was collected for analyses every 15 days. Natural ripening on standing plants, i.e. when the first yellow finger appears, determined the end of sampling.

Monitoring post-harvest fruit ripening

In the 2011 experiment, two harvest stages were studied. The stages were calculated so that each cultivar was at 70% and 90% of the average flowering-to-yellowing time (FYT) of the bunch on the tree. At each harvest stage, six bunches per cultivar and per treatment were harvested. In the 2012 experiment, only one harvest stage was studied. For each cultivar, this stage was calculated to be 75% of the average FYT of the bunch on the tree. Six bunches per cultivar and per treatment were harvested. After the bunches were harvested, the second proximal banana hand per bunch was rinsed and dipped in fungicide (bitertanol, 200 $mg.L^{-1}$) for 1 min. The fruits were placed in a plastic bag with 20 μm respiration holes and stored in boxes for 6 days at 18 °C. The fruits were then stored in a room at 18 °C and underwent ethylene treatment (1 $mL.L^{-1}$ for 24 h) to trigger the ripening process. After 24 h, the room was ventilated. Bananas were maintained at 18 °C during 13 days. One banana fruit was sampled before ethylene treatment, and at day 3, 6, 9 and 13 after ethylene treatment.

2.2.5 Biochemical measurements

The fresh and dry pulp of each sampled fruit was weighed. The dried pulp was then ground to obtain a dry powder for biochemical measurements. Citric acid and malic acid concentrations were determined according to Etienne et al. (2013a) using an enzymatic method and a microplate reader. The soluble oxalic acid concentration was determined using the LIBIOS Oxalic acid assay kit. Pulp soluble K, Mg, and Ca concentrations were determined by mass spectrometry, and soluble P was measured by colorimetry (Martin-Prével *et al.*, 1984). The Cl concentration in the pulp was determined by potentiometry using the automatic titrator TitroLine alpha (Walinga *et al.*, 1995).

2.2.6 Model solving and parameterization

The model was computed using R software (R Development Core Team, http://www.r-project.org). For each sampling date, the system was solved to calculate the concentration of malate in the pulp, using the "nleqslv" function of the R software, which solves a system of

non-linear equations using a Broyden method (http://cran.r-project.org/web/packages/nleqslv/index.html). (Mal^{2-}_{cyt}) was set at 0.001 mol.L^{-}1 which is within the range mentioned by Lobit et al. (2006). pH_{cyt} was set at 7 according to the common notion of a neutral cytosol. For parameters n_0, α, and β, which define the stoechiometry of the pump ATPase, Lobit et al. (2006) estimated values very close to those found by fitting equation 5 to the data of Davies et al. (1994) and Kettner et al. (2003). This suggests that these parameters correspond to a structural characteristic of ATPase and are unlikely to vary much, so we chose to set them to the values found by Lobit et al. (2006) (*Table III-4*).

2.2.7 Model calibration

Parameter ΔG_{ATP} was estimated by fitting the model to observed values of the pre-harvest 2011 dataset separated by cultivar. Parameters G_1, G_2, and G_3 were estimated by fitting the model to ΔG_{ATP} values calculated according to equation 9 from the 2011 post-harvest dataset separated by cultivar. The harvest stage was not taken into account since there were no differences in the variations in ΔG_{ATP} calculated with equation 9 between fruits harvested at 70% and 90% of FYT (data not shown). Parameters were estimated using the "hydroPSO" function of R software (Zambrano-Bigiarini et al., 2013). The hydroPSO function uses the computational method of particle swarm optimization (PSO) that optimizes a problem by iteratively trying to improve a candidate solution with regard to a given measure of quality. Parameters were estimated by minimizing the following criterion:

$$\sum_j \sum_i (x_{ij} - y_{ij})^2 \quad (14)$$

where x_{ij} is the predicted value and y_{ij} is the observed value of the fruit of the j^{th} banana plant at date t_i.

2.2.8 Goodness of fit and predictive quality of the model

The goodness of fit of the model was evaluated using two commonly used criteria, the root mean squared error (RMSE) and the relative root mean squared error (RRMSE), to compare the mean difference between simulated and observed results (Kobayashi and Salam, 2000). The smaller the value of RMSE and RRMSE, the better the fit.

$$\mathrm{RMSE} = \sqrt{\frac{(\sum (Y_i - X_i)^2)}{n}} \quad (15)$$

where Y_i is the predicted value of the fruit i, and X_i is the measured value of the fruit i. n is the data number.

$$\mathrm{RRMSE} = \frac{\mathrm{RMSE}}{\bar{x}} \quad (16)$$

where $\bar{x}$ is the mean of all observed values.

The predictive quality of the model, which ascertains model validity over various scenarios, was quantified by the RMSE and RRMSE calculated using the 2012 data set.

2.2.9 Sensitivity analysis of the model

The sensitivity of the malate model during banana growth and post-harvest ripening to variations in parameter and input values was quantified by normalized sensitivity coefficients, defined as the ratio between the variation in malate concentration (ΔM) relative to its standard value (M), and the variation in the parameter or input value (ΔP) relative to its standard value (P) (Monod et al., 2006).

$$\text{Normalized sensitivity coefficient} = \frac{\Delta M/M}{\Delta P/P} \quad (17)$$

The interpretation of the sensitivity coefficient is referred to as local sensitivity analysis since these coefficients provide information on the effect of small changes in the parameters on the model response. They do not provide information about the effect of simultaneous or large parameter changes. Normalized sensitivity coefficients were calculated by altering one parameter or input variable by ±0.1% while keeping all other parameters and inputs at their default values. Sensitivity analysis of the model to parameters was conducted by considering pH_{vac} as known (approximated by the measured pH of the pulp). Sensitivity analysis of the model to pulp composition and temperature was conducted by considering the total model, i.e. the combination of the malate and pH models.

2.3 Results

2.3.1 Overview of the effects of the cultivar and of the treatment

The effects of cultivar and treatments on malate concentration in banana pulp during the pre and post-harvest stages are detailed in a previous paper (Etienne *et al.*, 2014), so only the main conclusions are presented here. During banana growth, the concentration of malate increased and was significantly affected by the cultivar in both 2011 and 2012. During banana post-harvest ripening, the ripening stage and the cultivar had a significant effect on the concentrations of malate in 2011 and 2012. Fruits harvested later (at 90% of FYT) had significantly higher concentrations of malate at the beginning of ripening and lower concentrations at the end of ripening. Low fruit load and potassium fertilization significantly increased fruit fresh mass but had no effect on malate concentration in the three cultivars either during growth or post-harvest ripening.

2.3.2 Model calibration and evaluation

Values of the estimated parameters of the model are summarized in *Table III-4*. The values of ΔG_{ATP} estimated during banana growth were higher (less negative) than the values commonly found in the literature, which range between -50 and -58 KJ.mol^{-1} (Briskin and Reynolds-Niesman, 1991; Davies *et al.*, 1993; Rea and Sanders, 1987; Roberts *et al.*, 1985). The ΔG_{ATP} estimated for the PL cultivar was lower (more negative) than those estimated for the IDN and PJB cultivars. During post-harvest ripening, values of ΔG_{ATP} calculated from equation 10 with the estimated values of parameters G_1, G_2, and G_3 were in the range of values found in the literature (between -45 and -55 KJ.mol^{-1}) (data not shown). From day 6 to the end of ripening, cultivars PJB and PL had a lower (more negative) ΔG_{ATP} than cultivar IDN.

Table III-4 Values of model parameters

Parameter	Value			Unit	Description	Origin
	IDN	PJB	PL			
pH_{cyt}		7		Unit pH	Cytosolic pH	Literature
(Mal^{2-}_{cyt})		0.001		mol.L^{-1}	Cytosolic activity of the di-anion malate	Literature
n_0		4		dimensionless	Parameters to calculate the coupling ratio of the proton pump	Literature
α		0.3		dimensionless		Literature
β		-0.12		dimensionless		Literature
ΔG_{ATP}	-36.9*10^3	-39.1*10^3	-47.4*10^3	J.mol^{-1}	Free energy of ATP hydrolysis during banana growth	Estimated
G_1	75	69	110	J.mol^{-1}.day^{-2}	Parameters to calculate ΔG_{ATP} as a function of the number of days after ethylene treatment during banana post-harvest ripening	Estimated
G_2	-1176	-1108	-1959	J.mol.day^{-1}		Estimated
G_3	-45.2*10^3	-48.9*10^3	-46.3*10^3	J.mol^{-1}		Estimated

Simulated and observed malate concentrations during banana growth and post-harvest ripening are presented in *Fig. III.8* and *III.9* respectively. For the three cultivars, the goodness of fit of predictions of data from 2011 was satisfactory both during banana growth and post-harvest ripening. During growth, the RMSEs were between 2.86 and 3.43 mmol.Kg FW^{-1}, and RRMSEs between 0.25 and 0.38. During post-harvest ripening, the RMSEs were between 6.07 and 11.08 mmol.Kg FW^{-1}, and RRMSEs between 0.18 and 0.32. However, model validation during banana growth was not satisfactory in any of the three cultivars, as revealed by the RMSEs and RRMSEs of predictions of data from 2012, whose values ranged between 3.67 and 5.60 mmol.Kg FW^{-1}, and between 0.40 and 0.74 respectively. Model validation during banana post-harvest ripening for the three cultivars was satisfactory, as revealed by the RMSEs and RRMSEs of predictions of data from 2012, whose values ranged between 6.55 and 10.54 mmol.Kg FW^{-1}, and between 0.24 and 0.29 respectively. Statistical analysis revealed that the model predicted a large effect of the cultivar and of fruit age, and no effect of the fruit load and potassium fertilization on malate concentration during banana growth (*Appendix 2.1*) and post-harvest ripening (*Appendix 2.2*) which is in accordance with observed data. The model predicted a small effect of fruit age at harvest in agreement with observed data, but was not able to simulate the minor differences correctly (data not shown).

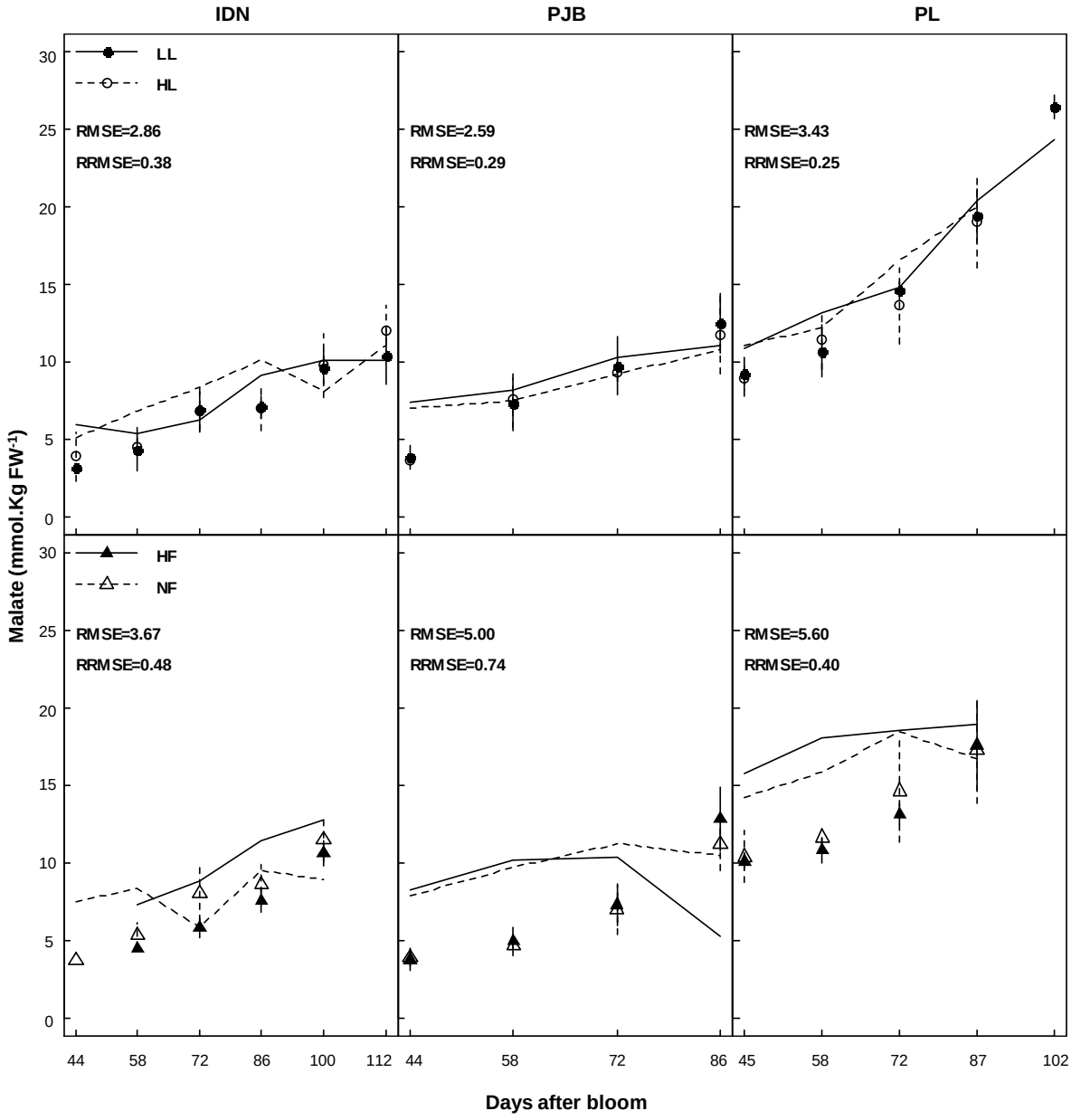

Figure III-8 Measured (symbols) and simulated (lines) malate concentrations in the pulp of banana of cultivars IDN, PJB, and PL during fruit growth. The cultivars were grown under two contrasted fruit loads in 2011 (LL: low fruit load; HL: high fruit load), and two contrasted levels of potassium fertilization in 2012 (NF: no potassium fertilization; HF: high potassium fertilization). Data are means ± s.d (*n*=6). The RMSE (mmol.100g FW^{-1}) and RRMSE are indicated in each graph.

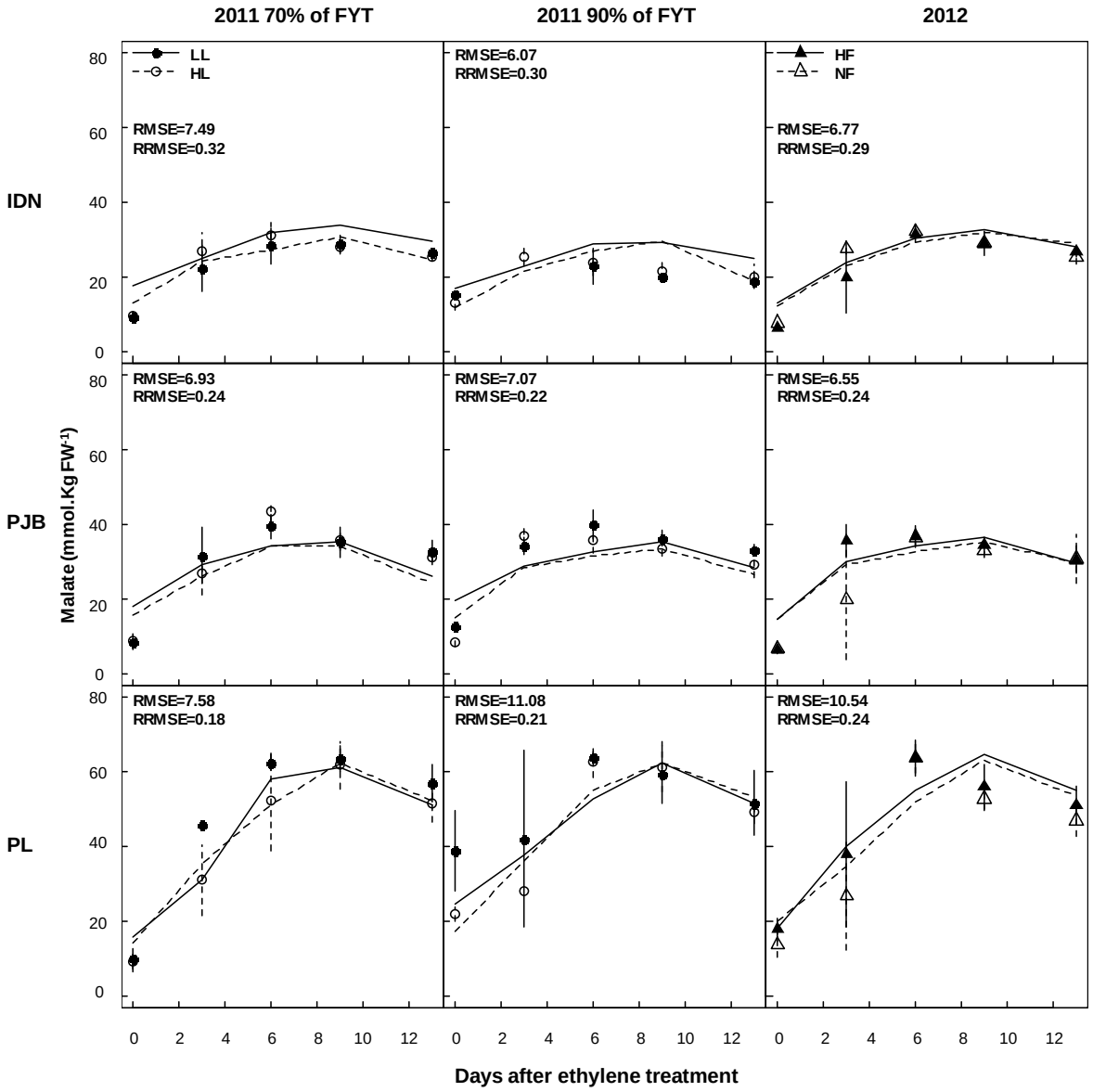

Figure III-9 Measured (symbols) and simulated (lines) malate concentrations in the pulp of banana of cultivars IDN, PJB, and PL during fruit post-harvest ripening. The cultivars were grown under two contrasted fruit loads in 2011 (LL: low fruit load; HL: high fruit load), and two contrasted levels of potassium fertilization in 2012 (NF: no potassium fertilization; HF: high potassium fertilization). In 2011, fruits were harvested at two different stages: early stage (70% of FYT) and late stage (90% of FYT). Data are means ± s.d (*n*=6). The RMSE (mmol.100g FW^{-1}) and RRMSE are indicated in each graph.

2.3.3 Sensitivity analysis of the model

A sensitivity coefficient (SC) was calculated to identify model responses to variations in parameters and inputs. A positive and negative sign of SC correspond, respectively, to a response in the same or reverse direction as the variation in the parameter or input. The larger the absolute value of SC, the more highly sensitive the model is to the parameter or input concerned. Since the SC behaved similarly between years with respect to a given cultivar, only results in 2011 are presented here. The SCs of model parameters behaved similarly with respect to the three cultivars and between banana growth (*Fig. III.10.A*) and post-harvest ripening (*Fig. III.10.B*). (Mal^{2-}_{cyt}) had a positive effect on malate concentration. This is as expected, since an increase in (Mal^{2-}_{cyt}) increases the gradient of concentration of the di-anion malate in favor of its transport into the vacuole. Malate concentration was greatly influenced by pH_{cyt} in a negative way. Malate accumulation decreases when cytosolic pH increases because the gradient of pH across the tonoplast increases, which depresses the $\Delta\psi$ (see equation 7). Increasing ΔG_{ATP}, i.e. a less negative ΔG_{ATP}, (which means increasing G_1, G_2, or G_3 during post-harvest ripening) depressed malate concentration, because it decreased proton pumping and consequently the $\Delta\psi$. The parameter n_0 had a strong negative effect on malate accumulation. This is as expected, since increasing n_0 decreases the $\Delta\psi$. The sensitivity to α was positive because increasing α increases the $\Delta\psi$. The sensitivity to β was negative because increasing β decreases the $\Delta\psi$.

The SCs of model inputs during banana growth and post-harvest ripening are shown in *Fig. III.11* and *III.12* respectively. Increasing citrate and oxalate concentration strongly depressed malate concentration during banana growth in all three cultivars. During post-harvest ripening, citrate and oxalate concentration also had a negative but less important effect on malate concentration. Increasing K concentration had a strong positive effect on malate concentration during growth and a lesser effect during post-harvest ripening in the three cultivars. Increasing P concentration slightly depressed malate concentration both during growth and post-harvest ripening in the three cultivars. Increasing the Mg concentration had a positive effect on malate concentration during growth and a lesser effect during post-harvest ripening in all three cultivars. Increasing the Ca concentration had a slight positive effect on malate concentration both during growth and post-harvest ripening in all three cultivars. Increasing the Cl concentration had a negative effect on malate concentration during banana growth, and a lesser effect during post-harvest ripening in all three cultivars. Increasing temperature depressed malate accumulation during banana growth and post-harvest ripening in all three cultivars.

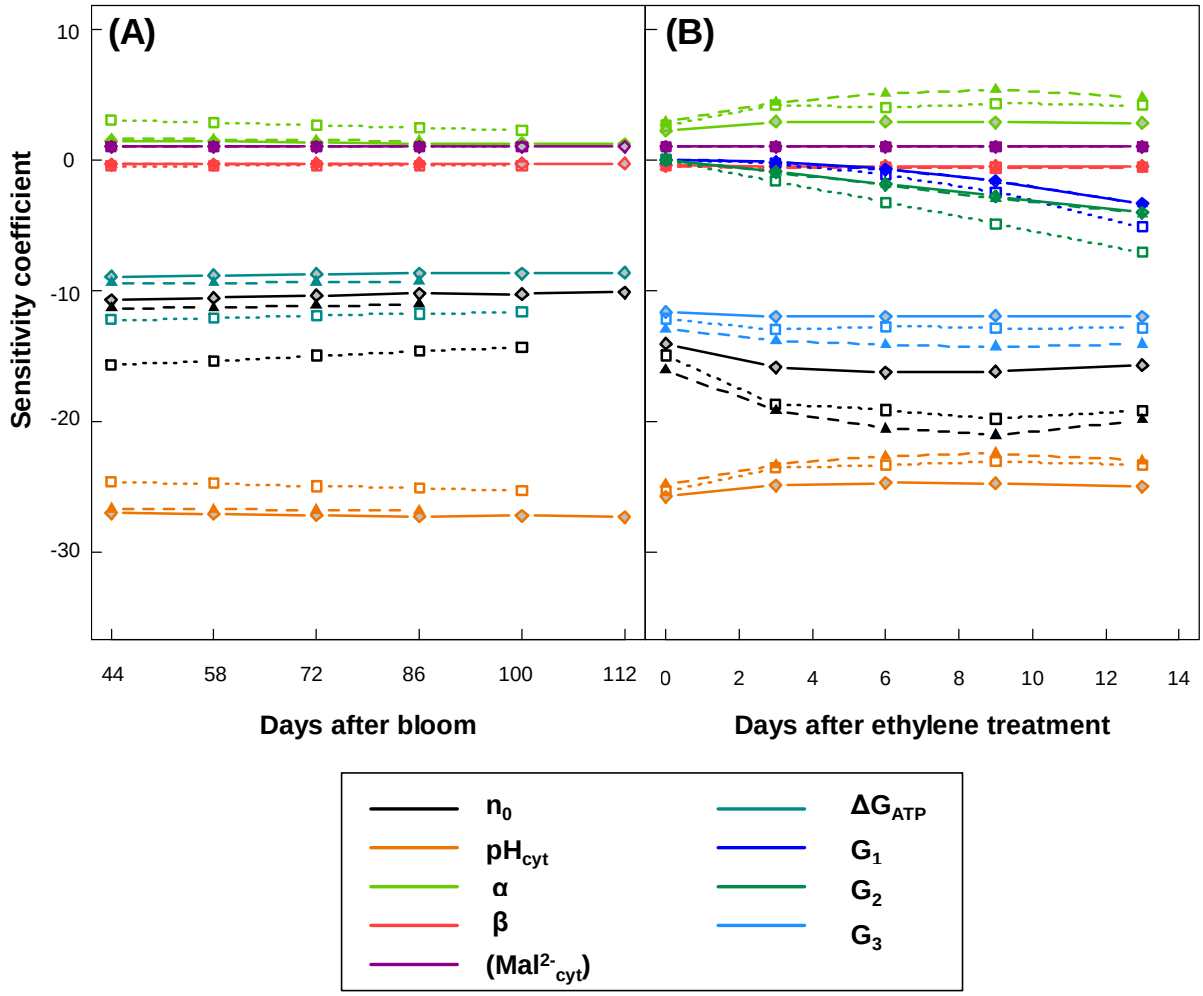

Figure III-10 Normalized sensitivity coefficients of the parameters of the malate model during (A) banana growth, and (B) post-harvest ripening for cultivar IDN (gray diamonds), PJB (black triangles), and PL (white squares).

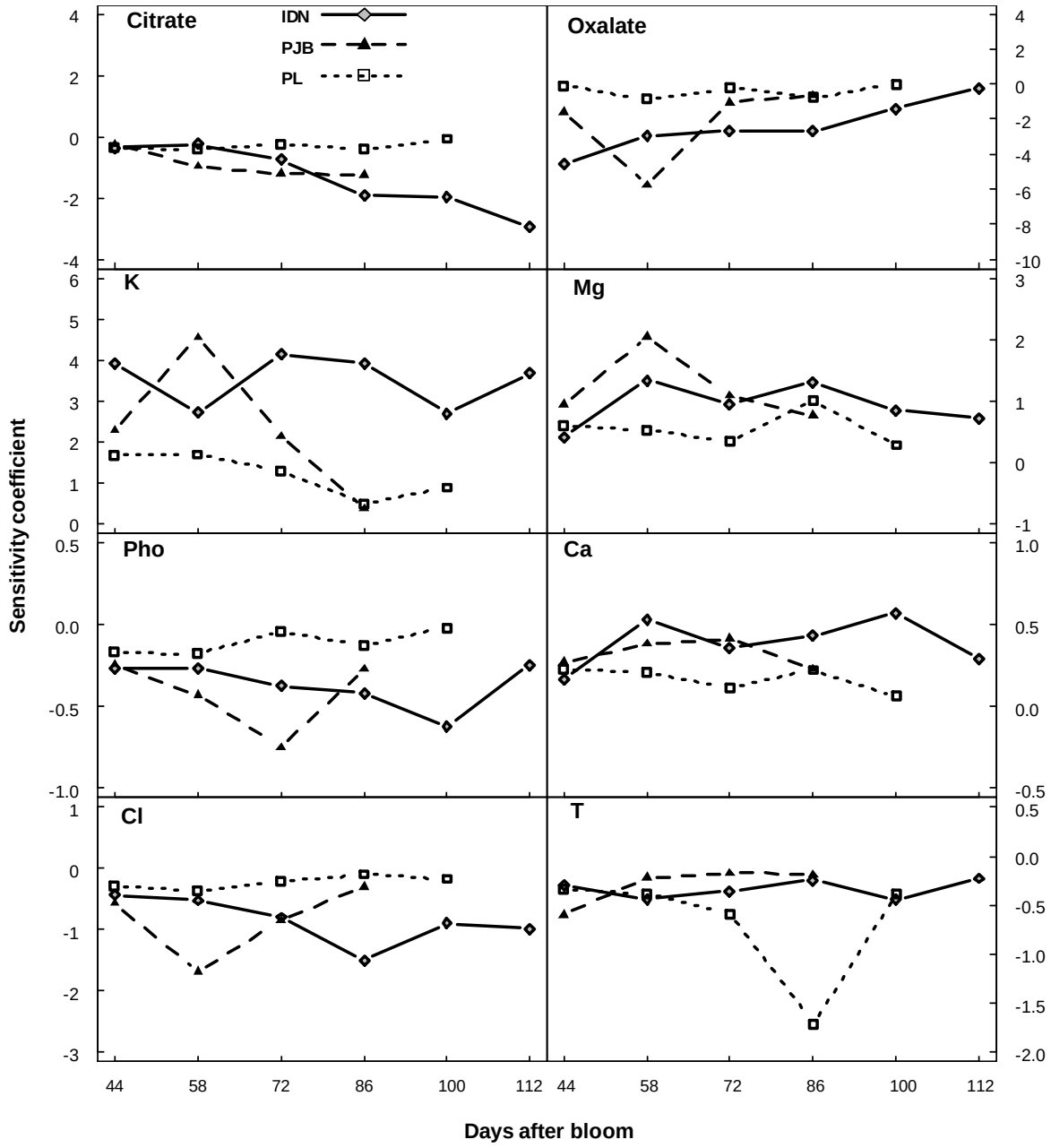

Figure III-11 Normalized sensitivity coefficients of the concentrations of citrate, oxalate, potassium (K), magnesium (Mg), phosphorus (P), calcium (Ca), and chloride (Cl) in the pulp, and of temperature (T) during banana growth for cultivars IDN, PJB, and PL.

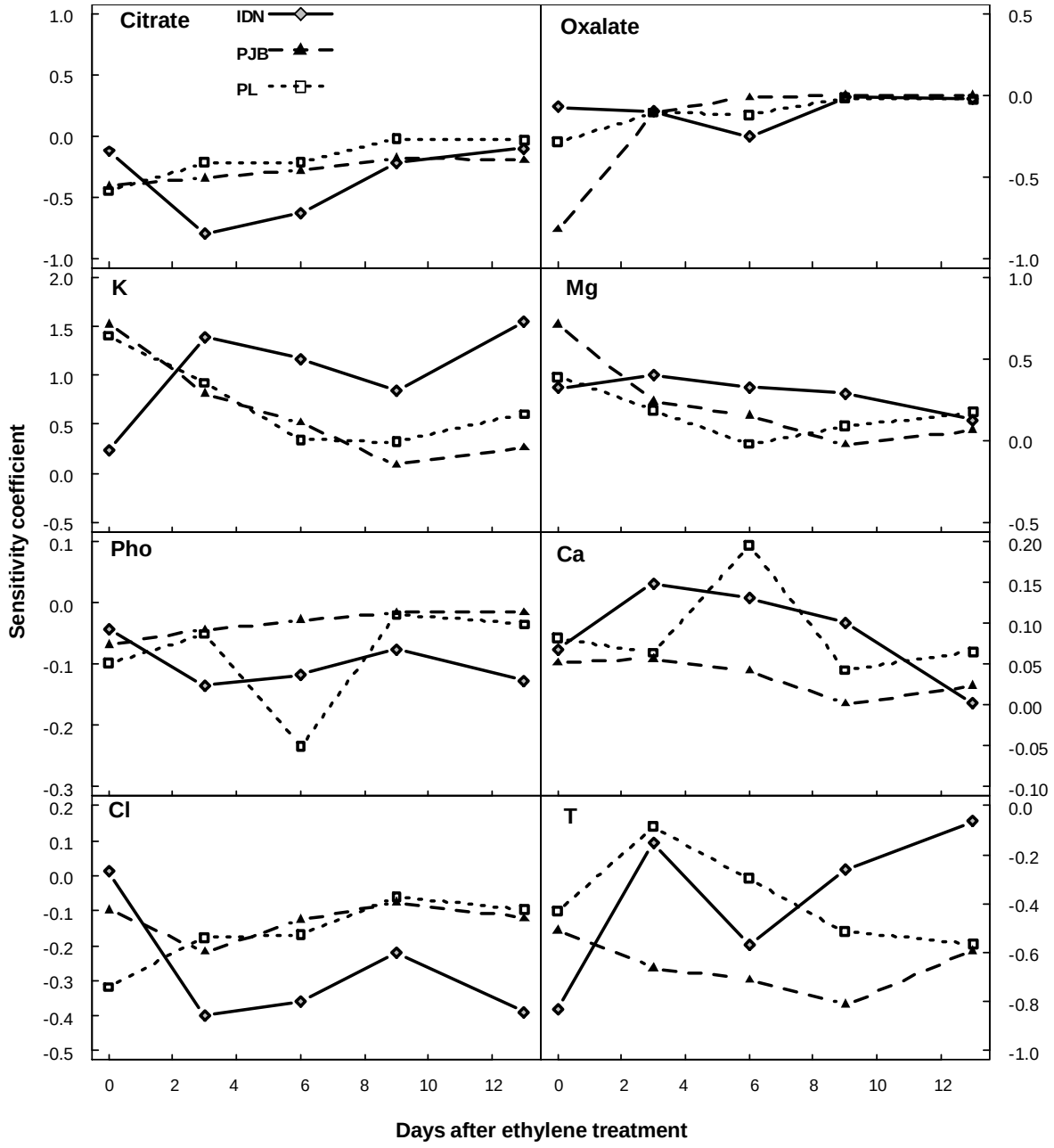

Figure III-12 Normalized sensitivity coefficients of the concentrations of citrate, oxalate, potassium (K), magnesium (Mg), phosphorus (P), calcium (Ca), and chloride (Cl) in the pulp, and of temperature (T) during banana post-harvest ripening for cultivars IDN, PJB, and PL.

2.4 Discussion

2.4.1 Quality of predictions and model simplifications

The concentrations of malate in the pulp were satisfactorily simulated by the model during post-harvest ripening in the two experimental years, whereas model validation during banana growth was not convincing. Differences in prediction quality between the pre and post-harvest stages have several possible explanations. First, the pH model was less accurate during banana growth than during post-harvest ripening (Etienne *et al.*, 2013a) which is certainly partially responsible for the discrepancies between observed and predicted malate concentrations during banana growth. Second, we assumed that the $\Delta\psi$ was determined only by the ATPase functioning, whereas in reality, $\Delta\psi$ may also depend on the transport of mineral ions across the tonoplast (which generate currents and/or proton movements) and on the contribution of the PPiase to proton pumping (Etienne *et al.*, 2013b). To check if this hypothesis is reasonable, we compared the $\Delta\psi$ required to reach the thermodynamic equilibrium of the di-anion malate across the tonoplast (by inverting equation 6) with the $\Delta\psi$ predicted by the ATPase model (by inverting equation 7). During post-harvest ripening, the changes in both $\Delta\psi$ were very similar (*Fig. III.13.B*). Therefore, the ATPase model appears to be adequate for post-harvest ripening. This is consistent with the fact that at this stage, when mineral concentrations in the pulp remain constant (Etienne *et al.*, 2013a), there should be no transport of minerals across the tonoplast. In addition, PPiase activity should be negligible since starch synthesis, which leads to the synthesis of PPi (Maeshima, 2000), has stopped. During banana growth, there were some discrepancies between the variations in the $\Delta\psi$ calculated with equations 6 and 7, especially for cultivars IDN and PJB, for which malate predictions were worst (*Fig. III.13.A*) and the ATPase model overestimated the $\Delta\psi$ required to sustain malate accumulation. During banana growth, minerals, especially potassium, accumulate in the vacuole of pulp cells (Etienne *et al.*, 2013a), which implies that electric currents may alter the $\Delta\psi$. Moreover, starch synthesis is high, so that PPi might be available in large quantities and PPiase activity might consequently be important (Maeshima, 2000), however, to our knowledge, no information is available concerning the tonoplastic PPiase of banana fruit cells. In the future, predictions of malate concentrations during banana growth might be improved by taking into account mineral fluxes and the possible contribution of the PPiase. Third, we assumed that pH_{cyt} and (Mal^{2-}_{cyt}) remained constant during banana development, whereas in reality they certainly fluctuate in response to the supply of acids and bases by the sap, their metabolism, and their vacuolar storage. Since the model was very

sensitive to cytosolic pH, one way to improve model predictions during fruit growth would be to take these possible fluctuations into account.

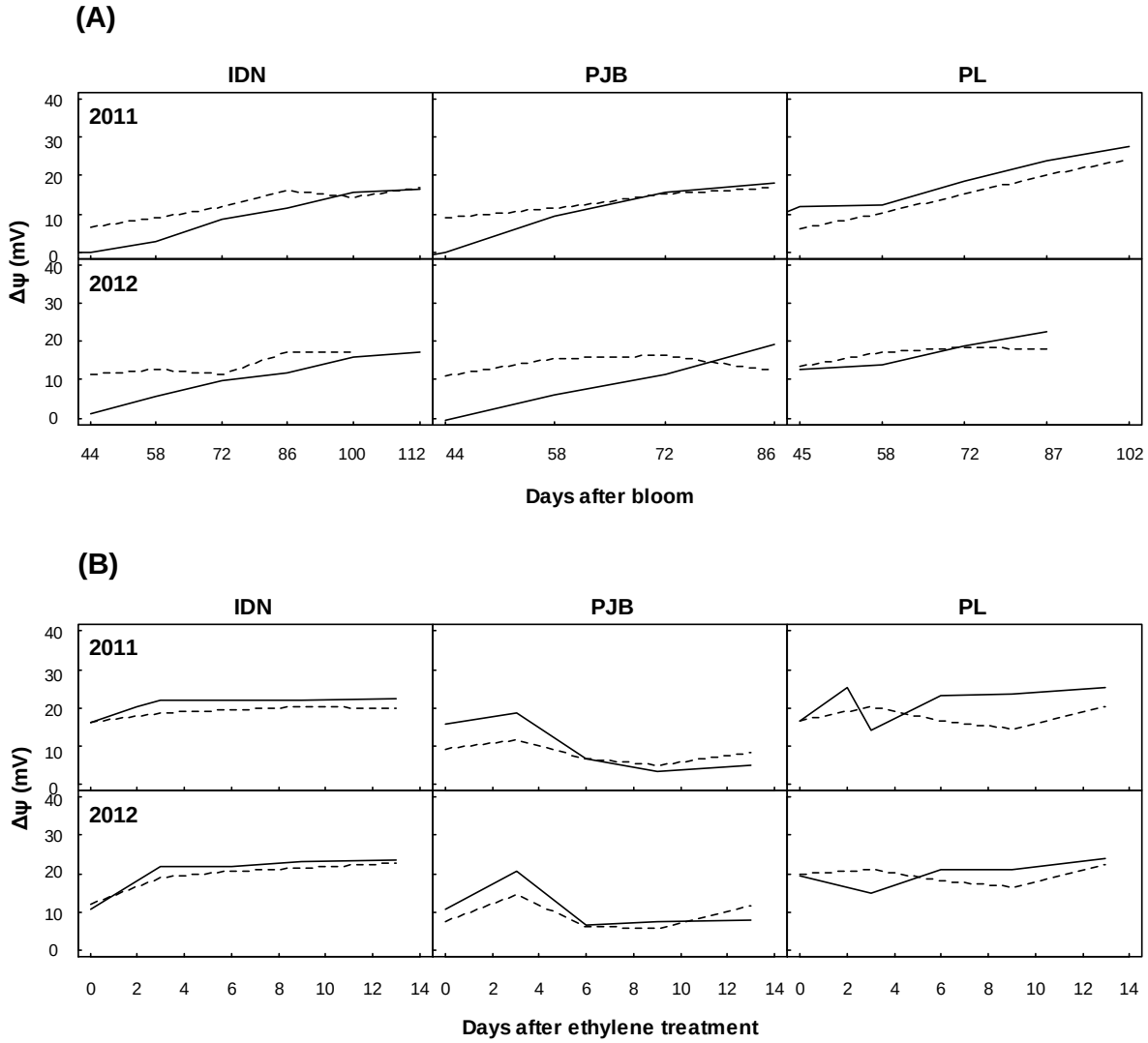

Figure III-13 Changes in Δψ calculated from equation 6 (solid line) and from equation 7 (dashed line) during (A) banana growth, and (B) post-harvest ripening for cultivars IDN, PJB, and PL in 2011 and 2012.

2.4.2 Predicted variability in vacuolar malate accumulation among cultivars and between pre and post-harvest stages

The model revealed possible differences in vacuolar malate accumulation among the three cultivars studied here. During banana growth, the value of estimated ΔG_{ATP} was a lot more negative for cultivar PL than for the two other cultivars, suggesting that the higher concentrations of malate in the fruits of cultivar PL could be the result of higher proton pumping due to a higher energy of ATP hydrolysis. During post-harvest ripening, the model predicted a more negative ΔG_{ATP} after ethylene treatment than before. This could be linked to

the climacteric crisis. Indeed, the dramatic increase in respiration in response to ethylene treatment might be associated with an enhanced level of ATP exceeding the needs of the cells (John and Marchal, 1995). Consequently, the ratio of ATP to ADP might increase greatly, making ΔG_{ATP} more negative, which would increase the activity of the proton pumps and the accumulation of malate. The predicted increase in the activity of the proton pumps during banana ripening is in agreement with the results of Terrier et al. (2001) on grape berry. The slight decrease in malate concentration at the end of ripening may be the consequence of a higher rate of malate leakage across the tonoplast, as observed in grape (Terrier *et al.*, 2001). However, since this phenomenon was not represented in the present model, it resulted in a less negative ΔG_{ATP} at the end of ripening. The model predicted a significantly less negative ΔG_{ATP} for cultivar IDN than for cultivars PL and PJB, suggesting that the lower concentrations of malate in cultivar IDN might be due to lower proton pump activity. Differences in malate accumulation between cultivars PL and PJB were not due to differences in ΔG_{ATP}, but to differences in vacuolar pH. Indeed, cultivar PL had a higher vacuolar pH than cultivar PJB during post-harvest ripening (Etienne *et al.*, 2013a). Vacuolar pH has contrasting effects on proton pump activity and malate dissociation. On one hand, increasing vacuolar pH decreases the di-anion concentration gradient, which reduces malate accumulation. On the other hand, it activates the proton pumps, which increases the $\Delta\psi$ and consequently malate accumulation. Finally, the positive effect on proton pump activity appears to prevail over the negative effect on malate dissociation. The possible involvement of vacuolar proton pumps in the difference in acidity among cultivars has been reported in peach (Etienne *et al.*, 2002) and in apple (Yao *et al.*, 2009). It should be noted that even though we assumed a common value of (Mal^{2-}_{cyt}) among cultivars, this parameter might be cultivar dependant, which would explain some of the differences in malate concentrations among cultivars. However, when we tried to fit the model with a common value of ΔG_{ATP} but different values of (Mal^{2-}_{cyt}) for the three cultivars, predictions were not in good agreement with the data (data not shown). This supports a role for ΔG_{ATP} in genotypic differences in malate accumulation.

2.4.3 Model behavior

The positive effect of potassium concentration on malate accumulation revealed by the sensitivity analysis is in agreement with the positive relationships found in ripe peaches between malate content and ash alkalinity, which is closely linked with potassium content (Genevois and Peynaud, 1974; Souty *et al.*, 1967). The model did not predict any effect of potassium fertilization on malate concentration, which is in agreement with observed data and

with the fact that no significant differences in potassium concentration in banana pulp were found between the two treatments (Etienne *et al.*, 2014). From a physiological point of view, increasing potassium concentration increases vacuolar pH (data not shown), which, according to the model, activates malate transport into the vacuole (see section 4.2). According to the model, magnesium and chloride concentrations can influence malate accumulation, especially during banana growth. Until now, no experiments have been conducted on the effects these minerals have on banana acidity, so it would be interesting to check the model predictions experimentally. The negative effect of organic acids (citrate and oxalate) on malate accumulation is the consequence of the decrease in vacuolar pH (see section 4.2). The negative effect of temperature on the concentration of malate predicted by the model is in agreement with the results of Lobit et al. (2006), and with some observations made in fields experiments on grape (Buttrose *et al.*, 1971; Kliewer, 1973; Rufner, 1982), and banana (Bugaud *et al.*, 2009). This is an interesting outcome of the model since temperature can easily be adjusted during post-harvest ripening. However, this result needs to be checked experimentally in post-harvest conditions.

2.4.4 Model validity

The model was based on the hypothesis that malate di-anion and proton transport across the tonoplast occurs in conditions that are close to their respective thermodynamic equilibrium. We can see if these hypotheses are reasonable by checking that a number of conditions are met. One condition is that the $\Delta\Psi$ calculated under the assumption of the model falls within the range expected from data cited in the literature. We found that the $\Delta\psi$ calculated with the equation of the thermodynamic equilibrium of the di-anion malate across the tonoplast (equation 6) or with the ATPase model (equation 7) was between 0 and 25 mV (*Fig. III.13*), i.e. comparable with the expected $\Delta\Psi$, which most authors estimate to be around 30 mV (Taiz and Zeiger, 2010). Therefore, the electric conditions of the vacuole appear to be compatible with the partitioning of the malate di-anion across the tonoplast in a state of thermodynamic equilibrium, and also with ATPase functioning in a state of thermodynamic equilibrium. Another condition is that the malate channel and the ATPase are not saturated; otherwise the transport of malate and proton would be limited by kinetic considerations and not just by thermodynamic considerations. In other words, the observed rate of malate accumulation must be lower than the maximum rate of malate transport through the di-anion channel, and the observed rate of proton accumulation must be lower than the maximum rate of proton transport through the ATPase. Concerning the malate channel, from the literature, Lobit et al. (2006) calculated a maximum rate of malate transport of around 20 $mmol.jour^{-1}.Kg\ FW^{-1}$.

From our data, it can be calculated that the maximum rate of malate accumulation during banana development was 15 mmol.jour^{-1}.Kg FW^{-1}. Therefore, the assumption that the activity of the malate transport system does not limit its storage appears to be reasonable. Concerning ATPase, from the literature, Lobit et al. (2006) calculated a maximum rate of proton transport of around 50 mmol.jour^{-1}.Kg FW^{-1}. From our data on titratable acidity (Etienne *et al.*, 2013a), it can be calculated that the maximum rate of proton accumulation during banana development was 27 mmol.jour^{-1}.Kg FW^{-1}. Therefore, the assumption that the activity of the ATPase does not limit proton pumping appears to be reasonable.

2.5 Conclusion

The model proposed in this study predicted the concentration of malate in banana pulp during post-harvest ripening with good accuracy for three cultivars. However, it needs to be improved to predict malate concentration during banana growth, maybe by taking into account the transport of minerals across the tonoplast, and/or the contribution of the PPiase, and/or possible fluctuations in cytosolic pH. The model suggested that the significant increase in malate concentration observed after the climacteric crisis could be due to an increase in ATPase activity in response to a higher free energy of ATP hydrolysis. The model also helped to dissect differences in malate accumulation among cultivars by highlighting the likely importance of the free energy of ATP hydrolysis and vacuolar pH. In the future, connecting such a model with a model of citrate prediction, and models relating titratable acidity and pulp composition (Etienne *et al.*, 2013a), would provide a useful tool to study banana acidity. Finally, the present adaptation of the malate model initially developed on peach, to banana fruit, highlights the possible generic quality of the model and its suitability for fleshy fruit.

3 Etude de l'accumulation du citrate par un modèle de fonctionnement du cycle de Krebs

Objectifs

Dans cette partie, l'accumulation du citrate dans la pulpe de banane a été modélisée dans le but (i) de comprendre les processus physiologiques qui pilotent la concentration en citrate dans la pulpe de banane pendant la croissance et la maturation post récolte, (ii) de proposer des hypothèses sur les origines des différences génotypiques au niveau cellulaire, et (iii) d'étudier les possibles effets des conditions de croissance du fruit sur l'accumulation du citrate. L'hypothèse de base de ce travail de modélisation est que l'accumulation du citrate dans la pulpe est pilotée par le fonctionnement du cycle de Krebs dans la mitochondrie (c.f. Chapitre I). Ainsi, un modèle mécaniste décrivant de manière simplifiée le fonctionnement de ce cycle a été développé. Cette partie a été rédigée sous la forme d'un article intitulé «A model of TCA cycle functioning to analyze citrate accumulation in pre and post-harvest fruits: application to banana fruit (*Musa* sp. AA)» qui a été soumis à **Plant Physiology**.

Principaux résultats

- Ce modèle permet de prédire la concentration en citrate dans la pulpe pendant la croissance et la maturation post récolte de la banane et de décrire la variabilité entre génotypes.
- Le cycle de Krebs apparaît comme un processus clé de l'accumulation du citrate dans la banane.
- Ce modèle suggère que la respiration et la température affectent la concentration en citrate pendant la maturation post récolte de manière différente selon le cultivar.
- L'enzyme malique mitochondriale et les transporteurs mitochondriaux du malate pourraient être des déterminants importants de l'accumulation du citrate et pourraient être à l'origine des différences de concentrations en citrate observées entre génotypes pendant les phases pré et post récolte.

A model of TCA cycle functioning to analyze citrate accumulation in pre and post-harvest fruits: application to banana fruit (*Musa* sp. AA)

A. Etienne[1], M. Génard[2], C. Bugaud[1]

[1] Centre de Coopération International en Recherche Agronomique pour le Développement (CIRAD), UMR QUALISUD, Pôle de Recherche Agronomique de Martinique, BP 214, 97 285 Lamentin Cedex 2, France

[2] INRA, UR 1115 Plantes et Systèmes de Cultures Horticoles, F-84914 Avignon, France

Abstract

Citrate concentration is a crucial determinant of banana pulp sourness and sweetness, two major drivers for consumer preferences. Banana fruit has the particularity of having separate growth and ripening stages, during which pulp citrate concentration changes. Our objective was to develop a mechanistic model of citrate accumulation based on a simplified representation of the TCA cycle to predict citrate concentration in banana pulp during the pre and post-harvest phases. The model was calibrated and validated separately on the pre and post-harvest phases, using data sets from three cultivars of dessert banana contrasting in terms of citrate accumulation, and incorporating different fruit load, potassium supply, and harvest stage. The model predicted the dynamic of citrate concentration in banana pulp with a fairly good accuracy for the three cultivars during the pre (mean RRMSE=0.22) and post-harvest phases (mean RRMSE=0.26). The sensitivity of the model to parameters and input variables were analyzed during the pre and post-harvest phases. According to the model, pulp respiration and temperature had no effect on citrate accumulation during the preharvest phase, whereas they affected citrate accumulation in a cultivar dependant manner during the post-harvest phase. Citrate accumulation was sensitive to pulp growth parameters in a cultivar dependant manner during the pre and post-harvest phases. The model helped to dissect differences of citrate concentration among cultivars during the pre and post-harvest phases. In particular, the model suggested major differences of TCA cycle functioning among cultivars during post-harvest ripening of banana, and pointed out the potential role of NAD-malic enzyme and mitochondrial malate carriers in the genotypic variability of citrate concentration. Finally, the model may be used as conceptual basis to study citrate accumulation in pre and post-harvest fleshy fruits.

3.1 Introduction

Citrate is one of the most important organic acids in many fruits (Seymour *et al.*, 1993), and its concentration in the pulp plays a critical role in organoleptic properties (Esti *et al.*, 2002; Harker *et al.*, 2002; Tieman *et al.*, 2012). The citrate concentration varies considerably among cultivars of many fruit species including citrus (Sadka *et al.*, 2001), peach (Moing *et al.*, 1998), pineapple (Saradhuldhat and Paull, 2007), and banana (Bugaud *et al.*, 2013). The accumulation of citrate in fruit cells is a complex phenomenon because it involves several metabolic pathways and transport mechanisms across different compartments, mainly cytosol, mitochondria, and vacuole (for review see (Etienne *et al.*, 2013b)). Ongoing transcriptomic (Cercos *et al.*, 2006), metabolomic (Katz *et al.*, 2011), proteomic (Katz *et al.*, 2007), and QTL studies (Schauer *et al.*, 2006) have begun to elucidate the complexity of the mechanisms involved in citrate accumulation. However, the regulation of citrate accumulation throughout fruit development, and the origins of the phenotypic variability of the citrate concentration within fruit species remain to be clarified. Given the complexity of the processes involved, ecophysiological process-based simulation models (PBSMs) could advance our understanding of the physiological mechanisms underlying citrate accumulation (Martre *et al.*, 2011). PBSMs could also help to elucidate the differences in citrate accumulation among and within fruit species, as it is the case for sugar accumulation in peach (Wu *et al.*, 2012), and grape berry (Dai *et al.*, 2009).

Attempts to mechanistically model citrate accumulation in fruits are rare. Lobit et al. (2003) proposed a mechanistic model to simulate the dynamics of citrate concentration in peach fruit. This model was based on the assumption that in fleshy fruits, citrate accumulation is driven by the tricarboxylic acid cycle (TCA cycle) located in the mitochondria, which is a convincing hypothesis (Etienne *et al.*, 2013b). This model was used to analyze the effects of temperature and pulp growth on citrate concentrations in two cultivars of peach (Lobit *et al.*, 2003; Wu *et al.*, 2007), and appeared to provide a good framework to study citrate accumulation in fleshy fruit. However, the approach used to solve the system of equations derived from the model led to a simple equation to predict the rate of net citrate production with parameters that had lost their real biological meaning. Thus, despite its good predictive quality, this model did not allow a complete study of the behavior and regulation of fruit mitochondrial citrate metabolism.

In the present study, we built a new, more mechanistic, model of citrate accumulation, with parameters that have biological meaning, based on a simplified representation of the TCA cycle adopted by Lobit et al. (2003). This model was developed for banana fruit because citrate concentration plays a crucial role in determining banana pulp sourness and sweetness

(Bugaud *et al.*, 2013), two major drivers of consumer preferences. Banana fruit has the particularity of having separate growth and ripening stages, during which citrate concentration undergoes substantial changes (Etienne *et al.*, 2014). We thus modeled the dynamics of citrate concentration during both the pre- and post-harvest stages. Because citrate concentration in banana pulp varies greatly among genotypes (Bugaud *et al.*, 2013; Etienne *et al.*, 2014), we chose to calibrate and validate the model on three cultivars with contrasting acidity. The physiological age of the fruit at harvest is known to affect the concentration of citrate in banana pulp during post-harvest ripening (Bugaud *et al.*, 2006). Fruit pruning and potassium fertilization, two cultural practices commonly used by banana growers, can also impact the concentration of citrate in fleshy fruits (for review see (Etienne *et al.*, 2013b)). For that reason, we used data sets incorporating different fruit loads, potassium supply, and harvest stages to study how these growing conditions affect citrate metabolism (or not). Model parameterization, model selection, and test of fit are presented for the pre- and post-harvest phases. The sensitivity of the model to the parameters and input variables were analyzed during the pre- and post-harvest stages. The model enabled us to (i) advance our understanding of citrate metabolism during growth and post-harvest ripening of banana fruit; (ii) propose a possible explanation for differences in citrate accumulation among cultivars and identify potential genotypic parameters (i.e. genotype-dependant parameters); and (iii) study the effects of fruit growth conditions on citrate metabolism. Finally, the model can be used as a conceptual basis to study citrate accumulation in pre- and post-harvest stages in fleshy fruits.

3.2 Materials and methods

3.2.1 Model description

The present model is based on the assumption that citrate accumulation in fleshy fruit is driven by the TCA cycle located in the mitochondria (Etienne *et al.*, 2013b). The TCA cycle results in the oxidation of pyruvate into CO_2 and a reduction in co-enzymes through a series of conversions between organic acids including malate and citrate (*Fig. III.14.A*). The maintenance of the pools of TCA cycle intermediates implies that for each metabolite exported, one is imported, and vice versa. These exchanges are achieved by a variety of mechanisms mediated by mitochondrial carrier proteins (for reviews, see (Haferkamp and Schmitz-Esser, 2012; Laloi, 1999)). The model presented here is based on the simplified representation of the TCA cycle used in the model of Lobit et al. (2003) (*Fig. III.14.B*)**.** The only metabolites considered, pyruvate, malate and citrate, were chosen because they are at

branch points between several reactions and because they are exchanged between the cytosol and the mitochondria. Pulp fruit was considered as a single big cell with mitochondrial and cytosolic compartments.

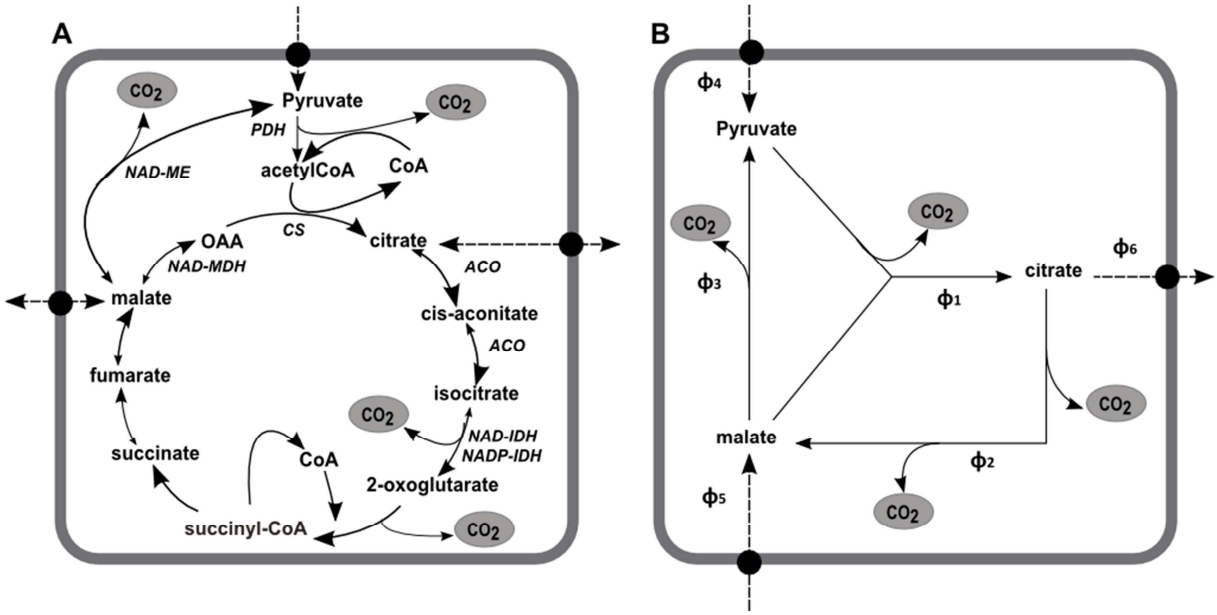

Figure III-14 (A) Reactions of the TCA cycle in the mitochondria and (B) the simplified representation used in the model of Lobit et al. (2003). Enzymes are in italics: ACO, aconitase; CS: citrate synthase; NAD-ME, NAD-malic enzyme; NAD-IDH, NAD-isocitrate dehydrogenase; NADP-IDH, NADP- isocitrate dehydrogenase; NAD-MDH, NAD-malate dehydrogenase; PDH, pyruvate dehydrogenase. Dashed arrows indicate transport across the mitochondrial membrane.

Stoichiometric equations:

Assuming the TCA cycle at steady-state implies that, for any given metabolite, the sum of metabolic fluxes that synthesizes it and the sum of metabolic fluxes that degrades it are equal (*Fig. III.14.B*).

$$\frac{dMpyr_{mt}}{dt} = \varphi_4 + \varphi_3 - \varphi_1 = 0 \quad (1)$$

$$\frac{dMmal_{mt}}{dt} = \varphi_5 + \varphi_2 - \varphi_3 - \varphi_1 = 0 \quad (2)$$

$$\frac{dMcit_{mt}}{dt} = \varphi_1 - \varphi_2 - \varphi_6 = 0 \quad (3)$$

The respiratory flux, approximated as the flux of CO_2 produced by the TCA cycle, is:

$$Resp = \varphi_1 + 2\varphi_2 + \varphi_3 \quad (4)$$

where $Mpyr_{mt}$, $Mmal_{mt}$, and $Mcit_{mt}$ (mmol) are respectively the amount of pyruvate, malate and citrate in the pulp mitochondrial compartment, φ_i are the metabolic fluxes of the TCA cycle (mmol.day^{-1}), and Resp is the respiratory flux of the pulp mitochondrial compartment (mmol.day^{-1}).

Mathematical representations of metabolic fluxes:

- *Enzymatic reactions:*

The metabolic flux between two compounds is described by enzyme kinetic rate laws, as a function that depends on the concentration of the reactants and on the k_i parameters called rate constants (Schallau and Junker, 2010).

$$\varphi_1 = k_1 Cmal_{mt} Cpyr_{mt} \quad (5)$$

$$\varphi_2 = k_2 Ccit_{mt} \quad (6)$$

$$\varphi_3 = k_3 Cmal_{mt} \quad (7)$$

where k_1 ($L^2.day^{-1}.mmol^{-1}$), k_2 ($L.day^{-1}$), k_3 ($L.day^{-1}$) are the rate constants, and $Cmal_{mt}$, $Cpyr_{mt}$, $Ccit_{mt}$ are the concentrations of malate, pyruvate and citrate in the pulp mitochondrial compartment, respectively ($mmol.L^{-1}$).

- *Transport reactions:*

Several carriers are present on the inner membrane of plant cell mitochondria and allow the exchange of metabolites of the TCA cycle between the cytosol and the mitochondrial matrix (for review see (Haferkamp and Schmitz-Esser, 2012)). For the sake of simplicity, we assumed that the transport of citrate, malate and pyruvate across the mitochondria depends mainly on the concentration gradients of the species transported between the cytosol and the mitochondrial matrix. Therefore, the formalism adopted to model the transport reactions was derived from Fick's law, which states that the diffusion flux of a compound is proportional to the concentration gradient of this compound across the membrane.

$$\varphi_4 = K_4(Cpyr_{cyt} - Cpyr_{mt}) \quad (8)$$

$$\varphi_5 = K_5(Cmal_{cyt} - Cmal_{mt}) \quad (9)$$

$$\varphi_6 = K_6(Ccit_{mt} - Ccit_{cyt}) \quad (10)$$

where K_4, K_5, K_6 are membrane permeability ($L.day^{-1}$); and $Cmal_{cyt}$, $Cpyr_{cyt}$, $Ccit_{cyt}$ are the respective concentrations of malate, pyruvate and citrate in the pulp cytosolic compartment ($mmol.L^{-1}$).

Solving the system and expressing the rate of net citrate production φ6 ($mmol.day^{-1}$):

Replacing the expressions of the different metabolic fluxes in equations 1 to 4 gives the following system:

$$K_4 Cpyr_{cyt} - K_4 Cpyr_{mt} + k_3 Cmal_{mt} - k_1 Cmal_{mt} Cpyr_{mt} = 0 \quad (11)$$

$$K_5 Cmal_{cyt} + k_2 Ccit_{mt} - (K_5 + k_3) Cmal_{mt} - k_1 Cmal_{mt} Cpyr_{mt} = 0 \quad (12)$$

$$K_6 Ccit_{cyt} + k_1 Cmal_{mt} Cpyr_{mt} - (k_2 + K_6) Ccit_{mt} = 0 \quad (13)$$

$$2k_2 Ccit_{mt} + k_3 Cmal_{mt} + k_1 Cmal_{mt} Cpyr_{mt} = Resp \quad (14)$$

where $Cpyr_{mt}$, $Cmal_{mt}$, $Ccit_{mt}$, $Ccit_{cyt}$ are the unknowns of the system, and K_i, k_i, $Cpyr_{cyt}$, $Cmal_{cyt}$ are parameters.

The system was solved by using the software Maple (Maple (16). Maplesoft, a division of Waterloo Maple Inc., Waterloo, Ontario). The solutions of $Ccit_{mt}$ and $Ccit_{cyt}$ were put into equation 10 which gave the following expression for φ_6:

$$\varphi_6 = -\frac{1}{4}\frac{(k_3+K_5)Resp}{3k_3+K_5} + \frac{1}{4}\frac{1}{k_1(3k_3+K_5)}(3K_4k_1(k_3+K_5)Cpyr_{cyt} + K_5k_1(2K_5+10k_3)Cmal_{cyt} - (k_3+K_5)\left(18K_4^2Cpyr_{cyt}k_1k_3 + 12K_4^2Cpyr_{cyt}k_1K_5 + 8K_4K_5^2Cmal_{cyt}k_1 + 9K_4^2k_3^2 + 4K_4^2K_5^2 + 9K_4^2Cpyr_{cyt}^2k_1^2 + 12K_4^2k_3K_5 + 4K_5^2Cmal_{cyt}^2k_1^2 - 12K_4Cpyr_{cyt}k_1^2K_5Cmal_{cyt} + 36K_4k_3K_5Cmal_{cyt}k_1 + \left(18K_4k_3k_1 - 6K_4Cpyr_{cyt}k_1^2 + 4K_4K_5k_1 + 4K_5Cmal_{cyt}k_1^2\right)Resp + Resp^2k_1^2\right)^{\frac{1}{2}} + K_4\left(5k_3K_5 + 3k_3^2 + 2K_5^2\right)) \quad (15)$$

Pulp respiration:

Pulp respiration during fruit growth was calculated using the growth-maintenance equation (Cannell and Thornley, 2000). Growth respiration is considered to be proportional to the fruit growth rate and maintenance respiration to dry mass and temperature (Penning de Vries and Laar, 1982; Thornley and Johnson, 1990). The effect of temperature is described with the Q_{10} concept. Pulp respiration (mmol CO_2.day^{-1}) was calculated as the sum of growth and maintenance respiration:

$$Resp = q_g\frac{dDW}{dt} + q_m DW\, Q_{10}^{\frac{\Theta-20}{10}} \quad (16)$$

where q_g is the growth respiration coefficient (mmol CO_2.g^{-1}), q_m is the maintenance coefficient at 20 °C (mmol CO_2.g^{-1}.day^{-1}), Q_{10} is the temperature ratio of maintenance respiration (dimensionless), DW is the pulp dry weight (g) and Θ is the temperature (°C).

Pulp respiration during post-harvest ripening was calculated by considering growth respiration equal to zero, since the fruit was detached.

Calculation of the concentration of citrate in the pulp:

Citrate concentration in the fruit was obtained by integrating φ_6 over the monitored period starting with citrate content observed at the beginning of the period, and by dividing it by the pulp fresh weight.

$$Ccit_t = \frac{100}{FW_t} * (Mcit_{t_0} + \int_{t_0}^{t}\varphi_6 dt) \quad (17)$$

where Ccit (mmol.100g FW^{-1}) is the citrate concentration in the pulp, $Mcit_{to}$ (mmol.fruit^{-1}) is the amount of citrate in the pulp at t_0, FW is pulp fresh weight (g), t is the time (days after

bloom or days after ethylene treatment), t_o is the time of the beginning of the experiment, and φ_6 the rate of net citrate production (mmol.day^{-1}).

Rate constants (k_i) and membrane permeability (K_i):

We hypothesized that k_i depends on enzyme activity, and K_i on transporter activity during fruit development. The activities of the TCA cycle enzymes and of the mitochondrial organic acid transporters can vary or remain constant during fruit growth (Chen *et al.*, 2009; Iannetta *et al.*, 2004; Katz *et al.*, 2011; Regalado *et al.*, 2013), and post-harvest ripening (Borsani *et al.*, 2009; Jeffery *et al.*, 1984; Liu *et al.*, 2004), suggesting that k_i and K_i are likely to vary during banana growth and post-harvest ripening. During fruit growth, variations in k_i and K_i may be due to changes in the number of mitochondria on one hand, and to the regulation of enzymes and transporter activities on the other hand. The first source of variation, i.e. the number of mitochondria, is likely to increase during fruit growth due to cell division and enlargement. Indeed, Winter et al. (1993 and 1994) found a positive linear relationship between the section area of the mitochondrial compartment and the section area of the leaf cells. Therefore, we chose to symbolize the link between the number of pulp mitochondria, and k_i and K_i by representing their variations during fruit growth as a function of the structural dry weight of the pulp, which represents the constitutive part of pulp cells and is therefore an indicator of pulp cell growth. Concerning the second source of variation, it is known that mitochondrial enzymes and transporters can be regulated by allosteric and post translational regulation, but little information is available on this subject (for review see (Araujo *et al.*, 2012)). Therefore, for the sake of simplicity, we included a regulatory factor (m_i) to modulate the relationship between the k_i and K_i, and the structural dry weight of the pulp:

$$k_{i,g}(t) = k_{i,g} * \left(\frac{SDW(t)}{SDW_{ref}}\right)^{m_i} \quad (18)$$

$$K_{i,g}(t) = K_{i,g} * \left(\frac{SDW(t)}{SDW_{ref}}\right)^{m_i} \quad (19)$$

where SDW is the structural dry weight of the pulp (g); SDW_{ref} is a reference structural dry weight equal to 1 g; $k_{i,g}$ (L.day^{-1} or L^2.day^{-1}.mmol^{-1}), $K_{i,g}$ (L.day^{-1}), and m_i (dimensionless) are fixed parameters, with $k_{i,g}$ and $K_{i,g}$ positives, and m_i positive, null or negative. Depending on the values of the parameter m_i, the patterns of $k_{i,g}(t)$ and $K_{i,g}(t)$ can remain constant, increase, or decrease, as shown in *Fig. III.15*.

During post-harvest ripening, the number of mitochondria of the pulp is likely to vary little since the fruit is no longer growing. Thus, changes in k_i and K_i are likely to be only due to the regulation of enzymes and transporters. We chose to represent the putative variations of

k_i and K_i during banana post-harvest ripening as a function of the number of days after ethylene treatment using the following mathematical expression:

$$k_{i,r}(t) = k_{i,r} * (\frac{DAE}{DAE_{ref}})^{j_i} \quad (20)$$

$$K_{i,r}(t) = K_{i,r} * (\frac{DAE}{DAE_{ref}})^{j_i} \quad (21)$$

where DAE is the day after ethylene treatment; DAE_{ref} is a reference day after ethylene treatment equal to 1; $k_{i,r}$ (L.day^{-2}), $K_{i,r}$ (L.day^{-2}), and j_i (dimensionless) are fixed parameters, with $k_{i,r}$ and $K_{i,r}$ positives, and j_i positive, null or negative. Depending on the values of the parameter j_i, $k_{i,r}(t)$ and $K_{i,r}(t)$ can remain constant, increase, or decrease during ripening.

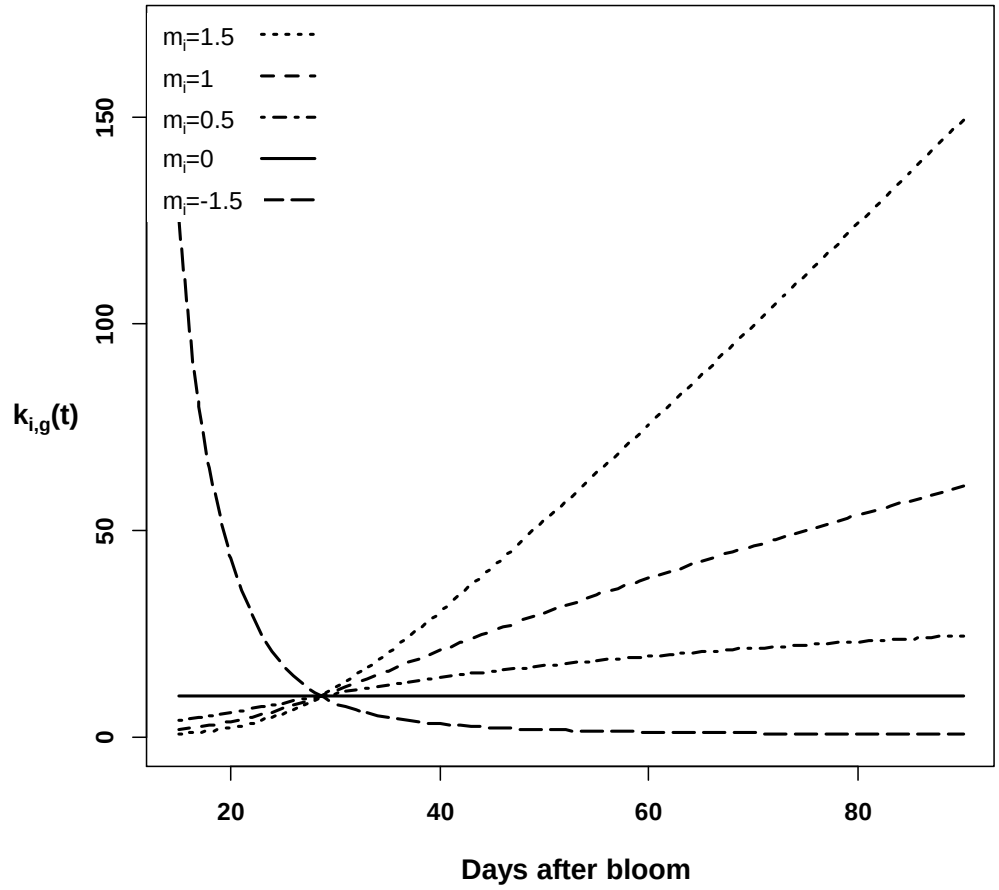

Figure III-15 Hypothetical changes in the rate constant $k_{i,g}(t)$ during fruit growth as a function of the value of parameter m_i. $k_{i,g}(t)=k_{i,g}*SDW^{mi}$, with $k_{i,g}$ arbitrarily equal to 10 and SDW (pulp structural dry weight) taking values of the PL cultivar. The different values of m_i correspond to the following situations: $m_i<0$: enzyme inhibition exceeds the increase in the number of mitochondria; $m_i=0$: enzyme inhibition compensates for the increase in the number of mitochondria; $0<m_i<1$: enzyme inhibition under-compensates for the increase in the number of mitochondria; $m_i>1$: activation of enzyme along with the increase in the number of mitochondria.

3.2.2 Model inputs and initial conditions

The model used daily pulp fresh weight, and daily pulp structural dry weight as input variables. Initial values were the amount of citrate in the fruit pulp on the first date of the modeled period. Equation 17 was numerically solved using the 'lsoda' function of the package 'dsolve' of the R software with a one-day time step (Soetaert *et al.*, 2010).

Daily pulp dry weight was estimated by fitting a growth expolinear function to pulp dry weight data (Goudriaan and Monteith, 1990).

$$DW = \left(\frac{C_m}{R_m}\right) * \ln(1 + \exp(R_m * (t - t_b))) \quad (22)$$

where C_m is the maximum absolute growth rate of pulp dry weight ($g.day^{-1}$), R_m is the maximum relative growth rate of pulp dry weight ($g.g^{-1}.day^{-1}$), t_b is the x axis intercept of the linear growth phase of pulp dry weight (day).

Daily pulp fresh weight was estimated using an empirical relationship with pulp dry weight (R^2=0.99 and *n*=488):

$$FW = 3.12 * DW + 3.47 \quad (23)$$

Daily pulp structural dry weight was estimated using an empirical relationship with pulp dry weight (R^2=0.98 and *n*=454):

$$SDW = 0.69 * DW^{0.73} \quad (24)$$

3.2.3 Plant Materials and experimental conditions

All experiments were conducted at the *Pôle de Recherche Agroenvironnementale de la Martinique* (PRAM, Martinique, French West Indies; latitude 14°37N, longitude 60°58W, altitude 16m) using three dessert banana cultivars (*Musa* spp.) diploids AA, that differ in their predominant organic acid at the eating stage: Indonesia 110 (IDN), Pisang Jari Buaya (PJB), and Pisang Lilin (PL). Experiments were conducted during the 2011 and 2012 growing seasons on continental alluvial soil. For the two growing seasons, irrigation was adjusted to the amount of rainfall to supply at least 5 mm of water per day, and non-systemic fungicide was applied to control foliar diseases. During the first period of bunch growth (March–November 2011) the mean daily temperature was 27 ± 1.2°C. During the second period of bunch growth (February-August 2012) the mean daily temperature was 26± 0.9°C.

2011 experiment: effect of fruit load on banana pulp acidity

For each cultivar, 36 plants were randomly chosen and tagged at inflorescence emergence. Two contrasted fruit loads were used: 18 plants of each cultivar were used as the control treatment i.e. high fruit load, and 18 other plants were highly pruned i.e. low fruit load. In the

control treatment, the number of leaves and hands left on the plants were calculated in order to have the same leaf area: fruit ratio among cultivars (approximately equal to 0.5 cm^2 leave. g $fruit^{-1}$). Thus, 15 days after inflorescence emergence, 8, 6, and 5 leaves were left on the plant for cultivars IDN, PL, and PJB respectively, and the top 10, 5 and 7 hands were left on the bunch for cultivars IDN, PL, and PJB respectively. To ensure the situation was the same among the three cultivars, fruit pruning in low fruit load treatment was calculated to increase the leaf area: fruit ratio by approximately 2.5. Consequently, 15 days after inflorescence emergence, the top 4, 2, and 3 hands were left on the bunch for cultivars IDN, PL, and PJB respectively. Banana plants received 12 g of nitrogen, 1.7 g of phosphorus, and 23 g of potassium at 4-week intervals during fruit growth.

2012 experiment: effect of potassium fertilization on banana pulp acidity

Two plots containing 50 banana plants of each cultivar were planted, i.e. each plot contained a total of 150 banana plants. Two contrasted levels of potassium fertilization were started six months before the beginning of fruit sampling. For each cultivar, one plot received 124 g of potassium per plant (high potassium fertilization) at 4-week intervals, while the other received no potassium at all. All the banana plants received 12 g of nitrogen and 10 g of phosphorus at 4-week intervals. Twenty-four plants of each cultivar were randomly chosen in each plot and tagged at inflorescence emergence. At 15 days after inflorescence emergence, 9, 7, and 9 leaves were left of cultivars IDN, PL, and PJB respectively, which corresponds to the average leaf number in 2012, and the top 10, 5, and 7 hands were left on the bunch of cultivars IDN, PL, and PJB respectively, which correspond to a high fruit load.

Monitoring fruit growth

In the two growing seasons, six bunches of each cultivar*treatment combination were selected. One fruit located in the internal row of the second proximal hand was collected for analyses every 15 days. Natural ripening on standing plants, i.e. when the first yellow finger appears, determined the end of sampling.

Monitoring post-harvest fruit ripening

Two harvest stages were studied in the 2011 experiment. The harvest stages were calculated for each cultivar to be 70% and 90% of the average flowering-to-yellowing time (FYT) of the bunch on the plant. For each harvest stage, six bunches of each cultivar*treatment combination were harvested. In the 2012 experiment, only one harvest stage was studied. The

harvest stage was calculated for each cultivar to be 75% of the average FYT of the bunch on the plant. Six bunches of each cultivar*treatment combination were harvested. After the bunches were harvested, the second proximal banana hand per bunch was rinsed and dipped in fungicide (bitertanol, 200 $mg.L^{-1}$) for 1 min. The fruits were placed in a plastic bag with 20 µm respiration holes and stored in boxes for 6 days at 18 °C. The fruits were then stored in a room at 18 °C and underwent ethylene treatment (1 $mL.L^{-1}$ for 24 h) to trigger the ripening process. After 24 h, the room was ventilated. Bananas were maintained at 18 °C for 13 days and a banana fruit was sampled before ethylene treatment, and at day 3, 6, 9 and 13 after ethylene treatment.

3.2.4 Biochemical and respiration measurements

For each fruit sampled, the fresh and dried pulp were weighed. The dried pulp was then mixed to obtain dry powder and to allow biochemical measurements. Citrate concentration was assessed according to the method described in Etienne et al. (2013a) using an enzymatic method and a microplate reader. Pulp structural dry weight was calculated as the difference between pulp dry weight and the sum of the weights of the main non-structural compounds (soluble sugars, starch, acids). To this end, concentrations of malate were assessed according to the method described in Etienne et al. (2013a), and concentrations of starch and soluble sugars (glucose, fructose, sucrose) were assessed according to Gomez et al. (2007), using an enzymatic method and a microplate reader. For measurements of respiration, each sampled fruit was placed in a closed plastic jar. The temperature of the room was set at 18 °C. After 1 hour, CO_2 concentration was measured with a gas analyzer (Vigaz, CANAL120).

3.2.5 Model parameterization

Based on information found in the literature, the value of $Cmal_{cyt}$ was set at 1 mM (Gerhardt and Heldt, 1984; Gout *et al.*, 1993), and the value of $Cpyr_{cyt}$ was set at 0.5 mM, (Beaudry *et al.*, 1989; Kubicek and Röhr, 1978).

Parameters of the pulp dry weight growth model (C_m, R_m, t_b) were estimated for each banana plant using a nonlinear least-squares regression method (Fox, 2002). The model explained 99% of the pulp dry weight variance in the three cultivars and in the two years of the experiment, and the RRMSE was satisfactory with mean values of 0.1 (*Appendix 3*).

According to the literature, the temperature ratio of maintenance respiration Q_{10} was set at 2 (Turner, 1995). The growth respiration coefficient of the pulp (q_g) was derived from construction cost measurements on banana pulp. In the three cultivars, the total nitrogen,

carbon and ash concentration of the banana pulp were measured at three different stages of fruit growth. The construction cost (CC; g glucose. g^{-1}) was calculated as a function of the carbon (C; g. g DW^{-1}), nitrogen (N; g. g DW^{-1}), and ash (A; g. g DW^{-1}) concentrations of banana pulp, and of the energetic costs of N assimilation and carbohydrate translocation (Vertregt and Penning de Vries, 1987; Wullschleger *et al.*, 1997):

$$CC = (5.39C + 0.80A + 5.64f_{Nh}N - 1.191)(1 + r_T) \quad (25)$$

where f_{Nh} is the fraction of N used in growth that is assimilated heterotrophically, assumed to be equal to 1 for fruits (Wullschleger *et al.*, 1997), and r_T is the added cost of translocating photosynthetates from sources to sinks, assumed to be equal to 5.3% (Vertregt and Penning de Vries, 1987).

The coefficient q_g (mmol $CO_2.g^{-1}$) was calculated using the following formula (Léchaudel *et al.*, 2005a):

$$q_g = \frac{(\alpha CC - C)}{M_C} * 1000 \quad (26)$$

where αCC is the carbon construction cost (α=0.4 is the concentration of carbon in glucose), and M_C is the molar mass of carbon equal to 12 $g.mol^{-1}$.

The calculated values of q_g were found to not significantly differ among cultivars and among developmental stages (data not shown). Thus, for q_g a value common to all cultivars and developmental stages was chosen as the mean value of the calculated values which was q_g=13 mmol $CO_2.g^{-1}$ ±1. This value is in the range of values found for tomato (9.3 mmol $CO_2.g^{-1}$; (Penning de Vries, 1989)), peach (7.0 mmol $CO_2.g^{-1}$; (DeJong and Goudriaan, 1989)), and mango (3.0 mmol $CO_2.g^{-1}$; (Léchaudel *et al.*, 2005a)).

The maintenance respiration coefficient (q_m) of the pulp during banana growth and post-harvest ripening were calculated respectively from measurements of respiration in harvested green fruits and in fruits subjected to ethylene treatment in the 2012 experiment (*n*=180). Since the fruits were harvested, the measured respiration corresponded only to maintenance respiration because growth respiration was null. Therefore, by inverting equation 16, q_m was calculated as follows:

$$q_m = \frac{Resp}{DW\, Q_{10}^{\frac{\theta-20}{10}}} \quad (27)$$

The value of q_m during fruit growth was estimated at q_m=0.15 mmol $CO_2.g^{-1}.day^{-1}$ ±0.02 for the three cultivars, a value close to those estimated for tomato (0.27 mmol $CO_2.g^{-1}.day^{-1}$; (Walker and Thornley, 1977)), peach (0.05 mmol $CO_2.g^{-1}.day^{-1}$; (DeJong and Goudriaan, 1989)), and mango (0.09 mmol $CO_2.g^{-1}.day^{-1}$; (Léchaudel *et al.*, 2005a)).

The values of calculated q_m during post-harvest ripening were plotted as a function of the number of days after ethylene treatment. In all three cultivars, q_m increased dramatically

during the first two days after ethylene treatment, and then remained constant until the end of ripening (*Appendix 4.A, B and C*). An appropriate expression to represent q_m was:

$$q_m = q_{m1} * (1 - q_{m2} * \exp^{-q_{m3} * DAE}) \quad (28)$$

where DAE is the day after ethylene treatment, and q_{m1}, q_{m2}, and q_{m3} are fitted coefficients.

The values of q_m differed significantly among cultivars, so we decided to fit the model of equation 28 to the three cultivars separately. Thus, parameters q_{m1}, q_{m2}, and q_{m3} were estimated for each cultivar by using a nonlinear least-squares regression method on the 2012 data (Fox, 2002) (*Table III-5***)**. The model allowed satisfactory prediction of fruit respiration during post-harvest ripening (R^2=0.72; RRMSE=0.10) (*Appendix 4.D*).

Table III-5 Estimated parameter values and standard errors (in parentheses) of the q_m model during post-harvest ripening in cultivars IDN, PJB, and PL. Parameters were estimated using the data from 2012 post-harvest ripening.

	q_{m1} (mmol $CO_2.g^{-1}.day^{-1}$)	q_{m2} (dimensionless)	q_{m3} (dimensionless)
IDN	0.61 (0.01)	0.71 (0.04)	1.08 (0.18)
PJB	0.48 (0.01)	0.68 (0.05)	0.65 (0.13)
PL	0.52 (0.01)	0.68 (0.04)	0.87 (0.13)

3.2.6 Model calibration

Parameters related to reaction rates $k_i(t)$ and membrane permeability $K_i(t)$ were estimated through the model calibration by fitting the predicted citrate concentrations to observed values of the 2011 dataset separately for each cultivar and developmental stage (growth and post-harvest ripening) using the hydroPSO function of the R software (Zambrano-Bigiarini *et al.*, 2013). The hydroPSO function uses the computational method of particle swarm optimization (PSO) that optimizes a problem by iteratively trying to improve a candidate solution with regard to a given measure of quality. Parameters were estimated by minimizing the following criterion:

$$\sum_j \sum_i (x_{ij} - y_{ij})^2 \quad (29)$$

where x_{ij} is the predicted value, and y_{ij} is the observed value of the fruit of the j^{th} banana plant at date t_i.

3.2.7 Sensitivity analysis of the models

Sensitivity analyses were conducted to help select the best model and to analyze the sensitivity of the best model to parameters and inputs during the pre- and post-harvest stages. The sensitivity of the model to variations in the parameters and input values was quantified by normalized sensitivity coefficients, defined as the ratio between variation in the citrate concentration (ΔC) relative to its standard value (C), and variation in the parameter or input value (ΔP) relative to its standard value (P) (Monod *et al.*, 2006).

$$\text{Normalized sensitivity coefficient} = \frac{\Delta C/C}{\Delta P/P} \quad (30)$$

The interpretation of the sensitivity coefficient is referred to as local sensitivity analysis since these coefficients provide information on the effect of small changes in the parameters on the response of the model. They do not provide information on the effect of simultaneous or large changes in parameters. Normalized sensitivity coefficients were calculated by altering one parameter or input variable by ±0.1% while maintaining all the other parameters and inputs at default values.

3.2.8 Model selection

We compared models to determine the best model to predict the concentration of citrate during the pre- and post-harvest stages of banana fruit development and to detect significant differences in parameter values among cultivars. We started by searching for the best model to predict citrate concentrations during the pre-harvest stage. We tested a full model in which all the $k_{i,g}(t)$ and $K_{i,g}(t)$ varied with SDW and were specific to cultivars (PREHARVEST1). Then, based on the values of the estimated parameters and on the sensitivity analysis of this full model (see 2.7), we tested a reduced model in which the less sensitive parameters $k_{i,g}(t)$ and $K_{i,g}(t)$ were kept constant throughout fruit growth and in which some of the parameters were supposed to be the same for some of the cultivars, thus reducing the number of parameters to be estimated (PREHARVEST2). For two models that do not significantly differ in fit quality, the one with fewer parameters is always preferred. In the second step, we searched for the best model to predict citrate concentrations during the post-harvest stage. Since the pre-harvest model did not correctly predict citrate concentration during the post-harvest stage (data not shown), we changed the equations $k_{i,r}(t)$ and $K_{i,r}(t)$ (equations 20 and 21). We thus tested a full model in which all the $k_{i,r}(t)$ and $K_{i,r}(t)$ varied with the number of days after ethylene treatment and were each specific to one cultivar (POSTHARVEST1). Then, based on the values of the estimated parameters and on the sensitivity analysis of this full model, we tested a reduced model in which the less sensitive parameters $k_{i,r}(t)$ and $K_{i,r}(t)$

were kept constant throughout fruit ripening and in which some of the parameters were assumed to be the same for some of the cultivars (POSTHARVEST2).

Models were selected using the Akaike information criterion (AIC), which allows the comparison of nested and non-nested models. In our case, the number of parameters exceeded *n*/40 (where *n* is sample size), so a second order derivative AICc, which contained a bias correction term for small sample size, was applied, as suggested by Johnson and Omland (2004). The model with smaller AICc was preferred.

$$AIC_c = n\ln\left(\frac{RSS}{n}\right) + 2k\left(\frac{n}{n-k-1}\right) \quad (31)$$

where n is the number of observations, RSS is the residual sum of squares, and k is the number of estimated parameters of the model.

3.2.9 Goodness-of-fit and predictive quality of the models

The goodness-of-fit of the pre- and post-harvest models was evaluated using two commonly used criteria, the root mean squared error (RMSE) and the relative root mean squared error (RRMSE), to compare the mean difference between simulated and observed results (Kobayashi and Salam, 2000). The smaller the value of RMSE and RRMSE, the better the fit.

$$RMSE = \sqrt{\frac{(\sum(Y_i - X_i)^2)}{n}} \quad (32)$$

where Y_i is the predicted value of the fruit i, and X_i is the measured value of the fruit i. n is the number of data.

$$RRMSE = \frac{RMSE}{\bar{x}} \quad (33)$$

where $\bar{x}$ is the mean of all observed values.

The predictive quality of the model, which ascertains the validity of the model in different scenarios, was quantified by the RMSE and RRMSE calculated on the 2012 data set.

3.3 Results

3.3.1 Overview of cultivar and treatment effects

The effects of cultivar and treatments on citrate concentration in banana pulp during the pre- and post-harvest stages are detailed in a previous paper (Etienne *et al.*, 2014), so only the main conclusions are presented here. During banana growth, citrate concentration increased and was significantly affected by cultivar both in 2011 and 2012. During banana post-harvest ripening, both the ripening stage and the cultivar had a significant effect on the concentrations of citrate in 2011 and 2012. Fruits harvested later (at 90% of FYT) had significantly higher concentration of citrate throughout ripening. Low fruit load and potassium fertilization had

significant effects on fruit fresh mass but not on citrate concentration during either growth or post-harvest ripening in the three cultivars.

3.3.2 Model comparison and calibration

The full PREHARVEST1 model was fitted to observed data by estimating 24 parameters, and predictions were in good agreement with observed data for the three cultivars (mean RRMSE=0.19). Sensitivity analysis of the model PREHARVEST1 showed that $K_{5,g}$ and m_5 had strong effects on the concentration of citrate in the three cultivars whereas $k_{1,g}$, $k_{3,g}$, $K_{4,g}$, m_1, m_3, and m_4 did not (data not shown). AICc comparison showed that $k_{1,g}$, $k_{3,g}$, and $K_{4,g}$ did not differ significantly among cultivars, but that $K_{5,g}$ and m_5 did (data not shown). Therefore, a reduced model (PREHARVEST2) was tested where m_1, m_3 and m_4 were null; $k_{1,g}$, $k_{3,g}$, $K_{4,g}$ were the same for the three cultivars; and $K_{5,g}$ and m_5 were specific to cultivars, thus reducing the number of estimated parameters to nine. The PREHARVEST2 model had a lower AICc than PREHARVEST1, meaning that the PREHARVEST2 model was the best (*Table III-6*). Values of the estimated parameters of the model PREHARVEST2 are summarized in *Table III-7*.

The full POSTHARVEST1 model was fitted to observed data by estimating 24 parameters, and predictions were in good agreement with observed data for the three cultivars (mean RRMSE=0.27). For parameter $k_{1,r}(t)$, sensitivity analysis of the model POSTHARVEST1 showed that $k_{1,r}$ and j_1 had strong effects on citrate concentration in cultivars IDN and PL, but not in cultivar PJB (data not shown). These results suggested that $k_{1,r}(t)$ could be assumed to be constant in cultivar PJB (i.e. $j_1=0$). Comparison of AICc showed that $k_{1,r}$ differed significantly among the three cultivars, and that j_1 differed significantly between cultivars IDN and PL (data not shown). For parameter $k_{3,r}(t)$, sensitivity analysis showed that $k_{3,r}$ had a strong effect on citrate concentration in the three cultivars, but not j_3. These results suggested that $k_{3,r}(t)$ could be assumed to be constant in the three cultivars (i.e. $j_3=0$). Comparison of AICc values showed that $k_{3,r}$ differed significantly among cultivars. For parameter $K_{4,r}(t)$, sensitivity analysis showed that $K_{4,r}$ had a strong effect on citrate concentration in the three cultivars but not j_4. These results suggested that $K_{4,r}(t)$ could be assumed to be constant in the three cultivars (i.e. $j_4=0$). Comparison of AICc values showed that $K_{4,r}$ did not significantly differ between cultivars IDN and PL. For parameter $K_{5,r}(t)$, sensitivity analysis showed that $K_{5,r}$ had a strong effect on citrate concentration in the three cultivars, and that j_5 had no effect on citrate concentration in cultivars IDN and PL but was highly influential in cultivar PJB. These results suggested that $K_{5,r}(t)$ could be assumed to be constant in cultivars IDN and PL (i.e. $j_5=0$). Comparison of AICc values showed that $K_{5,r}$

did not significantly differ between cultivars IDN and PL. For that reason, a reduced model (POSTHARVEST2) was tested where j_3 and j_4 were null for the three cultivars; j_5 was null for cultivars IDN and PL; j_1 was null for cultivar PJB; and $K_{4,r}$ and $K_{5,r}$ were the same for cultivars IDN and PL, reducing the number of estimated parameters to 13. Based on the comparison of AICc values, the POSTHARVEST2 model was the best (*Table III-6*). Values of the estimated parameters of the model POSTHARVEST2 are summarized in *Table III-7*.

Table III-6 Results of model selection using AICc criteria. The superscript names following the parameters refer to banana cultivars IDN, PJB and PL. Parameters followed by more than one superscript name have the same values as the corresponding cultivars.

Model	Estimated parameters	Fixed parameters	AICc
PRE-HARVEST1	$k_{1,g}^{idn}$,m_1^{idn},$k_{3,g}^{idn}$,m_3^{idn},$K_{4,g}^{idn}$,m_4^{idn},$K_{5,g}^{idn}$,m_5^{idn}, $k_{1,g}^{pjb}$,m_1^{pjb},$k_{3,g}^{pjb}$,m_3^{pjb},$K_{4,g}^{pjb}$,m_4^{pjb},$K_{5,g}^{pjb}$,m_5^{pjb}, $k_{1,g}^{pl}$,m_1^{pl},$k_{3,g}^{pl}$,m_3^{pl},$K_{4,g}^{pl}$,m_4^{pl},$K_{5,g}^{pl}$,m_5^{pl}		-795
PRE-HARVEST2	$k_{1,g}^{idn,pjb,pl}$,$k_{3,g}^{idn,pjb,pl}$,$K_{4,g}^{idn,pjb,pl}$, $K_{5,g}^{idn}$,m_5^{idn}, $K_{5,g}^{pjb}$,m_5^{pjb}, $K_{5,g}^{pl}$,m_5^{pl}	$m_1^{idn,pjb,pl}$=$m_3^{idn,pjb,pl}$= $m_4^{idn,pjb,pl}$=0	**-877**
POST-HARVEST1	$k_{1,r}^{idn}$,j_1^{idn},$k_{3,r}^{idn}$,j_3^{idn},$K_{4,r}^{idn}$,j_4^{idn},$K_{5,r}^{idn}$,j_5^{idn}, $k_{1,r}^{pjb}$,j_1^{pjb},$k_{3,r}^{pjb}$,j_3^{pjb},$K_{4,r}^{pjb}$,j_4^{pjb},$K_{5,r}^{pjb}$,j_5^{pjb}, $k_{1,r}^{pl}$,j_1^{pl},$k_{3,r}^{pl}$,j_3^{pl},$K_{4,r}^{pl}$,j_4^{pl},$K_{5,r}^{pl}$,j_5^{pl}		-180
POST-HARVEST2	$k_{1,r}^{idn}$,j_1^{idn},$k_{3,r}^{idn}$, $k_{1,r}^{pl}$,j_1^{pl},$k_{3,r}^{pl}$, $K_{4,r}^{idn,pl}$,$K_{5,r}^{idn,pl}$, $k_{1,r}^{pjb}$,$k_{3,r}^{pjb}$,$K_{4,r}^{pjb}$,$K_{5,r}^{pjb}$,j_5^{pjb}	j_1^{pjb}=$j_5^{idn,pl}$=$j_4^{idn,pjb,pl}$= $j_3^{idn,pjb,pl}$=0	**-223**

Table III-7 Estimated parameter values for the cultivars IDN, PJB, and PL according to the best models during growth (model PREHARVEST2) and post-harvest ripening (model POSTHARVEST2).

Parameter	Unit	Value		
		PL	IDN	PJB
Model PREHARVEST2				
$k_{1,g}(t)$	$L.day^{-1}$	9000		
$k_{3,g}(t)$	$L.day^{-1}$	2		
$K_{4,g}(t)$	$L.day^{-1}$	4000		
$K_{5,g}(t)$	$L.day^{-1}$	$0.0048*SDW(t)^{0.98}$	$0.0012*SDW(t)^{1.99}$	$0.0017*SDW(t)^{1.95}$
Model POSTHARVEST2				
$k_{1,r}(t)$	$L.day^{-1}$	$5634*t^{1.36}$	$4904*t^{-1.99}$	9887
$k_{3,r}(t)$	$L.day^{-1}$	531	0.17	0.08
$K_{4,r}(t)$	$L.day^{-1}$	3965		6889
$K_{5,r}(t)$	$L.day^{-1}$	1.0e-04		$1.03*t^{-1.26}$

3.3.3 Evaluation of the PREHARVEST2 and POSTHARVEST2 models

Citrate concentrations simulated by the models PREHARVEST2 (*Fig. III.16***)** and POSTHARVEST2 (*Fig. III.17*) were in good agreement with values observed in the three cultivars. RMSEs and RRMSEs of predictions of data from 2011, quantifying the goodness of fit, were satisfactory, with values ranging between 0.14 and 1.08 mmol.100g FW^{-1}, and between 0.15 and 0.40 respectively. Model validation was also satisfactory, as revealed by RMSEs and RRMSEs of predictions of data from 2012, with values ranging between 0.20 and 0.98 mmol.100g FW^{-1}, and between 0.17 and 0.35 respectively. Statistical analysis revealed that the PREHARVEST2 and POSTHARVEST2 models correctly simulated the strong effect of cultivar and fruit age on citrate concentration during banana development (*Appendix 5.1 and 5.2*). The PREHARVEST2 and POSTHARVEST2 models predicted little or no effect of fruit load and potassium fertilization on citrate concentration during banana development,

consistent with observed data. The POSTHARVEST2 model predicted a small effect of fruit age at harvest, consistent with observed data, but was not able to simulate the minor differences correctly (data not shown).

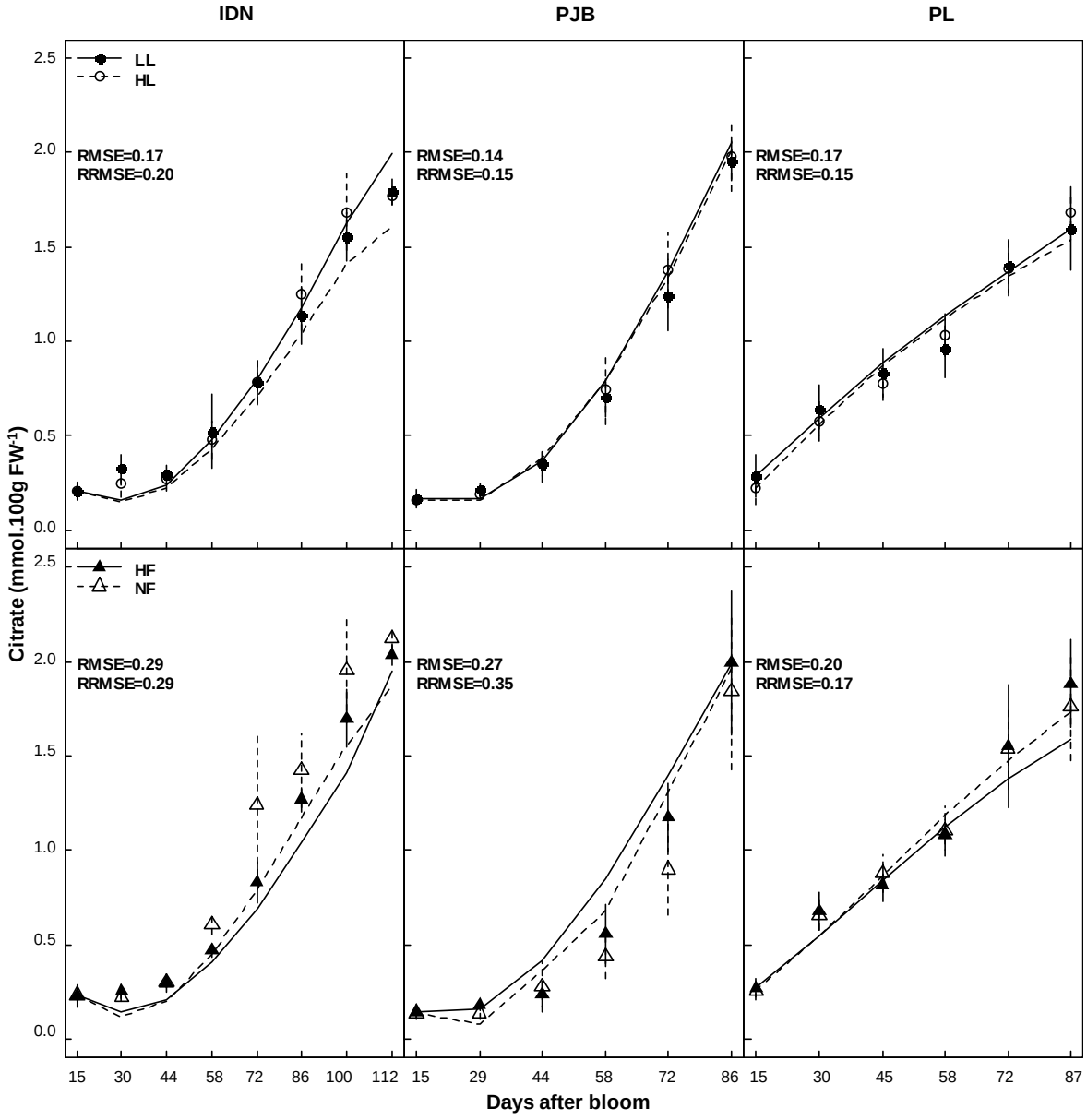

Figure III-16 Measured (dots) and simulated (lines) citrate concentrations in the banana pulp of cultivars IDN, PJB, and PL during fruit growth. The cultivars were grown under two contrasted fruit loads in 2011 (LL: low fruit load; HL: high fruit load), and two contrasted levels of potassium fertilization in 2012 (NF: no potassium fertilization; HF: high level of potassium fertilization). Data are means ± s.d (*n*=6). The RMSE (mmol.100 g FW^{-1}) and RRMSE are indicated in each graph.

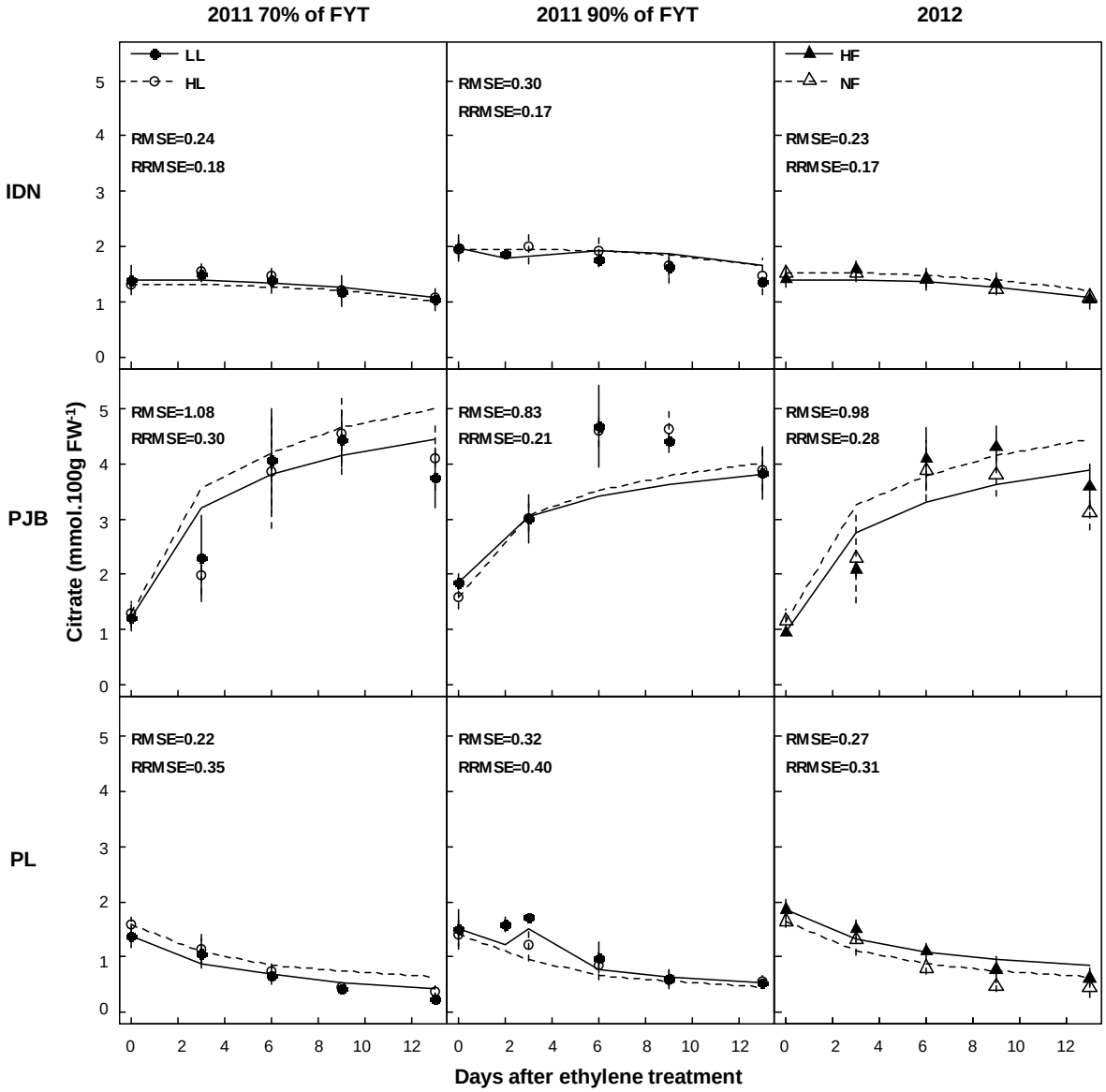

Figure III-17 Measured (dots) and simulated (lines) citrate concentrations in the banana pulp of cultivars IDN, PJB, and PL during fruit post-harvest ripening. The cultivars were grown under two contrasted fruit loads in 2011 (LL: low fruit load; HL: high fruit load), and two contrasted levels of potassium fertilization in 2012 (NF: no potassium fertilization; HF: high level of potassium fertilization). In 2011, fruits were harvested at two different stages: early stage (70% of FYT) and late stage (90% of FYT). Data are means ± s.d (*n*=6). The RMSE (mmol.100g FW^{-1}) and RRMSE are indicated in each graph.

3.3.4 Predictions of metabolic fluxes

The metabolic fluxes of the TCA cycle predicted by the models PREHARVEST2 and POSTHARVEST2 are presented in *Fig. III.18* for the three cultivars. During banana growth, all the metabolic fluxes underwent a continuous increase in the three cultivars. φ_1, φ_2, φ_4, and φ_3 followed the same pattern, but φ_3 was a lot lower. φ_5 and φ_6 followed the same pattern. All the metabolic fluxes were highest in cultivar PJB, then in cultivar PL and lastly in cultivar IDN. During post-harvest ripening, φ_1, φ_2, and φ_4 dramatically increased in the first two days after ethylene treatment and then remained constant in all three cultivars. φ_1, φ_2, and φ_4 were highest in cultivar PJB, then in cultivar IDN and lastly in cultivar PL. There were great differences in the pattern of φ_3, φ_5, and φ_6 among cultivars during ripening. φ_3 increased from 0 to almost 0.05 mmol.day^{-1} in cultivar IDN, decreased from 0.12 to almost 0 mmol.day^{-1} in cultivar PL, and was equal to zero in cultivar PJB. φ_5 decreased from 1 to almost 0 mmol.day^{-1} in cultivar PJB, and was equal to zero in cultivars IDN and PL. φ_6 decreased from 1 to almost 0 mmol.day^{-1} in cultivar PJB, increased from -0.1 to 0 in cultivar PL, and decreased slightly from 0 to negative values in cultivar IDN.

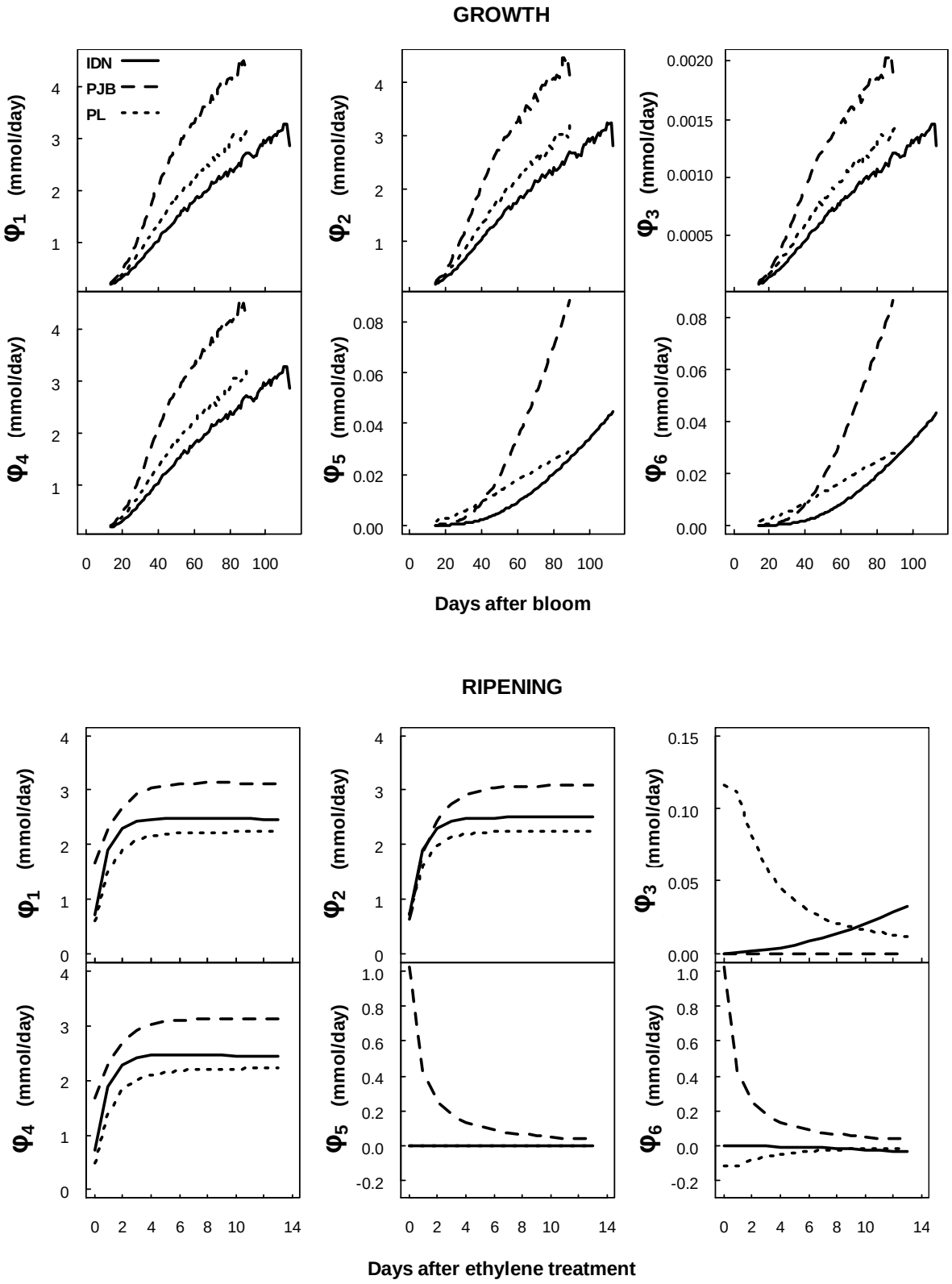

Figure III-18 Metabolic fluxes of the TCA cycle predicted by the citrate model during fruit growth and post-harvest ripening for the cultivars IDN, PJB, and PL.

3.3.5 Sensitivity analysis of the PREHARVEST2 and POSTHARVEST2 models

A normalized sensitivity coefficient (SC) was calculated to identify model responses to variations in parameters and inputs. A positive and negative sign of SC correspond, respectively, to a response in the same or reverse direction as the variation in the parameter or input. The larger the absolute value of SC, the more sensitive the model is to the parameter or input. Since the SC behaved similarly between years for a given cultivar, only results in 2011 are presented. For the sensitivity analysis during post-harvest ripening, the SCs behaved similarly between the two harvest stages in a given cultivar, so only results for 70% of FYT are presented. During banana growth, the SCs of parameters of the PREHARVEST2 model showed globally the same pattern among cultivars (*Fig. III.19*). Parameters $Cmal_{cyt}$, $K_{5,g}$ and m_5 greatly influenced citrate concentration in all three cultivars, whereas other parameters had little effect. The SCs of $Cmal_{cyt}$ and $K_{5,g}$ increased during the first part of growth and remained almost constant at about +1.0 in the second part. The SC of m_5 was slightly negative in the early stage of growth, and then dramatically increased to reach +1, +3, and +3.5 at the end of growth in cultivars PL, IDN and PJB respectively. During post-harvest ripening, the SCs of parameters of the POSTHARVEST2 model differed greatly among cultivars (*Fig. III.20*). In cultivar PL, parameters $Cpyr_{cyt}$, $k_{1,r}$, j_1, and $k_{3,r}$ greatly influenced citrate concentration since the absolute value of their SCs reached 2.5 at the end of ripening. The SC of $k_{3,r}$ became more and more negative during ripening, whereas the SCs of $Cpyr_{cyt}$, $k_{1,r}$, and j_1 became more and more positive. In cultivar IDN, all the parameters had little influence on citrate concentration, except for j_1 for which the SC increased to +1 at the end of ripening. In cultivar PJB, parameters $Cmal_{cyt}$, $K_{5,r}$ and j_5 were the most influential. The SCs of these three parameters were positive and increased during ripening but remained lower than +1.

During banana growth, growth parameters influenced citrate concentration in a cultivar dependant manner (*Fig. III.21*). The sensitivity of the PREHARVEST2 model to C_m was higher in cultivars IDN and PJB, than in cultivar PL. The SC of C_m increased in the first part of growth, and remained almost constant thereafter. The PREHARVEST2 model was very sensitive to R_m and t_b at the beginning of growth, and less at the end. To analyze the sensitivity of the POSTHARVEST2 model to pulp growth parameters, we combined the models PREHARVEST2 and POSTHARVEST2. We took into account the six days of fruit storage at 18 °C between harvest and ethylene treatment, and assumed that, during that period, fruit respiration was equal to growth maintenance respiration. During post-harvest ripening, C_m had a positive effect on citrate concentration in the cultivar IDN, and a negative effect in cultivars PJB and PL (*Fig. III.21*). R_m had a negative effect on citrate concentration

in all three cultivars. t_b had a negative effect on citrate concentration in cultivar IDN, and a positive effect in cultivars PJB and PL.

We analyzed the effect of changes in pulp respiration on citrate accumulation by studying the sensitivity of the two models to respiration parameters and temperature (*Fig. III.21*). During banana growth, respiration parameters and temperature had no effect on citrate concentration in any of the three cultivars. During post-harvest ripening, q_m and storage temperature greatly influenced citrate accumulation in a negative way in cultivar PL and to a lesser extent in cultivar IDN, but had no effect in cultivar PJB. Q_{10} had a positive effect on citrate accumulation in cultivar PL, a limited effect in cultivar IDN, and no effect in cultivar PJB.

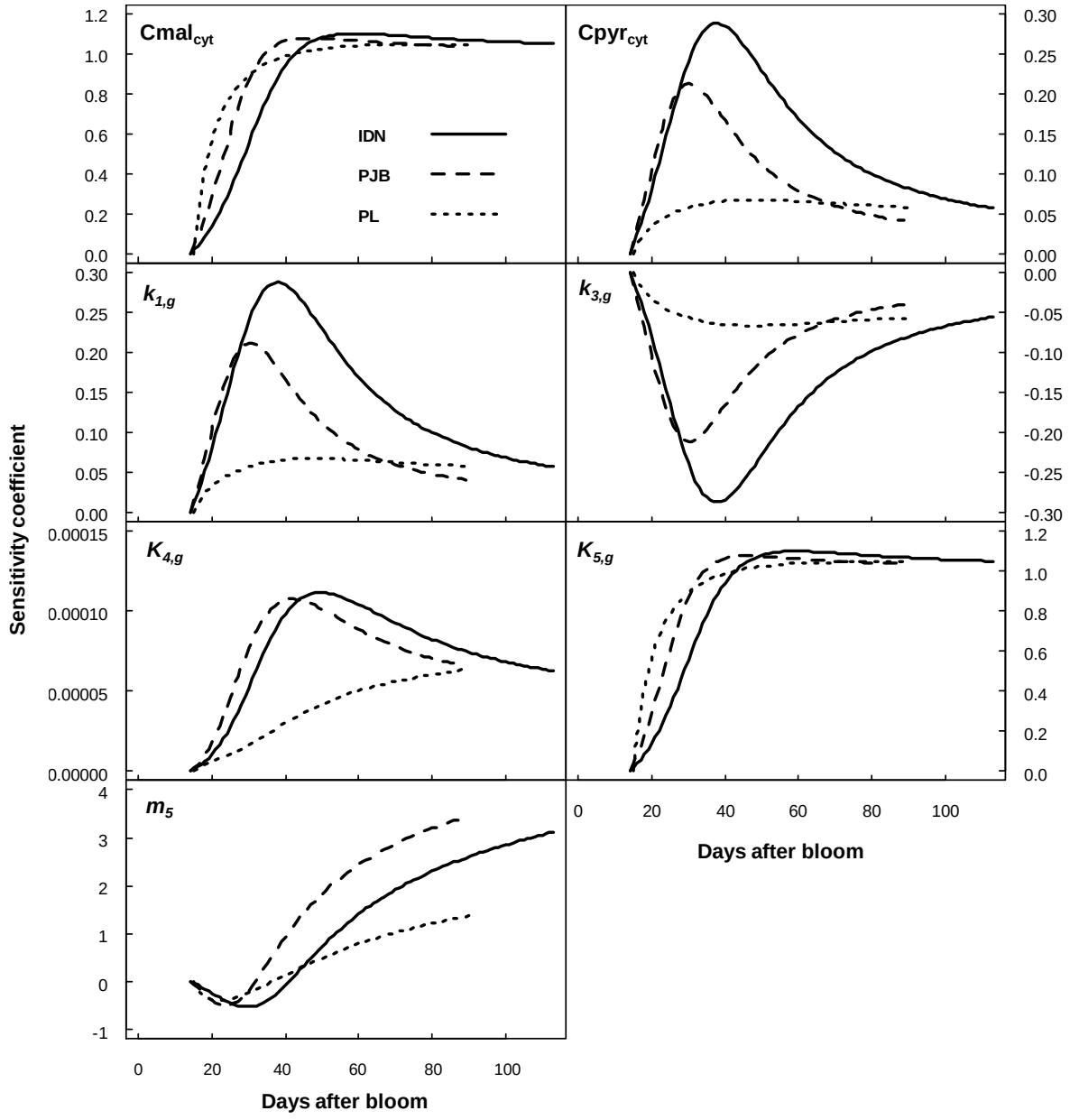

Figure III-19 Normalized sensitivity coefficients of the parameters of the citrate model during fruit growth for the cultivars IDN, PJB, and PL.

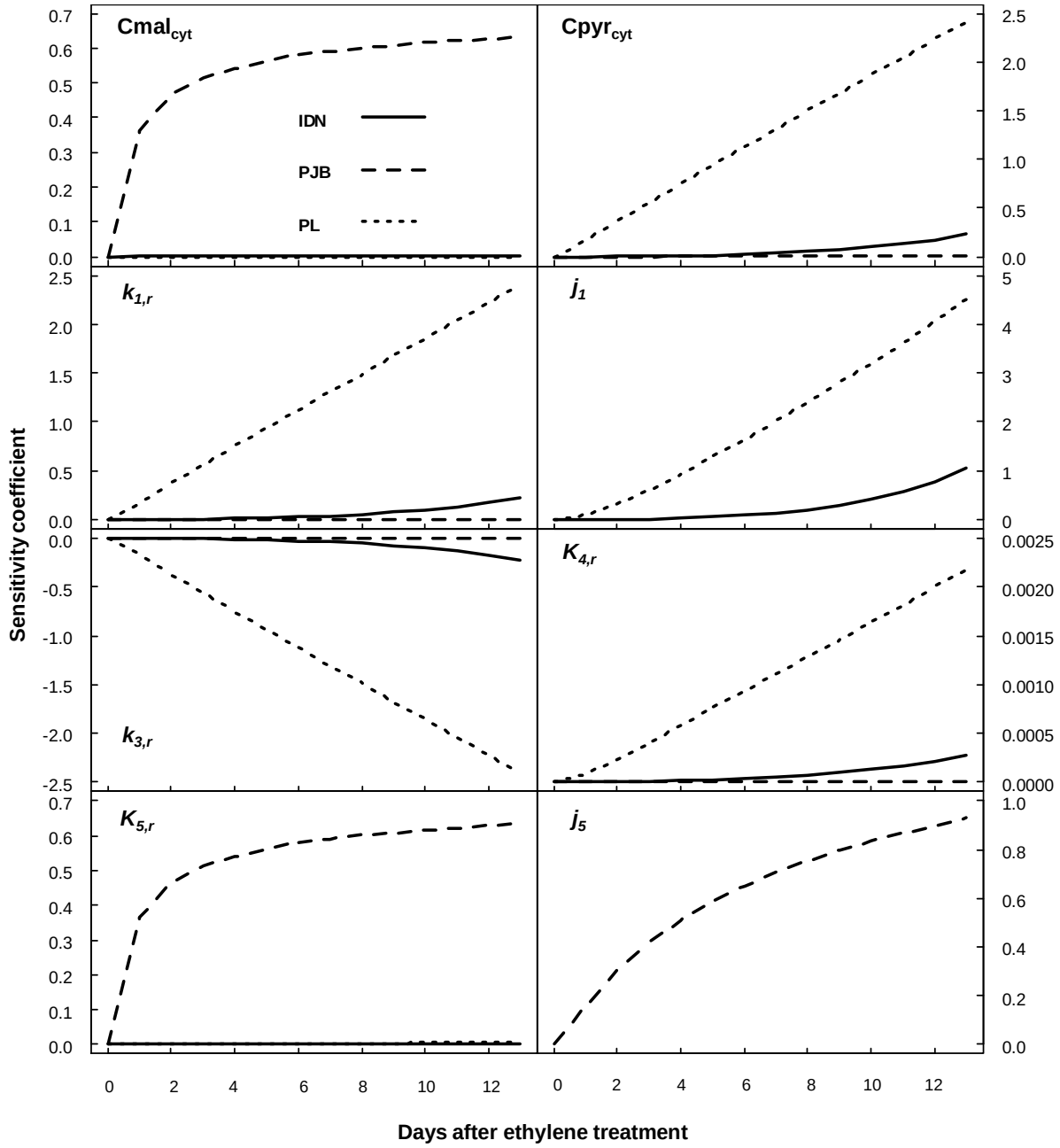

Figure III-20 Normalized sensitivity coefficients of the parameters of the citrate model during fruit post-harvest ripening in the cultivars IDN, PJB, and PL.

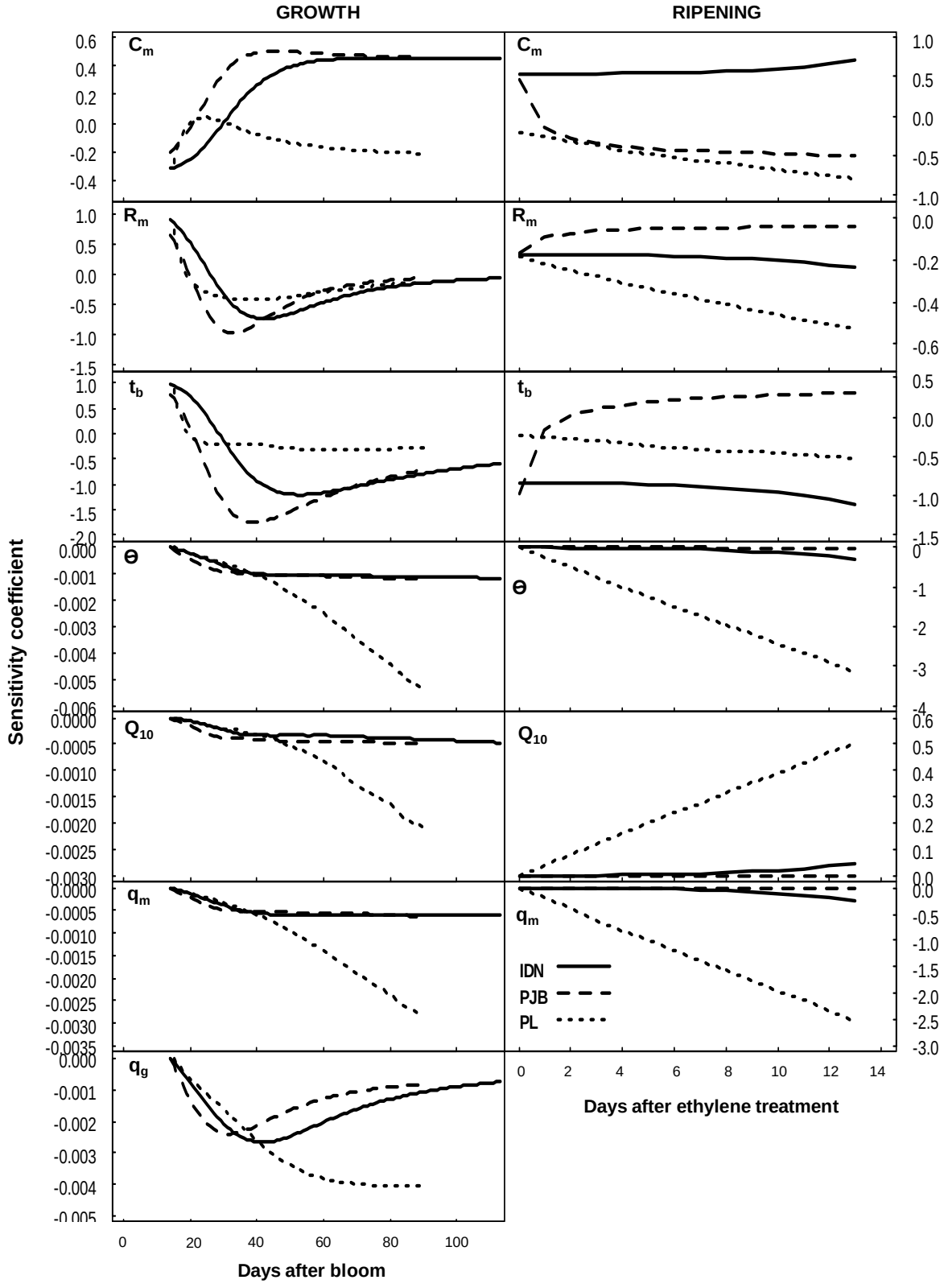

Figure III-21 Normalized sensitivity coefficients of the growth parameters, temperature (air temperature during fruit growth and storage temperature during fruit ripening), and respiration parameters during growth and post-harvest ripening in the cultivars IDN, PJB, and PL.

3.4 Discussion

3.4.1 Predicted variability in citrate metabolism among cultivars and between pre- and post-harvest stages

The model proposed in this study satisfactorily simulated the dynamics of citrate concentration during the pre- and post-harvest stages of banana development, despite the fact that they do not account for every detailed physiological process involved in citrate accumulation (e.g. the GABA shunt (Liu *et al.*, 2004), vacuolar storage (for review see (Etienne *et al.*, 2013b)). The main advantage of this model is that it gives a possible explanation for differences in citrate accumulation between the pre- and post-harvest stages, and among cultivars **(***Fig. III.22***).** During banana growth, the model predicted a common metabolic scheme for the three cultivars with φ_3 close to zero, and consequently φ_6 was equal to φ_5. Thus, during the pre-harvest stage, the import of malate into the mitochondria drove citrate production. This result was consistent with the fact that the most influential parameters were those related to the transport of malate across the mitochondrial membrane, namely $Cmal_{cyt}$ and $K_{5,g}(t)$. The model suggested that differences in citrate accumulation among cultivars during banana growth were due to differences in φ_5, and in particular in $K_{5,g}(t)$, which reflects the activity of malate mitochondrial transporters. In the three cultivars, $K_{5,g}(t)$ increased during banana growth but increased more in cultivar PJB than in the two other cultivars (data not shown). It is known that the expression of mitochondrial malate transporters varies during fruit development (Regalado *et al.*, 2013). The absence of φ_3 suggests that the pyruvate imported into the mitochondria through φ_4 could completely satisfy the fruit energy demand, with no need to produce any pyruvate via the mitochondrial malic enzyme reaction.

During post-harvest ripening, the model predicted the same metabolic scheme as during growth in the cultivar PJB, i.e. φ_3 close to zero and thus φ_6 equal to φ_5. Therefore, in cultivar PJB, the import of malate into the mitochondria drove citrate production during post-harvest ripening, which is consistent with $Cmal_{cyt}$ and $K_{5,g}(t)$ being the most influential parameters. In cultivar PJB, $K_{5,g}(t)$ was important at the beginning of ripening and then decreased dramatically (data not shown), explaining why the concentration of citrate increased significantly in the first days after ethylene treatment and then remained almost constant. In cultivars IDN and PL, φ_3 was positive and φ_5 was equal to zero during post-harvest ripening. Consequently, φ_6 was equal to $-\varphi_3$ and was therefore negative, explaining the decrease in citrate concentration, and the negative sensitivity of the model to $k_{3,r}(t)$. Comparison of the models and sensitivity analysis indicated that $k_{3,r}(t)$, which reflects

mitochondrial NAD-malic enzyme activity, can be assumed to remain constant during post-harvest ripening in the three banana cultivars, suggesting that NAD-malic enzyme activity is likely to vary little during this stage. Borsani et al. (2009) observed no significant changes in NAD-malic enzyme activity during post-harvest ripening in peach. Differences in citrate concentrations between cultivars IDN and PL were due to differences in φ_3, and in particular in $k_{3,r}(t)$. There is no information in the literature concerning the possible involvement of mitochondrial NAD-malic enzyme in the difference in acidity among fruit cultivars, but the model suggests this could be an interesting avenue to explore. In the end, it appears that screening for a genotype with low mitochondrial malate transport activity or high mitochondrial NAD-malic enzyme activity could be the most promising way to achieve a low citrate concentration in ripe banana fruit.

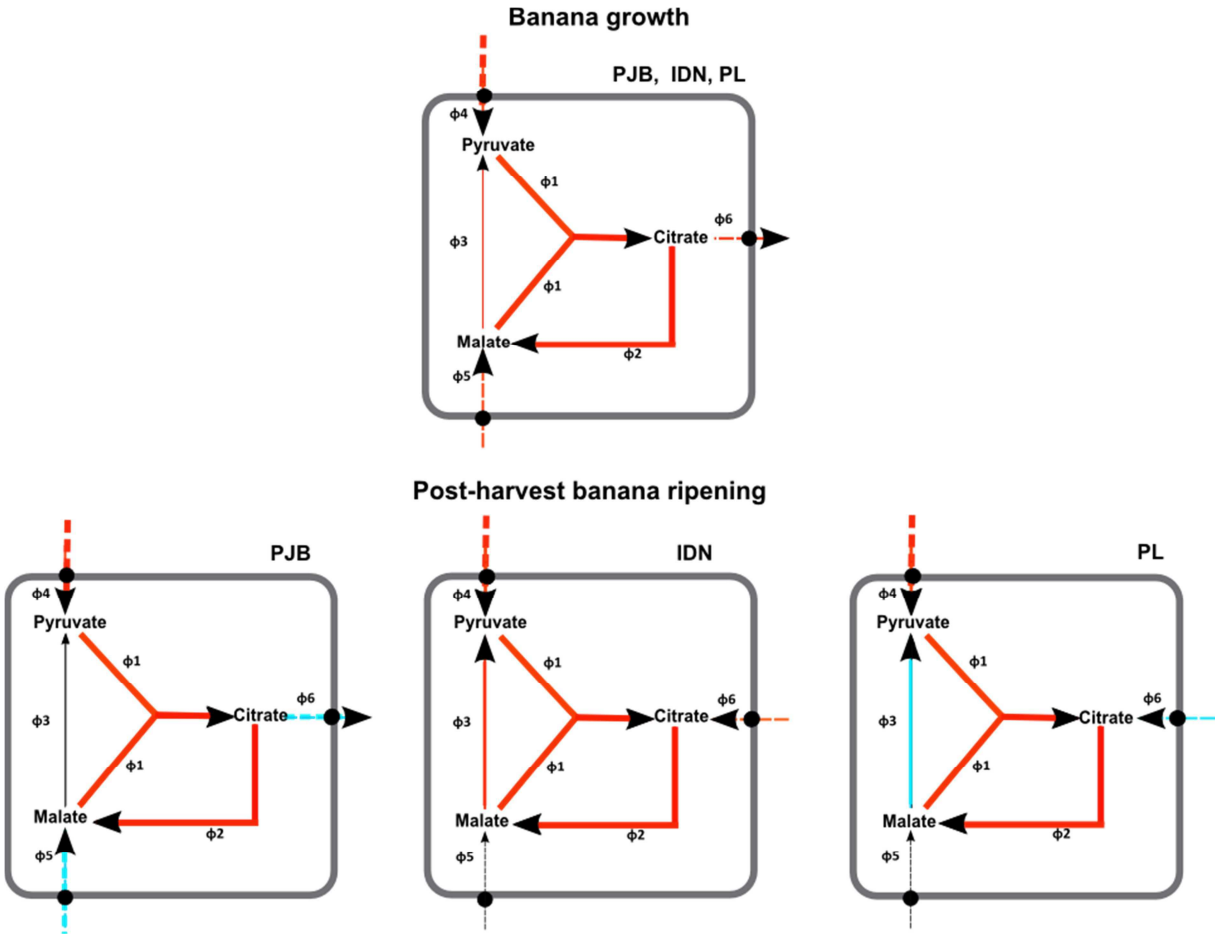

Figure III-22 Schematic diagram of the differences in organic acid metabolism in the mitochondria predicted by the model between cultivars IDN, PJB, and PL during banana growth and post-harvest ripening. The thickness of the arrow shows the importance of the metabolic flux. The color of the arrow indicates changes in the metabolic flux over time: blue means decrease, red means increase, and black means almost no change.

3.4.2 Model behavior

Citrate concentration was not sensitive to pulp respiration during banana growth, as also observed in simulations on peach by Wu et al. (2007) using the citrate model of Lobit et al. (2003). Indeed, their simulations showed little or no effect of fruit respiration on citrate concentration during the first part of peach growth, i.e. before ripening. During post-harvest ripening in our study, the sensitivity of citrate concentration to pulp respiration differed among cultivars. In cultivar PJB, citrate concentration was not affected by pulp respiration, whereas in cultivars IDN and PL, there was a negative relationship between pulp respiration and citrate accumulation in agreement with simulations on peach by Wu et al. (2007). According to our model, in these two cultivars, increasing pulp respiration increased φ_3 without replenishment of the pool of mitochondrial malate via φ_5. Therefore, citrate must have been imported into the mitochondria and converted into malate, leading to a decrease in citrate concentration. Temperature, which is one of the parameters that drives pulp respiration, negatively affected the concentration of citrate during post-harvest ripening in cultivars IDN and PL. This is in accordance with the fact that, as frequently observed in field experiments, high temperatures reduce fruit acidity (for review see (Etienne *et al.*, 2013b)). This is an interesting outcome of the model since temperature is a variable that is easy to control during post-harvest ripening. However, this result first needs to be checked experimentally to see if model simulations correctly reproduce the effect of storage temperature in a cultivar dependant manner.

According to the model, increasing fruit loads lead to higher citrate concentrations during fruit growth and to lower citrate concentrations during ripening. These predictions are in agreement with observations in agronomic experiments on peach (Wu *et al.*, 2002) and mango (Léchaudel *et al.*, 2005b). The effects of fruit load predicted by the model varied in intensity depending on the cultivar. The simulations performed by Wu et al. (2007) on peach using the citrate model of Lobit et al. (2003) also predicted different responses of citrate concentration to pulp growth between two cultivars. The effects of fruit load on citrate concentration predicted by our model were the result of a modification in pulp growth. In the three cultivars, fruits grown under low fruit load had higher C_m, which represents the maximum absolute growth rate of the pulp during the pulp cell filling period (Jullien *et al.*, 2001a) (*Appendix 6*). In the second part of banana growth, increasing C_m led to an increase in pulp fresh weight, and in net citrate production because of the increase in $K_{5,g}(t)$ due to higher pulp structural dry weight (data not shown). In the end, the effect of C_m on citrate concentration depended on whether the dilution effect was greater than the increase in citrate production (or not). If the increase in citrate production is comparable to the increase in pulp

fresh weight, the concentration of citrate will not change, which may explain the lack of influence of fruit load on citrate concentration observed in our field experiment. During post-harvest ripening, in addition to increasing the amount of pulp citrate and pulp fresh weight at harvest, increasing C_m affected post-harvest citrate metabolism in a cultivar dependant manner. In cultivars IDN and PL, increasing C_m increased pulp respiration, which in turn, increased citrate degradation. On the contrary, in cultivar PJB, C_m had no effect on citrate metabolism because in this case, the model was not sensitive to respiration (data not shown). The minor effect of potassium fertilization on citrate concentration predicted by the model during post-harvest ripening was the result of modifications in pulp growth. Fruits grown under contrasted potassium fertilization had different growth parameters (*Appendix 7*) that affected citrate concentration during post-harvest ripening in a cultivar dependant manner (see. sensitivity analysis).

3.4.3 Model validation

Globally, the model presented in this study fairly satisfactorily reproduced the absence of an effect of fruit load and potassium fertilization on citrate concentration during the pre- and post-harvest stages of banana development, and thus may be adequate for agronomical purposes. However, the robustness of the model needs to be tested on further replications of study over several years, and with growing conditions that lead to significant differences in citrate concentration. The validity of flux predictions could be tested by comparing them to experimental measurements of metabolic fluxes. This kind of approach is commonly used to model metabolic flux and helps constrain the flux solution space (Sweetlove *et al.*, 2013). Moreover, Sweetlove et al. (2013) suggested that metabolic input and output are the key drivers of flux distribution, more than enzyme regulation. Consequently, the precise determination of the input metabolites considered in our model (cytosolic malate and pyruvate concentrations) should help improve metabolic predictions. In the present model, cytosolic malate and pyruvate concentrations were assumed to be constant during banana development, whereas in reality they certainly fluctuate since they play a role in the regulation of cytosolic pH (Smith and Raven, 1979).

3.5 Conclusion

The model of TCA cycle functioning proposed in this study predicted the concentration of citrate in banana pulp with fairly good accuracy in a range of cultivars. The model helped to dissect differences in citrate concentration among cultivars. In particular, the model suggested

major differences in TCA cycle functioning among cultivars during post-harvest ripening of banana, and pointed to the potential role of NAD-malic enzyme and mitochondrial malate carriers in the genotypic variability of citrate concentration. In the future, linking such models with a model for malate (Lobit *et al.*, 2006), and a model relating titratable acidity and pulp composition (Etienne *et al.*, 2013a), would be a useful way to study fruit acidity. Moreover, the present model could be incorporated in a biophysical fruit growth model to simulate the dynamics of fruit fresh and dry mass (Dai *et al.*, 2008; Fishman and Génard, 1998), the main inputs of the model. The integrated model would facilitate identification of the key physiological processes responsible for the responses of banana growth and citrate concentration to environmental and management conditions. Finally, the model proposed in the present study can be used as a conceptual basis for modeling citrate accumulation in other fruit species.

Chapitre IV Conclusion générale et perspectives de recherche

1 Bilan des connaissances acquises

Dans ce travail, des approches expérimentales et de modélisation écophysiologiques ont été utilisées pour analyser et disséquer les processus qui pilotent l'acidité de la banane en pré et post récolte, et étudier les effets du génotype et des conditions de croissance du fruit.

1.1 L'acidité de la banane est fortement influencée par le génotype et peu par les conditions de croissance du fruit

L'approche expérimentale (Chapitre II) a permis de quantifier l'effet de la charge en fruit, de la fertilisation potassique et du stade de récolte sur les concentrations en citrate et malate dans le fruit au cours des phases pré et post récolte chez trois génotypes contrastés en acidité. Nous avons choisi dans cette approche de décomposer la concentration du citrate et du malate par gramme de matière fraîche en trois composantes :

- la concentration par gramme de matière sèche structurale de chaque acide qui est liée au métabolisme et transport des acides,
- le rapport de la matière sèche non structurale sur la matière sèche totale qui permet de quantifier la dilution des acides parmi les composés non structuraux stockés dans les cellules (sucres, amidon, minéraux,…),
- la teneur en eau de la pulpe qui permet de quantifier la dilution des acides par accumulation d'eau.

Cette décomposition a permis de disséquer l'effet du génotype et des facteurs agronomiques sur l'accumulation des acides dans la pulpe.

Des différences de profils d'accumulation du citrate et du malate ont été observées entre les trois génotypes aussi bien pendant la croissance que pendant la maturation post récolte des fruits. La phase de croissance correspond à une phase d'accumulation des acides chez les trois génotypes mais à des vitesses différentes. Durant la maturation post récolte, d'importantes différences d'évolution des teneurs en acides dans la pulpe sont apparues entre génotypes. La teneur en malate a fortement augmenté en début de maturation pour atteindre des niveaux différents selon le génotype. La teneur en citrate a quant à elle diminué tout au long de la maturation chez deux génotypes (IDN et PL), et a augmenté chez le troisième (PJB). La décomposition des teneurs en acides dans la pulpe en trois composantes (décrites précédemment) a montré que cette variabilité génotypique était principalement due à des différences au niveau du métabolisme et/ou transport des acides.

Les effets des facteurs agronomiques sur chacune des composantes décrites précédemment ont été les suivants :

Effet de la charge en fruit :

- La teneur en eau a légèrement diminué avec la charge en fruit en pré et post récolte pour les trois génotypes.
- Le rapport de la matière sèche non structurale sur la matière sèche totale, ainsi que la concentration des acides par gramme de matière sèche structurale n'ont pas été affectés par la charge en fruit pour les trois génotypes.
- Finalement, pour les trois génotypes, la concentration des acides par gramme de matière fraîche n'a pas été significativement affectée par la charge en fruit.

Effet de la fertilisation potassique :

- La teneur en eau et le rapport de la matière sèche non structurale sur la matière sèche totale n'ont pas été affectés par la fertilisation potassique pour les trois génotypes.
- Pour le génotype IDN, la concentration des acides par gramme de matière sèche structurale a légèrement diminué dans les fruits des bananiers ayant reçus une dose élevée de fertilisation potassique. Pour les génotypes PJB et PL, il n'y a eu aucun effet significatif observé.
- Finalement, pour les trois génotypes, la concentration des acides par gramme de matière fraîche n'a pas été significativement affectée par la fertilisation potassique.

Effet du stade de récolte :

- La teneur en eau des fruits récoltés tardivement a été légèrement plus élevée pour le génotype IDN et légèrement plus faible pour les génotypes PJB et PL.
- Le rapport de la matière sèche non structurale sur la matière sèche totale a été plus faible dans les fruits récoltés tardivement pour les trois génotypes.
- Les concentrations des acides par gramme de matière sèche structurale et par gramme de matière fraîche ont été affectées par le stade de récolte chez les trois génotypes: en fin de maturation post récolte, les concentrations en citrate ont été plus élevées dans les fruits récoltés tardivement alors que celles en malate ont globalement été plus faibles.

Ces études indiquent que les concentrations en malate et citrate dans la banane dépendent fortement du génotype et peu des conditions de croissance du fruit. Concernant les effets de la charge en fruit sur l'acidité des fruits, il n'y a pas eu d'autre étude à notre connaissance réalisée sur la banane. Chez la mangue et la pêche, il a été observé un effet du rapport feuille : fruit sur les teneurs en malate et citrate pendant la croissance du fruit (Lechaudel, 2005 ; Souty, 1999 ; Wu, 2002). Une étude sur la mangue n'a pas mis en évidence d'effet significatif

du rapport feuille : fruit sur l'acidité des fruits en post récolte (Joas, 2012). Concernant l'effet de la fertilisation potassique, nos résultats sont en désaccord avec ceux de Kumar et Kumar (2007) qui ont observé une diminution de l'acidité titrable des bananes mûres en réponse à un niveau élevé de fertilisation potassique. Les effets du stade de récolte que nous avons observés sur l'acidité des fruits pendant la maturation sont en accord avec les résultats obtenus sur Cavendish par Bugaud et al. (2006). Les expérimentations agronomiques présentées dans ce travail ayant été réalisées dans des conditions agro-environnementales particulières et sur un nombre restreint de génotypes, les résultats obtenus devront être confirmés dans d'autres environnements et pour d'autres génotypes.

1.2 Identification des paramètres génotypiques et processus physiologiques qui pilotent l'acidité de la banane grâce à la modélisation

Les données expérimentales acquises ont permis de construire et de valider des modèles de prédiction des paramètres d'acidité de la banane (Chapitre III). Un modèle basé sur la représentation des équilibres acido-basiques a permis de prédire le pH et l'acidité titrable de la pulpe. Ce modèle a montré que les déterminants majeurs de l'acidité de la banane sont les teneurs en acides organiques (citrate, malate, oxalate) et en potassium de la pulpe. Un modèle d'accumulation du malate, basé sur une représentation simplifiée des mécanismes de stockage vacuolaire du malate et faisant appel au modèle pH, a permis de simuler l'évolution des teneurs en malate dans la pulpe au cours des phases pré et post récolte chez les trois génotypes. Un modèle d'accumulation du citrate, basé sur une représentation simplifié du cycle de Krebs, a permis de prédire l'évolution des teneurs en citrate dans la pulpe au cours des phases pré et post récolte chez les trois génotypes.

Cette approche de modélisation a permis d'apporter des éléments de compréhension sur les processus physiologiques qui pilotent l'acidité de la banane en pré et post récolte, et sur les paramètres génotypiques à l'origine des variations d'acidité entre génotypes. Le modèle de fonctionnement du cycle de Krebs a permis de prédire de manière satisfaisante l'évolution de la teneur en citrate, indiquant la fonction clé de ce processus dans l'accumulation du citrate dans la pulpe des fruits. Le modèle suggère également le rôle déterminant de l'enzyme malique mitochondriale et des transporteurs mitochondriaux du malate dans les différences de teneurs en citrate observées entre génotypes pendant les phases pré et post récolte. Le modèle de stockage vacuolaire a permis de simuler de manière correcte la teneur en malate, indiquant la fonction clé de ce processus dans l'accumulation du malate dans la pulpe des fruits. Le modèle a mis en évidence le rôle déterminant de la variation

d'énergie libre d'hydrolyse de l'ATP et du pH vacuolaire dans les différences de teneurs en malate observées entre génotypes et entre les phases pré et post récolte.

L'analyse de sensibilité des modèles a permis de quantifier l'effet de certains facteurs liés aux pratiques pré et post récolte sur les teneurs en acides dans la pulpe. Ainsi, le modèle d'accumulation du citrate prédit un effet différent de la température de conservation selon le cultivar sur la concentration en citrate pendant la maturation du fruit. Le modèle d'accumulation du malate prédit quant à lui un effet négatif de la température sur le stockage du malate dans la vacuole pendant les phases pré et post récolte et quelque soit le génotype. Ces résultats sont intéressants car la température est une variable facilement manipulable et pourrait donc être un facteur sur lequel jouer pour modifier l'acidité des fruits. Cependant, à notre connaissance, aucune étude expérimentale n'a été menée a ce jour pour étudier l'effet de la température de stockage sur l'acidité de la banane en post récolte. Il serait donc intéressant dans le futur de vérifier expérimentalement les simulations des modèles. Le modèle d'accumulation du malate suggère que les concentrations en acides organiques et en potassium de la pulpe ont un effet important sur l'accumulation du malate dans la vacuole. Dans les conditions de notre expérimentation en 2012, la fertilisation potassique n'a pas modifié la teneur en potassium dans les fruits, ne nous permettant donc pas de vérifier l'effet prédit par le modèle. L'acquisition future de données expérimentales obtenues dans différents scénarii agro-environnementaux conduisant à des teneurs en potassium dans les fruits contrastées permettrait de tester ces prédictions.

1.3 Hypothèses et limites des modèles écophysiologiques développés

Les modèles développés ont été construits sur la base des conclusions de la synthèse bibliographique réalisée au début de ce travail (Chapitre I). Nous avons ainsi choisi de modéliser le cycle de Krebs et le stockage vacuolaire, qui apparaissent comme les processus déterminants de l'accumulation du citrate et du malate respectivement. La qualité des prédictions des modèles développés nous confortent à posteriori dans le choix de ces hypothèses. Dans le futur, avec de meilleures connaissances sur la compartimentation intra cellulaire du citrate et du malate dans les cellules du fruit, ces modèles pourraient être améliorés en considérant les différents compartiments cellulaires, ce qui permettrait de simuler les teneurs en acides dans le cytosol, la mitochondrie et la vacuole. De tels modèles qui restent certes beaucoup plus difficiles à construire et à paramétrer, donneraient une image globale de la régulation de l'accumulation du citrate et du malate dans le fruit.

Une amélioration envisageable du modèle d'accumulation du citrate en post récolte pourrait être de considérer le rôle de l'éthylène dans la maturation des fruits climactériques

comme la banane. La maturation de la banane est déclenchée par un pic précoce de production d'éthylène qui s'accompagne de la conversion de l'amidon en sucre associée à une augmentation importante de l'activité respiratoire (Bapat *et al.*, 2010). Plusieurs études ont révélé le rôle de l'éthylène dans la régulation de nombreux gènes contrôlant la fermeté, le goût, la couleur et les arômes du fruit (Bapat *et al.*, 2010). Il serait peut être donc plus pertinent de représenter l'évolution des paramètres $k_{i,r}(t)$ et $K_{i,r}(t)$ non pas comme une fonction du nombre de jours après traitement éthylénique, mais comme une fonction de la concentration en éthylène dans le fruit. La prise en compte de l'éthylène pourrait peut-être permettre de mieux simuler la variabilité des teneurs en citrate entre les fruits. Evidemment, cela nécessiterait de faire des mesures d'émissions d'éthylène des fruits qui seraient utilisées comme entrées du modèle (ce que nous n'avions pas dans le cas présent). On pourrait aussi imaginer utiliser un modèle pour prédire la concentration en éthylène dans la banane basé, sur le modèle ETHY développé sur la pêche par Génard et Gouble (2005).

Concernant le modèle d'accumulation du malate, nous avons uniquement considéré la pompe à proton vacuolaire ATPase et négligé la PPiase. A notre connaissance, aucune étude n'a été réalisée à ce jour sur l'activité de la PPiase au cours du développement de la banane. Il serait donc intéressant d'étudier expérimentalement la contribution des deux types de pompes afin de modéliser plus justement la génération du potentiel électrique tonoplastique.

2 Perspectives de recherche

2.1 Modèle intégré d'élaboration de l'acidité : le modèle MUSACIDE

Les modèles développés dans ce travail (pH/acidité titrable, malate et citrate) sont interdépendants puisque certains ont pour entrées des variables prédites par d'autres modèles. Il est donc possible de construire un modèle intégré (MUSACIDE) prédisant les différentes composantes de l'acidité de la banane en combinant ces trois modèles. Les relations entre les différents modèles intégrés sont présentées dans la Fig. IV.1. Les variables d'entrées du modèle MUSACIDE sont le poids frais et sec de la pulpe, la température, et les teneurs en oxalate et minéraux de la pulpe. Les teneurs en citrate et malate prédites sont des entrées du modèle de pH et d'acidité titrable. Le pH prédit par ce dernier modèle est une entrée du modèle malate.

Afin de valider le modèle MUSACIDE, il faut vérifier que l'association des différents modèles n'entraîne pas une accumulation d'erreurs de prédictions. Pour ce faire, les prédictions du modèle MUSACIDE à partir des variables d'entrées des données des expérimentations de 2011 et 2012 pour les trois génotypes ont été comparées aux données

observées (Fig. IV.2). Le modèle MUSACIDE prédit de manière correcte les concentrations en citrate et malate dans la pulpe ainsi que son acidité titrable en pré et post récolte. On peut noter que le RRMSE élevé pour les acidités titrables prédites pendant la phase de croissance n'est pas du à l'intégration des modèles puisque la qualité des prédictions était la même dans le modèle d'acidité titrable simple (cf. Chapitre III.1).

Le modèle MUSACIDE permet donc de prédire l'évolution de l'ensemble des critères d'acidité de la banane en fonction de la croissance de la pulpe, de la température, de la nutrition minérale du fruit, et de sa teneur en oxalate. Il peut donc être utilisé pour simuler l'effet de ces différents facteurs sur l'acidité de la banane en pré et post récolte chez les différents génotypes. Par exemple, nous avons simulé l'effet de la température de conservation sur les paramètres d'acidité pendant la maturation post récolte chez les trois génotypes étudiés (Fig. IV.3). Le modèle MUSACIDE prédit une diminution des teneurs en citrate et malate, et de l'acidité titrable en réponse à une augmentation de la température. Il est intéressant de noter que l'effet simulé de la température n'a pas la même intensité selon les génotypes. Le modèle MUSACIDE pourrait donc être, sous réserve de sa validation sur d'autres jeux de données et pour d'autres génotypes, un outil intéressant pour étudier les interactions entre le génotype et l'environnement en pré et post récolte. De plus, ce modèle devrait être transposable à d'autres espèces de fruits sous réserve de quelques modifications puisque les processus décrits sont communs à tous les fruits.

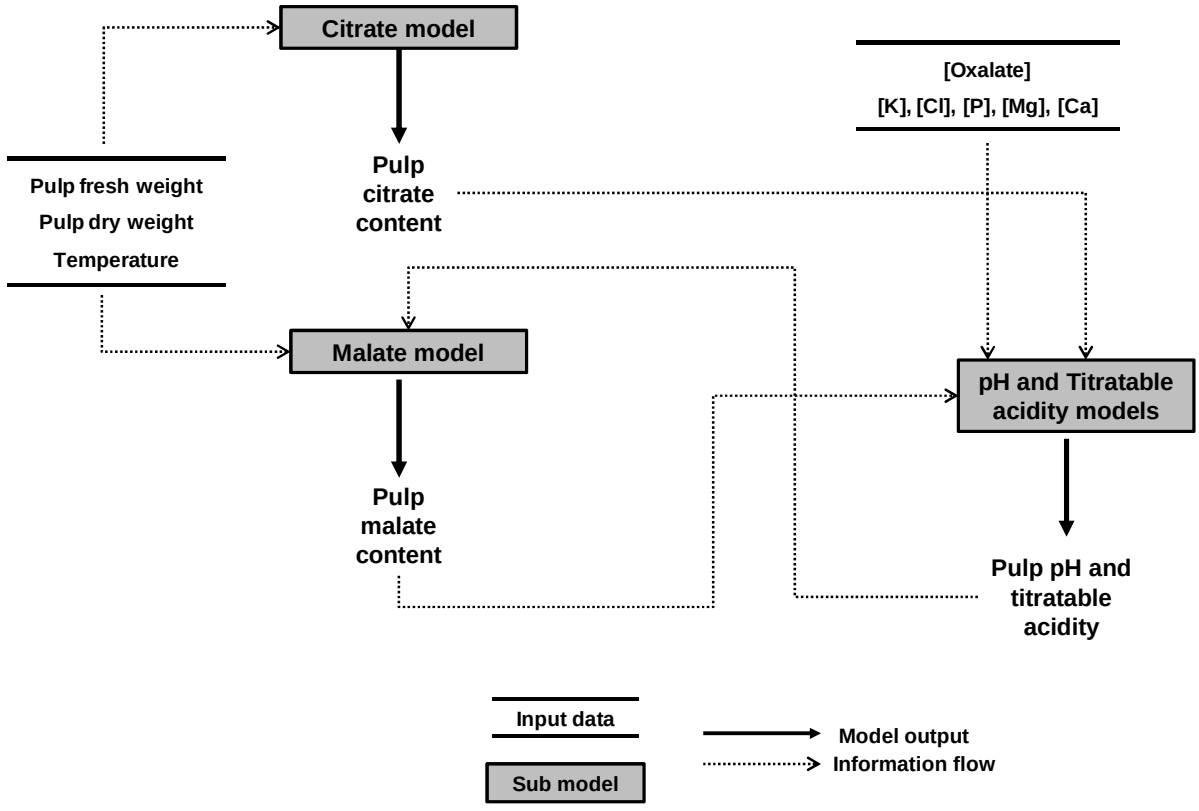

Figure IV-1 Schematic representation of the MUSACIDE model.

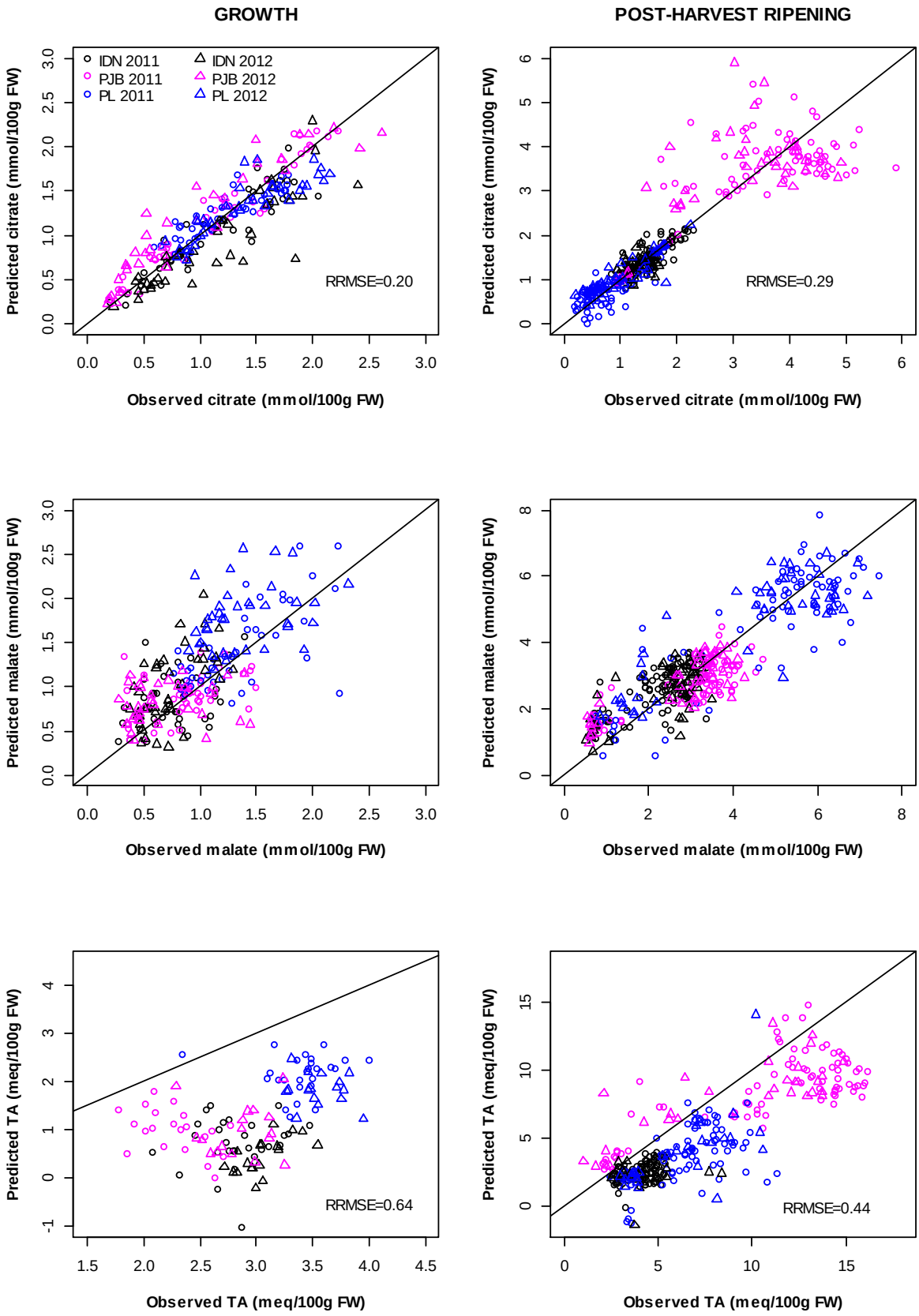

Figure IV-2 Observed vs. predicted citrate concentrations, malate concentrations, and titratable acidity (TA) of banana pulp of cultivars IDN, PJB, and PL during fruit growth and post-harvest ripening. Each symbol represents a fruit. The RRMSE is indicated in each graph.

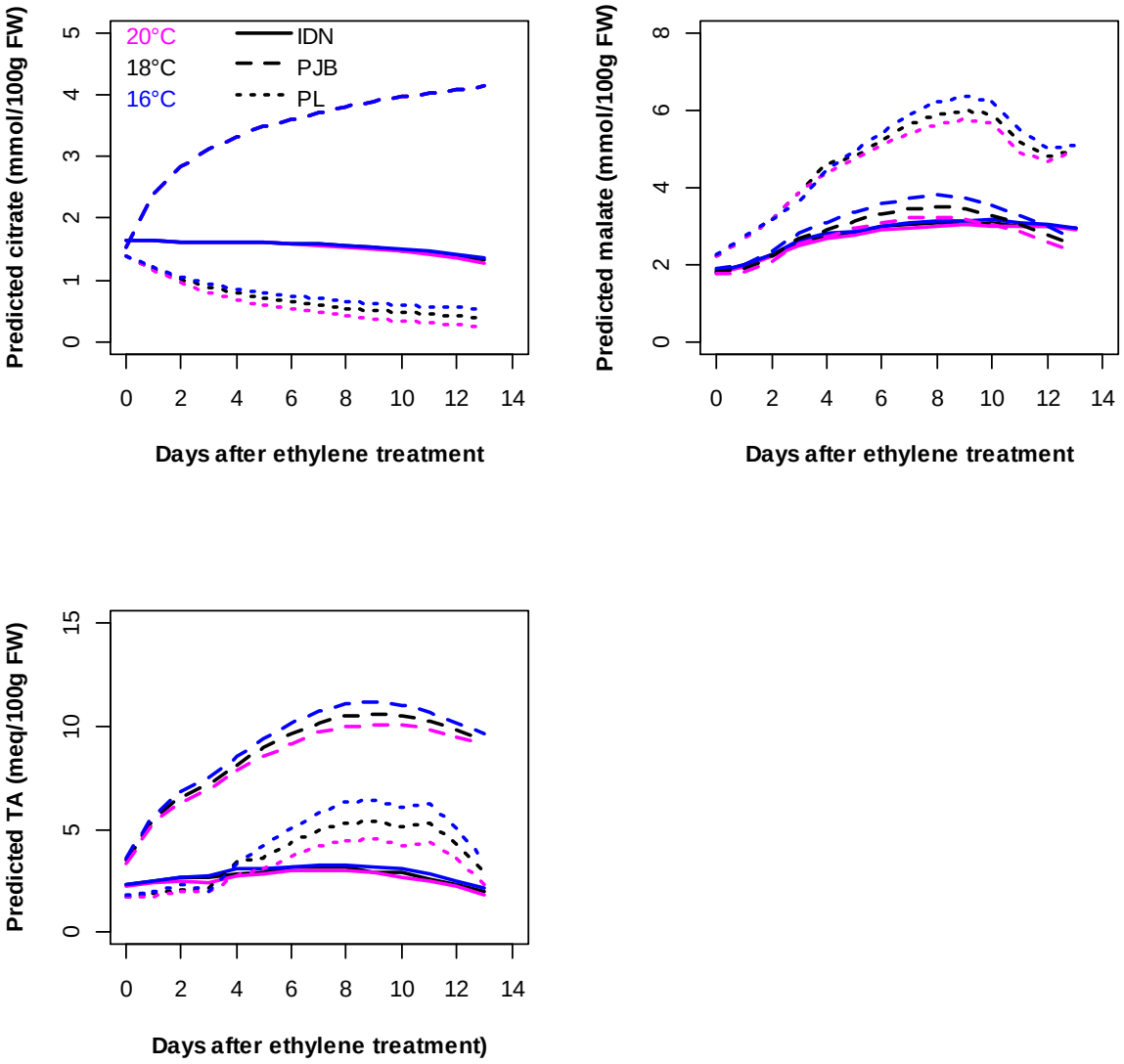

Figure IV-3 Simulated responses of pulp citrate concentration, pulp malate concentration and pulp titratable acidity to changes in temperature during post-harvest ripening of cultivars IDN, PJB, and PL.

2.2 Apport du modèle MUSACIDE pour l'étude de la physiologie du fruit

La démarche de modélisation que nous avons effectuée s'avère bénéfique pour différentes disciplines puisqu'elle apporte des informations sur la physiologie du fruit mais révèle également des lacunes dans nos connaissances. Pour les généticiens et les physiologistes, l'identification des processus et des paramètres importants pour l'accumulation du citrate et du malate dans le fruit fournit des pistes de recherche prioritaires. Ainsi, dans le but d'étudier les déterminants de l'accumulation du citrate, il serait intéressant d'axer les recherches sur les transporteurs mitochondriaux du malate et sur l'enzyme malique mitochondriale. Concernant l'accumulation du malate, les recherches pourraient se focaliser sur l'étude des pompes à protons vacuolaires, dont l'activité dépend entre autre de l'énergie libre d'hydrolyse de l'ATP et du pH vacuolaire. Pour les modélisateurs, il apparait nécessaire de se concentrer sur les processus identifiés comme importants pour décrire l'élaboration de l'acidité du fruit. Nous avons proposé des modèles décrivant de manière simplifiée le fonctionnement du cycle de Krebs et du transport du malate à travers le tonoplaste. Dans l'objectif de mieux comprendre la physiologie du fruit, il pourrait être intéressant de construire un modèle métabolique décrivant par exemple beaucoup plus finement les différents flux du cycle de Krebs. Ce type de modèle pourrait se rapprocher des modèles de flux métaboliques proposé par Alvarez-Vasquez et al. (2000) et Williams et al. (2010). Cependant, la construction d'un tel modèle requiert des données expérimentales de flux métaboliques et ne peut donc se faire sans une collaboration étroite avec les physiologistes.

Ce travail a donc fait ressortir la nécessité d'une forte coopération entre modélisateurs, physiologistes et généticiens. En effet, nous avons été confrontés au manque de données (en particulier chez la banane) concernant l'évolution des activités enzymatiques au cours du développement du fruit ainsi que le contrôle génétique et environnemental de ces activités. L'interaction entre modélisateurs et biologistes moléculaires seraient bénéfique pour les deux partis. En effet, cela apporterait aux modélisateurs des renseignements précieux pour représenter plus finement les processus physiologiques, et donnerait aux biologistes moléculaires une vision intégrée des effets des changements observés au niveau cellulaire (gènes, protéines, métabolites) sur le fonctionnement de la plante. Cette approche pluridisciplinaire est en train de se développer dans le but de construire de modèles multi-échelles intégrant des données moléculaires à des modèles de croissance et de développement des plantes (Baldazzi *et al.*, 2012).

Le modèle MUSACIDE peut être un outil intéressant pour tester des hypothèses physiologiques et évaluer la contribution de certains mécanismes sur l'élaboration de l'acidité. En effet, en comparant le modèle actuel à des versions plus complexes intégrant des

processus supplémentaires, il serait possible de tester l'effet de ces processus sur l'élaboration de l'acidité. L'analyse du fonctionnement de modèles écophysiologiques décrivant différents processus permet de dégager des propriétés émergentes du système décrit et de mieux comprendre les interactions entre processus (Hennig, 2007). L'analyse du modèle MUSACIDE devrait donc permettre d'apporter des informations sur les liens entre les différents processus interdépendants décrits. Par exemple, on pourra analyser l'effet de la concentration cytosolique en malate sur l'accumulation du citrate et du malate puisque ce paramètre intervient dans les deux sous-modèles. Le modèle MUSACIDE pourrait être également utilisé pour explorer *in silico* l'effet de mutations sur les mécanismes physiologiques liés à l'acidité du fruit. Il s'agirait de faire varier la valeur d'un ou plusieurs paramètres pour créer différents mutants virtuels, chacun défini par une combinaison de valeurs de paramètres, et voir l'impact de ces mutations sur les différentes variables du modèle. Cette approche a notamment été utilisée par Génard et al. (2010) sur le modèle de fruit virtuel et par Luquet et al. (2012) sur le modèle Ecomeristem appliqué à la croissance du riz.

Dans le futur, le modèle MUSACIDE pourrait être combiné à des modèles écophysiologiques décrivant d'autres critères importants de la qualité de la banane tels que sa teneur en sucres et sa teneur en matière sèche (Bugaud *et al.*, 2013). Cela permettrait d'obtenir un modèle complet de la qualité de la banane qui serait un outil puissant pour la compréhension de l'élaboration de la qualité du fruit du point de vue physiologique comme cela a déjà été démontré sur la pêche (Génard *et al.*, 2010). Pour prédire la teneur en matière sèche, il faudrait développer un modèle de croissance du fruit prédisant l'accumulation en matière sèche et en eau dans la pulpe. Un modèle biophysique d'accumulation de l'eau dans le fruit (Fishman and Génard, 1998) a déjà été développé sur la pêche et des travaux sont actuellement en cours pour l'adapter au cas de la banane. Un modèle de prédiction du poids sec de la pulpe de banane, basé sur une estimation du nombre de cellules de la pulpe et de la vitesse de remplissage de celles-ci, a été proposé par Jullien (2000) et pourrait donc être utilisé sous réserve de sa validation sur d'autres jeux de données. Pour prédire la teneur en sucres, le modèle d'accumulation des sucres proposé par Génard et al. (2003) sur la pêche pourrait être utilisé. La banane étant un fruit qui stocke beaucoup d'amidon pendant la croissance (Jullien *et al.*, 2001a) contrairement à la pêche, des modifications du modèle initial seraient à envisager pour prendre en compte cette particularité.

2.3 Apport du modèle MUSACIDE pour l'amélioration variétale

Notre travail a montré que le modèle MUSACIDE est un outil intéressant pour analyser la variabilité de l'acidité entre génotypes. Nous avons pu identifier des paramètres génotype-dépendants ayant une grande influence sur les sorties du modèle (ΔG_{ATP} et pHvac pour la teneur en malate ; $K_{5,g}(t)$, $K_{5,r}(t)$, $k_{3,r}(t)$ pour la teneur en citrate). Ces paramètres sont donc des cibles potentiellement intéressantes pour la recherche de QTLs en vue d'améliorer la qualité gustative de la banane par sélection assistée par marqueurs. Pour envisager la recherche de QTLs de ces paramètres, il sera nécessaire de les estimer chez un grand nombre d'individus. La recherche de QTLs de paramètres de modèles écophysiologiques a déjà été réalisée avec succès sur la pêche (Quilot *et al.*, 2005) et la tomate (Prudent *et al.*, 2013).

Ces dernières années, de nombreuses études ont montré l'utilité des modèles écophysiologiques combinés à des modèles génétiques pour disséquer les interactions entre le génotype, l'environnement et les pratiques culturales, et proposer des idéotypes ayant des caractéristiques particulières, adaptés à des conditions spécifiques ou conduisant à des systèmes de production durables (Letort *et al.*, 2008; Quilot-Turion *et al.*, 2011; Tardieu, 2003). Cette approche consiste à estimer la valeur des paramètres du modèle écophysiologique pour n'importe quel individu en fonction de l'allèle présent à chaque locus associé aux QTLs détectés. Les premiers travaux présentant ce type d'approche ont été appliqués à un modèle architectural de l'orge (Buck-Sorlin and Bachmann, 2000). La combinaison de modèles génétiques et écophysiologiques permet une bonne prédiction de l'association entre le génotype et le phénotype (Hammer *et al.*, 2006). Lifeng et al. (2012) sont même allés plus loin en proposant un modèle écophysiologique de croissance du riz intégrant un modèle génétique reproduisant les processus de la reproduction sexuelle. Cette étude a permis de montrer qu'il était pertinent d'intégrer des modèles QTLs dans les modèles écophysiologiques dans une optique de sélection variétale virtuelle. Dans le cas du modèle MUSACIDE, si des QTLs sont détectés pour les paramètres génotype-dépendants, on pourrait donc envisager de créer un modèle génétique pour calculer les valeurs de ces paramètres en fonction de l'allèle présent à chaque locus associé aux QTLs détectés. Ces valeurs de paramètres pourraient ensuite être introduites dans le modèle MUSACIDE. La combinaison des modèles génétiques et écophysiologiques pourrait alors permettre de définir une stratégie d'amélioration de la qualité gustative de la banane, comme cela a été proposé sur la pêche (Quilot *et al.*, 2005). Il s'agirait dans un premier temps de définir l'objectif de qualité multicritère à atteindre, par exemple des valeurs précises d'acidité titrable et de concentrations en acides. Ensuite, il faudrait déterminer grâce au modèle MUSACIDE, les jeux de paramètres qui permettent de parvenir à cet objectif. Dans une troisième étape, les génotypes

qui permettent d'obtenir ces valeurs de paramètres seraient caractérisés en identifiant les combinaisons d'allèles nécessaires aux locus associés à chaque paramètre. Enfin, les individus de la population possédant les génotypes caractérisés à l'étape précédente seraient identifiés afin de réaliser des croisements pour rassembler les allèles favorables et améliorer la qualité gustative de la banane. Si un modèle global de la qualité de la banane est construit dans le futur, il pourra également être utilisé pour définir des idéotypes répondant à des objectifs multicritères de qualité plus complexes et/ou adaptés à des systèmes de productions particuliers (Quilot-Turion *et al.*, 2011).

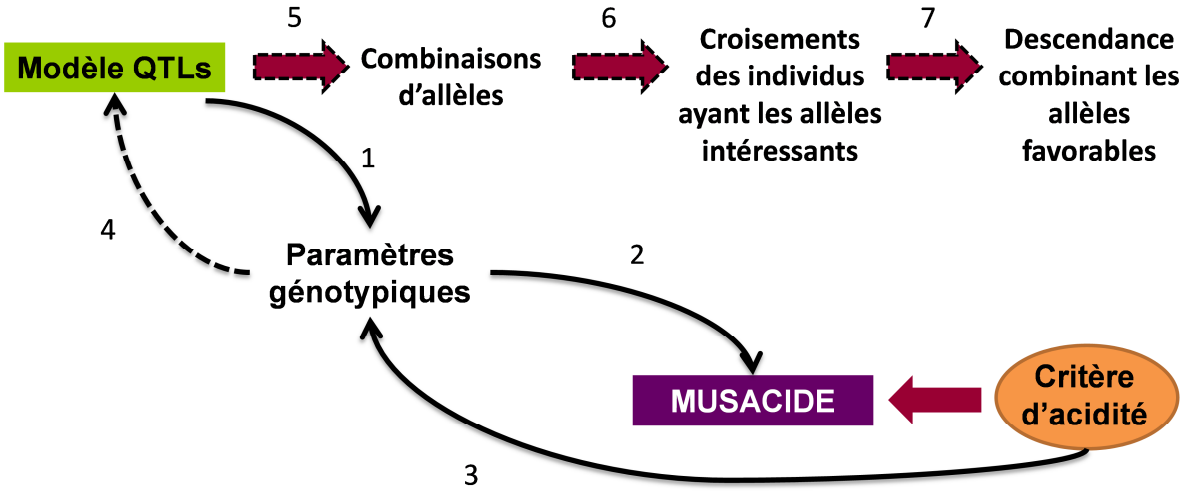

Figure IV-4 Combining the QTLs and MUSACIDE models to define ideotypes of dessert bananas. The QTLs model would allow prediction of the value of the genotypic parameters of the MUSACIDE model for any combination of alleles (1). Then the MUSACIDE model would predict the corresponding parameters of acidity (2). Once the combined model (QTLs and MUSACIDE) will be validated, it could be potentially used as follow to design ideotypes: First, by inverting the MUSACIDE model, the values of genotypic parameters that lead to a certain criteria of acidity could be found (3), then the allelic combination leading to this set of parameters could be identified (4 and 5). The next step would be to cross the individuals carrying the favorable alleles (6) and identifying in the offspring the individuals gathering the larger number of favorable alleles (7).

Bibliographie

Abadie C, Chilin-Charles Y, Huat J, Salmon F, Pignolet L, Carlier J, Lescot T, Côte F, Jenny C. 2007. New approaches to select cultivars of banana with durable resistance to Mycosphaerella leaf spot diseases. *International Symposium on Recent Advances in Banana Crop Protection for Sustainable Production and Improved Livelihoods 828*, Vol. 58, 171-178.
Abou-Zamzama A, Wallace A. 1970. Some characteristics of the mitochondrial and soluble forms of malate dehydrogenase in lemon fruits. *Biochimica and Biophysica Acta* **220**, 396-409.
Albertini MV, Carcouet E, Pailly O, Gambotti C, Luro F, Berti L. 2006. Changes in organic acids and sugars during early stages of development of acidic and acidless citrus fruit. *Journal of agricultural and food chemistry* **54**, 8335-8339.
Allen GJ, Sanders D. 1997. Vacuolar ion channels of higher plants. *Advances in Botanical Research* **25**, 217-252.
Alva AK, Mattos Jr D, Paramasivam S, Patil B, Dou H, Sajwan KS. 2006. Potassium management for optimizing citrus production and quality. *International journal of fruit science* **6**, 3-43.
Alvarez-Vasquez F, González-Alcón C, Torres NV. 2000. Metabolism of citric acid production by *Aspergillus niger*: Model definition, steady-state analysis and constrained optimization of citric acid production rate. *Biotechnology and Bioengineering* **70**, 82-108.
Aprile A, Federici C, Close TJ, De Bellis L, Cattivelli L, Roose ML. 2011. Expression of the H^+-ATPase AHA10 proton pump is associated with citric acid accumulation in lemon juice sac cells. *Functional and Integrative Genomics* **11**, 551-563.
Araujo WL, Nunes-Nesi A, Nikoloski Z, Sweetlove LJ, Fernie AR. 2012. Metabolic control and regulation of the tricarboxylic acid cycle in photosynthetic and heterotrophic plant tissues. *Plant, Cell & Environment* **35**, 1-21.
Ashraf MY, Gul A, Ashraf M, Hussain F, Ebert G. 2010. Improvement in yield and quality of Kinnow (*Citrus deliciosa* x *Citrus nobilis*) by potassium fertilization. *Journal of plant nutrition* **33**, 1625-1637.
Bahrami AR, Chen Z-H, Walker RP, Leegood RC, Gray JE. 2001. Ripening-related occurrence of phosphoenolpyruvate carboxykinase in tomato fruit. *Plant Molecular Biology* **47**, 499-506.
Bai Y, Dougherty L, Li M, Fazio G, Cheng L, Xu K. 2012. A natural mutation-led truncation in one of the two aluminum-activated malate transporter-like genes at the *Ma* locus is associated with low fruit acidity in apple. *Molecular Genetics and Genomics* **287**, 663-678.
Baldazzi V, Bertin N, De Jong H, Génard M. 2012. Towards multiscale plant models: integrating cellular networks. *Trends in Plant Science* **17**, 728-736.
Bapat VA, Trivedi PK, Ghosh A, Sane VA, Ganapathi TR, Nath P. 2010. Ripening of fleshy fruit: molecular insight and the role of ethylene. *Biotechnology advances* **28**, 94-107.
Beaudry RM, Severson RF, Black CC, Kays SJ. 1989. Banana ripening: implications of changes in glycolytic intermediate concentrations, glycolytic and gluconeogenic carbon flux, and fructose 2, 6-bisphosphate concentration. *Plant Physiology* **91**, 1436-1444.
Benzioni A, Vaadia Y, Lips SH. 1971. Nitrate uptake by roots is regulated by nitrate reduction products of shoot. *Physiologia plantarum* **24**, 288-290.
Bergmeyer HU. 1983. *Methods of enzymatic analysis*. Weinheim: Verlag Chemie.
Bertin N, Martre P, Génard M, Quilot B, Salon C. 2010. Under what circumstances can process-based simulation models link genotype to phenotype for complex traits? Case-study of fruit and grain quality traits. *Journal of experimental botany* **61**, 955-967.
Berüter J. 2004. Carbohydrate metabolism in two apple genotypes that differ in malate accumulation. *Journal of Plant Physiology* **161**, 1011-1029.

Bollard E. 1970. The physiology and nutrition of developing fruits. *The biochemistry of fruits and their products* **1**, 387-425.

Borsani J, Budde CO, Porrini L, Lauxmann MA, Lombardo VA, Murray R, Andreo CS, Drincovich MF, Lara MV. 2009. Carbon metabolism of peach fruit after harvest: changes in enzymes involved in organic acid and sugar level modifications. *Journal of experimental botany* **60**, 1823-1837.

Bown AW, Shelp BJ. 1997. The Metabolism and Functions of [gamma]-Aminobutyric Acid. *Plant Physiology* **115**, 1.

Briskin DP, Reynolds-Niesman I. 1991. Determination of H^+/ATP stoichiometry for the plasma membrane H^+-ATPase from red beet (*Beta vulgaris L.*) storage tissue. *Plant Physiology* **95**, 242-250.

Brune A, Gonzalez P, Goren R, Zehavi U, Echeverria E. 1998. Citrate uptake into tonoplast vesicles from acid lime (*Citrus aurantifolia*) juice cells. *Journal of Membrane Biology* **166**, 197-203.

Buck-Sorlin GH, Bachmann K. 2000. Simulating the morphology of barley spike phenotypes using genotype information. *Agronomie* **20**, 691-702.

Bugaud C, Chillet M, Beaute MP, Dubois C. 2006. Physicochemical analysis of mountain bananas from the French West Indies. *Scientia Horticulturae* **108**, 167–172.

Bugaud C, Daribo M-O, Beauté M-P, Telle N, Dubois C. 2009. Relative importance of location and period of banana bunch growth in carbohydrate content and mineral composition of fruit. *Fruits* **64**, 63-74.

Bugaud C, Deverge E, Daribo MO, Ribeyre F, Fils-Lycaon B, Mbéguié-A-Mbéguié D. 2011. Sensory characterisation enabled the first classification of dessert bananas. *Journal of the Science of Food and Agriculture* **91**, 992-1000.

Bugaud C, Belleil T, Daribo M-O, Génard M. 2012. Does bunch trimming affect dry matter content in banana? *Scientia Horticulturae* **144**, 125-129.

Bugaud C, Cazevieille P, Daribo MO, Telle N, Julianus P, Fils-Lycaon B, Mbéguié-A-Mbéguié D. 2013. Rheological and chemical predictors of texture and taste in dessert banana (*Musa* spp.). *Post harvest biology and technology* **84**, 1-8.

Burdon J, Lallu N, Yearsley C, Osman S, Billing D, Boldingh H. 2007. Postharvest conditioning of Satsuma mandarins for reduction of acidity and skin puffiness. *Postharvest Biology and Technology* **43**, 102-114.

Burström H. 1945. Studies on the buffer systems of cells. *Arkiv botanik* **32**, 1-18.

Buttrose M, Hale C, Kliewer WM. 1971. Effect of temperature on the composition of 'Cabernet Sauvignon' berries. *American Journal of Enology and Viticulture* **22**, 71-75.

Canel C, Bailey-Serres JN, Roose ML. 1995. In vitro [^{14}C] citrate uptake by tonoplast vesicles of acidless *Citrus* juice cells. *Journal of American Society of Horticultural Science* **120**, 510-514.

Canel C, Bailey-Serres JN, Roose ML. 1996. Molecular characterization of the mitochondrial citrate synthase gene of an acidless pummelo (*Citrus maxima*). *Plant Molecular Biology* **31**, 143-147.

Cannell M, Thornley J. 2000. Modelling the components of plant respiration: some guiding principles. *Annals of Botany* **85**, 45-54.

Carrari F, Baxter C, Usadel B, Urbanczyk-Wochniak E, Zanor M-I, Nunes-Nesi A, Nikiforova V, Centero D, Ratzka A, Pauly M, Sweetlove LJ, Fernie AR. 2006. Integrated analysis of metabolite and transcript levels reveals the metabolic shifts that underlie tomato fruit development and highlight regulatory aspects of metabolic network behavior. *Plant Physiology* **142**, 1380-1396.

Cercos M, Soler G, Iglesias DJ, Gadea J, Forment J, Talon M. 2006. Global analysis of gene expression during development and ripening of *citrus* fruit flesh. A proposed mechanism for citric acid utilization. *Plant Molecular Biology* **62**, 513-527.

Chacón SI, Víquez F, Chacón G. 1987. Escala físico-química de maduración de banano. Physico-chemical banana ripening scale. *Fruits* **42**, 95-102.
Chandler S. 1995. The nutritional value of bananas. In: Gowen S, ed. *Bananas and plantains*, Vol. 15. London: Chapman & Hall, 468-480.
Chen FX, Liu XH, Chen LS. 2009. Developmental changes in pulp organic acid concentration and activities of acid-metabolising enzymes during the fruit development of two loquat (*Eriobotrya japonica Lindl.*) cultivars differing in fruit acidity. *Food Chemistry* **114**, 657-664.
Chen R, Gadal P. 1990. Structure, functions and regulation of NAD and NADP dependent isocitrate dehydrogenases in higher plants and in other organisms. *Plant physiology and biochemistry* **28**, 411-427.
Chen R. 1998. Plant NADP-dependent isocitrate dehydrogenases are predominantly localized in the cytosol. *Planta* **207**, 280-285.
Chillet M, de Lapeyre de Bellaire L, Hubert O, Mbeguie-A-Mbeguie D. 2008. Measurement of banana green life. *Fruits* **63**, 125-128.
Coombe B. 1976. The development of fleshy fruits. *Annual Review of Plant Physiology* **27**, 207-228.
Cummings GA, Reeves J. 1971. Factors influencing chemical characteristics of peaches. *Journal of American Society of Horticultural Science* **96**, 320-322.
Dai ZW, Vivin P, Génard M. 2008. Modelling the effects of leaf-to-fruit ratio on dry and fresh mass accumulation in ripening grape berries. *Acta Horticulturae* **803**, 283-291.
Dai ZW, Vivin P, Robert T, Milin S, Li SH, Génard M. 2009. Model-based analysis of sugar accumulation in response to source–sink ratio and water supply in grape (*Vitis vinifera*) berries. *Functional Plant Biology* **36**, 527–540.
Davies CW. 1962. *Ion association*. London: Butterworths.
Davies DD. 1986. The fine control of cytosolic pH. *Plant Physiology* **67**, 702-706.
Davies JM, Poole RJ, Sanders D. 1993. The computed free energy change of hydrolysis of inorganic pyrophosphate and ATP: apparent significance for inorganic-pyrophosphate-driven reactions of intermediary metabolism. *Biochimica et Biophysica Acta (BBA)-Bioenergetics* **1141**, 29-36.
Davies JM, Hunt I, Sanders D. 1994. Vacuolar H (+)-pumping ATPase variable transport coupling ratio controlled by pH. *Proceedings of the National Academy of Sciences* **91**, 8547.
Day DA, Neuburger M, Douce R. 1984. Activation of NAD-linked malic enzyme in intact plant mitochondria by exogenous coenzyme A. *Archives of Biochemistry and Biophysics* **231**, 233-242.
De Angeli A, Baetz U, Francisco R, Zhang J, Chaves MM, Regalado A. 2013. The vacuolar channel VvALMT9 mediates malate and tartrate accumulation in berries of *Vitis vinifera*. *Planta* **238**, 283-291.
De la Hera-Orts M, Martinez-Cutillas A, Lopez-Roca J, Gomez-Plaza E. 2005. Effect of moderate irrigation on grape composition during ripening. *Spanish journal of agricultural research* **3**, 352-361.
Degu A, Hatew B, Nunes-Nesi A, Shlizerman L, Zur N, Katz E, Fernie AR, Blumwald E, Sadka A. 2011. Inhibition of aconitase in *citrus* fruit callus results in a metabolic shift towards amino acid biosynthesis. *Planta* **234**, 501-513.
DeJong T, Goudriaan J. 1989. Modeling peach fruit growth and carbohydrate requirements: reevaluation of the double-sigmoid growth pattern. *Journal of the American Society for Horticultural Science* **114**, 800-804.
Deluc LG, Grimplet J, Wheatley MD, Tillett RL, Quilici DR, Osborne C, Schooley DA, Schlauch KA, Cushman JC, Cramer GR. 2007. Transcriptomic and metabolite analyses of Cabernet Sauvignon grape berry development. *BMC genomics* **8**, 429.

Deng W, Luo K, Li Z, Yang Y. 2008. Molecular cloning and characterization of a mitochondrial dicarboxylate/tricarboxylate transporter gene in *Citrus junos* response to aluminum stress. *Mitochondrial DNA* **19**, 376-384.

des Gachons CP, Leeuwen CV, Tominaga T, Soyer JP, Gaudillère JP, Dubourdieu D. 2004. Influence of water and nitrogen deficit on fruit ripening and aroma potential of *Vitis vinifera* L cv Sauvignon blanc in field conditions. *Journal of the Science of Food and Agriculture* **85**, 73-85.

Diakou P, Svanella L, Raymond P, Gaudillère JP, Moing A. 2000. Phosphoenolpyruvate carboxylase during grape berry development: protein level, enzyme activity and regulation. *Functional Plant Biology* **27**, 221-229.

Dilley DR. 1962. Malic enzyme activity in apple fruit. *Nature* **196**, 387-388.

Douce R. 1985. *Mitochondria in higher plants: Structure, function, and biogenesis*. Orlando: Academic Press.

Du Preez M. 1985. Effect of fertilization on fruit quality. *Deciduous fruit Grower* **April**, 138-140.

Echeverria E, Gonzales PC, Brune A. 1997. Characterization of proton and sugar transport at the tonoplast of sweet lime (*Citrus limmetioides*) juice cells. *Physiologia plantarum* **101**, 291-300.

Embleton T, Jones W, Pallares C, Platt R. 1978. Effects of fertilization of *citrus* on fruit quality and ground water nitrate-pollution potential. *International citrus congress*. Sidney, 280-285.

Emmerlich V, Linka N, Reinhold T, Hurth MA, Traub M, Martinoia E, Neuhaus HE. 2003. The plant homolog to the human sodium/dicarboxylic cotransporter is the vacuolar malate carrier. *Proceedings of the National Academy of Sciences* **100**, 11122-11126.

Epimashko S, Meckel T, Fischer-Schliebs E, Luttge U, Thiel G. 2004. Two functionally different vacuoles for static and dynamic purposes in one plant mesophyll leaf cell. *Plant journal* **37**, 294-300.

Esteban MA, Villanueva MJ, Lissargue JR. 1999. Effect of irrigation on changes in berry composition of Tempranillo during maturation. Sugars, organic acids, and mineral elements. *American Journal of Enology and Viticulture* **50**, 418-434.

Esti M, Cinquanta L, Sinesio F, Moneta E, Di Matteo M. 2002. Physicochemical and sensory fruit characteristics of two sweet cherry cultivars after cool storage. *Food Chemistry* **76**, 399-405.

Etienne A, Génard M, Bancel D, Benoit S, Bugaud C. 2013a. A model approach revealed the relationship between banana pulp acidity and composition during growth and post harvest ripening. *Scientia Horticulturae* **162**, 125-134.

Etienne A, Génard M, Lobit P, Mbeguié-A-Mbéguié D, Bugaud C. 2013b. What controls fleshy fruit acidity? A review of malate and citrate accumulation in fruit cells. *Journal of experimental botany* **64**, 1451-1469.

Etienne A, Génard M, Bancel D, Benoit S, Lemire G, Bugaud C. 2014. Citrate and malate accumulation in banana fruit (*Musa* sp. AA) is highly affected by genotype and fruit age, but not by cultural practices *Scientia Horticulturae* **(*in press*)**.

Etienne C, Moing A, Dirlewanger E, Raymond P, Monet R, Rothan C. 2002. Isolation and characterization of six peach cDNAs encoding key proteins in organic acid metabolism and solute accumulation: involvement in regulating peach fruit acidity. *Physiologia plantarum* **114**, 259-270.

Etxeberria E, Pozueta-Romero J, Gonzales P. 2012. In and out of the plant storage vacuole. *Plant Science* **190**, 52-61.

Fait A, Hanhineva K, Beleggia R, Dai N, Rogachev I, Nikiforova VJ, Fernie AR, Aharoni A. 2008. Reconfiguration of the achene and receptacle metabolic networks during strawberry fruit development. *Plant Physiology* **148**, 730-750.

Famiani F, Walker RP, Tecsi L, Chen ZH, Proietti P, Leegood RC. 2000. A immunohistochemical study of the compartmentation of metabolism during the development of grape (*Vitis vinifera* L.) berries. *Journal of experimental botany* **51**, 675-683.
Famiani F, Cultrera NGM, Battistelli A, Casulli V, Proietti P, Standardi A, Chen ZH, Leegood RC, Walker RP. 2005. Phosphoenolpyruvate carboxykinase and its potential role in the catabolism of organic acids in the flesh of soft fruit during ripening. *Journal of experimental botany* **56**, 2959-2969.
Fatland BL, Ke J, Anderson MD, Mentzen WI, Cui LW, Allred CC, Johnston JL, Nikolau BJ, Wurtele ES. 2002. Molecular characterization of a heteromeric ATP-citrate lyase that generates cytosolic acetyl-coenzyme A in Arabidopsis. *Plant Physiology* **130**, 740-756.
Fishman S, Génard M. 1998. A biophysical model of fruit growth: simulation of seasonal and diurnal dynamics of mass. *Plant, Cell & Environment* **21**, 739-752.
Fontes N, Gerós H, Delrot S. 2011. Grape berry vacuole: a complex and heterogeneous membrane system specialized in the accumulation of solutes. *American Journal of Enology and Viticulture* **62**, 270-278.
Fox J. 2002. Non linear regression and non linear least squares. In: oaks T, ed. *Appendix to an R and S-PLUS companion to applied regression.* CA: Sage publications
Gałecki A, Burzykowski T. 2013. Linear Mixed-Effects Model. *Linear Mixed-Effects Models Using R.* New York: Springer, 245-273.
Gálvez S, Gadal P. 1995. On the function of the NADP-dependent isocitrate dehydrogenase isoenzymes in living organisms. *Plant Science* **105**, 1-14.
Gautier H, Rocci A, Buret M, Grassely D, Causse M. 2005. Fruit load or fruit position alters response to temperature and subsequently cherry tomato quality. *Journal of the Science of Food and Agriculture* **85**, 1009-1016.
Génard M, Bruchou C, Souty M. 1991. Variabilité de la croissance et de la qualité chez la pêche (*Prunus persica L Batsch*) et liaison entre croissance et qualité. *Agronomie* **11**, 829-845.
Génard M, Bruchou C. 1993. A functionnal and explanatory approach to studying growth: the example of the peach fruit. *Journal of American Society of Horticultural Science* **118**, 317-323.
Génard M, Souty M, Holmes S, Reich M, Breuils L. 1994. Correlations among quality parameters of peach fruit. *Journal of the Science of Food and Agriculure* **66**, 241-245.
Génard M, Souty M. 1996. Modeling the Peach Sugar Contents in Relation to Fruit Growth. *Journal of American Society of Horticultural Science* **121**, 1122–1131.
Génard M, Reich M, Lobit P, Besset J. 1999. Correlations between sugar and acid content and peach growth. *Journal of horticultural science & biotechnology* **74**, 772-776.
Génard M, Lescourret F, Gomez L, Habib R. 2003. Changes in fruit sugar concentrations in response to assimilate supply, metabolism and dilution: a modeling approach applied to peach fruit (*Prunus persica*). *Tree Physiology* **23**, 373–385.
Génard M, Gouble B. 2005. ETHY. A Theory of Fruit Climacteric Ethylene Emission. *Plant Physiology* **139**, 531–545.
Génard M, Bertin N, Borel C, Bussières P, Gautier H, Habib R, Léchaudel M, Lecomte A, Lescourret F, Lobit P, Quilot B. 2007. Towards a virtual fruit focusing on quality: modelling features and potential uses. *Journal of experimental botany* **58**, 917–928.
Génard M, Bertin N, Gautier H, Lescourret F, Quilot B. 2010. Virtual profiling: a new way to analyse phenotypes. *Plant journal* **62**, 344-355.
Genevois L, Peynaud E. 1974. Composition de 16 variétés de pêches. *Revue Horticole* **30**, 295-298.
Gerhardt R, Heldt HW. 1984. Measurement of subcellular metabolite levels in leaves by fractionation of freeze-stopped material in nonaqueous media. *Plant Physiology* **75**, 542-547.

Giovannoni JJ. 2004. Genetic regulation of fruit development and ripening. *The plant cell* **16**, 170-180.
Givan CV. 1999. Evolving concepts in plant glycolysis: two centuries of progress. *Biological reviews* **74**, 277-309.
Gomez L, Bancel D, Rubio E, Vercambre G. 2007. The microplate reader: an efficient tool for the separate enzymatic analysis of sugars in plant tissues—validation of a micro-method. *Journal of the Science of Food and Agriculture* **87**, 1893-1905.
Gonzales-Altozano P, Castel JR. 1999. Regulated deficit irrigation in 'Clementina De Nules' *citrus* trees. I. Yield and fruit quality effects. *Journal of horticultural science & biotechnology* **74**, 706-713.
Goodenough PW, Prosser IM, Young K. 1985. NADP-linked malic enzyme and malate metabolism in ageing tomato fruit. *Phytochemistry* **24**, 1157-1162.
Goudriaan J, Monteith J. 1990. A mathematical function for crop growth based on light interception and leaf area expansion. *Annals of Botany* **66**, 695-701.
Gout E, Bligny R, Pascal N, Douce R. 1993. 13C nuclear magnetic resonance studies of malate and citrate synthesis and compartmentation in higher plant cells. *Journal of Biological Chemistry* **268**, 3986-3992.
Gurrieri F, Audergon JM, Albagnac G, Reich M. 2001. Soluble sugars and carboxylic acids in ripe apricot fruit as parameters for distinguishing different cultivars. *Euphytica* **117**, 183-189.
Haferkamp I, Schmitz-Esser S. 2012. The plant mitochondrial carrier family: functional and evolutionary aspects. *Frontiers in plant science* **3**, 1-19.
Hafke JB, Hafke Y, Smith JAC, Lüttge U, Thiel G. 2003. Vacuolar malate uptake is mediated by an anion-selective inward rectifier. *The Plant Journal* **35**, 116-128.
Halestrap AP. 1975. The mitochondrial pyruvate carrier. Kinetics and specificity for substrates and inhibitors. *Biochemical Journal* **148**, 85.
Hammer G, Cooper M, Tardieu F, Welch S, Walsh B, van Eeuwijk F, Chapman S, Podlich D. 2006. Models for navigating biological complexity in breeding improved crop plants. *Trends in Plant Science* **11**, 587-593.
Hardy PJ. 1968. Metabolism of sugars and organic acids in immature grape berries. *Plant Physiology* **43**, 224-228.
Harker F, Marsh K, Young H, Murray S, Gunson F, Walker S. 2002. Sensory interpretation of instrumental measurements 2: sweet and acid taste of apple fruit. *Postharvest Biology and Technology* **24**, 241-250.
Hawker JS. 1969. Changes in the activities of malic enzyme, malate dehydrogenase, phosphopyruvate carboxylase and pyruvate decarboxylase during the development of a non-climacteric fruit (the grape). *Phytochemistry* **8**, 19-23.
Hennig L. 2007. Patterns of beauty–omics meets plant development. *Trends in Plant Science* **12**, 287-293.
Hudina M, Stampar F. 2000. Influence of water regimes and mineral contents in soil upon the contents of minerals, sugars and organic acids in pear fruits (*Pyrus communis L.*) cv.Williams'. *Phyton* **40**, 91-96.
Hummel I, Pantin F, Sulpice R, Piques M, Rolland G, Dauzat M, Christophe A, Pervent M, Bouteillé M, Stitt M, Gibon Y, Muller B. 2010. *Arabidopsis* plants acclimate to water deficit at low cost through changes of carbon usage: an integrated perspective using growth, metabolite, enzyme, and gene expression analysis. *Plant Physiology* **154**, 357-372.
Hunsche M, Brackmann A, Ernani PR. 2003. Effect of potassium fertilization on the postharvest quality of 'Fuji' apples. *Pesquisa Agropecuaria Brasileira* **38**, 489-496.
Hurth MA, Suh SJ, Kretzschmar T, Geis T, Bregante M, Gambale F, Martinoia E, Neuhaus HE. 2005. Impaired pH homeostasis in *Arabidopsis* lacking the vacuolar dicarboxylate transporter and analysis of carboxylic acid transport across the tonoplast. *Plant Physiology* **137**, 901-910.

Iannetta PPM, Escobar NM, Ross HA, Souleyre EJF, Hancock RD, Witte C-P, Davies HV. 2004. Identification, cloning and expression analysis of strawberry (*Fragaria* × *ananassa*) mitochondrial citrate synthase and mitochondrial malate dehydrogenase. *Physiologia plantarum* **121**, 15-26.

Isayenkov S, Isner JC, Maathuis FJM. 2010. Vacuolar ion channels: Roles in plant nutrition and signalling. *FEBS letters* **584**, 1982-1988.

Izonfuo W-AL, Omuaru VOT. 1988. Effect of ripening on the chemical composition of Plantain peels and pulps (*Musa paradisiaca*). *Journal of the Science of Food and Agriculture* **45**, 333-336.

Jeffery D, Smith C, Goodenough P, Prosser I, Grierson D. 1984. Ethylene-Independent and Ethylene-Dependent Biochemical Changes in Ripening Tomatoes. *Plant Physiology* **74**, 32-38.

Jeger MJ, Eden-Green S, Thresh JM, Johanson A, Waller JM, Brown AE. 1995. Banana diseases. In: S. G, ed. *Bananas and Plantains*. London: Chapman & Hall, 317-381.

Jia H, Hirano K, Okamoto G. 1999. Effects of fertilizer levels on tree growth and fruit quality of 'Hakuho' peaches (*Prunux persica*). *Journal of the Japanese Society for Horticultural Science* **68**, 487-493.

Joas J, Vulcain E, Desvignes C, Morales E, Léchaudel M. 2012. Physiological age at harvest regulates the variability in postharvest ripening, sensory and nutritional characteristics of mango (*Mangifera indica* L.) cv. Coghshall due to growing conditions. *Journal of the Science of Food and Agriculture* **92**, 1282-1290.

John P, Marchal J. 1995. Ripening and biochemistry of the fruit. In: Gowen S, ed. *Bananas and Plantains*. London: Chapman and Hall, 434-467.

Johnson JB, Omland KS. 2004. Model selection in ecology and evolution. *Trends in ecology & evolution* **19**, 101-108.

Jullien A. 2000. Croissance, développement et qualité des fruits du bananier (*Musa* spp groupe AAA cv Grande Naine). Modélisation de la répartition des assimilats entre les fruits du régime., INA-PG, Paris.

Jullien A, Malézieux E, Michaux-Ferrière N, Chillet M, Ney B. 2001a. Within-bunch variability in banana fruit weight: importance of developmental lag between fruits. *Annals of Botany* **87**, 101-108.

Jullien A, Munier-Jolain NG, Malézieux E, Chillet M, Ney B. 2001b. Effect of pulp cell number and assimilate availability on dry matter accumulation rate in a banana fruit [*Musa* sp. AAA group 'Grande Naine'(Cavendish subgroup)]. *Annals of Botany* **88**, 321-330.

Jullien A, Chillet M, Malezieux E. 2008. Pre-harvest growth and development, measured as accumulated degree days, determine the post-harvest green life of banana fruit. *Journal of Horticultural Science and Biotechnology* **83**, 506-512.

Kallsen CE, Sanden B, Arpaia ML. 2011. Early navel orange fruit yield, quality, and maturity in response to late-season water stress. *HortScience* **46**, 1163-1169.

Katz E, Fon M, Lee Y, Phinney B, Sadka A, Blumwald E. 2007. The *citrus* fruit proteome: insights into *citrus* fruit metabolism. *Planta* **226**, 989-1005.

Katz E, Boo KH, Kim HY, Eigenheer RA, Phinney BS, Shulaev V, Negre-Zakharov F, Sadka A, Blumwald E. 2011. Label-free shotgun proteomics and metabolite analysis reveal a significant metabolic shift during *citrus* fruit development. *Journal of experimental botany* **62**, 5367-5384.

Kettner C, Bertl A, Obermeyer G, Slayman C, Bihler H. 2003. Electrophysiological analysis of the yeast V-type proton pump: variable coupling ratio and proton shunt. *Biophysical journal* **85**, 3730-3738.

Kliewer WM. 1973. Berry composition of *Vitis Vinifera* cultivars as influenced by photo- and nycto-temperature during maturation. *Journal of the American Society for Horticultural Science* **98**, 153-159.

Kobayashi K, Salam MU. 2000. Comparing simulated and measured values using mean squared deviation and its components. *Agronomy journal* **92**, 345-352.
Kovermann P, Meyer S, Hörtensteiner S, Picco C, Scholz-Starke J, Ravera S, Lee Y, Martinoia E. 2007. The *Arabidopsis* vacuolar malate channel is a member of the ALMT family. *The Plant Journal* **52**, 1169-1180.
Kubicek C, Röhr M. 1978. The role of the tricarboxylic acid cycle in citric acid accumulation by Aspergillus niger. *European journal of applied microbiology and biotechnology* **5**, 263-271.
Lakso AN, Kliewer WM. 1975a. Physical properties of phosphoenolpyruvate carboxylase and malic enzyme in grape berries. *American Journal of Eonology and Viticulture* **26**, 75-78.
Lakso AN, Kliewer WM. 1975b. The influence of temperature on malic acid metabolism in grape berries: I. Enzyme responses 1. *Plant Physiology* **56**, 370-372.
Laloi M. 1999. Plant mitochondrial carriers: an overview. *Cellular and Molecular Life Sciences* **56**, 918-944.
Léchaudel M, Génard M, Lescourret F, Urban L, Jannoyer M. 2002. Leaf-to-fruit ratio affects water and dry-matter content of mango fruit. *Journal of horticultural science & biotechnology* **77**, 773-777.
Léchaudel M, Génard M, Lescourret F, Urban L, Jannoyer M. 2005a. Modeling effects of weather and source–sink relationships on mango fruit growth. *Tree Physiology* **25**, 583–597.
Léchaudel M, Joas J, Caro Y, Génard M, Jannoyer M. 2005b. Leaf:fruit ratio and irrigation supply affect seasonal changes in minerals, organic acids and sugars of mango fruit. *Journal of the Science of Food and Agriculture* **85**, 251–260.
Léchaudel M, Vercambre G, Lescourret F, Normand F, Génard M. 2007. An analysis of elastic and plastic fruit growth of mango in response to various assimilate supplies. *Tree Physiology* **27**, 219-230.
Leegood RC, Walker RP. 2003. Regulation and roles of phospho*enol*pyruvate carboxykinase in plants. *Archives of Biochemistry and Biophysics* **414**, 204-210.
Leidi EO, Barragán V, Rubio L, El-Hamdaoui A, Ruiz MT, Cubero B, Fernández JA, Bressan RA, Hasegawa PM, Quintero FJ. 2010. The AtNHX1 exchanger mediates potassium compartmentation in vacuoles of transgenic tomato. *The Plant Journal* **61**, 495-506.
Leigh RA. 2001. Potassium homeostasis and membrane transport. *Journal of Plant Nutrition and Soil Science* **164**, 193-198.
Lerceteau-Köhler E, Moing A, Guérin G, Renaud C, Petit A, Rothan C, Denoyes B. 2012. Genetic dissection of fruit quality traits in the octoploid cultivated strawberry highlights the role of homoeo-QTL in their control. *Theoretical and Applied Genetics* **124**, 1059-1077.
Lescourret F, Ben Mimoun B, Génard M. 1998. A simulation model of growth at the shoot-bearing fruit level I. Description and parameterization for peach. *European Journal of Agronomy* **9**, 173–188.
Lester GE, Jifon JL, Makus DJ. 2010. Impact of potassium nutrition on postharvest fruit quality: Melon (*Cucumis melo L*) case study. *Plant and soil* **335**, 117-131.
Letort V, Mahe P, Cournède P-H, De Reffye P, Courtois B. 2008. Quantitative genetics and functional–structural plant growth models: simulation of quantitative trait loci detection for model parameters and application to potential yield optimization. *Annals of Botany* **101**, 1243-1254.
Lifeng X, Weilong D, Jun Z, Henke M, Kurth W, Buck-Sorlin G. 2012. Simulating superior genotypes for plant height based on QTLs: Towards virtual breeding of rice. *IEEE Plant Growth Modeling, Simulation, Visualization and Applications (PMA) 2012*, 447-454.
Liu H-F, Génard M. 2007. Model-assisted analysis of tomato fruit growth in relation to carbon and water fluxes. *Journal of experimental botany* **58**, 3567–3580.

Liu S, Yang Y, Murayama H, Taira S, Fukushima T. 2004. Effects of CO_2 on respiratory metabolism in ripening banana fruit. *Postharvest Biology and Technology* **33**, 27-34.
Lobit P. 1999. Etude et modélisation de l'acidité des pêches (*Prunus persica L. Batsch*, cv. Fidelia). Application à l'étude des effets de la nutrition azotée. PhD thesis, Ecole nationale superieure agronomique de Montpellier, Montpellier, 237.
Lobit P, Soing P, Génard M, Habib R. 2002. Theoretical analysis of relationships between composition, pH, and titratable acidity of peach fruit. *Journal of plant nutrition* **25**, 2775–2792.
Lobit P, Génard M, Wu BH, Soing P, Habib R. 2003. Modelling citrate metabolism in fruits: responses to growth and temperature. *Journal of experimental botany* **54**, 2489-2501.
Lobit P, Génard M, Soing P, Habib R. 2006. Modelling malic acid accumulation in fruits: relationships with organic acids, potassium, and temperature. *Journal of experimental botany* **57**, 1471–1483.
Loeillet D. 2008. Fiche pays producteur : la banane en Martinique. *Fruitrop* **155**, 23-28.
Lopez-Bucio J, Nieto-Jacobo MF, Ramirez-Rodriguez V, Herrera-Estrella L. 2000. Organic acid metabolism in plants: from adaptative physiology to transgenic varieties for cultivation in extreme soils. *Plant Science* **160**, 1-13.
Lu X-P, Liu Y-Z, Zhou G-F, Wei Q-J, Hu H-J, Peng S-A. 2011. Identification of organic acid-related genes and their expression profiles in two pear (*Pyrus pyrofolia*) cultivars with difference in predominant acid type at fruit ripening stage. *Scientia Horticulturae* **129**, 680-687.
Luquet D, Soulié J, Rebolledo M, Rouan L, Clément-Vidal A, Dingkuhn M. 2012. Developmental dynamics and early growth vigour in rice 2. Modelling genetic diversity using Ecomeristem. *Journal of Agronomy and Crop Science* **198**, 385-398.
Lüttge U, Ball E. 1979. Electrochemical investigation of active malic acid transport at the tonoplast into the vacuoles of the CAM plant Kalanchoë daigremontiana. *Journal of Membrane Biology* **47**, 401-422.
Lyon BG, Robertson JA, Meredith FI. 1993. Sensory descriptive analysis of cv. Cresthaven peaches: maturity, ripening, and storage effects. *Journal of Food Science* **58**, 177-181.
Macrae AR, Moorhouse R. 1970. The oxidation of malate by mitochondria isolated from cauliflower buds. *European Journal of Biochemistry* **16**, 96-102.
Madshus IH. 1988. Regulation of intracellular pH in eukaryotic cells. *Biochemical Journal* **250**, 1-8.
Maeshima M, Hara-Nishimura I, Takeuchi Y, Nishimura M. 1994. Accumulation of vacuolar H^+-pyrophosphatase and H^+-ATPase during reformation of the central vacuole in germinating pumpkin seeds. *Plant Physiology* **106**, 61-69.
Maeshima M. 2000. Vacuolar H^+-pyrophosphatase. *Biochimica et Biophysica Acta (BBA)-Biomembranes* **1465**, 37-51.
Maeshima M. 2001. Tonoplast transporters: organization and function. *Annual review of plant biology* **52**, 469-497.
Maillard J-C. 2002. Le commerce international de la banane: marché, filière, système. *Les Cahiers d'Outre-Mer. Revue de géographie de Bordeaux* **55**, 371-392.
Martin-Prével P. 1973. Influence de la Nutrition Potassique sur les Fonctions Physiologiques et la Qualité de la Production chez Quelques plantes Tropicales. *10th Colloquium of the international potash institute*. Abidjan, 233-248.
Martin-Prével P. 1977. Echantillonnage du bananier pour l'analyse foliaire: Consequences des differences de techniques. *Fruits* **32**, 151-166.
Martin-Prével P, Gagnard J, Gautier P. 1984. *L'analyse végétale dans le contrôle de l'alimentation des plantes tempérées et tropicales.* Paris: Lavoisier.
Martınez-Esteso MJ, Selles-Marchart S, Lijavetzky D, Angeles Pedren M, Bru-Martınez R. 2011. A DIGE-based quantitative proteomic analysis of grape berry flesh development and

ripening reveals key events in sugar and organic acid metabolism. *Journal of experimental botany* **62**, 2521-2569.
Martinoia E, Maeshima M, Neuhaus HE. 2007. Vacuolar transporters and their essential role in plant metabolism. *Journal of experimental botany* **58**, 83-102.
Martre P, Bertin N, Salon C, Génard M. 2011. Modelling the size and composition of fruit, grain and seed by process-based simulation models. *New Phytologist* **191**, 601-618.
Mattoo A, Modi V. 1970. Citrate cleavage enzyme in mango fruit. *Biochemical and Biophysical Research Communications* **39**, 895-904.
Medina-Suárez R, Manning K, Fletcher J, Aked J, Bird CR, Seymour GB. 1997. Gene expression in the pulp of ripening bananas (two-dimensional sodium dodecyl sulfate-polyacrylamide gel electrophoresis of in vitro translation products and cDNA cloning of 25 different ripening-related mRNAs). *Plant Physiology* **115**, 453-461.
Mehinagic E, Charles M, Vigneau E, Symoneaux R, Maitre I. 2012. Segmentation des consommateurs de pommes selon des critères gustatifs. *Revue Suisse de Viticulture Arboriculture et Horticulture* **44**, 360-366.
Meyer S, Scholz-Starke J, De Angeli A, Kovermann P, Burla B, Gambale F, Martinoia E. 2011. Malate transport by the vacuolar AtALMT6 channel in guard cells is subject to multiple regulation. *The Plant Journal* **67**, 247-257.
Mills TM, Behboudian MH, and Clothier BE. 1996. Water relations, growth, and the composition of 'Braeburn' apple fruit under deficit irrigation. *Journal of the American Society for Horticultural Science* **121**, 286-291
Moing A, Svanella L, Monet R, Rothan C, Just D, Diakou P, Gaudillère JP, Rollin D. 1998. Organic acid metabolism during the fruit development of two peach cultivars. *Acta Horticulturae* **465**, 425-430.
Moing A, Rothan C, Svanella L, Just D, Diakou P, Raymond P, Gaudillère JP, Monet R. 2000. Role of phosphoenolpyruvate carboxylase in organic acid accumulation during peach fruit development. *Physiologia plantarum* **108**, 1-10.
Monod H, Naud C, Makowski D. 2006. *Uncertainty and sensitivity analysis for crop models.* Amsterdam: Elsevier.
Moreira R, Hiroce R, Saes L. 1986. An analysis of twelve nutrients in the internal and external leaf samples of fifty banana cultivars. *Fruits* **41**, 669-673.
Morgan MM, Osorio S, Gehl B, Baxter CJ, Kruger NJ, Ratcliffe RG, Fernie AR, Sweetlove L. 2013. Metabolic engineering of tomato fruit organic acid content guided by biochemical analysis of an introgression line. *Plant Physiology* **161**, 397-407.
Moskowitz AH, Hrazdina G. 1981. Vacuolar contents of fruit subepidermal cells from *Vitis* species. *Plant Physiology* **68**, 686-692.
Mpelasoka BS, Schachtman DP, Treeby MT, Thomas MR. 2003. A review of potassium nutrition in grapevines with special emphasis on berry accumulation. *Australian Journal of Grape and Wine Research* **9**, 154-168.
Müller M, Taiz L. 2002. Regulation of the lemon-fruit V-ATPase by variable stoichiometry and organic acids. *Journal of Membrane Biology* **185**, 209-220.
Müller ML, Irkens-Kiesecker U, Rubinstein B, Taiz L. 1996. On the mechanism of hyperacidification in lemon. Comparison of the vacuolar H^+-ATPase activities of fruits and epicotyls. *The journal of biological chemistry* **271**, 1916-1924.
Müller ML, Irkens-Kiesecker U, Kramer D, Taiz L. 1997. Purification and reconstitution of the vacuolar H^+-ATPases from lemon fruits and epicotyls. *Journal of Biological Chemistry* **272**, 12762-12770.
Murata N, Los DA. 1997. Membrane fluidity and temperature perception. *Plant Physiology* **115**, 875-879.
Mustaffa R, Osman A, Yusof S, Mohamed S. 1998. Physico-chemical Changes in Cavendish Banana (*Musa* cavendishii L var Montel) at Different Positions within a Bunch

during Development and Maturation. *Journal of the Science of Food and Agriculture* **78**, 201-207.

N'Ganzoua KR, Camara B, Dick E. 2010. Evaluation des changements physico-chimiques caractérisant le mûrissement au cours de l'entreposage de trois variétés de bananes *Musa* spp. (AAB, cv. Corne 1; AAA, cv. Poyo et AA, cv. Figue sucrée). *Sciences & Nature* **7**, 155-163.

Oleski N, Mahdavi P, Bennett AB. 1987. Transport Properties of the Tomato Fruit Tonoplast : II. Citrate Transport. *Plant Physiology* **84**, 997-1000.

Or E, BAYBIK J, Sadka A, SAKS Y. 2000. Isolation of mitochondrial malate dehydrogenase and phosphoenolpyruvate carboxylase cDNA clones from grape berries and analysis of their expression pattern throughout berry development. *Journal of Plant Physiology* **157**, 527-234.

Osuji JO, Ndukwu BC. 2005. Probable functions and remobilisation of calcium oxalates in *Musa L*. *African journal of biotechnology* **4**, 1139-1141.

Palmer J, Schwitzguebel J, Møller I. 1982. Regulation of malate oxidation in plant mitochondria. Response to rotenone and exogenous NAD^+. *Biochemical Journal* **208**, 703-711.

Penning de Vries F, Laar Hv. 1982. Simulation of growth processes and the model BACROS. In: Pudoc FWTPdVaHHVL, ed. *Simulation of plant growth and crop production.* Wageningen, 114-135.

Penning de Vries F. 1989. *Simulation of ecophysiological processes of growth in several annual crops*. Wageningen: IRRI

Pinheiro J, Bates D, DebRoy S, Sarkar D. 2013. Package 'nlme': Linear and Nonlinear Mixed Effects Models.

Possner D, Ruffner HP, Rast DM. 1981. Isolation and biochemical characterization of grape malic enzyme. *Planta* **151**, 549-554.

Pracharoenwattana I, Smith SM. 2008. When is a peroxysome not a peroxysome ? *Trends in Plant Science* **13**, 522-525.

Prudent M, Dai ZW, Génard M, Bertin N, Causse M, Vivin P. 2013. Resource competition modulates the seed number–fruit size relationship in a genotype-dependent manner: A modeling approach in grape and tomato. *Ecological Modelling* **(*in press*)**.

Pua EC, Chandramouli S, Han P, Liu P. 2003. Malate synthase gene expression during fruit ripening of Cavendish banana (*Musa acuminata* cv. Williams). *Journal of experimental botany* **54**, 309-316.

Quaggio JA, Mattos Junior D, Boaretto RM. 2011. Sources and rates of potassium for sweet orange production. *Scientia Agricola* **68**, 369-375.

Quilot-Turion B, Ould-Sidi MM, Kadrani A, Hilgert N, Génard M, Lescourret F. 2011. Optimization of parameters of the 'Virtual Fruit' model to design peach genotype for sustainable production systems. *European Journal of Agronomy* **42**, 34-48.

Quilot B, Génard M. 2005. Simulating genotypic variation of fruit quality in an advanced peach3Prunus davidiana cross. *Journal of experimental botany* **56**.

Quilot B, Kervella J, Génard M, Lescourret F. 2005. Analysing the genetic control of peach fruit quality through an ecophysiological model combined with a QTL approach. *Journal of experimental botany* **56**, 3083-3092.

Radi M, Mahrouz M, Jaouad A, Amiot MJ. 2003. Influence of mineral fertilization (NPK) on the quality of apricot fruit (cv. Canino). The effect of the mode of nitrogen supply. *Agronomie* **23**, 737-745.

Ramesh Kumar A, Kumar N. 2007. Sulfate of potash foliar spray effects on yield, quality, and post-harvest life of banana. *Better crops* **91**, 22-24.

Ratajczak R. 2000. Structure, function and regulation of the plant vacuolar H+-translocating ATPase. *Biochemica and Biophysica Acta* **1465**, 17-36.

Ratajczak R, Lüttge U, Gonzalez P, Etxeberria E. 2003. Malate and malate-channel antibodies inhibit electrogenic and ATP-dependent citrate transport across the tonoplast of citrus juice cells. *Journal of Plant Physiology* **160**, 1313-1317.

Rea PA, Sanders D. 1987. Tonoplast energization: two H^+ pumps, one membrane. *Physiologia plantarum* **71**, 131-141.

Regalado A, Pierri CL, Bitetto M, Laera VL, Pimentel C, Francisco R, Passarinho J, Chaves MM, Agrimi G. 2013. Characterization of mitochondrial dicarboxylate/tricarboxylate transporters from grape berries. *Planta* **237**, 693-703.

Reitz HJ, Koo RCJ. 1960. Effect of nitrogen and potassium fertilization on yield, fruit quality, and leaf analysis of Valencia orange. *American society for horticultural science*, Vol. 75, 244-252.

Rentsch D, Martinoia E. 1991. Citrate transport into barley mesophyll vacuoles-comparison with malate uptake activity. *Planta* **184**, 532-537.

Rienmüller F, Dreyer I, Schönknecht G, Schulz A, Schumacher K, Nagy R, Martinoia E, Marten I, Hedrich R. 2012. Luminal and Cytosolic pH Feedback on Proton Pump Activity and ATP Affinity of V-type ATPase from *Arabidopsis*. *Journal of Biological Chemistry* **287**, 8986-8993.

Roberts JK, Lane AN, Clark RA, Nieman RH. 1985. Relationships between the rate of synthesis of ATP and the concentrations of reactants and products of ATP hydrolysis in maize root tips, determined by ^{31}P nuclear magnetic resonance. *Archives of Biochemistry and Biophysics* **240**, 712-722.

Rongala J. 2008. Identification and localization of vacuolar organic acid carriers in grapevine berries. PhD thesis, University of Adelaide, Faculty of Science, School of Agriculture, food and wine, Waite Campus, Adelaide.

Rottensteiner H, Theodoulou FL. 2006. The ins and outs of peroxisomes: co-ordination of membrane transport and peroxisomal metabolism. *Biochimica et Biophysica Acta* **1763**, 1527-1540.

Ruffner HP, Hawker JS, Hale CR. 1976. Temperature and enzymic control of malate metabolism in berries of *Vitis vinifera*. *Phytochemistry* **15**, 1877-1880.

Rufner HP. 1982. Metabolism of tartaric and malic acids in *vitis*: a review,-part B. *Vitis* **21**, 346-358.

Ruhl EH. 1989. Effect of potassium and nitrogen supply on the distribution of minerals and organic acids and the composition of grape juice of Sultana vines. *Australian Journal of Experimental Agriculture* **29**, 133-137.

Sacher J. 1966. Permeability characteristics and amino acid incorporation during senescence (ripening) of banana tissue. *Plant Physiology* **41**, 701-708.

Sadka A, Dahan E, Cohen L, Marsh KB. 2000a. Aconitase activity and expression during the development of lemon fruit. *Physiologia plantarum* **108**, 255-262.

Sadka A, Dahan E, Or E, Cohen L. 2000b. $NADP^+$-isocitrate dehydrogenase gene expression and isozyme activity during citrus fruit development. *Plant Science* **158**, 173-181.

Sadka A, Dahan E, Or E, Roose ML, Marsh KB, Cohen L. 2001. Comparative analysis of mitochondrial citrate synthase gene structure, transcript level and enzymatic activity in acidless and acid-containing Citrus varieties. *Functional Plant Biology* **28**, 383-390.

Saradhuldhat P, Paull RE. 2007. Pineapple organic acid metabolism and accumulation during fruit development. *Scientia Horticulturae* **112**, 297-303.

Sathiamoorthy S, Jeyabaskaran K. 2001. Potassium management of banana. In: IPI/NARCTT, ed. *Regional workshop: potassium and water management in West Asia and North Africa*. Amman.

Schallau K, Junker BH. 2010. Simulating plant metabolic pathways with enzyme-kinetic models. *Plant Physiology* **152**, 1763-1771.

Schauer N, Semel Y, Roessner U, Gur A, Balbo I, Carrari F, Pleban T, Perez-Melis A, Bruedigam C, Kopka J. 2006. Comprehensive metabolic profiling and phenotyping of interspecific introgression lines for tomato improvement. *Nature biotechnology* **24**, 447-454.
Scheible WR, Gonzales-Fontes A, Lauerer M, Müller-Röber B, Caboche M, Stitt M. 1997. Nitrate acts as a signal to induce organic acid metabolism and repress starch metabolism in Tobacco. *The plant cell* **9**, 783-798.
Seymour GB, Taylor J, Tucker GA. 1993. *Biochemistry of fruit ripening*. London: Chapman & Hall.
Sha SF, Li JC, Wu J, Zhang SL. 2011. Changes in the organic acid content and related metabolic enzyme activities in developing 'Xinping' pear fruit. *African Journal of Agricultural Research* **6**, 3560-3567.
Shimada T, Nakano R, Shulaev V, Sadka A, Blumwald E. 2006. Vacuolar citrate/H^+ symporter of citrus juice cells. *Planta* **224**, 472-480.
Shiratake K, Kanayama Y, Maeshima M, Yamaki S. 1997. Changes in H^+-pumps and a tonoplast intrinsic protein of vacuolar membranes during the development of pear fruit. *Plant Cell physiology* **38**, 1039-1045.
Shiratake K, Martinoia E. 2007. Transporters in fruit vacuoles. *Plant Biotechnology* **24**, 127-133.
Smith FA, Raven JA. 1979. Intracellular pH and its regulation. *Annual review of plant physiology and plant molecular biology* **30**, 289-311.
Soetaert K, Petzoldt T, Setzer RW. 2010. Solving differential equations in R: Package deSolve. *Journal of Statistical Software* **33**, 1-25.
Souty M, Perret A, André P. 1967. Premières observations sur quelques variétés de pêches destinées à la conserve. *Annales de technologies agricoles* **6**, 775-791.
Souty M, Génard M, Reich M, Albagnac G. 1999. Effect of assimilate supply on peach fruit maturation and quality. *Canadian Journal of Plant Science* **79**, 259-268.
Spironello A, Quaggio JA, Teixeira LAJ, Furlani PR, Sigrist JMM. 2004. Pineapple yield and fruit quality effected by NPK fertilization in a tropical soil. *Revista Brasileira de Fruticultura* **26**, 155-159.
Steuer R, Nesi AN, Fernie AR, Gross T, Blasius B, Selbig J. 2007. From structure to dynamics of metabolic pathways: application to the plant mitochondrial TCA cycle. *Bioinformatics* **23**, 1378-1385.
Struik PC, Yin X, Visser P. 2005. Complex quality traits: now time to model. *Trends in Plant Science* **10**, 513-516.
Surendranathan KK, Nair PM. 1976. Stimulation of the glyoxylate shunt in gamma-irradiated banana. *Phytochemistry* **15**, 371-373.
Suzuki Y, Shiratake K, Yamaki S. 2000. Seasonal changes in the activities of vacuolar H^+-pumps and their gene expression in the developping japanese pear fruit. *Journal of the Japanese Society of Horticultural Science* **69**, 15-21.
Sweetlove LJ, Beard KFM, Nunes-Nesi A, Fernie AR, Ratcliffe RG. 2010. Not just a circle: flux modes in the plant TCA cycle. *Trends in Plant Science* **15**, 462-470.
Sweetlove LJ, Obata T, Fernie AR. 2013. Systems analysis of metabolic phenotypes: what have we learnt? . *Trends in Plant Science* **(*in press*)**.
Sweetman C, Deluc LG, Cramer GR, Ford CM, Soole KL. 2009. Regulation of malate metabolism in grape berry and other developing fruits. *Phytochemistry* **70**, 1329–1344.
Taiz L, Zeiger E. 2010. Plant Physiology, Ed Fifth. Sinauer Associates, USA.
Tang M, Bie ZL, Wu MZ, Yi HP, Feng JX. 2010. Changes in organic acids and organic acids metabolism enzymes in melon fruit during development. *Scientia Horticulturae* **123**, 360-365.
Tardieu F. 2003. Virtual plants: modelling as a tool for the genomics of tolerance to water deficit. *Trends in Plant Science* **8**, 9-14.

Taureilles-Saurel C, Romieu C, Robin JP, Flanzy C. 1995. Grape (*Vitis vinifera* L.) malate dehydrogenase. II. Characterization of the major mitochondrial and cytosolic isoforms and their role in ripening. *American Journal of Enology and Viticulture* **46**, 29-36.
Terol J, Soler G, Talon M, Cercos M. 2010. The aconitate hydratase family from *Citrus*. *BMC plant biology* **10**, 222.
Terrier N, Deguilloux C, Sauvage F-X, Martinoia E, Romieu C. 1998. Proton pumps and anion transport in *Vitis vinifera:* The inorganic pyrophosphatase plays a predominant role in the energization of the tonoplast. *Plant physiology and biochemistry* **36**, 367-377.
Terrier N, Sauvage F-X, Ageorges A, Romieu C. 2001. Changes in acidity and in proton transport at the tonoplast of grape berries during development. *Planta* **213**, 20-28.
Terrier N, Glissant D, Grimplet J, Barrieu F, Abbal P, Couture C, Ageorges A, Atanassova R, Renaudin JP, Dedaldechamp F, Romieu C, Delrot S, S. H. 2005. Isogene specific oligo arrays reveal multifaceted changes in gene expression during grape berry (*Vitis vinifera L.*) development. *Planta* **222**, 832-847.
Thakur A, Singh Z. 2012. Responses of 'Spring Bright' and 'Summer Bright' nectarines to deficit irrigation: Fruit growth and concentration of sugars and organic acids. *Scientia Horticulturae* **135**, 112-119.
Thornley JH, Johnson IR. 1990. *Plant and crop modelling: a mathematical approach to plant and crop physiology*. New York Oxford university press.
Tieman D, Bliss P, McIntyre LM, Blandon-Ubeda A, Bies D, Odabasi AZ, Rodríguez GR, van der Knaap E, Taylor MG, Goulet C. 2012. The chemical interactions underlying tomato flavor preferences. *Current Biology* **22**, 1035-1039.
Turner D. 1995. The response of the plant to the environment. In: S. G, ed. *Bananas and Plantains*. London: Chapman & Hall, 206-229.
Ulrich JI. 1970. Organic acids. In : The Biochemistry of fruits and their products (Ed. A.C. Hulme). *Academic press London and New York* **1**, 89-117.
Vadivel E, Shanmugavelu KG. 1978. Effect of increasing rates of potash on banana quality cv. Robusta. *Revue de la potasse* **24**, 1-4.
Veit-Köhler U, Krumbein A, Kosegarten H. 1999. Effect of different water supply on plant growth and fruit quality of *Lycopersicon esculentum*. *Journal of Plant Nutrition and Soil Science* **162**, 583-588.
Vertregt N, Penning de Vries F. 1987. A rapid method for determining the efficiency of biosynthesis of plant biomass. *Journal of Theoretical Biology* **128**, 109-119.
Walinga I, Lee J, Houba V, Vark Wv, Novozamsky I. 1995. *Plant analysis manual*. Dordrecht: Kluwer Academic.
Walker A, Thornley J. 1977. The tomato fruit: import, growth, respiration and carbon metabolism at different fruit sizes and temperatures. *Annals of Botany* **41**, 977-985.
Wang SY, Camp MJ. 2000. Temperature after bloom affects plant growth and fruit quality of strawberry. *Scientia Horticulturae* **85**, 183-199.
Watanabe K, Takahashi B. 1998. Determination of soluble and insoluble oxalate contents in kiwifruit (*Actinidia deliciosa*) and related species. *Journal of the Japanese Society for Horticultural Science* **67**, 299-305.
Wen T, Qing EX, Zeng W, Liu Y. 2001. Study on the change of organic acid synthetase activity during fruit development of navel orange (*Citrus sinensis* Osbeck). *Journal of Sichuan Agricultural University* **19**, 27-30.
Williams TC, Poolman MG, Howden AJ, Schwarzlander M, Fell DA, Ratcliffe RG, Sweetlove LJ. 2010. A genome-scale metabolic model accurately predicts fluxes in central carbon metabolism under stress conditions. *Plant Physiology* **154**, 311-323.
Wu BH, Génard M, Lescourret F, Gomez L, Li SH. 2002. Influence of assimilate and water supply on seasonal variation of acids in peach (cv Suncrest). *Journal of the Science of Food and Agriculture* **82**, 1829-1836.

Wu BH, Quilot B, Génard M, Kervella J, Li SH. 2005. Changes in sugar and organic acid concentrations during fruit maturation in peaches, *P. davidiana* and hybrids as analyzed by principal component analysis. *Scientia Horticulturae* **103**, 429-439.
Wu BH, Génard M, Lobit P, Longuenesse JJ, Lescourret F, Habib R, Li SH. 2007. Analysis of citrate accumulation during peach fruit development via a model approach. *Journal of experimental botany* **58**, 2583–2594.
Wu BH, Quilot B, Genard M, Li S, Zhao J, Yang J, Wang Y. 2012. Application of a SUGAR model to analyse sugar accumulation in peach cultivars that differ in glucose–fructose ratio. *Journal of Agricultural Science-London* **150**, 53-63.
Wullschleger S, Norby R, Love J, Runck C. 1997. Energetic Costs of Tissue Construction in Yellow-poplar and White Oak Trees Exposed to Long-term CO_2 Enrichment. *Annals of Botany* **80**, 289-297.
Wyn Jones R, Pollard A. 1983. Proteins, enzymes and inorganic ions. *Encyclopedia of plant physiology, new series* **15**, 528-562.
Xu K, Wang A, Brown S. 2012. Genetic characterization of the *Ma* locus with pH and titratable acidity in apple. *Molecular Breeding* **30**, 899-912.
Yakushiji H, Morinaga K, Nonami H. 1998. Sugar accumulation and partitioning in Satsuma mandarin tree tissues and fruit in response to drought stress. *Journal of the American Society for Horticultural Science* **123**, 719-726.
Yamaki S. 1984. Isolation of vacuoles from immature apple fruit flesh and compartmentation of sugars, organic acids, phenolic compounds and amino acids. *Plant and cell physiology* **25**, 151-166.
Yamaki YT. 1989. Organic acids in the juice of citrus fruits. *Journal of the Japanese Society for Horticultural Science* **58**, 587-594.
Yang LT, Xie CY, Jiang HX, Chen LS. 2011. Expression of six malate-related genes in pulp during the fruit development of two loquat (*Eriobotrya japonica*) cultivars differing in fruit acidity. *African journal of biotechnology* **10**, 2414-2422.
Yao YX, Li M, Liu Z, You CX, Wang DM, Zhai H, Hao YJ. 2009. Molecular cloning of three malic acid related genes *MdPEPC, MdVHA-A, MdcyME* and their expression analysis in apple fruits. *Scientia Horticulturae* **122**, 404-408.
Yao YX, Li M, Zhai H, You CX, Hao YJ. 2011. Isolation and characterization of an apple *cytosolic malate dehydrogenase* gene reveal its function in malate synthesis. *Journal of Plant Physiology* **168**, 474-480.
Young RE, Biale JB. 1968. Carbon dioxide effects on fruits. *Planta* **81**, 253-263.
Zambrano-Bigiarini M, Rojas R, Zambrano-Bigiarini MM. 2013. Package 'hydroPSO'.
Zhao YH, Li XL, Jiang ZS, Wang CJ, Yang FL. 2007. Organic acid metabolism in nectarine fruit development under protected cultivation. *Chinese Journal of Eco-Agriculture* **15**, 87-89.
Zuur AF, Ieno EN, Walker N, Saveliev AA, Smith GM. 2009. *Mixed effects models and extensions in ecology with R*. New York: Springer.

Annexes

Appendix 1 Pictures of the fruits of three cultivars of dessert bananas used in the 2011 and 2012 field experiments and graphics showing the repartition of the different organic acids present in the pulp of ripe banana fruit.

Indonésia 110 (IDN) **Pisang Lilin (PL)** **Pisang Jari Buaya (PJB)**

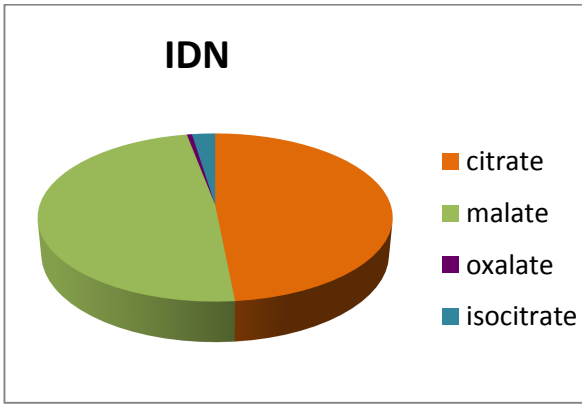

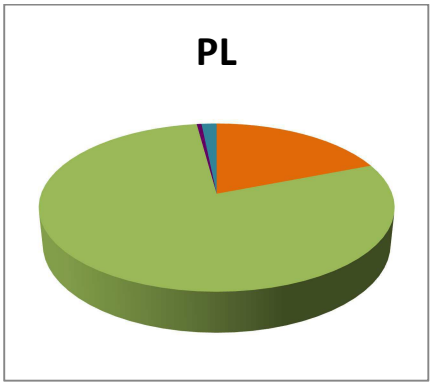

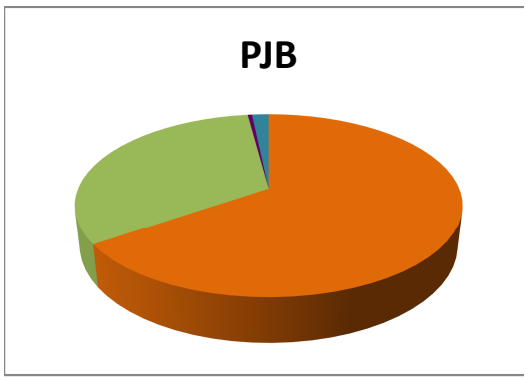

Appendix 2 LMM analysis of predicted and measured concentrations of malate (mmol. Kg FW^{-1}) during fruit growth and post-harvest ripening.

Linear mixed-effects models [LMMs (Gałecki and Burzykowski, 2013)] were used to examine the relationship between malate concentration and explanatory variables (fruit age, cultivar, treatment), and interactions. We used quadratic and cubic terms of fruit age when the curve passed through a maximum and had an asymmetrical shape. We used the lme function in the 'nlme' library (Pinheiro et al., 2013) in the statistical program R 2.14.0. "Banana plant" was treated as a random effect because banana plants were assumed to contain unobserved heterogeneity, which is impossible to model. A temporal correlation structure was used to account for temporal pseudo-replication. Model selection was made using the top-down strategy (Zuur et al., 2009): starting with a model in which the fixed component contains all the explanatory variables and interactions, we found the optimal structure of the random component. We then used the F-statistic obtained with restricted maximum likelihood (REML) estimation to find the optimal fixed structure. Finally, the significance of each factor kept in the optimal model was assessed using the F-statistic obtained with REML estimation.

Appendix 2.1 LMM analysis of predicted and measured concentrations of malate (mmol. Kg FW^{-1}) during fruit growth. The factors studied were fruit age, cultivar, and pruning treatment in the 2011 experiment, and fruit age, cultivar, and potassium fertilization in the 2012 experiment.

		F-value [a] and significance [b]	
Year	Factors [c]	Predicted malate concentration	Measured malate concentration
2011			
	c	51***	79***
	p	Ns	Ns
	a	78***	1599***
	a^2	Ns	44***
	a^3	Ns	9**
	p : a	Ns	Ns
	c : a	10***	155***
	c : p	Ns	Ns
	c: p : a	Ns	Ns
2012			
	c	77***	92***
	f	Ns	Ns
	a	8**	560***
	a^2	7**	70***
	a^3	5*	6**
	c : a	Ns	54***
	c : f	Ns	Ns
	f: a	Ns	Ns
	c: f: a	Ns	Ns

[a] The F-value is given only for the factors kept in the optimal model.

[b] *** p-value < 0.001; ** p-value < 0.01; * p-value<0.05 ; Ns : not significant.

[c] Codes for factors: c=cultivar; p=pruning treatment; a=fruit age (in % of flowering-to-yellowing time); f=potassium fertilization treatment.

Appendix 2.2 LMM analysis of predicted and measured malate concentration (mmol. Kg FW^{-1}) during post-harvest fruit ripening. The factors studied were ripening stage, fruit age at harvest, cultivars, and pruning treatment in the 2011 experiment, and ripening stage, cultivars, and potassium fertilization treatment in the 2012 experiment.

		F-value [a] and significance [b]	
Year	Factors	Predicted malate concentration	Measured malate concentration
2011			
	c	199***	284***
	p	Ns	Ns
	a	6*	11**
	r	363***	327***
	r^2	563***	241***
	r^3	12***	Ns
	p : r	Ns	Ns
	a : c	4*	15***
	a : r	Ns	15***
	c : r	92***	50***
	p : a	Ns	Ns
	p : c	Ns	Ns
	a:c:r	Ns	Ns
	p :a :c	Ns	Ns
	p:a:r	Ns	Ns
	p:a:c:r	Ns	Ns
2012			
	c	139***	73***
	f	Ns	Ns
	r	473***	386***
	r^2	341***	184***
	r^3	Ns	Ns
	c : f	Ns	Ns
	c : r	46***	51***
	f : r	Ns	Ns
	c: f : r	Ns	Ns

[a] The F-value is given only for the factors retained from the optimal model.

[b] *** p-value < 0.001; ** p-value < 0.01; * p-value<0.05; Ns: not significant.

[c] Codes for factors: c=cultivar; p=pruning treatment; a=fruit age at harvest; r=ripening stage; f=potassium fertilization treatment.

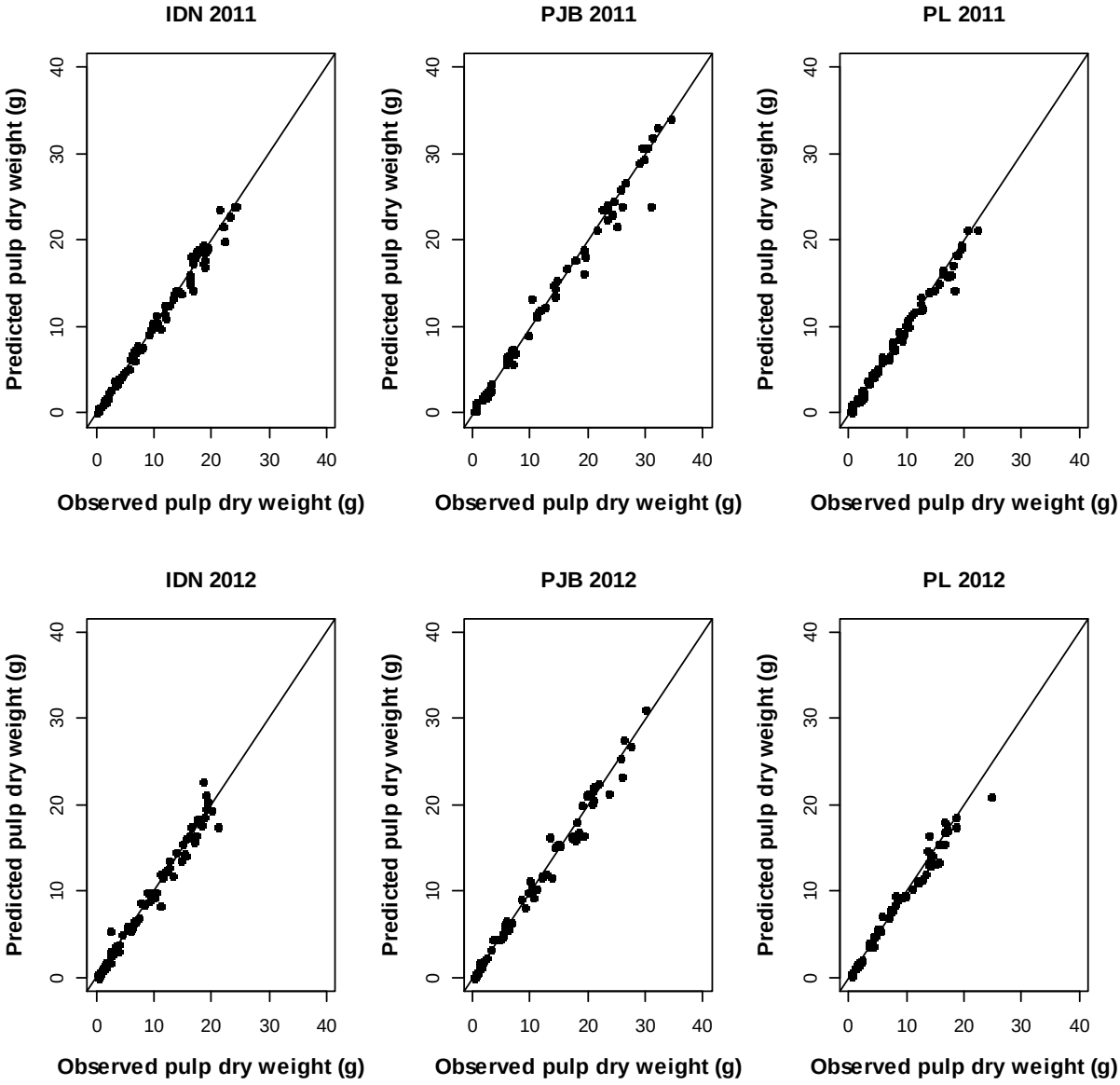

Appendix 3 Observed pulp dry weight vs. pulp dry weight predicted by the growth expolinear model for cultivars IDN, PJB, and PL in 2011 and 2012.

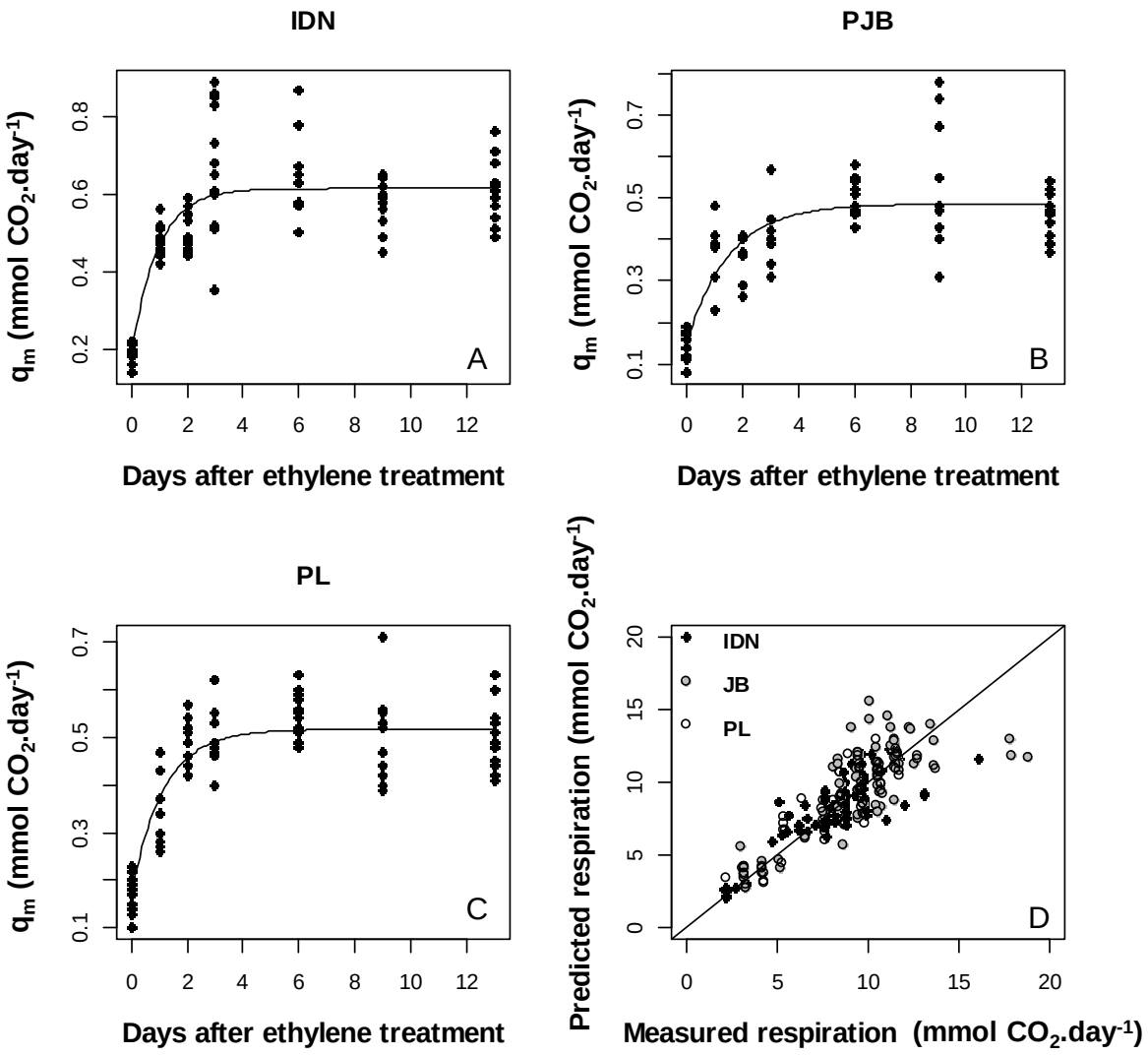

Appendix 4 Variations in the maintenance respiration coefficient q_m during post-harvest ripening of banana in cultivars IDN, PJB, and PL (A, B, and C), and predicted vs. measured fruit respiration (D).

Appendix 5 LMM analysis of predicted and measured citrate concentration (g. 100 g FW^{-1}) during fruit growth and post-harvest fruit ripening.

Linear mixed-effects models [LMMs (Gałecki and Burzykowski, 2013)] were used to examine the relationship between citrate concentration and explanatory variables (fruit age, cultivar, treatment), and interactions. We used quadratic and cubic terms of fruit age when the curve passed through a maximum and had an asymmetrical shape. We used the lme function in the 'nlme' library (Pinheiro et al., 2013) in the statistical program R 2.14.0. "Banana plant" was treated as a random effect because banana plants were assumed to contain unobserved heterogeneity, which is impossible to model. A temporal correlation structure was used to account for temporal pseudo-replication. Model selection was made using the top-down strategy (Zuur *et al.*, 2009): starting with a model in which the fixed component contains all the explanatory variables and interactions, we found the optimal structure of the random component. We then used the F-statistic obtained with restricted maximum likelihood (REML) estimation to find the optimal fixed structure. Finally, the significance of each factor kept in the optimal model was assessed using the F-statistic obtained with REML estimation.

Appendix 5.1 LMM analysis of predicted and measured citrate concentration (g. 100 g FW^{-1}) during fruit growth. The factors studied were fruit age, cultivar, and pruning treatment in the 2011 experiment, and fruit age, cultivar, and potassium fertilization in the 2012 experiment.

		F-value [a] and significance [b]	
Year	Factors [c]	Predicted citrate concentration	Measured citrate concentration
2011			
	c	20***	16***
	p	6*	Ns
	a	5649***	2703***
	a^2	224***	184***
	a^3	Ns	Ns
	p : a	22***	Ns
	c : a	27***	7***
	c : p	Ns	Ns
	c: p : a	Ns	Ns
2012			
	c	5*	28***
	f	Ns	Ns
	a	4239***	1603***
	a^2	208***	142***
	a^3	15***	Ns
	c : a	36***	8***
	c : f	Ns	Ns
	f: a	Ns	Ns
	c: f: a	Ns	Ns

[a] The F-value is given only for the factors kept in the optimal model.

[b] *** p-value < 0.001; ** p-value < 0.01; * p-value<0.05 ; Ns : not significant.

[c] Codes for factors: c=cultivar; p=pruning treatment; a=fruit age (in % of flowering-to-yellowing time); f=potassium fertilization treatment.

Appendix 5.2 LMM analysis of predicted and measured citrate concentration (g. 100 g FW^{-1}) during post-harvest fruit ripening. The factors studied were ripening stage, fruit age at harvest, cultivars and pruning treatment in the 2011 experiment, and ripening stage, cultivars and potassium fertilization treatment in the 2012 experiment.

		F-value [a] and significance [b]	
Year	Factors	Predicted citrate concentration	Measured citrate concentration
2011			
	c	517***	496***
	p	Ns	Ns
	a	Ns	23***
	r	241***	21***
	r^2	36***	45***
	r^3	6*	5*
	p : r	10**	Ns
	a : c	15***	Ns
	a : r	21***	Ns
	c : r	1204***	212***
	p : a	Ns	Ns
	p : c	Ns	Ns
	a:c:r	35***	Ns
	p :a :c	Ns	Ns
	p:a:r	Ns	Ns
	p:a:c:r	Ns	Ns
2012			
	c	147***	252***
	f	Ns	Ns
	r	106***	6*
	r^2	20***	29***
	r^3	7**	Ns
	c : f	6**	Ns
	c : r	564***	104***
	f : r	Ns	Ns
	c: f : r	Ns	Ns

[a] The F-value is given only for the factors retained from the optimal model.

[b] *** p-value < 0.001; ** p-value < 0.01; * p-value<0.05 ; Ns : not significant.

[c] Codes for factors: c=cultivar; p=pruning treatment; a=fruit age at harvest; r=ripening stage; f=potassium fertilization treatment.

Appendix 6 Estimated parameter values and standard errors (in parentheses) of the expolinear growth model of pulp dry weight for the three cultivars (IDN, PJB, and PL) and two contrasted fruit loads (LL: low fruit load; HL: high fruit load) in 2011.

Cultivar	Fruit load	C_m	R_m	t_b
IDN	LL	0.34 (0.02)	0.11 (0.03)	30.1 (2.4)
IDN	HL	0.28(0.02)	0.11 (0.04)	29.7 (3.7)
JB	LL	0.54 (0.03)	0.11 (0.03)	36.1 (3.0)
JB	HL	0.40 (0.02)	0.13 (0.04)	30.4 (2.6)
PL	LL	0.36 (0.02)	0.11 (0.03)	29.9 (2.7)
PL	HL	0.32 (0.02)	0.12 (0.04)	30.92 (3.4)

Appendix 7 Estimated parameter values and standard errors (in parentheses) of the expolinear growth model of pulp dry weight in the three cultivars (IDN, PJB, and PL) and the two contrasted levels of potassium fertilization (NF: no potassium fertilization; HF: high potassium fertilization) in 2012.

Cultivar	Potassium fertilization	C_m	R_m	t_b
IDN	NF	0.29 (0.02)	0.15 (0.08)	26.5 (2.9)
IDN	HF	0.26 (0.03)	0.13 (0.08)	28.5 (5.0)
JB	NF	0.34 (0.02)	0.21 (0.14)	28.4 (2.2)
JB	HF	0.40 (0.04)	0.12 (0.07)	32.5 (5.3)
PL	NF	0.31 (0.02)	0.14 (0.06)	27.2 (3.0)
PL	HF	0.33 (0.02)	0.16 (0.10)	25.2 (3.5)